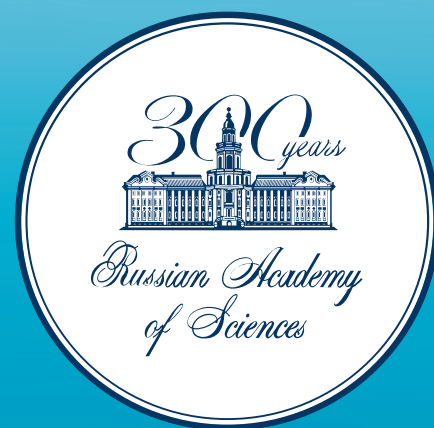




ISSN 2499-9768 print

МОРСКОЙ
БИОЛОГИЧЕСКИЙ
ЖУРНАЛ
MARINE BIOLOGICAL JOURNAL

Vol. 8 No. 4
2023



**МОРСКОЙ БИОЛОГИЧЕСКИЙ ЖУРНАЛ
MARINE BIOLOGICAL JOURNAL**

Выпуск посвящён 300-летию Российской академии наук.

Журнал включён в перечень рецензируемых научных изданий, рекомендованных ВАК Российской Федерации, а также в базу данных Russian Science Citation Index (RSCI).

Журнал реферируется международной библиографической и реферативной базой данных Scopus (Elsevier), международной информационной системой по водным наукам и рыболовству ASFA (ProQuest), Всероссийским институтом научно-технической информации (ВИНИТИ),

а также Российским индексом научного цитирования (РИНЦ) на базе Научной электронной библиотеки elibrary.ru. Все материалы проходят независимое двойное слепое рецензирование.

Редакционная коллегия

Главный редактор

Егоров В. Н., акад. РАН, д. б. н., проф., ФИЦ ИнБЮМ

Заместитель главного редактора

Солдатов А. А., д. б. н., проф., ФИЦ ИнБЮМ

Ответственный секретарь

Корнийчук Ю. М., к. б. н., ФИЦ ИнБЮМ

Адрианов А. В., акад. РАН, д. б. н., проф.,
ННЦМБ ДВО РАН

Азовский А. И., д. б. н., проф., МГУ

Васильева Е. Д., д. б. н., МГУ

Генкал С. И., д. б. н., проф., ИБВВ РАН

Денисенко С. Г., д. б. н., ЗИН РАН

Довгаль И. В., д. б. н., проф., ФИЦ ИнБЮМ

Зуев Г. В., д. б. н., проф., ФИЦ ИнБЮМ

Коновалов С. К., чл.-корр. РАН, д. г. н., ФИЦ МГИ

Мильчакова Н. А., к. б. н., ФИЦ ИнБЮМ

Неврова Е. Л., д. б. н., ФИЦ ИнБЮМ

Празукин А. В., д. б. н., ФИЦ ИнБЮМ

Руднева И. И., д. б. н., проф., ФИЦ МГИ

Рябушко В. И., д. б. н., ФИЦ ИнБЮМ

Самышев Э. З., д. б. н., проф., ФИЦ ИнБЮМ

Санжарова Н. И., чл.-корр. РАН, д. б. н., ВНИИРАЭ

Совга Е. Е., д. г. н., проф., ФИЦ МГИ

Стельмах Л. В., д. б. н., ФИЦ ИнБЮМ

Трапезников А. В., д. б. н., ИЭРиЖ УрО РАН

Фесенко С. В., д. б. н., проф., ВНИИРАЭ

Arvanitidis Chr., D. Sc., HCMR, Greece

Bat L., D. Sc., Prof., Sinop University, Turkey

Ben Souissi J., D. Sc., Prof., INAT, Tunis

Kociolek J. P., D. Sc., Prof., CU, USA

Magni P., PhD, CNR-IAS, Italy

Moncheva S., D. Sc., Prof., IO BAS, Bulgaria

Pešić V., D. Sc., Prof., University of Montenegro,
Montenegro

Zaharia T., D. Sc., NIMRD, Romania

Адрес учредителя, издателя и редакции:

ФИЦ «Институт биологии южных морей
имени А. О. Ковалевского РАН».

Пр-т Нахимова, 2, Севастополь, 299011, РФ.

Тел.: +7 8692 54-41-10. E-mail: mbj@imbr-ras.ru.

Сайт журнала: <https://marine-biology.ru>.

Адрес соиздателя:

Зоологический институт РАН.

Университетская наб., 1, Санкт-Петербург, 199034, РФ.

Editorial Board

Editor-in-Chief

Egorov V. N., Acad. of RAS, D. Sc., Prof., IBSS, Russia

Assistant Editor

Soldatov A. A., D. Sc., Prof., IBSS, Russia

Managing Editor

Korneychuk Yu. M., PhD, IBSS, Russia

Adrianov A. V., Acad. of RAS, D. Sc., Prof.,
NSCMB FEB RAS, Russia

Arvanitidis Chr., D. Sc., HCMR, Greece

Azovsky A. I., D. Sc., Prof., MSU, Russia

Bat L., D. Sc., Prof., Sinop University, Turkey

Ben Souissi J., D. Sc., Prof., INAT, Tunis

Denisenko S. G., D. Sc., ZIN, Russia

Dovgal I. V., D. Sc., Prof., IBSS, Russia

Fesenko S. V., D. Sc., Prof., RIRAE, Russia

Genkal S. I., D. Sc., Prof., IBIW RAS, Russia

Kociolek J. P., D. Sc., Prof., CU, USA

Konovalev S. K., Corr. Member of RAS, D. Sc., Prof.,

MHI RAS, Russia

Magni P., PhD, CNR-IAS, Italy

Milchakova N. A., PhD, IBSS, Russia

Moncheva S., D. Sc., Prof., IO BAS, Bulgaria

Nevrova E. L., D. Sc., IBSS, Russia

Pešić V., D. Sc., Prof., University of Montenegro, Montenegro

Prazukin A. V., D. Sc., IBSS, Russia

Rudneva I. I., D. Sc., Prof., MHI RAS, Russia

Ryabushko V. I., D. Sc., IBSS, Russia

Samyshev E. Z., D. Sc., Prof., IBSS, Russia

Sanjharova N. I., Corr. Member of RAS, D. Sc., RIRAE, Russia

Sovga E. E., D. Sc., Prof., MHI RAS, Russia

Stelmakh L. V., D. Sc., IBSS, Russia

Trapeznikov A. V., D. Sc., IPAE UB RAS, Russia

Vasil'eva E. D., D. Sc., MSU, Russia

Zaharia T., D. Sc., NIMRD, Romania

Zuyev G. V., D. Sc., Prof., IBSS, Russia

Founder, Publisher, and Editorial Office address:

A. O. Kovalevsky Institute of Biology of the Southern Seas
of Russian Academy of Sciences.

2 Nakhimov ave., Sevastopol, 299011, Russia.

Тел.: +7 8692 54-41-10. E-mail: mbj@imbr-ras.ru.

Journal website: <https://marine-biology.ru>.

Co-publisher address:

Zoological Institute Russian Academy of Sciences.

1 Universitetskaya emb., Saint Petersburg, 199034, Russia.

МОРСКОЙ БИОЛОГИЧЕСКИЙ ЖУРНАЛ

MARINE BIOLOGICAL JOURNAL

2023 Vol. 8 no. 4

Established in February 2016

SCIENTIFIC JOURNAL

4 issues per year

CONTENTS

Scientific communications

- Boltachova N. A., Podzorova D. V., and Lisitskaya E. V.*
Distribution of polychaetes of the family Spionidae (Annelida)
on the shelf of the northwestern part of the Black Sea 3–22
- Bondarev I. P.*
Functional morphology and morphological variability of the operculum
of *Rapana venosa* (Gastropoda, Muricidae) 23–39
- Zaytsev A. A., Troshichev A. R., Pakhomov M. V., and Yakovlev A. P.*
Marine mammals of the Kola Bay, Barents Sea 40–51
- Kovalyova I. V., Finenko Z. Z., and Suslin V. V.*
Spatial and temporal dynamics of the phytoplankton biomass
in the surface layer of the Black Sea 52–63
- Melnik L. A., Melnik A. V., Mashukova O. V., and Melnikov V. V.*
Using the vertical sounding method for recording bioluminescence
in the Antarctic sector of the Atlantic Ocean 64–73
- Mukhametova O. N.*
The structure of coastal ichthyoplankton in the area of the Dudinka River confluence
(Eastern Sakhalin) 74–93
- Sazykina T. G. and Kryshev A. I.*
Assessment of radiation effect of ^{137}Cs , ^{134}Cs , and ^{90}Sr on biota of the Barents Sea
in the vicinity of hypothetical accident with the sunken nuclear submarine K-159 94–105
- #### Notes
- Brunetti J., De Maddalena A., Eliceche Constantini M. A., and Calatayud C.*
On a large shortfin mako shark *Isurus oxyrinchus* (Lamnidae) observed at Cabo San Lucas,
Mexico (eastern central Pacific Ocean) 106–109
- Koroliesova D. D.*
Restoration of the *Chara aculeolate* Kützing phytocenosis
in the Tendrovsky Bay (Black Sea) 110–115
- Selivanova O. N. and Zhigadlova G. G.*
Finding of *Acrosorium yendoii* Yamada (Delesseriaceae, Rhodophyta),
a new to Kamchatka species, in Avacha Gulf 116–120

SCIENTIFIC COMMUNICATIONS

UDC [595.142.241:551.462.32](262.5-16)

**DISTRIBUTION OF POLYCHAETES OF THE FAMILY SPIONIDAE (ANNELIDA)
ON THE SHELF OF THE NORTHWESTERN PART OF THE BLACK SEA**

© 2023 N. A. Boltachova, D. V. Podzorova, and E. V. Lisitskaya

A. O. Kovalevsky Institute of Biology of the Southern Seas of RAS, Sevastopol, Russian Federation

E-mail: nboltacheva@mail.ru

Received by the Editor 09.03.2021; after reviewing 14.09.2021;
accepted for publication 04.08.2023; published online 01.12.2023.

The northwestern part of the Black Sea (NWBS) is a vast shallow water area, biocenoses of which are an important component of the Black Sea ecosystem. Since the benthos of this region has not been studied in recent decades, data on its current state are relevant. A significant contribution to the taxonomic composition of macrozoobenthos is made by polychaetes of the family Spionidae, which are represented by a large number of species and are characterized by high abundance rates. The aim of the research is to study the species composition, distribution, and quantitative representation of polychaetes of the family Spionidae in the NWBS at depths of more than 10–15 m. The material used was macrozoobenthos sampled from 160 stations (230 samples) during research cruises of the RV “Maria S. Merian” and the RV “Professor Vodyanitsky” in 2010–2017 at depths from 10 to 137 m. Bottom sediments were sampled with an Ocean-25 bottom grab (capture area of 0.25 m²) and a box corer (S = 0.1 m²). Bottom sediments were washed through sieves with the smallest mesh diameter of 1 mm. On the surveyed shelf area of the NWBS, 83 Polychaeta species were found, including 12 Spionidae species. Polychaetes were recorded at all the stations performed, while spionids were noted at 66% of their total number. At single stations, up to 6 Spionidae species were registered, but more often, there were 2–3 species. In total, 11 species were identified: *Aonides paucibranchiata* Southern, 1914, *Dipolydora quadrilobata* (Jacobi, 1883), *Microspio mecznikowiana* (Claparède, 1869), *Prionospio* cf. *cirrifer* Wirén, 1883, *Polydora cornuta* Bosc, 1802, *Pygospio elegans* Claparède, 1863, *Scolelepis tridentata* (Southern, 1914), *Scolelepis (Scolelepis) cantabra* (Rioja, 1918), *Spio decorata* Bobretzky, 1871, *Laonice* cf. *cirrata* (M. Sars, 1851), and *Marenzelleria neglecta* Sikorski & Bick, 2004. Non-identified specimens of the genus *Prionospio* were registered as well. Spionidae distribution in the water area of the NWBS is uneven, which is due to the response of certain species to various environmental factors. The maximum density of spionids was 2,984 ind.·m⁻², and the average density was (477 ± 126) ind.·m⁻². The highest density of Spionidae was observed in the depth range of 20–40 m. In terms of density, *P.* cf. *cirrifer*, *A. paucibranchiata*, and *D. quadrilobata* predominated. Out of identified species, three (*M. neglecta*, *P. cornuta*, and *D. quadrilobata*) are non-native for the Black Sea. In the taxonomic composition of Polychaeta of the NWBS, Spionidae accounted for 14%, while in the quantitative representation, their contribution reached 42% of the total density of polychaetes. This indicates a significant role of this family in the functioning of the benthic ecosystem of the NWBS.

Keywords: Polychaeta, Spionidae, *Dipolydora quadrilobata*, density, distribution, northwestern part of the Black Sea

In the second half of the XX century, 192 species were known in the Polychaeta fauna of the Black Sea [Mordukhai-Boltovskoi, 1972]; later, 195 species [Kiseleva, 2004]. In recent decades, the intensification of benthic research (especially in Turkish waters), the development of taxonomy,

and the introduction of non-native species into the Black Sea resulted in a rapid increase in this number to 238 [Kurt-Şahin, Çinar, 2012] and then to 256 [Kurt Şahin et al., 2019]. Polychaetes were recorded at all depths inhabited by macrozoobenthos in the Black Sea – from 0 to 150 m. In terms of the species number, one of the most represented families in the Black Sea is Spionidae Grube, 1850: in 1972, 19 species were known (9.7% of the Polychaeta fauna); by the end of the XX century, 34 species (13.3%) [Kurt-Şahin, Çinar, 2012; Kurt Şahin et al., 2019; Mordukhai-Boltovskoi, 1972].

Spionidae is a family of small, predominantly detritivorous polychaetes that are found in a wide variety of biotopes from intertidal to deep-sea zone, but most of the species inhabit shallow waters. Spionids mainly inhabit soft bottoms, moving freely in sediments near the surface or living in temporary or permanent tubes. The density of such tube-dwelling polychaetes can reach thousands of individuals *per m*² [Blake, 1996; Radashevsky, 2012]. Some species of the genus *Polydora* Bosc, 1802 are borers in various substrates. Most spionids live in marine environments with oceanic salinity; at the same time, certain species exhibit low-salinity tolerance, and some representatives of the genera *Prionospio* Malmgren, 1867, *Pseudopolydora* Czerniavsky, 1881, and *Streblospio* Webster, 1879 are recorded only in estuaries or lakes [Blake, 1996; Radashevsky, 2012]. The larval development of spionids is varied – from pelagic and planktotrophic to almost entirely capsule-based and lecithotrophic [Blake, Arnofsky, 1999]. Larvae of shallow-water sublittoral species, especially those found in estuaries (often used as port areas), easily survive in ballast waters and are transported throughout the world [Radashevsky, 2012; Surugiu, 2012]. As a result, the proportion of spionids is significant in the number of non-native polychaetes in various areas of the World Ocean [Boltachova et al., 2015; Dağlı et al., 2011; Radashevsky, Selifonova, 2013]. For the northern part of the Black Sea, 11 non-native Polychaeta species are known, and 5 out of them belong to the family Spionidae [Boltachova et al., 2021].

The northwestern part of the Black Sea (hereinafter NWBS) is its largest shallow bay, boarded by Romania, Ukraine, and Crimea. Its southern border has been drawn in different ways – along the line connecting Cape Kaliakra (Bulgaria) with Cape Tarkhankut on the Crimean coast [Biologiya, 1967], along the edge of the continental shelf or 100-m isobath [Samyshev, Zolotarev, 2018], and along the parallel 44°40'N [Severo-zapadnaya chast', 2006]. The bottom surface of the NWBS is flat, with a slight slope to the south; it is crossed by the trenches of the Odessa, Dnieper, and Karkinit basins, as well as by river paleochannels and sandbars. The predominant type of sediments in the NWBS are shell debris of varying degree of siltation, which occupy the central part of the area (depths of 10–30 m). In the north for the Odessa–Tendrovskaya depression and in the east for the Karkinit one, the characteristic type of sediments is fine aleurite silts. In the southern part of the area, at depths of 50–100 m, silts with a high content of pelite fraction are common [Samyshev, Zolotarev, 2018]. The NWBS is characterized by variations in water temperature and salinity over a wider range than that in other parts of the Black Sea. At a 20-m horizon, the minimum temperature is +4 °C in winter and +10 °C in summer. The water salinity at depths exceeding 10 m in the warm season varies from 16.6‰ in the west to 19.5‰ in the east. The oxygen content in autumn–winter is close to normal; in summer, its concentration can decrease, causing suffocation death [Biologiya, 1967; Samyshev, Zolotarev, 2018].

By the early 1960s, 63 species of polychaetes were known for the NWBS, *inter alia* 7 species of spionids [Biologiya, 1967]. Subsequently, numerous studies of shallow waters of the Romanian shelf, as well as estuaries and bays of the Odessa region and the western coast of Crimea, led to an increase in the faunal list of polychaetes to 132 species (out of them, 12 belonged to Spionidae) [Kiseleva, 2004; Marinov, 1977].

Serious disturbances in the Black Sea ecosystem in the 1970–1980s, related to anthropogenic eutrophication of the basin and its consequences (decrease in water transparency and formation of zones

with near-bottom hypoxia), as well as siltation of the bottom substrate resulting from seafood fishing, were most disastrous for the NWBS. This led to a drop in species richness in benthic communities, sharp fluctuations in the density and biomass of benthos, a change in the role of some common species, the disappearance of certain species, and the appearance of new ones in the benthic fauna of the area [Losovskaya, 1977; Revkov et al., 2018; Severo-zapadnaya chast', 2006]. Specifically, in the 1980s compared to 1953–1960, in the areas between the Danube and Dnieper rivers, the number of polychaete species decreased from 29 to 17. However, in quantitative terms, mass development of some species was registered, including representatives of the genera *Spio*, *Prionospio*, and *Polydora*, identified as *Spio filicornis*, *Prionospio cirrifera*, and *Polydora limicola*, respectively [Losovskaya, 1991; Severo-zapadnaya chast', 2006]. De-eutrophication of the Black Sea basin since the mid-1990s [Zaika, 2011], the prohibition of bottom fishing for sprat and mussel dredging in the late 1980s in Ukraine, and subsequent stricter control over the use of bottom fishing gear gave rise to improved general indicators of zoobenthos representation [Revkov et al., 2018]. The benthic research in the last decade of the XX century and the first decades of the XXI century in the NWBS was mainly carried out in shallow bays, bights, and estuaries. The same applies to special studies of the polychaete fauna: those were mostly carried out in the Odessa region, Sevastopol bays, and shallow coastal areas of Romania [Boltachova, Lisitskaya, 2007; Boltachova et al., 2015; Bondarenko, 2009, 2017; Surugiu, 2005, 2012]. In the central region of the NWBS at depths of more than 10–15 m, benthic investigations were rare. Thus, in 2012, in the Zernov *Phyllophora* Field area (the central region of the NWBS), 14 species of polychaetes (*inter alia* 2 species of spionids) were noted in the composition of macrobenthos [Kovalishina, Kachalov, 2015]. In 2003, when studying meiobenthos along the western coast of the Black Sea (off the coast of Romania and Ukraine), 24 Polychaeta species were recorded (including 5 Spionidae species) [Vorobyova, Bondarenko, 2009]. In 2006–2007, a detailed investigation of the benthic fauna was carried out in a small area of the Romanian shelf, covering all depths inhabited by macrobenthos. It resulted in registration of 43 species of polychaetes (out of them, 10 spionids). Interestingly, mass development of a new species non-native for the Black Sea, *Dipolydora quadrilobata* (Jacobi, 1883), was observed [Begun et al., 2010; Surugiu, 2012].

Thus, we have to admit that the bottom fauna of the most extensive part of the Black Sea shelf, which is under ever-increasing anthropogenic load, has remained virtually out of the spotlight of researchers over the past 30 years. A significant part of macrobenthos, and often the predominant one in terms of density, are Polychaeta species, and out of them, in turn, Spionidae representatives usually dominate. The aim of our research is to study the species composition, distribution, and quantitative development of polychaetes of the family Spionidae in the northwestern part of the Black Sea at depths of more than 10–15 m.

MATERIAL AND METHODS

The material was macrobenthos sampled in the NWBS during the cruise no. 15/2 of the RV “Maria S. Merian” (May 2010) and cruises no. 64, 68, 70, 72, 84, 86, 90, and 96 of the RV “Professor Vodyanitsky” (July and November 2010, August 2011, May 2013, April, June, and October 2016, and July 2017). The stations were performed in the depth range of 10–137 m (Table 1). From the RV “Professor Vodyanitsky,” bottom sediments were sampled with Ocean-25 bottom grabs (capture area of 0.25 m²); from the RV “Maria S. Merian,” using a box corer (capture area of 0.1 m²). Bottom sediments were washed through sieves with the smallest diameter of 1 mm. The material was fixed with a 4% formaldehyde solution and further processed in a laboratory. In total, 230 samples from 160 stations were taken and processed. Golden Software Surfer 2011 was used to create species distribution maps.

Table 1. Coordinates of stations in the northwestern part of the Black Sea, performed in 2010–2017 on the RV “Maria S. Merian” (*) and “Professor Vodyanitsky,” where Spionidae were found

| Cruise no., date | Sta. no. | Coordinates | | Depth, m | Cruise no., date | Sta. no. | Coordinates | | Depth, m | |
|---------------------|----------|-------------|---------|----------|---------------------|----------------|-------------|---------|----------|----|
| | | °N | °E | | | | °N | °E | | |
| 15/2*, 05.2010 | 361 | 44.8123 | 31.9220 | 82 | 70, 07.2011 | 35 | 45.9822 | 33.2445 | 10 | |
| | 362 | 44.8000 | 31.9167 | 83 | | 36 | 45.8966 | 33.1836 | 11 | |
| | 533 | 44.6427 | 33.0012 | 137 | | 37 | 45.9187 | 33.2030 | 11 | |
| 64, 07.2010 | 10 | 44.5637 | 33.3487 | 87 | | 39 | 45.6855 | 32.7660 | 27 | |
| | 14 | 44.9425 | 33.1562 | 93 | | 43 | 45.0499 | 33.0611 | 87 | |
| | 15 | 45.0163 | 33.2269 | 70 | | 25 | 45.3927 | 30.9839 | 44 | |
| | 16 | 45.0639 | 33.2757 | 30 | 27 | 45.5261 | 32.4353 | 29 | | |
| | 16a | 45.0602 | 33.2408 | 46 | 28 | 45.5008 | 32.4574 | 30 | | |
| 68, 11.2010 | 1 | 45.2987 | 30.4802 | 39 | 72, 05.2013 | 29 | 45.5513 | 32.5885 | 25 | |
| | 2 | 45.2991 | 30.7001 | 37 | | 33 | 46.0380 | 31.5362 | 17 | |
| | 3 | 45.2917 | 30.9250 | 41 | | 34 | 45.5929 | 31.6435 | 41 | |
| | 4 | 45.2986 | 31.3889 | 52 | | 35 | 45.2912 | 32.6741 | 38 | |
| | 5 | 45.2937 | 31.6469 | 48 | | 42 | 45.2904 | 32.9596 | 19 | |
| | 6 | 45.6448 | 31.7874 | 39 | | 43 | 44.9267 | 33.1849 | 86 | |
| | 7 | 45.6351 | 31.5076 | 43 | | 46 | 45.1206 | 33.2371 | 12 | |
| | 8 | 45.6365 | 31.2552 | 44 | | 47 | 45.0747 | 33.2365 | 33 | |
| | 9 | 45.6290 | 31.0414 | 36 | | 48 | 45.0397 | 33.4934 | 18 | |
| | 10 | 45.6356 | 30.8020 | 36 | | 84, 04.2016 | 6 | 32.7348 | 45.3332 | 25 |
| | 11 | 45.6403 | 30.6059 | 27 | | | 7 | 33.1420 | 45.1580 | 22 |
| | 12 | 45.8440 | 30.7423 | 19 | | | 9 | 33.4366 | 44.9882 | 31 |
| | 13 | 45.8467 | 30.8700 | 23 | 1 | | 33.1095 | 45.2032 | 18 | |
| | 14 | 45.9829 | 30.8871 | 21 | 2 | | 32.8980 | 45.2643 | 44 | |
| | 15 | 46.0883 | 31.0988 | 34 | 4 | | 32.7493 | 45.6053 | 22 | |
| | 16 | 45.9818 | 31.0895 | 35 | 5 | 32.7767 | 45.6183 | 21 | | |
| | 17 | 45.8706 | 31.0942 | 35 | 6 | 32.7617 | 45.6407 | 22 | | |
| | 18 | 45.7575 | 31.1146 | 36 | 7 | 33.0298 | 45.7457 | 20 | | |
| | 19 | 45.5013 | 31.1370 | 46 | 8 | 33.0653 | 45.7542 | 15 | | |
| | 20 | 45.4717 | 31.3650 | 48 | 9 | 33.0360 | 45.7805 | 18 | | |
| | 21 | 45.7565 | 31.3578 | 41 | 10 | 33.0725 | 45.7917 | 14 | | |
| | 22 | 45.8446 | 31.3595 | 25 | 11 | 33.0402 | 45.8167 | 15 | | |
| | 23 | 45.9671 | 31.3588 | 22 | 12 | 32.5667 | 45.4955 | 23 | | |
| | 24 | 46.0685 | 31.3507 | 20 | 46 | 32.8333 | 44.8667 | 117 | | |
| | 25 | 46.0675 | 31.5848 | 20 | 86, 06.2016 | 5 | 45.0898 | 32.5528 | 81 | |
| | 26 | 45.9552 | 31.5824 | 23 | | 7 | 45.0375 | 32.2256 | 72 | |
| | 27 | 45.8411 | 31.9533 | 26 | | 8 | 45.1638 | 32.1172 | 57 | |
| | 28 | 45.8470 | 31.5804 | 26 | | 9 | 45.2914 | 32.0502 | 50 | |
| | 29 | 45.7458 | 31.5857 | 33 | | 12 | 44.9757 | 31.9271 | 59 | |
| | 30 | 45.4820 | 31.5827 | 49 | | 2 | 32.7175 | 45.6037 | 27 | |
| 70, 07.2011 | 18 | 45.5061 | 31.4006 | 46 | 3 | 32.7698 | 45.5877 | 20 | | |
| | 19 | 45.5074 | 30.7159 | 38 | 4 | 32.7602 | 45.6324 | 20 | | |
| | 20 | 45.6205 | 30.6288 | 24 | 5 | 32.7684 | 45.6963 | 27 | | |
| | 21 | 45.6237 | 30.8368 | 35 | 6 | 32.9815 | 45.7229 | 20 | | |
| | 22 | 45.7381 | 30.9173 | 32 | 7 | 33.0648 | 45.7547 | 19 | | |
| | 23 | 45.6188 | 31.0552 | 35 | 8 | 32.9976 | 45.7855 | 19 | | |
| | 24 | 46.0582 | 31.2220 | 31 | 9 | 32.7175 | 45.7372 | 28 | | |
| | 25 | 46.4474 | 31.3842 | 15 | 14 | 33.3472 | 45.0042 | 30 | | |
| | 26 | 46.0482 | 31.5383 | 20 | 15 | 33.3581 | 44.8797 | 74 | | |
| | 27 | 46.6195 | 31.6360 | 45 | 41 | 32.2197 | 45.6271 | 34 | | |
| | 28 | 45.7008 | 31.9797 | 33 | 42 | 31.9658 | 45.5478 | 40 | | |
| | 30 | 45.8130 | 32.4892 | 31 | 44 | 31.6527 | 45.2310 | 59 | | |
| | 32 | 45.9190 | 33.0002 | 11 | 45 | 31.4489 | 45.1643 | 61 | | |
| | 33 | 45.9690 | 33.2062 | 11 | 48 | 32.5612 | 45.0892 | 79 | | |
| | 34 | 45.9224 | 33.2708 | 11 | | | | | | |

RESULTS

Representatives of the family Spionidae were found in almost the entire surveyed shelf area – at 105 out of 160 stations performed (Fig. 1). In total, 20,263 Spionidae specimens were recorded, and 11 species were identified: *Aonides paucibranchiata* Southern, 1914, *Dipolydora quadrilobata* (Jacobi, 1883), *Microspio mecznikowiana* (Claparède, 1869), *Prionospio* cf. *cirrifera* Wirén, 1883, *Polydora cornuta* Bosc, 1802, *Pygospio elegans* Claparède, 1863, *Scolelepis tridentata* (Southern, 1914), *Scolelepis (Scolelepis) cantabra* (Rioja, 1918), *Laonice* cf. *cirrata* (M. Sars, 1851), *Marenzelleria neglecta* Sikorski & Bick, 2004, and *Spio decorata** Bobretzky, 1871. *Prionospio* sp. (non-identified down to a species level) were registered as well.

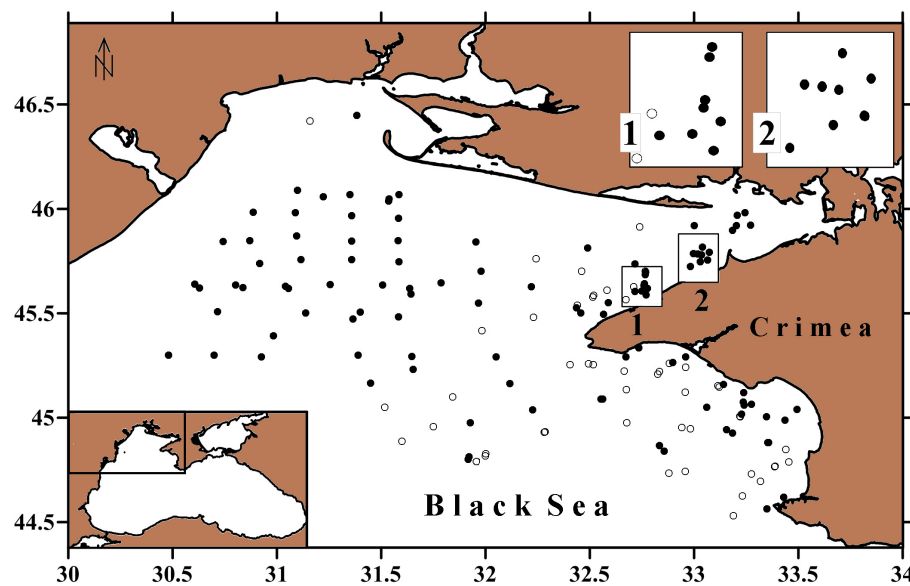


Fig. 1. Spionidae distribution on the shelf of the northwestern part of the Black Sea in 2010–2017: ○, benthic stations; ●, stations where Spionidae representatives were found

Spionidae were noted at all surveyed depths – down to 137 m. As known, in the Black Sea, the maximum depths suitable for macrozoobenthos habitat are limited by isobaths of 150–170 m; in the NWBS, 110–125 m [Kiseleva, 1981, 2004]. Thus, representatives of this family inhabit the entire depth range of the NWBS. Spionids were recorded on various sediments, but preferred coarse sand with shell debris; there, their average density was 729 ind. \cdot m⁻², while on finer silted sand, the value was 399 ind. \cdot m⁻². On aleurite and pelite silts, spionids were less common, and their density was minimum, 33 ind. \cdot m⁻². At individual stations, Spionidae density reached 2,984 ind. \cdot m⁻², and the average value was (477 \pm 126) ind. \cdot m⁻². Especially high density of spionids was registered in the west of the central region of the NWBS and in some coastal areas of the Karkinitzky and Kalamitsky bays (Fig. 2).

***Aonides paucibranchiata* Southern, 1914.** The material was 619 ind. The RV “Professor Vodyanitsky”: cruise no. 64, sta. 14; cruise no. 68, sta. 2–4, 7–10, 12, 14, 19, 24, 25, 28, 30; cruise no. 70, sta. 19–22, 26, 43; cruise no. 72, sta. 25, 47; cruise no. 84, sta. 6, 7; cruise no. 86, sta. 5, 12, 46; cruise no. 90, sta. 8, 12; cruise no. 96, sta. 14, 44, 45. The RV “Maria S. Merian”: cruise no. 15/2, sta. 361, 362.

*A thorough examination of polychaetes of the genus *Spio*, previously attributed by us, as well as by most other researchers, to the species *S. filicornis* (Müller, 1776), led to the conclusion that this is *S. decorata* Bobretzky, 1871 [Boltachova, Lisitskaya, 2019]. The opinion that the Black Sea is inhabited by the latter species is currently shared by a number of authors [V. Radashevsky, oral report; Surugiu, 2005].

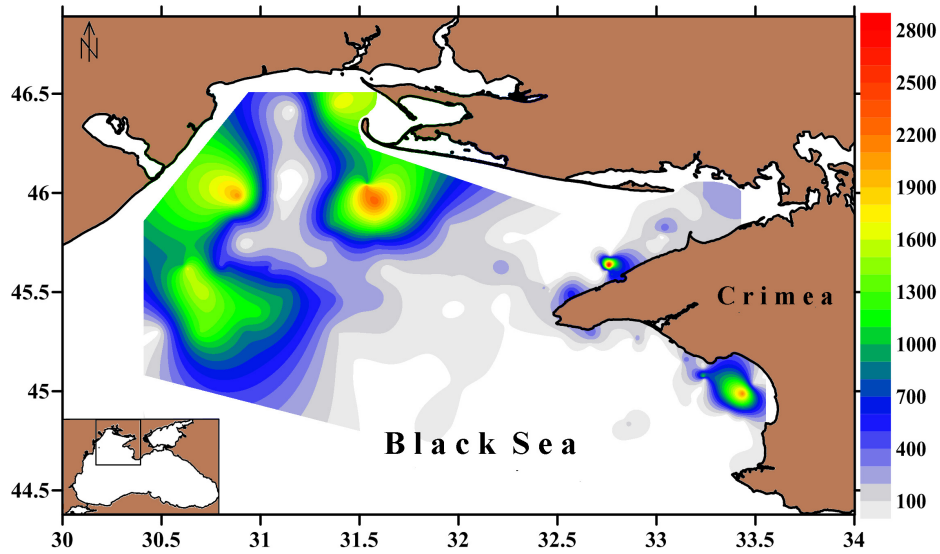


Fig. 2. Spionidae density on the shelf of the northwestern part of the Black Sea in 2010–2017

Amphi-Atlantic species. It is distributed in the White and North seas, off the Atlantic coast of Europe, in the Mediterranean Sea, and in the Gulf of Mexico [Dauvin et al., 2003; Fauchald et al., 2009; Fauvel, 1927]. In the Black Sea, it is recorded everywhere – off the coasts of Bulgaria, Romania, and Turkey [Marinov, 1977; Kurt-Şahin, Çinar, 2012; Surugiu, 2005], in the NWBS [Biologiya, 1967], and off the Crimean and Caucasian coasts [Kiseleva, 2004; Vinogradov, Losovskaya, 1968].

We found this species at 35 stations in a wide depth range (19–117 m) on sand, shell debris, and their mixture, sometimes slightly silted (Fig. 3). A higher frequency of occurrence was revealed at depths of 20–60 and 80–100 m. The density varied in the range of 2–260 ind.·m⁻², with the average value of (44 ± 20) ind.·m⁻². The maximum density for *A. paucibranchiata* was registered in the western region of the NWBS – 260 and 192 ind.·m⁻² (cruise no. 70, sta. 21, depth of 35 m; cruise no. 72, sta. 25, depth of 44 m). The species had relatively low density and frequency of occurrence at the lowest (less than 20 m) and greatest (more than 100 m) depths.

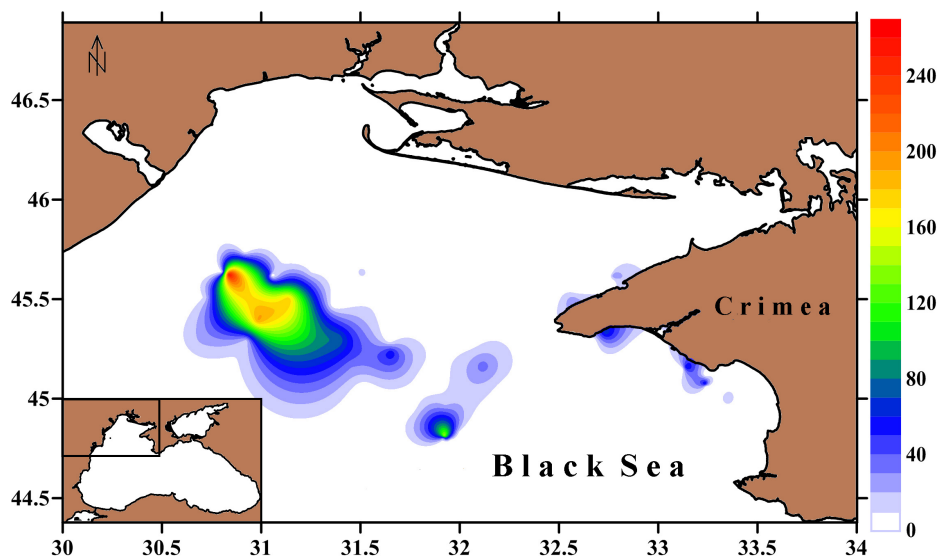


Fig. 3. *Aonides paucibranchiata* distribution on the shelf of the northwestern part of the Black Sea in 2010–2017

There are contradictory data on *A. paucibranchiata* confinement to various depths and sediments. According to K. Vinogradov, this species is found primarily on coarse sand with shell debris at depths of 10–22 m [Vinogradov, Losovskaya, 1968]. At the same time, its large accumulations were revealed by M. Băcescu off the Romanian coast on silty sediments at depths of 110 and 124 m, where its density reached 1,000 and 3,000 ind. \cdot m⁻², respectively [Kiseleva, 2004]. Our data confirm the wide ecological range of *A. paucibranchiata* distribution in the Black Sea.

***Dipolydora quadrilobata* (Jacobi, 1883).** The material was 2,560 ind. The RV “Professor Vodyanitsky”: cruise no. 64, sta. 10, 14, 15; cruise no. 68, sta. 1–4, 9–13, 16–20, 22–24, 28–30; cruise no. 70, sta. 18–24, 43; cruise no. 72, sta. 33, 34, 43; cruise 90, sta. 5. The RV “Maria S. Merian”: cruise no. 15/2, sta. 362.

Arctic-boreal species. It is known for the Atlantic coast of Europe and North America [Blake, 1969; Dauvin et al., 2003; Fauvel, 1927], the Okhotsk Sea, the Sea of Japan, and the Bering Sea [Radashkevsky, 1993; Ushakov, 1955], the Pacific coast of North America [Blake, 1996], and the Adriatic Sea [Castelli et al., 1995]. This species is a recent invader into the Black Sea [Todorova, Panayotova, 2006, cited from: Surugiu, 2012].

We found *D. quadrilobata* at 36 stations in a wide depth range (17–93 m) on sandy and shell debris sediments of varying degree of siltation. The species was most often registered in the central region of the NWBS; its maximum density was also recorded there (cruise no. 70, sta. 2, depth of 37 m) (Fig. 4). *D. quadrilobata* frequency of occurrence was higher at depths of 20–40 and 80–100 m (Fig. 5). However, high density was noted in the range of 20–60 m, while at depths exceeding 80 m, the value was low. In general, the density varied from 4 to 1,184 ind. \cdot m⁻², and the average was (177 \pm 99) ind. \cdot m⁻².

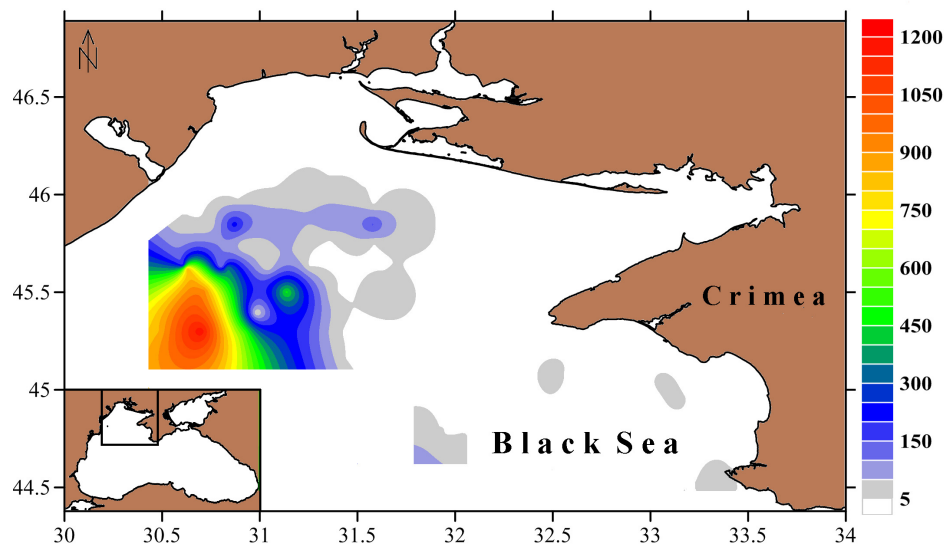


Fig. 4. *Dipolydora quadrilobata* distribution on the shelf of the northwestern part of the Black Sea in 2010–2017

Despite the fact that *D. quadrilobata* was recorded on various sediments, its distribution was uneven. Specifically, on silty sediments, the minimum density was registered, on average 14 ind. \cdot m⁻². On silted shell debris, the value was an order of magnitude higher, 142 ind. \cdot m⁻². On sandy and shell debris, the average density of this species was 277 ind. \cdot m⁻².

The high (50%) frequency of occurrence of *D. quadrilobata* at great depths is of interest. Studies of this species off the Atlantic coast of North America showed the existence of two ecological forms that differ in the type of larval development [Blake, 1969]. Those were characterized by different temperature

optimums for larval growth – +6...+10 and +10...+15 °C [Blake, 1969]. In the Black Sea, at a depth of more than 50–55 m, water temperature is constant, about +8 °C, while at lower depths, 30–40 m, it rises to +11...+13 °C [Ivanov, Belokopytov, 2011]. These temperatures correspond to the optimal ones for the indicated ecological forms of *D. quadrilobata*. In the very surface layer, the water can warm up to +28...+29 °C, which may explain the absence of this species at depths less than 20 m. It can be assumed that the Black Sea is inhabited by both ecological forms of *D. quadrilobata*, the taxonomic status of which requires further research.

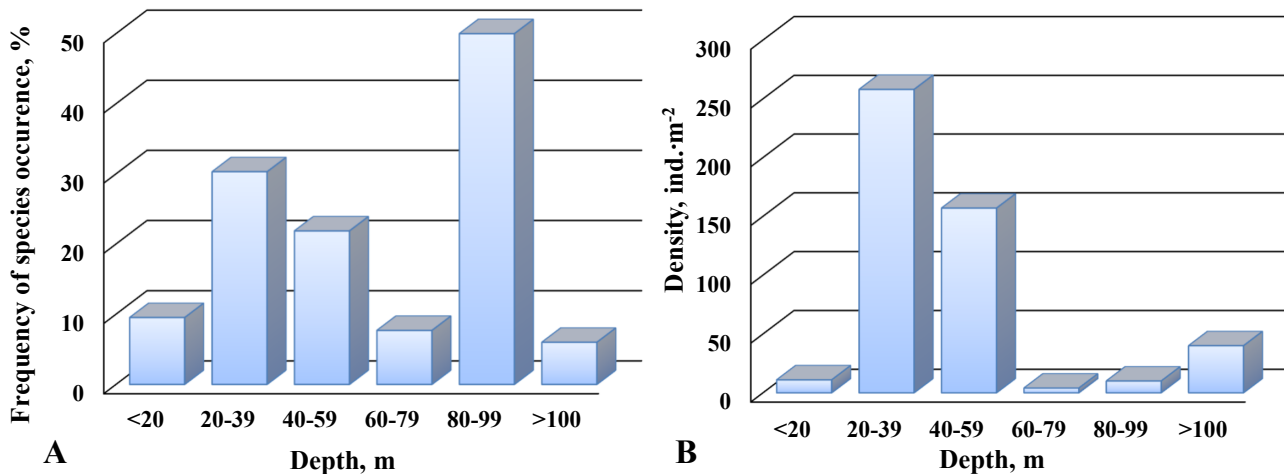


Fig. 5. *Dipolydora quadrilobata* frequency of occurrence (A) and density (B) on the shelf of the north-western part of the Black Sea in 2010–2017

***Laonice cf. cirrata* (M. Sars, 1851).** The material was 2 ind. The RV “Professor Vodyanitsky”: cruise no. 96, sta. 2, 5.

The species is distributed in the Arctic seas, the northern Pacific Ocean, the Atlantic, and the Mediterranean and Marmara seas [Blake, 1996; Fauvel, 1927; Rullier, 1963; Sikorski, 2003; Zhirkov, 2001; Çinar et al., 2014]. In the Black Sea, single finds are known for the Karadag water area [Vinogradov, 1949], the Bosphorus outlet area, and the coast of Bulgaria [Kurt-Şahin, Çinar, 2012; Rullier, 1963].

We noted *L. cf. cirrata* off the coast of Crimea in the Karkinitzky Bay (Fig. 6) at a depth of 27 m on silted shell debris.

***Marenzelleria neglecta* Sikorski & Bick, 2004.** The material was 1 ind. The RV “Professor Vodyanitsky”: cruise no. 84, sta. 6.

The species is listed for the Atlantic coast of North America, the Canadian Arctic, and the North and Baltic seas [Sikorski, Bick, 2004]. *M. neglecta* is a non-native species widely distributed in the Baltic Sea; in 2014, it was revealed in the Sea of Azov, where it seemed to arrive with the ballast waters of ships passing the Volga-Baltic and Volga-Don channels on their way from the North Atlantic and the Baltic Sea [Syomin et al., 2016]. The species is spreading rapidly in the Sea of Azov and has already been registered in the Kerch Strait and off the coast of the Taman Peninsula [Syomin et al., 2017].

We recorded *M. neglecta* near the Tarkhankut Peninsula (western coast of Crimea) at a depth of 25 m on sand with shell debris (Fig. 6). This find is the first for the NWBS. Considering the rapid distribution of this species, in the coming years, we can expect its naturalization throughout the Sea of Azov–Black Sea basin.

***Microspio mecznikowiana* (Claparède, 1869).** The material was 15 ind. The RV “Professor Vodyanitsky”: cruise no. 68, sta. 1, 11; cruise no. 70, sta. 33; cruise no. 96, sta. 41 (Fig. 6).

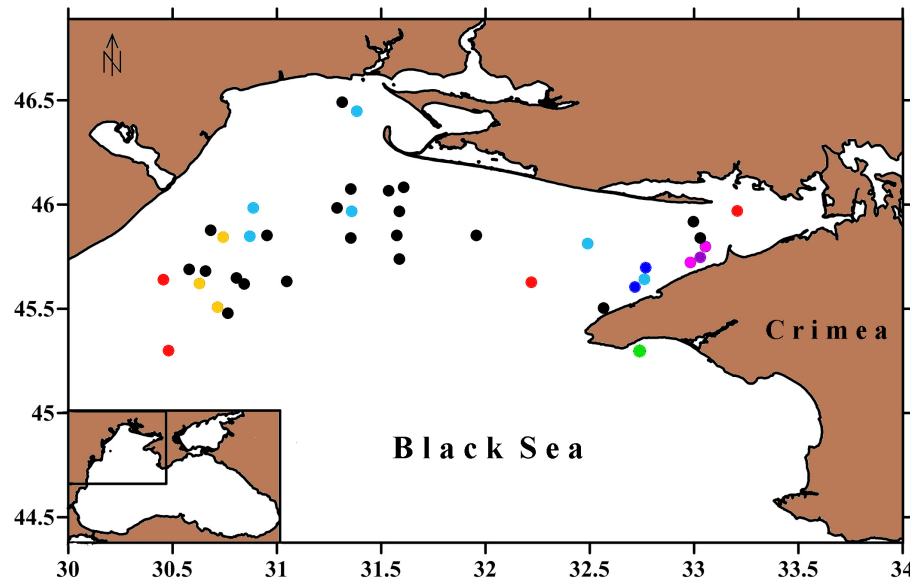


Fig. 6. Finds on the shelf of the northwestern part of the Black Sea in 2010–2017: ●, *Polydora cornuta*; ●, *Laonice cf. cirrata*; ●, *Microspio mecznikowiana*; ●, *Marenzelleria neglecta*; ●, *Scolelepis tridentata*; ●, *Pygospio elegans*; ●, *Scolelepis (Scolelepis) cantabra*; ●, *Spio decorata*

The species is noted off the Atlantic coast of Europe, in the Mediterranean, Red, Marmara, and Black seas, and in the Sea of Azov [Dauvin et al., 2003; Kiseleva, 2004; Çinar et al., 2014]. In the Black Sea, it is recorded in different areas at depths of 0–49 m [Kiseleva, 1981, 2004; Marinov, 1977; Samyshev, Zolotarev, 2018; Vinogradov, 1949; Vinogradov, Losovskaya, 1968].

We found *M. mecznikowiana* at depths of 11–39 m on silted shell debris; its density did not exceed 20 ind. \cdot m⁻² (Fig. 6). Since this species prefers shallow-water areas [Vinogradov, 1949], it was extremely rarely identified in cruise material.

***Polydora cornuta* Bosc, 1802.** The material was 30 ind. The RV “Professor Vodyanitsky”: cruise no. 68, sta. 13, 14, 23; cruise no. 70, sta. 25, 30; cruise no. 86, sta. 6.

Widespread species, cosmopolitan. It is especially abundant in estuaries and seaports, in eutrophicated water areas [Blake, 1996; Radashevsky, Selifonova, 2013]. It is one of the first invaders to spread massively in the Black Sea [Boltachova, Lisitskaya, 2007; Losovskaya, Nesterova, 1964; Boltachova et al., 2021; Radashevsky, Selifonova, 2013; Surugiu, 2012].

In our samples, *P. cornuta* was found singly at depths of 15–31 m on silted shell debris and sand mixed with silt. Its density did not exceed 30 ind. \cdot m⁻². This can be explained by the fact that our studies were carried out mainly at depths exceeding 20 m in open waters, remote from bays, estuaries, and ports (see Fig. 6). Meanwhile, as known, in shallow bays, at depths of 0–33 m, *P. cornuta* is a widespread species; off the Romanian coast, in the Gulf of Mangalia, its density reached 150 thousand ind. \cdot m⁻² [Surugiu, 2012].

***Prionospio cf. cirrifera* Wiren, 1883.** The material was 15,611 ind. The RV “Professor Vodyanitsky”: cruise no. 64, sta. 14, 15, 16, 16a; cruise no. 68, sta. 1–30; cruise no. 70, sta. 18–21, 23–28, 32–37, 39, 43; cruise no. 72, sta. 25–29, 33–35, 42, 46–48; cruise no. 84, sta. 6, 7, 9; cruise no. 86, sta. 1, 2, 4–8, 10–12; cruise no. 90, sta. 7, 9, 12; cruise no. 96, sta. 3, 4, 6–9, 14, 15, 41, 42, 44, 48. The RV “Maria S. Merian”: cruise no. 15/2, sta. 533.

For a long time, the species was considered as widespread and cosmopolitan. It was first described from the Arctic Ocean; it is known for the North Atlantic [Dauvin et al., 2003; Zhirkov, 2001], the coasts of Asia and South Africa [Day, 1967; Shen et al., 2010], and the Mediterranean Sea [Castelli et al., 1995;

Çinar, Ergen, 1999]. Some researchers consider the species to be cold-water and question the fact of its habitat in the Mediterranean basin [Faulwetter et al., 2017; Maciolek, 1985; Mackie, 1984]. In the Black Sea, *P. cf. cirrifera* is noted everywhere – off the coasts of Bulgaria, Romania, and Turkey [Kurt-Şahin, Çinar, 2012; Marinov, 1977; Surugiu, 2005; Çinar et al., 2014], as well as off the Crimean and Caucasian coasts [Biologiya, 1967; Kiseleva, 1981, 2004; Vinogradov, Losovskaya, 1968].

We found this species at 92 stations over the entire range of depths studied (10–137 m) on a variety of sediments (shell debris, sand, their mixture, silted sand or shell debris, and silt). *P. cf. cirrifera* was especially widespread in the central region of the NWBS and in the Karkinitzky and Kalamitsky bays (Fig. 7).

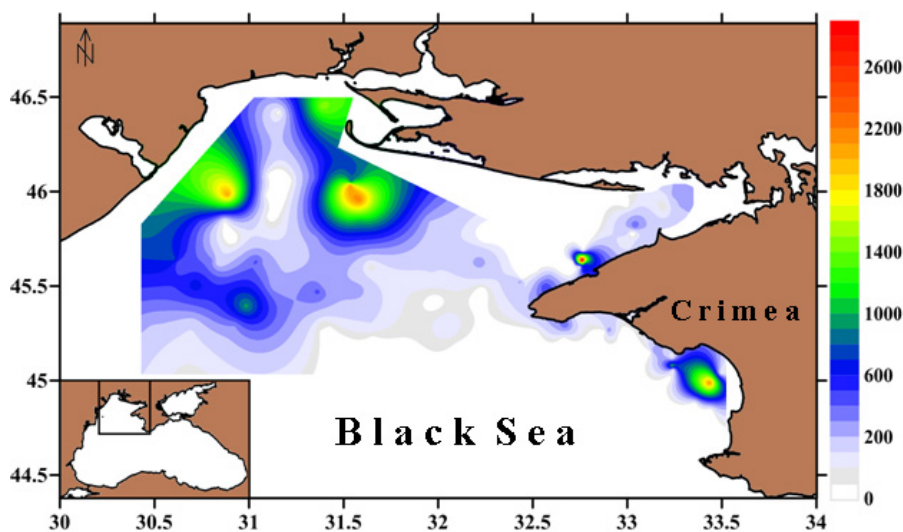


Fig. 7. *Prionospio cf. cirrifera* distribution on the shelf of the northwestern part of the Black Sea in 2010–2017

Analysis of *P. cf. cirrifera* bathymetric distribution showed as follows. Despite the fact that the species occurs at all depths studied, its frequency of occurrence drops with increasing depth. The frequency of occurrence exceeding 50% (indicator of the fact that the species was one of the leading in communities) was registered at depths of down to 60 m (Fig. 8).

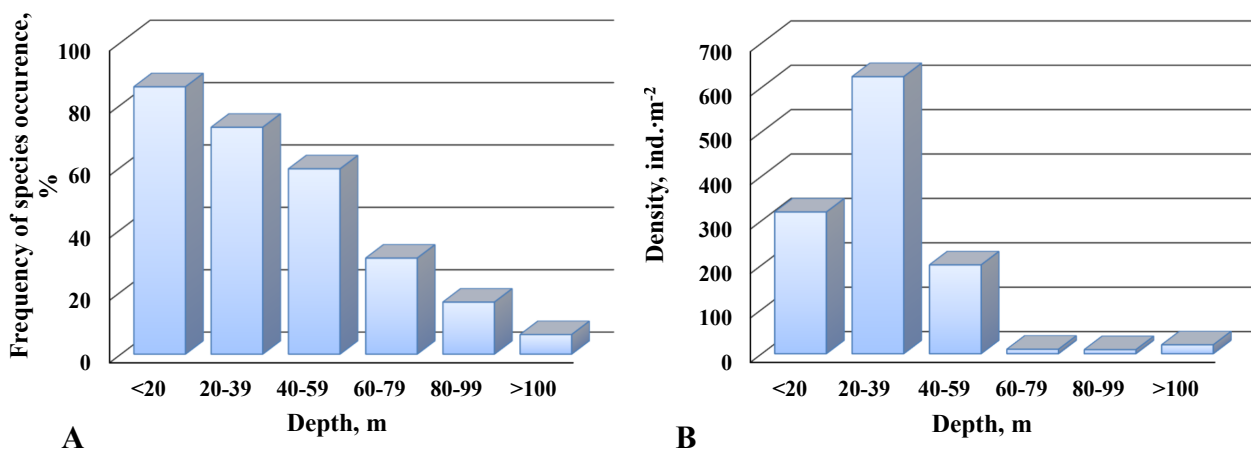


Fig. 8. *Prionospio cf. cirrifera* frequency of occurrence (A) and density (B) on the shelf of the northwestern part of the Black Sea in 2010–2017

Average density of this species at the site was (419 ± 126) ind. \cdot m⁻². The maximum density of *P. cf. cirrifera* was recorded in the Karkinitzky Bay, in the area of the Small *Phyllophora* Field – 2,984 ind. \cdot m⁻² (cruise no. 96, sta. 4, depth of 20 m). The species was most abundant in shallow waters; at depths of more than 60 m, its density was extremely low. This depth distribution is likely to result from the fact that these polychaetes prefer denser sediments, which lie at lower depths. When comparing the density of *P. cf. cirrifera* on various sediments, the values turned out to be maximum on shell debris with an admixture of silt [(653 ± 213) ind. \cdot m⁻²] and minimum on purely silty sediments [(104 ± 61) ind. \cdot m⁻²]. The confinement of this species to silted sands is also revealed for the eastern Mediterranean basin [Dağlı et al., 2011]. The values obtained during our research on the maximum density of *P. cf. cirrifera* exceed those known for the Black Sea. Specifically, off the Crimean coast on sandy sediments, *P. cf. cirrifera* density was 396 ind. \cdot m⁻², while in the NWBS off the coast of Bulgaria on shell debris–sandy sediments, the value was 267 ind. \cdot m⁻² [Kiseleva, 2004; Marinov, 1977].

***Pygospio elegans* Claparède, 1863.** The material was 15 ind. The RV “Professor Vodyanitsky”: cruise no. 68, sta. 12; cruise no. 70, sta. 19, 20. Depths were 19–24 m; sediments were sand with shell debris.

The species is distributed very widely – the Arctic seas, the Baltic Sea, the Atlantic coast of Europe and North America [Dauvin et al., 2003; Radashevsky et al., 2016; Zhirkov, 2001], the Pacific coast of Asia and North America [Blake, 1996; Ushakov, 1955], the Mediterranean, Marmara, and Black seas, and the Sea of Azov [Kiseleva, 2004; Rullier, 1963]. Genetic studies confirmed that *P. elegans* is an amphiboreal species [Radashevsky et al., 2016].

We found it in the central region of the NWBS at depths of 19–38 m on sand and silted shell debris; the density did not exceed 52 ind. \cdot m⁻² (Fig. 6). In the Black Sea, *P. elegans* is known to inhabit sandy-silty sediments at depths of 0–100 m [Kiseleva, 1981]. It does not form large aggregations. The species tolerates a wide range of salinity and is more often registered in desalinated zones [Vinogradov, Losovskaya, 1968].

***Scolelepis (Scolelepis) cantabra* (Rioja, 1918).** The material was 1 ind. The RV “Professor Vodyanitsky”: cruise no. 86, sta. 7.

It is distributed in the Atlantic off the coast of Portugal, France, and Ireland [Dauvin et al., 2003; Kiseleva, 2004; Rioja, 1918], as well as in the Mediterranean Sea. In the Black Sea, it is a rare species recorded only off the western coast of Crimea and off the coast of Romania [Boltachova et al., 2022; Marinov, 1977; Mokievsky, 1949].

We found *S. cantabra* at a depth of 16 m on silted sand in the southern area of the Karkinitzky Bay, west of the Bakal Spit (Fig. 6). In the Black Sea, the species is typical for sandy shallow waters. According to O. Mokievsky [1949], it was widespread in the pseudolitoral zone of the western coast of Crimea, where its density reached 325 ind. \cdot m⁻².

***Scolelepis tridentata* (Southern, 1914).** The material was 5 ind. The RV “Professor Vodyanitsky”: cruise no. 86, sta. 9; cruise no. 96, sta. 6.

The species is distributed off the coast of Ireland, in the northern Atlantic Ocean, and in the Mediterranean Sea [Dauvin et al., 2003; Faulwetter et al., 2017; Southern, 1914; Çinar et al., 2014]. In the Black Sea and the Sea of Azov, it is recorded for almost all areas at depths of down to 27 m, but its occurrence and density are low [Kiseleva, 2004; Kurt-Şahin, Çinar, 2012; Marinov, 1977; Vorobyova, Bondarenko, 2009].

We noted *S. tridentata* at a depth of 18–20 m, on silted sand with shell debris in the southern Karkinitzky Bay, in the area of the Small *Phyllophora* Field (Fig. 6).

***Spio decorata* Bobretzky, 1871.** The material was 1,404 ind. The RV “Professor Vodyanitsky”: cruise no. 68, sta. 9, 11–14, 22–29; cruise no. 70, sta. 19–21, 25, 26, 32; cruise no. 86, sta. 10, 12.

The species is distributed along the Atlantic coast of Europe [Bick et al., 2010; Dauvin, 1989; Dauvin et al., 2003], in the Mediterranean Sea [Faulwetter et al., 2017; Giordanella, 1969; Simboura, Nicolaidou, 2001], and in the Black Sea – off the Caucasian coast [Chernyavskii, 1880], in Turkey [Kurt Şahin et al., 2017; Çinar, Gönügür-Demirci, 2005] and Romania [Surugiu, 2005]. Assuming that for a long time researchers of the Black Sea mistakenly attributed *Spio decorata* to *Spio filicornis* [Boltachova, Lisitskaya, 2019], *S. decorata* should be considered as widespread along all the shores of the Black Sea and in the Sea of Azov [Kiseleva, 2004; Marinov, 1977; Vinogradov, Losovskaya, 1968].

We registered the species at 21 stations at depths from 11 to 38 m on sandy-shell debris sediments (Fig. 6). The highest frequency of occurrence of *S. decorata* was recorded at a depth of 20–30 m (Fig. 10). Its density ranged within 2–556 ind. \cdot m⁻², averaging (136 \pm 72) ind. \cdot m⁻². The species is especially widespread in the central region of the NWBS, in the Zernov *Phyllophora* Field area; there, its maximum density was registered (cruise no. 68, sta. 12, depth of 19 m). The maximum density, in contrast to the frequency of occurrence, was noted in the range of 10–20 m; the value decreased with increasing depth (Fig. 9).

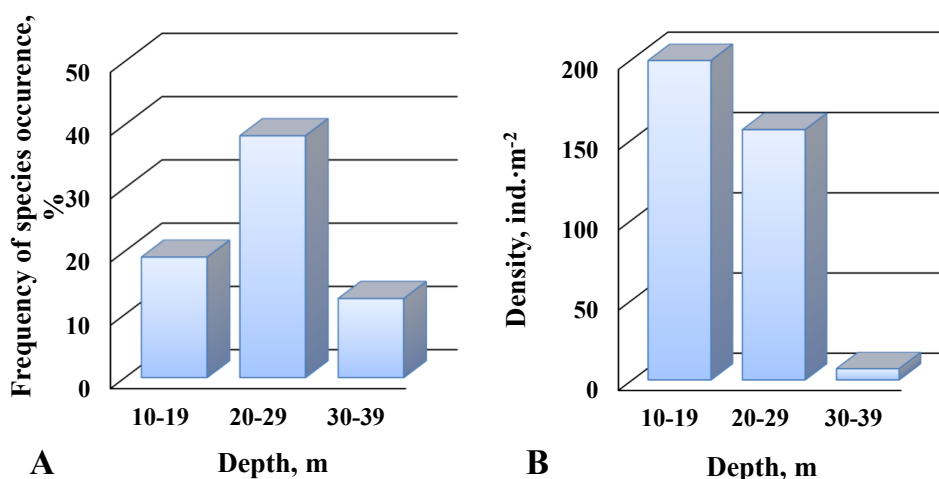


Fig. 9. *Spio decorata* frequency of occurrence (A) and density (B) on the shelf of the northwestern part of the Black Sea in 2010–2017

It is known that *S. decorata* (listed as *S. filicornis*) is common in the Black Sea at depths of down to 30 m at a salinity of 10.5–18.08‰ [Kiseleva, 2004; Vinogradov, Losovskaya, 1968]. Considering that *S. decorata* reproduction occurs at water temperatures above +8 °C, it can be assumed that the lower limit of the species distribution is determined by the position of the thermocline [Boltachova, Lisitskaya, 2019]. In the shallow NWBS, the boundary of the upper layer, heated in the summer season to +28...+29 °C, lies at a depth of about 30 m; deeper, there is a quasi-homogeneous layer with water temperature of about +8 °C [Ivanov, Belokopytov, 2011].

DISCUSSION

In recent years, numerous studies have been carried out in the field of the taxonomy of the family Spiroidea. New species have been identified, some of the previously described ones have been redescribed, and ranges have been clarified. Specifically, the redescription of *Spio filicornis* Müller, 1776 [Bick et al., 2010], as noted above, led to the revision of the Black Sea specimens of the genus *Spio* and to the conclusion that this is *S. decorata* Bobretzky, 1871 [Boltachova, Lisitskaya, 2019].

The features of the systematic status of the Black Sea spionids *Prionospio* cf. *cirrifer*a and *Laonice* cf. *cirr*ata also raise questions. Both species were previously considered as widespread, but some researchers, as mentioned earlier, are of the opinion that these are cold-water species and doubt the fact of their occurrence in the Mediterranean Sea [Maciolek, 1985; Mackie, 1984; Sikorski, 2003]. To date, *P. cirrifer*a and *L. cirr*ata from the seas of the Mediterranean basin have uncertain systematic status (questionable) [Faulwetter et al., 2017]. Finds of *L. cirr*ata in the Mediterranean may be finds of another species – *Laonice bahusiensis* Söderström, 1920 [Sikorski, 2003]. The distribution of the first one is limited to subpolar territories, but *L. bahusiensis*, a very similar species, has a more southern distribution and is also present in the Central and Eastern Mediterranean [Sikorski, 2003; Çinar et al., 2014]. The specimens of this genus we found were not well preserved, so we tentatively assigned them to *L. cf. cirr*ata.

Some authors believe that *P. cirrifer*a is a species from the seas of the Arctic Ocean and is unlikely to occur south of Portugal [Maciolek, 1985]. A. Mackie [1984] assumed that the Mediterranean specimens belong to other, endemic species. From the Mediterranean specimens of *Prionospio*, a new species was isolated – *Prionospio maciolekae* Dağlı & Çinar, 2011. Other *P. cirrifer*a specimens, from Italy, were revised by Dağlı and Çinar [2011] and classified as a non-native species *Prionospio pulchra* Imaijima, 1990. However, *P. cirrifer*a retains the status of the widespread *Prionospio* species in the region [Çinar et al., 2014]. Recently, several species of the genus *Prionospio* (the group *Minuspio*) have been recorded off the Turkish coast of the Black Sea [Kurt Şahin et al., 2017; Çinar et al., 2014]. However, *P. cirrifer*a is still considered as one of the most abundant Spionidae representatives in the Black Sea [Kiseleva, 2004; Kurt-Şahin, Çinar, 2012; Surugiu, 2005]. Recent studies of *Prionospio* specimens sampled off the Caucasian coast led the authors to conclude the presence of two species – *P. pulchra* and *Prionospio* cf. *multibranchiata* Berkeley, 1927 [Syomin, Simakova, 2020]. In our material, there was a small number of *Prionospio* sp. (non-identified down to a species level). Those, according to morphological characteristics, were rather close to *P. maciolekae*, but it was impossible to accurately identify them. Most of *Prionospio* (the group *Minuspio*) could not be assigned to these three species (*P. pulchra*, *P. multibranchiata*, and *P. maciolekae*), and we, in anticipation of further studies, more detailed, *inter alia* genetic ones, left the name *P. cf. cirrifer*a for them.

In the Black Sea macrozoobenthos, the group of polychaetes, as a rule, is the most abundant among all the taxa – both in the number of species and in quantitative terms, *i. e.*, in the number of specimens. On the surveyed area of the NWBS shelf, we noted 83 Polychaeta species, and out of them, 12 species were Spionidae, which accounted for 14% of the taxonomic composition of this group. Polychaetes were registered at all performed stations, spionids – at 66% of their total number. At most stations, 2–3 species were recorded, and at single stations, up to 6 Spionidae species were found. The density of polychaetes at stations ranged from 66 to 17,708 ind.·m⁻², averaging 1,127 ind.·m⁻². At the same time, the density of spionids varied from 4 to 2,984 ind.·m⁻², and the average value was (477 ± 126) ind.·m⁻². Thus, while spionids accounted only for 14% of the taxonomic composition of polychaetes in the NWBS, their contribution in quantitative representation reached 42%, which may indicate a significant role of polychaetes of this family in the functioning of the benthic ecosystem of the NWBS.

The distribution of spionids in the NWBS is uneven, which is due to the response of individual species to various environmental factors. In the Black Sea, such important factors for the life of hydrobionts, as water temperature, in coastal areas water salinity as well, and the composition of sediments, vary naturally with changes in depth. Consequently, it is of some interest to fix the bathymetric boundaries of species habitat, although it is not always clear, which environmental factor limits the depth distribution of a certain species. In the NWBS, spionids were recorded at depths of 10–137 m. Depths of 11–40 m,

which warm up well in the warm season, limited the distribution of the Atlantic–Mediterranean species *M. mecznikowiana*, *S. decorata*, *S. tridentata*, and *S. cantabra*, as well as amphiboreal *P. elegans*, inhabiting warm waters of temperate latitudes. In the widest range of depths in the NWBS, the species of Arctic-boreal origin were found – *D. quadrilobata* (17–93 m) and *A. paucibranchiata* (19–117 m).

The highest density of spionids was noted in the range of 20–40 m – (721 ± 206) ind. \cdot m $^{-2}$ (Fig. 10). At depths exceeding 60 m, spionids were not abundant – from (15 ± 10) ind. \cdot m $^{-2}$ at 60–80 m to (44 ± 38) ind. \cdot m $^{-2}$ at 80–100 m. The proportion of thermophilic species (*S. decorata*, *M. mecznikowiana*, *S. tridentata*, and *S. cantabra*) in the total density of spionids accounted for 33% at a depth of 10–20 m and 12% at 21–40 m. The maximum density of Spionidae was determined by a small number of species. The density of cold-water *A. paucibranchiata* at a depth of down to 60 m did not exceed 15%, but deeper than 60 m, it ranged from 30 to 60% of the total density.

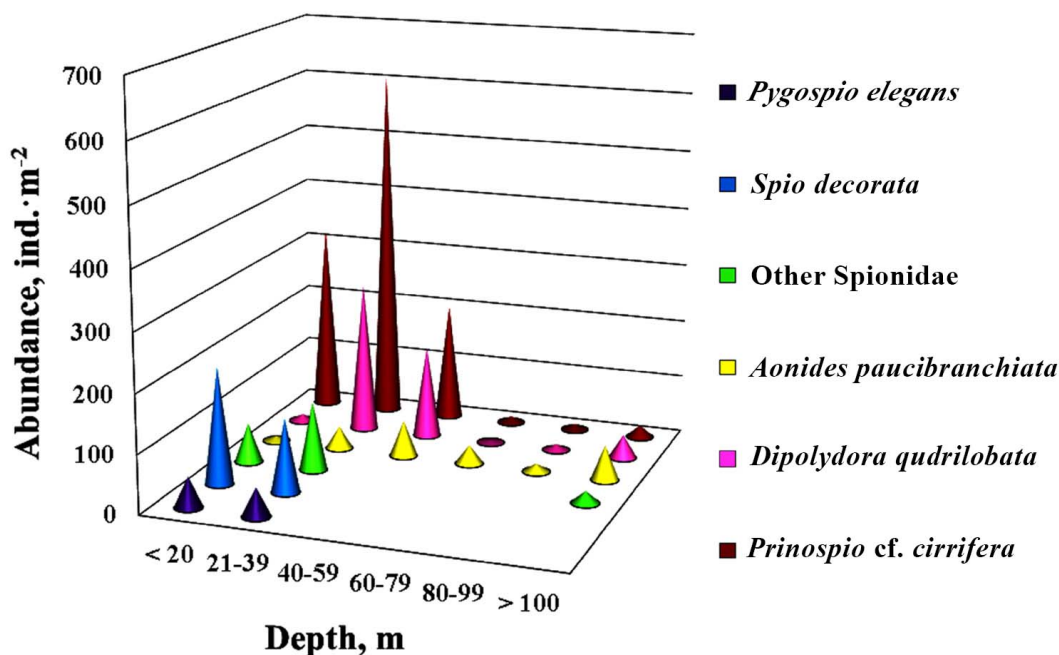


Fig. 10. Density of common Spionidae species at different depths on the shelf of the northwestern part of the Black Sea in 2010–2017

The density of the most abundant species, *P. cf. cirrifera*, at depths of down to 60 m accounted for about 50%, while deeper, it accounted for 15–30% of the total density of spionids. The density of another common species, *D. quadrilobata*, was maximum at a depth of 20–60 m [(232 ± 127) ind. \cdot m $^{-2}$], but its frequency of occurrence was relatively high both at 20–39 m [30%] and 80–99 m [50%]. Such a wide bathymetric distribution of *P. cf. cirrifera*, as well as the previously discussed complexities of *P. cf. cirrifera* systematic status and the features of *D. quadrilobata* reproductive biology, allow suggesting that the NWBS is inhabited by several species of the genera *Prionospio* and *Dipolydora*.

Conclusion:

1. In 2010–2017, during the research, 12 Polychaeta species belonging to the family Spionidae were recorded on the shelf of the northwestern part of the Black Sea. In total, 11 species were identified: *Aonides paucibranchiata*, *Dipolydora quadrilobata*, *Microspio mecznikowiana*, *Prionospio cf. cirrifera*, *Polydora cornuta*, *Pygospio elegans*, *Scoelepis tridentata*, *Scoelepis (Scoelepis) cantabra*, *Spio decorata*, *Laonice cf. cirrata*, and *Marenzelleria neglecta*. *Prionospio* sp. were registered as well.

2. Spionids were found at depths from 10 to 137 m, on different bottom sediments, and in various communities. The highest values of their density and frequency of occurrence were noted in the depth range of 20–40 m. The maximum density of Spionidae reached 2,984 ind.·m⁻², the average value was (477 ± 126) ind.·m⁻². *P. cf. cirrifera*, *A. paucibranchiata*, and *D. quadrilobata* dominated in terms of density.
3. Out of the species we recorded, three are non-native. Thus, *P. cornuta* is a species known since the middle of the XX century and now widely distributed throughout the Black Sea. *D. quadrilobata* is a species introduced in the early XXI century and rapidly distributing from the coast of Romania in the eastern direction. *M. neglecta* is a species registered in the Black Sea in 2017 and not yet widespread.
4. In the taxonomic composition of polychaetes of the northwestern part of the Black Sea, Spionidae accounted for only 14%, while in quantitative representation, their contribution reached 42% of the total density of Polychaeta. It indicates a significant role of this family in the functioning of the benthic ecosystem of the surveyed area.

This work was carried out within the framework of IBSS state research assignment “Regularities of formation and anthropogenic transformation of biodiversity and biological resources of the Sea of Azov–Black Sea basin and other areas of the World Ocean” (No. 121030100028-0) and “Investigation of mechanisms of controlling production processes in biotechnological complexes with the aim of developing scientific foundations for production of biologically active substances and technical products of marine genesis” (No. 121030300149-0).

Acknowledgment. We would like to thank the participants of the research cruises – N. Sergeeva, N. Revkov, V. Timofeev, I. Bondarev, V. Kopyy, Kh. Kharkevich, A. Nadolny, and M. Makarov – for their assistance in sampling, as well as L. Lukyanova, V. Kopytova, I. Anninskaya, and G. Dobrotina for their participation in the analysis of the material. We express our gratitude to highly respected reviewers for their detailed analysis of our work and valuable advice on improving the final version of the article.

REFERENCES

1. *Biologiya severo-zapadnoi chasti Chernogo morya* / K. A. Vinogradov (Ed). Kyiv : Naukova dumka, 1967, 266 p. (in Russ.). <https://repository.marine-research.ru/handle/299011/1107>
2. Boltachova N. A., Lisitskaya E. V. About species of *Polydora* (Polychaeta: Spionidae) from the Balaklava Bay (the Black Sea). *Morskoy ekologicheskij zhurnal*, 2007, vol. 6, no. 3, pp. 33–35. (in Russ.). <https://repository.marine-research.ru/handle/299011/917>
3. Boltachova N. A., Lisitskaya E. V. On the taxonomic classification of *Spio* (Annelida, Spionidae) species from the Sea of Azov – Black Sea basin. *Morskoy biologicheskij zhurnal*, 2019, vol. 4, no. 3, pp. 26–36. (in Russ.). <https://doi.org/10.21072/mbj.2019.04.3.03>
4. Bondarenko A. S. Species composition and features of polychaete distribution in the western Black Sea. *Ekologiya morya*, 2009, iss. 78, pp. 22–27. (in Russ.). <https://repository.marine-research.ru/handle/299011/4852>
5. Bondarenko O. S. Structure and long-term dynamics of polychaete taxocene of Odesa Sea region (Black Sea). *Naukovi zapysky Ternopilskoho natsionalnoho pedahohichnoho universytetu imeni Volodymyra Hnatiuka. Seriya: biolohiia*, 2017, no. 3 (70), pp. 70–74. (in Russ.)
6. Vinogradov K. A. K faune kol'chatykh chervei (Polychaeta) Chernogo morya. *Trudy Karadagskoi biologicheskoi stantsii*, 1949, iss. 8, pp. 3–84. (in Russ.). <https://repository.marine-research.ru/handle/299011/6859>
7. Vinogradov K. A., Losovskaya G. V. Tip kol'chatye chervi – Annelida. In: *Opredelitel' fauny Chernogo i Azovskogo morei*. Vol. 1 : *Svobodnozhivushchie bespozvonochnye*. Kyiv : Naukova dumka, 1968,

- pp. 251–405. (in Russ.). <https://repository.marine-research.ru/handle/299011/6076>
8. Zaika V. E. De-evtrofikatsiya Chernogo morya i vliyanie klimaticheskikh ostsillyatsii. In: *Sostoyanie ekosistemy shel'fovoi zony Chernogo i Azovskogo morei v usloviyakh antropogennogo vozdeistviya* : sb. st., posvyashch. 90-letiyu Novorossiiskoi morskoi biologicheskoi stantsii im. prof. V. M. Arnol'di. Krasnodar, 2011, pp. 88–93. (in Russ.)
 9. Zhirkov I. A. *Polikhety Severnogo Ledovitogo okeana*. Moscow : Yanus-K, 2001, 632 p. (in Russ.)
 10. Ivanov V. A., Belokopytov V. N. *Oceanography of the Black Sea*. Sevastopol : EKOSI-Gidrofizika, 2011, 212 p. (in Russ.)
 11. Kiseleva M. I. *Bentos rykhlykh gruntov Chernogo morya*. Kyiv : Naukova dumka, 1981, 165 p. (in Russ.). <https://repository.marine-research.ru/handle/299011/8133>
 12. Kiseleva M. I. *Mnogoshchetinkovye chervi (Polychaeta) Chernogo i Azovskogo morei*. Apatity : Izd-vo KNTs RAN, 2004, 409 p. (in Russ.). <https://repository.marine-research.ru/handle/299011/5647>
 13. Kovalishina S. P., Kachalov O. G. Makrozoobentos fillofornogo polya Zernova v mae – iyune 2012. *Naukovi zapysky Ternopilskoho natsionalnoho pedahohichnoho universytetu imeni Volodymyra Hnatiuka. Seriya: biolohiia*, 2015, no. 3–4 (64), pp. 309–313. (in Russ.)
 14. Losovskaya G. V. *Ekologiya polikhet Chernogo morya*. Kyiv : Naukova dumka, 1977, 90 p. (in Russ.). <https://repository.marine-research.ru/handle/299011/5662>
 15. Losovskaya G. V. Small detritivorous polychaetes in benthic communities of the north-western part of the Black Sea. *Gidrobiologicheskii zhurnal*, 1991, vol. 27, no. 6, pp. 24–29. (in Russ.)
 16. Losovskaya G. V., Nesterova D. A. On the mass development of a form of Polychaeta, *Polydora ciliata* ssp. *limicola* Annenkova, new for the Black Sea in Sukhoi liman (north-western part of the Black Sea). *Zoologicheskii zhurnal*, 1964, vol. 43, no. 10, pp. 1559–1560. (in Russ.)
 17. Marinov T. M. *Mnogochetinesti chervei (Polychaeta)*. Sofiya : Izd-vo B"lg. AN, 1977, 258 p. (Fauna na B"lgariya ; vol. 6). (in Bulg.)
 18. Mokievsky O. B. Fauna rykhlykh gruntov litorali zapadnykh beregov Kryma. *Trudy Instituta okeanologii*, 1949, vol. 4, pp. 124–159. (in Russ.)
 19. Mordukhai-Boltovskoi F. D. Obshchaya kharakteristika fauny Chernogo i Azovskogo morei. In: *Opredelitel' fauny Chernogo i Azovskogo morei*. Vol. 3 : *Chlenistonogie (krome rakoobraznykh), mollyuski, iglokozhe, shchetinkochelyustnye, khordovye*. Kyiv : Naukova dumka, 1972, pp. 316–324. (in Russ.). <https://repository.marine-research.ru/handle/299011/6078>
 20. Samyshev E. Z., Zolotarev P. N. *Pattern of Anthropogenic Impact on Benthos and Structure of Bottom Biocenoses in the North-West Part of the Black Sea* / Kovalevsky Institute of Marine Biological Research of RAS. Sevastopol : OOO "Kolorit", 2018, 208 p. (in Russ.). <https://doi.org/10.21072/978-5-6042012-2-0>
 21. *Severo-zapadnaya chast' Chernogo morya: biologiya i ekologiya* / Yu. P. Zaitsev, B. G. Aleksandrov, G. G. Minicheva (Eds). Kyiv : Naukova dumka, 2006, 703 p. (in Russ.). <https://repository.marine-research.ru/handle/299011/10163>
 22. Syomin V. L., Simakova U. V. Polikhety rodov *Spio* i *Prionospio* kavkazskogo shel'fa Chernogo morya. In: *Marine Research in Education (MARESEDU-2019)* : proceedings of the VIII International Conference, Moscow, 28–31 October, 2019. Tver : OOO "PoliPRESS", 2020, vol. II (III), pp. 356–359. (in Russ.)
 23. Ushakov P. V. *Mnogoshchetinkovye chervi dal'nevostochnykh morei SSSR*. Moscow ; Leningrad : Izd-vo AN SSSR, 1955, 445 p. (Opredeliteli po faune SSSR ; vol. 56). (in Russ.)
 24. Chernyavskii V. I. Materialy dlya sravnitel'noi zoografii Ponta = Materialia ad Zoographiam Ponticam Comparatam. Fasc. 3. Vermes. *Bulletin Société Impériale des Naturalistes de Moscou*, 1880, vol. 55, no. 4, pp. 213–363. (in Russ.)
 25. Begun T., Teacă A., Gomoiu M. T. State of the macrobenthos within *Modiolus phaseolinus* biocenosis from Romanian Black Sea continental shelf. *Geo-Eco-Marina*, 2010, vol. 16, pp. 5–18. <https://doi.org/10.5281/zenodo.56945>

26. Bick A., Otte K., Meißner K. A contribution to the taxonomy of *Spio* (Spionidae, Polychaeta, Annelida) occurring in the North and Baltic seas, with a key to species recorded in this area. *Marine Biodiversity*, 2010, vol. 40, iss. 3, pp. 161–180. <http://doi.org/10.1007/s12526-010-0040-5>
27. Blake J. A. Reproduction and larval development of *Polydora* from northern New England (Polychaeta: Spionidae). *Ophelia*, 1969, vol. 7, pp. 1–63. <https://doi.org/10.1080/00785326.1969.10419288>
28. Blake J. A. Family Spionidae Grube, 1850. Including a review of the genera and species from California and a revision of the genus *Polydora* Bosc, 1802. In: *Taxonomic Atlas of the Benthic Fauna of the Santa Maria Basin and Western Santa Barbara Channel. The Annelida* / J. A. Blake, B. Hilbig, P. H. Scott (Eds), Santa Barbara, California : Santa Barbara Museum of Natural History, 1996, vol. 6, pt 3: Polychaeta: Orbiniidae to Cosuridae, pp. 81–223.
29. Blake J. A., Arnofsky P. L. Reproduction and larval development of the spioniform Polychaeta with application to systematics and phylogeny. *Hydrobiologia*, 1999, vol. 402, pp. 57–106. <https://doi.org/10.1023/A:1003784324125>
30. Boltachova N. A., Lisitskaya E. V., Podzorova D. V. The population dynamics and reproduction of *Streblospio gynobranchiata* (Annelida, Spionidae), an alien polychaete worm, in the Sevastopol Bay (the Black Sea). *Ecologica Montenegrina*, 2015, vol. 4, pp. 22–28. <https://doi.org/10.37828/em.2015.4.5>
31. Boltachova N. A., Lisitskaya E. V., Podzorova D. V. Distribution of alien polychaetes in biotopes of the northern part of the Black Sea. *Russian Journal of Biological Invasions*, 2021, vol. 12, no. 1, pp. 11–26. <https://doi.org/10.1134/S2075111721010033>
32. Boltachova N. A., Lisitskaya E. V., Revkov N. K., Podzorova D. V. Polychaetes in benthos of Karkinit Bay, northwestern Black Sea. *Ekosistemy*, 2022, no. 30, pp. 5–21.
33. Castelli A., Abbiati M., Badalamenti F., Bianchi C. N., Cantone G., Gambi M. C., Giangrande A., Gravina M. F., Lanera P., Lardicci C., Somaschini A., Sordino P. Annelida: Polychaeta, Pogonophora, Echiura, Sipuncula. In: *Checklist delle specie della fauna italiana* / A. Minelli, S. Ruffo, S. La Posta (Eds). Bologna : Edizioni Calderini, 1995, vol. 19, pp. 1–45.
34. Çınar M. E., Ergen Z. Occurrence of *Prionospio saccifera* (Spionidae: Polychaeta) in the Mediterranean Sea. *Cahiers de Biologie Marine*, 1999, vol. 40, pp. 105–112.
35. Çınar M. E., Gönlüğü-Demirci G. Polychaete assemblage on shallow water benthic habitats along the Sinop Peninsula (Black Sea, Turkey). *Cahiers de Biologie Marine*, 2005, vol. 46, pp. 253–263.
36. Çınar M. E., Dağlı E., Kurt Şahin G. Checklist of Annelida from the coasts of Turkey. *Turkish Journal of Zoology*, 2014, vol. 38, no. 6, pp. 734–764. <https://doi.org/10.3906/zoo-1405-72>
37. Day J. H. *A Monograph on the Polychaeta of Southern Africa. Pt 2 : Sedentaria*. London : The British Museum (Natural History), 1967, pp. 459–878. <https://doi.org/10.5962/bhl.title.8596>
38. Dağlı E., Çınar M. E., Ergen Z. Spionidae (Annelida: Polychaeta) from the Aegean Sea (eastern Mediterranean). *Italian Journal of Zoology*, 2011, vol. 78, iss. sup1, pp. 49–64. <https://doi.org/10.1080/11250003.2011.567828>
39. Dauvin J.-C. Sur la présence de *Spio decoratus* Bobretzky, 1871 en Manche et remarques sur *Spio martinensis* Mesnil, 1896 et *Spio filicomis* (O. F. Müller, 1776). *Cahiers de Biologie Marine*, 1989, vol. 30, pp. 167–180.
40. Dauvin J.-C., Dewarumez J.-M., Gentil F. Liste actualisée des espèces d'Annélides Polychètes présentes en Manche. *Cahiers de Biologie Marine*, 2003, vol. 44, pp. 67–95.
41. Fauchald K., Granados-Barba A., Solís-Weiss V. Polychaeta (Annelida) of the Gulf of Mexico. In: *Gulf of Mexico. Origin, Waters, and Biota. Vol. 1 : Biodiversity* / D. L. Felder, D. K. Camp (Eds). Texas : Texas A&M University Press, 2009, pp. 751–788.
42. Faulwetter S., Simboura N., Katsiaras N., Chatzigeorgiou G., Arvanitidis C. Polychaetes of Greece: An updated and annotated checklist. *Biodiversity Data Journal*, 2017, vol. 5, art. no. e20997 (230 p.). <https://doi.org/10.3897/BDJ.5.e20997>

43. Fauvel P. *Polychetes sedentaires. Addenda aux Errantes, Archiannelides, Myzostomaires*. Paris : Paul Lechevalier Editeur, 1927, 494 p. (Faune de France ; vol. 16).
44. Giordanella E. Contribution a l'étude de quelques *Spionidae*. *Recueil des Travaux de la Station Marine d'Endoume*, 1969, bull. 45, fasc. 61, pp. 325–349.
45. Kurt-Şahin G., Çinar M. E. A check-list of polychaete species (Annelida: Polychaeta) from the Black Sea. *Journal of the Black Sea / Mediterranean Environment*, 2012, vol. 18, no. 1, pp. 10–48.
46. Kurt Şahin G., Dağlı E., Sezgin M. Spatial and temporal variations of soft bottom polychaetes of Sinop Peninsula (southern Black Sea) with new records. *Turkish Journal of Zoology*, 2017, vol. 41, no. 1, pp. 89–101. <https://doi.org/10.3906/zoo-1510-15>
47. Kurt Şahin G., Çinar M. E., Dağlı E. New records of polychaetes (Annelida) from the Black Sea. *Cahiers de Biologie Marine*, 2019, vol. 60, no. 2, pp. 153–165. <https://doi.org/10.21411/cbm.a.2d8cec7b>
48. Maciolek N. J. A revision of the genus *Prionospio* Malmgren, with special emphasis on species from the Atlantic Ocean, and new records of species belonging to the genera *Apoprionospio* Foster and *Paraprionospio* Caullery (Polychaeta: Spionidae). *Zoological Journal of the Linnean Society*, 1985, vol. 84, iss. 4, pp. 325–383. <https://doi.org/10.1111/j.1096-3642.1985.tb01804.x>
49. Mackie A. S. Y. On the identity and zoogeography of *Prionospio cirrifera* Wirén, 1883 and *Prionospio multibranchiata* Berkeley, 1927 (Polychaeta: Spionidae). In: *Proceedings of the First International Polychaete Conference, Sydney, 1983* / P. A. Hutchings (Ed.). Sydney : The Linnean Society of New South Wales, 1984, pp. 35–47.
50. Radashevsky V. I. Revision of the genus *Polydora* and related genera from the northwest Pacific (Polychaeta: Spionidae). *Publications of the Seto Marine Biological Laboratory*, 1993, vol. 36, no. 1–2, pp. 1–60. <https://doi.org/10.5134/176224>
51. Radashevsky V. I. Spionidae (Annelida) from shallow waters around the British Islands: An identification guide for the NMBAQC Scheme with an overview of spionid morphology and biology. *Zootaxa*, 2012, vol. 3152, no. 1, pp. 1–35. <https://doi.org/10.11646/zootaxa.3152.1.1>
52. Radashevsky V. I., Selifonova Zh. P. Records of *Polydora cornuta* and *Streblospio gynobranchiata* (Annelida, Spionidae) from the Black Sea. *Mediterranean Marine Science*, 2013, vol. 14, no. 2, pp. 261–269. <http://dx.doi.org/10.12681/mms.415>
53. Radashevsky V. I., Pankova V. V., Neretina T. V., Stupnikova A. N., Tzetlin A. B. Molecular analysis of the *Pygospio elegans* group of species (Annelida: Spionidae). *Zootaxa*, 2016, vol. 4083, no. 2, pp. 239–250. <https://doi.org/10.11646/zootaxa.4083.2.4>
54. Revkov N. K., Boltacheva N. A., Timofeev V. A., Bondarev I. P., Bondarenko L. V. Macrozoobenthos of the Zernov's *Phyllophora* Field, northwestern Black Sea: Species richness, quantitative representation and long-term variations. *Nature Conservation Research*, 2018, vol. 3, no. 4, pp. 32–43. <https://doi.org/10.24189/ncr.2018.045>
55. Rioja E. Adiciones a la fauna de anélidos del Cantábrico. *Revista de la Real Academia de Ciencias Exactas, Físicas y Naturales de Madrid*, 1918, vol. 17, pp. 54–79.
56. Rullier F. Les annelides polychetes du Bosphore, de la Mer de Marmara et de la Mer Noire, en relation avec celles de la Méditerranée. *Rapports et Procès-verbaux des réunions de la Commission Internationale pour l'Exploration Scientifique de la Mer Méditerranée*, 1963, vol. 17, no. 2, pp. 161–260.
57. Shen P. P., Zhou H., Gu J.-D. Patterns of polychaete communities in relation to environmental perturbations in a subtropical wetland of Hong Kong. *Journal of the Marine Biological Association of the United Kingdom*, 2010, vol. 90, iss. 5, pp. 923–932. <https://doi.org/10.1017/S0025315410000068>
58. Sikorski A. V. *Laonice* (Polychaeta, Spionidae) in the Arctic and the North Atlantic. *Sarsia*, 2003, vol. 88, iss. 5, pp. 316–345. <https://doi.org/10.1080/00364820310002551>

59. Sikorski A. V., Bick A. Revision of *Marenzelleria* Mesnil, 1896 (Spionidae, Polychaeta). *Sarsia*, 2004, vol. 89, iss. 4, pp. 253–275. <https://doi.org/10.1080/00364820410002460>
60. Simboura N., Nicolaidou A. *The Polychaetes (Annelida, Polychaeta) of Greece: Checklist, Distribution and Ecological Characteristics*. Athens : National Centre for Marine Research, 2001, 115 p. (Monographs on Marine Sciences ; no. 4).
61. Southern R. Archannelida and Polychaeta. In: *Proceedings of the Royal Irish Academy*, [1914], vol. 31, sec. 2 : A biological survey of Clare Island in the county of Mayo, Ireland and of the adjoining district, pt 47, pp. 3–160.
62. Surugiu V. Inventory of inshore polychaetes from Romanian coast (Black Sea). *Mediterranean Marine Science*, 2005, vol. 6, no. 1, pp. 51–73. <https://doi.org/10.12681/mms.193>
63. Surugiu V. Systematics and ecology of species of the *Polydora*-complex (Polychaeta: Spionidae) of the Black Sea. *Zootaxa*, 2012, vol. 3518, no. 1, pp. 45–65. <http://dx.doi.org/10.11646/zootaxa.3518.1.3>
64. Syomin V. L., Sikorski A. V., Kovalenko E. P., Bulysheva N. I. Introduction of species of genus *Marenzelleria* Mensil, 1896 (Polychaeta: Spionidae) in the Don River delta and Taganrog Bay. *Russian Journal of Biological Invasions*, 2016, vol. 7, no. 2, pp. 174–181. <https://doi.org/10.1134/S2075111716020107>
65. Syomin V., Sikorski A., Bastrop R., Köhler N., Stradomsky B., Fomina E., Matishov D. The invasion of the genus *Marenzelleria* (Polychaeta: Spionidae) into the Don River mouth and the Taganrog Bay: Morphological and genetic study. *Journal of the Marine Biological Association of the United Kingdom*, 2017, vol. 97, spec. iss. 5, pp. 975–984. <https://doi.org/10.1017/S0025315417001114>
66. Vorobyova L. V., Bondarenko O. S. Meiobenthic bristle worms (Polychaeta) of the western Black Sea shelf. *Journal of the Black Sea / Mediterranean Environment*, 2009, vol. 15, no. 2, pp. 109–121.

РАСПРОСТРАНЕНИЕ ПОЛИХЕТ СЕМЕЙСТВА SPIONIDAE (ANNELIDA) НА ШЕЛЬФЕ СЕВЕРО-ЗАПАДНОЙ ЧАСТИ ЧЁРНОГО МОРЯ

Н. А. Болтачева, Д. В. Подзорова, Е. В. Лисицкая

ФГБУН ФИЦ «Институт биологии южных морей имени А. О. Ковалевского РАН»,

Севастополь, Российская Федерация

E-mail: nboltacheva@mail.ru

Северо-западная часть Чёрного моря (СЗЧМ) — обширная мелководная акватория, биоценозы которой являются важной частью экосистемы Чёрного моря. Поскольку в последние десятилетия бентос этого региона практически не был исследован, сведения о его современном состоянии актуальны. Существенный вклад в таксономический состав макрозообентоса вносят полихеты семейства Spionidae, которые представлены большим количеством видов и характеризуются высокими показателями численности. Цель исследования — изучить видовой состав, распределение и количественное развитие полихет семейства Spionidae в СЗЧМ на глубинах более 10–15 м. Материалом послужили пробы макрозообентоса, собранные с 160 станций (230 проб) в рейсах НИС Maria S. Merian и «Профессор Водяницкий» в 2010–2017 гг. на глубинах от 10 до 137 м. Отбор донных осадков осуществляли с помощью дночерпателей «Океан-25» (площадь захвата 0,25 м²) и box corer (S = 0,1 м²). Грунт промывали через сита с наименьшим диаметром 1 мм. На обследованной части шельфа СЗЧМ обнаружено 83 вида Polychaeta, в том числе 12 Spionidae. Полихеты отмечены на всех выполненных станциях, спиониды — на 66 % их общего количества. На отдельных станциях зарегистрировано до 6 видов спионид, но чаще встречалось 2–3 вида. Идентифицировано 11 видов: *Aonides paucibranchiata* Southern, 1914, *Dipolydora quadrilobata* (Jacobi, 1883), *Microspio mecznikowiana* (Claparède, 1869),

Prionospio cf. *cirrifera* Wirén, 1883, *Polydora cornuta* Bosc, 1802, *Pygospio elegans* Claparède, 1863, *Scolelepis tridentata* (Southern, 1914), *Scolelepis (Scolelepis) cantabra* (Rioja, 1918), *Spio decorata* Bobretzky, 1871, *Laonice* cf. *cirrata* (M. Sars, 1851) и *Marenzelleria neglecta* Sikorski & Bick, 2004. Зарегистрированы не идентифицированные до вида экземпляры *Prionospio* sp. Распределение спионид в акватории СЗЧМ неравномерно, что обусловлено реакцией отдельных видов на различные экологические факторы. Максимальная плотность Spionidae достигала 2984 экз. \cdot м⁻², средняя составляла (477 \pm 126) экз. \cdot м⁻². Наиболее высокую плотность спионид наблюдали в диапазоне глубин 20–40 м. По плотности доминировали *P.* cf. *cirrifera*, *A. paucibranchiata* и *D. quadrilobata*. Из идентифицированных видов три (*M. neglecta*, *P. cornuta* и *D. quadrilobata*) являются вселенцами в Чёрном море. В таксономическом составе полихет СЗЧМ Spionidae занимали 14 %, тогда как в количественном развитии их вклад достигал 42 % суммарной плотности Polychaeta, что свидетельствует о существенной роли этого семейства в функционировании донной экосистемы СЗЧМ.

Ключевые слова: Polychaeta, Spionidae, *Dipolydora quadrilobata*, плотность, распределение, северо-западная часть Чёрного моря

UDC 594.329.65-147.124(262.2)

**FUNCTIONAL MORPHOLOGY
AND MORPHOLOGICAL VARIABILITY
OF THE OPERCULUM OF *RAPANA VENOSA* (GASTROPODA, MURICIDAE)**

© 2023 I. P. Bondarev

A. O. Kovalevsky Institute of Biology of the Southern Seas of RAS, Sevastopol, Russian Federation
E-mail: igor.p.bondarev@gmail.com

Received by the Editor 29.03.2021; after reviewing 05.08.2021;
accepted for publication 04.08.2023; published online 01.12.2023.

The gastropod *Rapana venosa* has spread from the Western Pacific to the Black Sea, Mediterranean Sea, and coastal areas on both sides of the Atlantic Ocean largely due to its ecological and morphological plasticity. Numerous works have been devoted to the study of the variability of the rapa whelk shell. The functional morphology and morphological variability of the *R. venosa* operculum have been insufficiently studied, and the description of this exosomatic organ is given only schematically. Based on the analysis of 190 *R. venosa* specimens sampled in two areas of the Black Sea, detailed description is given, and trends in the morphological variability of the operculum are shown depending on the specimen age and size. The characteristics determining the normal and aberrant development of the operculum are evaluated. It is shown for the first time that *R. venosa* has regenerative capabilities, up to the restoration of the lost operculum, and morphogenetic adaptive potential. A manifestation of this potential is the formation of a hypertrophied large operculum, with the shape that is not characteristic of any other Muricidae species and gastropods in general. Apparently, the abnormal size and shape of the operculum are a defensive response to pressure from predators, especially crabs. The previously unknown ability to regenerate the operculum broadens the understanding of the physiological capabilities of the rapa whelk. The phenomenon of operculum formation with a unique shape for gastropods is another manifestation of morphological plasticity, which made *R. venosa* one of the most successful invasive species in the modern marine environment.

Keywords: variability, operculum, morphology, regeneration, *Rapana venosa*

The Western Pacific predatory gastropod *Rapana venosa* (Valenciennes, 1846), being transferred by ships, entered the Black Sea in the early 1940s and successfully adapted there [Bondarev, 2010, 2014; Chukhchin, 1961, 1984; Drapkin, 1953]. Then, this species spread its expansion to the Mediterranean Sea and the Atlantic Ocean waters off the coast of Europe and North and South America [Alien Species Alert, 2004; Bondarev, 2010; Xue et al., 2018].

The success of colonization of a wide range by the rapa whelk was due to the features of its biology: high fertility, development of eggs in durable capsules, the possibility of a long stay in the planktonic phase, and tolerance to abiotic environmental factors [Alien Species Alert, 2004; Chukhchin, 1984; Drapkin, 1953]. Successful adaptation to new habitat conditions and to their changes is largely determined both by ecological and morphological plasticity of *R. venosa* [Bondarev, 2010, 2013, 2015, 2016; Chukhchin, 1961; Kosyan, 2013]. The functional morphology

and morphological variability of the species shell are most studied [Bondarev, 2010, 2013, 2016; Chukhchin, 1961, 1970; Kosyan, 2013]. Much less attention is paid to the analysis of the operculum. The monograph devoted to the functional morphology of the rapa whelk [Chukhchin, 1970] contains just a mention of the presence of a horny operculum, and the figure shows its position on a mollusc foot. “The Guide to Fauna of the Black Sea and the Sea of Azov” [Golikov et al., 1972] provides a brief description of the operculum for the genus *Rapana* Schumacher, 1817; however, the operculum is not described in the diagnosis of the species *R. venosa*. The features of the rapa whelk operculum morphology are discussed in several publications in terms of the possibility of determining the age of individuals by growth lines (“rings”) [Choi, Ryu, 2009; Chukhchin, 1961; Kosyan, Antipushkina, 2011]. A detailed analysis in this field was carried out for the banded dye-murex *Hexaplex trunculus* (Linnaeus, 1758) [Vasconcelos et al., 2012]. The variability and functionality of the operculum under different ecological conditions were investigated in the Atlantic dogwinkle *Nucella lapillus* (Linnaeus, 1758). Based on the studies, it was concluded that *N. lapillus* operculum plays a more significant role in defense against predators, especially crabs, than in defense against desiccation on the littoral [Keppens et al., 2008].

R. venosa operculum also has an important protective function, but its functional morphology and variability have not been well investigated and have not been described. The aim of this study is to fill the gap based on the analysis of material that allows to trace age-related changes, sex-driven differences, and anomalies in the operculum development under the effect of external factors.

MATERIAL AND METHODS

The material was sampled in summer and autumn, 28.06.2020–28.11.2020, using freediving equipment at depths of 1.0–6.0 m in the Donuzlav Bay (the Northwestern Crimea) and in the bays of Sevastopol (the Southwestern Crimea) of the Black Sea (Fig. 1). In the Donuzlav Bay, 49 specimens (14 females and 35 males), and in Sevastopol bays, 145 specimens (10 juveniles, 48 females, and 87 males). *R. venosa* sample for statistical analysis of the operculum characteristics consists of 190 specimens (10 juveniles, 62 females, and 118 males), with a shell height from 10.4 to 135.0 mm and age from 5–6 months to 15 years.



Fig. 1. Schematic map of sampling areas: 1, the Donuzlav Bay; 2, Sevastopol bays

The main morphological parameters of *R. venosa* shell and operculum are shown in Fig. 2A and 3A: Hs, shell height; Ds, width or maximum diameter of the last whorl of the shell; Ha, aperture height; Da, aperture width; Ho, operculum height; and Do, operculum width. The sex of individuals (F, female; M, male; and J, juveniles) was determined by the presence/absence of a penis in males/females, respectively, and the color of the gonads (Fig. 2B); the age was determined by spawning marks [Bondarev, 2010, 2015; Chukhchin, 1961, 1970; Kosyan, Antipushkina, 2011].

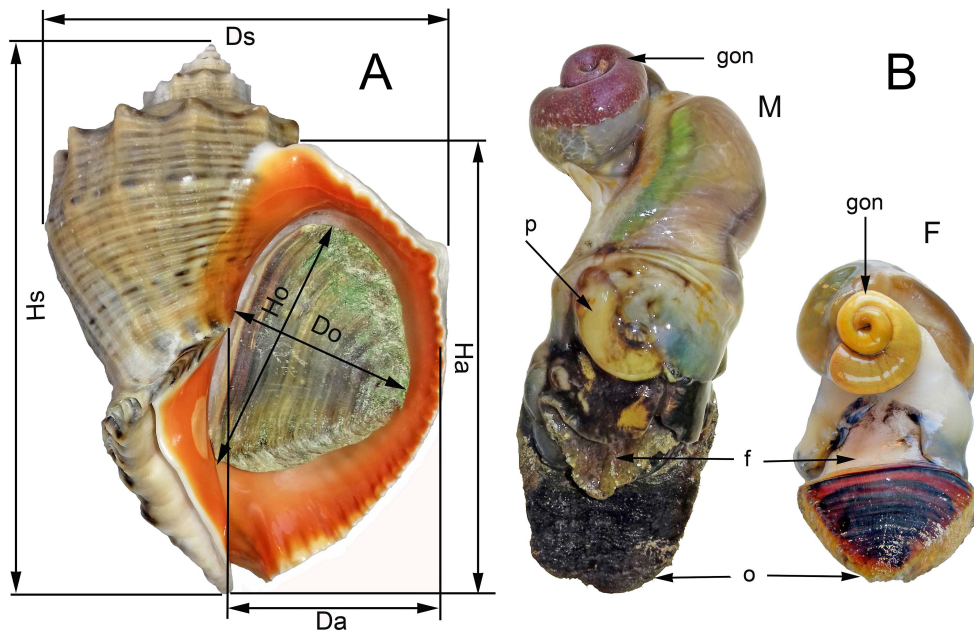


Fig. 2. A, main morphological parameters of *Rapana venosa* shell and operculum (in parentheses, there are the dimensions of the pictured specimen, male, 3 years old): Hs, shell height (108.8 mm); Ds, width or maximum diameter of the last whorl (77 mm); Ha, aperture height (91 mm); Da, aperture width (39 mm); Ho, operculum height (50.3 mm); Do, operculum width (33.8 mm). B, *R. venosa* soft body with operculum (o): M, male, 12 years old, ventral view (p, penis; f, foot; gon, gonad); F, female, 3 years old, dorsal view

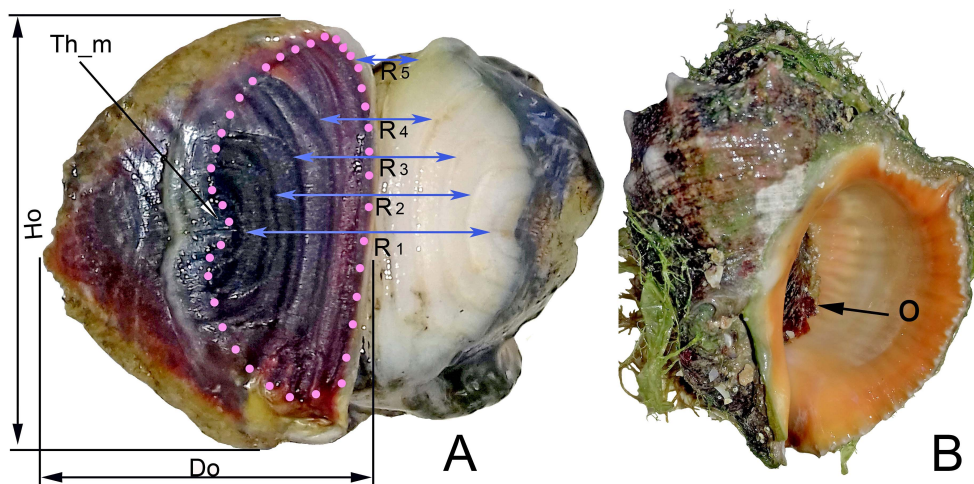


Fig. 3. A, the inner side of *Rapana venosa* operculum (Ho, 28.5 mm; Do, 23 mm) with 5 “rings” (shown by arrows R1–R5) and the imprint of its attachment site (light-colored surface) on the dorsal side of the foot. The arrow indicates the point of measurement of the operculum thickness (Th_m); the outline of light (pink) dots shows the area of the operculum attachment. B, *R. venosa* specimen (M; 4 years old; Hs, 68 mm; Ds, 48 mm) with the operculum (the parameters are given above, see A) retracted inside the aperture

The linear dimensions of shells and opercula were determined with a caliper with an accuracy of 0.1 mm. The operculum thickness (Tho) was measured with a caliper to the nearest 0.01 mm in the location shown by an arrow (Th_m) in Fig. 3A. To study Tho variability, we used 60 rapa whelk specimens (10 juveniles, 20 females, and 30 males) representing the entire size and age range of the general sample and reflecting the structure of the modern Black Sea metapopulation of *R. venosa*, where the proportion of males usually exceeds the proportion of females [Bondarev, 2010, 2014, 2016].

Morphometric characteristics of opercula regenerated after predator damage were not included in the data analysis.

Graphs were plotted and raw data were statistically processed applying standard algorithms of parametric and rank analysis with the use of SigmaPlot for Windows [2023] and MS Office Excel (v10).

RESULTS

R. venosa operculum consisting of a horn-like substance is located on the dorsal side of the mollusc massive foot (Figs 2B, 3A). The operculum is attached to the rapa whelk foot not by its entire inner surface, but only by its part (Fig. 3A). The operculum is the thickest outside the attachment site, where horn-like substance layering is maximum (shown by an arrow in Fig. 3A). The thickness naturally increases with mollusc shell size (Hs) and age (Fig. 4).

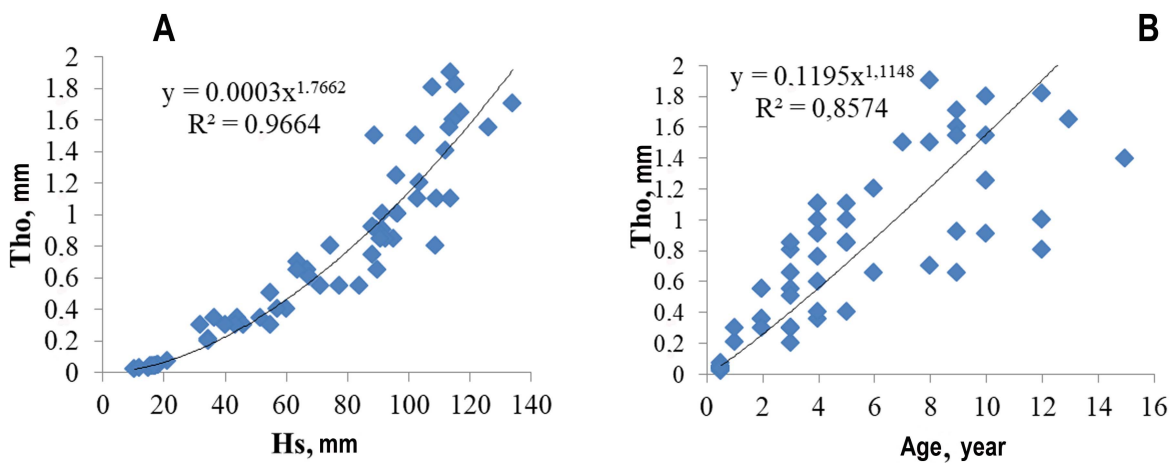


Fig. 4. Graphs of the dependence of *Rapana venosa* operculum thickness: A, on the shell height (Hs); B, on the age of the mollusc

The dependence of *R. venosa* operculum thickness on shell height is well approximated by a power function ($R^2 = 0.9664$) (Fig. 4A). The plot of the dependence on aperture height (no plot is shown) looks similar, but the coefficient of determination is slightly lower ($R^2 = 0.9627$). The operculum thickness correlates well with age ($R^2 = 0.8574$), but there are pronounced individual deviations (Fig. 4B).

In our sample, Tho values varied from 0.02 mm in a juvenile individual with a size (Hs) of 10.4 mm to 1.9 mm in an 8-year-old male with a shell height (Hs) of 114.0 mm. The operculum thickness of juvenile *R. venosa* about 5–6 months old with Hs ranging from 10.4 to 21.3 mm was 0.02–0.07 mm. The largest specimen in our sample (Hs of 135 mm), a 12-year-old male, had Tho of 1.62 mm. The mean thickness and the range of variation in the operculum thickness in females are lower than in males (Table 1).

Table 1. Indicators of *Rapana venosa* operculum thickness (Tho) by sex and age groups (*N*, number of individuals; F, females; M, males; J, juveniles; Hs, shell height, mm; *M*, mean values; σ , standard deviation)

| Sex | <i>N</i> | Age, years (min–max) | Hs, mm (min–max) | Tho | | | |
|-----------|----------|----------------------|------------------|------|------|----------|----------|
| | | | | min | max | <i>M</i> | σ |
| J | 10 | 0.5 | 10.4–21.3 | 0.02 | 0.07 | 0.04 | 0.014 |
| F | 20 | 1–15 | 34.6–126.0 | 0.2 | 1.55 | 0.76 | 0.46 |
| M | 30 | 1–12 | 36.8–135.0 | 0.3 | 1.90 | 0.97 | 0.50 |
| J + F + M | 60 | 0.5–15 | 10.4–135.0 | 0.02 | 1.90 | 0.74 | 0.55 |

Toward the periphery, the operculum decreases in terms of its thickness to a thin flexible film, which is minimum in the zone of growth on the inner edge, thinner than 0.01 mm. The flexibility and smooth surface of the peripheral zone ensure a tight adhesion of the operculum edges to the inner surface of the shell aperture. Moreover, such a structure of the operculum allows the mollusc to retract it deep inside the shell (Fig. 3B) and more effectively block the access of predators to the soft body.

The outer surface of the operculum is streaked with growth lines of varying relief [Figs 2A, B (F), 5A, D, 6A].

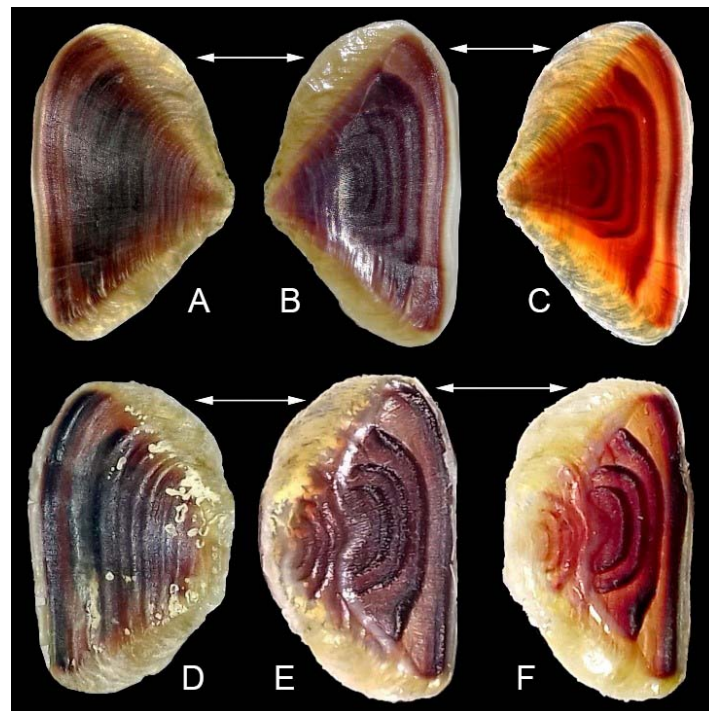


Fig. 5. A–F, opercula of two different-aged individuals of *Rapana venosa*. A–C, 2+ years; Hs, 64.2 mm; Ho, 27 mm; Do, 16.5 mm; number of “rings” (RN), 6. D–F, 4 years; Hs, 36.8 mm; Ho, 15.2 mm; Do, 9.3 mm; RN, 4. A, D, outer surface; B, C, E, F, inner surface (B, E, in reflected light; C, F, in transmitted light)

On the inner side of the operculum, the attachment site has a relief of concentric horseshoe-shaped ridges mirrored on the corresponding section of the dorsal side of the mollusc foot (Fig. 3A). The number of these ridges, commonly referred to as “rings” in the literature [Choi, Ryu, 2009; Chukhchin, 1961; Kosyan, Antipushkina, 2011], increases with age as the mollusc grows, as shown in Table 2.

Table 2. The number of “rings” (RN) on the inner side of *Rapana venosa* operculum for individuals of different age (years) and size (Hs, mm) (*N*, the number of individuals in the sample)

| RN | 2 | 3 | 4 | 5 | 6 | 7 | 8 | 9 | 10 | 11 | 12 |
|----------|---------------|---------------|---------------|---------------|------------|--------------|--------------|---------------|----------------|---------------|--------------|
| Age | 0.5 | 0.5 | 2–4 | 1–8 | 2–9 | 3–12 | 4–9 | 10–12 | 8–13 | 9–15 | 8–12 |
| Hs | 10.4– 16.4 | 16.8– 21.3 | 36.8– 60.8 | 35.2– 96.5 | 44– 114 | 64– 109.5 | 88.2– 103 | 74.5– 91.5 | 63.3– 117.3 | 112.2– 126 | 91.5– 135 |
| <i>N</i> | 5 | 5 | 3 | 85 | 47 | 23 | 3 | 3 | 9 | 3 | 4 |

As follows from Table 2, the operculum of juvenile specimens has 2–3 “rings.” Most (82%) of examined *R. venosa* have 5 to 7 “rings” on the operculum; out of them, 55% have 5 “rings.” The age of those individuals varies from 1 to 12 years, and the size (Hs) ranges from 35.2 to 114 mm. The highest number of “rings” (8–12) is typical for large old individuals (Table 2). In molluscs up to and including 5 years, the “rings” on the inner side of the operculum usually differ quite clearly (Figs 3A, 5B, C, E, F). The “rings” are distinctly visible in transmitted light due to thickening relative to the base surface of the operculum (Fig. 5C, F). On the operculum of older individuals, the lines of “rings” are more often “intertwined” (Fig. 6B); sometimes, those are indistinguishable, and less often those are clearly distinguishable (Fig. 6C).

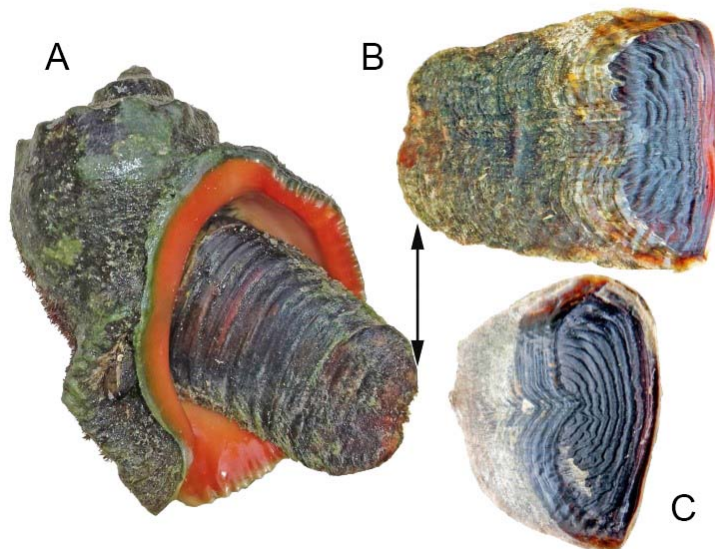


Fig. 6. A, *Rapana venosa*; male; 12 years old; Hs, 91.5 mm; with an abnormally wide operculum. B, its operculum (Ho, 45 mm; Do, 50.2 mm; RN, 12), inner view. C, operculum (Ho 62.5 mm; Do, 55.5 mm; RN, 10) of 12-year-old male *R. venosa* (Hs, 115.7 mm), inner view

Initially, the operculum of juvenile *R. venosa* has the shape of a triangle with rounded corners; this shape is typical for individuals up to 2–3 years old (Figs 2A, 5A–C). The long (inner) side of the triangle, oriented along the shell columella, is the growth zone of the operculum, and its nucleus is located on the opposite apex of the outer edge. With increasing age of the mollusc, the apexes of the corners become more and more rounded (Fig. 5D–F), and the operculum shape changes from subtriangular to irregularly oval, corresponding to the aperture shape. Such a change occurs due to abrasion of the nucleus area and a gradual decrease in the growth rate of the rapa whelk and its operculum as the mollusc becomes older.

The operculum height and width increase as *R. venosa* shell grows. The operculum height (Ho) correlates better with the aperture height (Ha) (Fig. 7A) than with the shell height, where the coefficient of determination is slightly lower ($R^2 = 0.9764$) (no plot is shown). The operculum width (Do) is more closely ($R^2 = 0.9497$) related to the width of the last whorl of the shell (Ds) (Fig. 7B) than to the aperture width (Da) ($R^2 = 0.9199$) (no plot is shown).

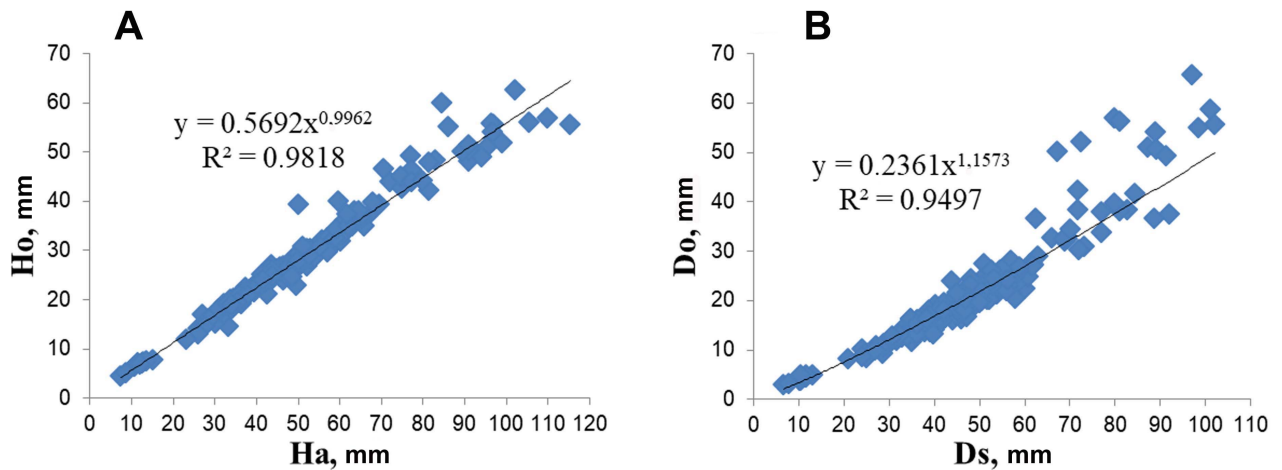


Fig. 7. Graphs of correspondence between the size of the operculum and the size of *Rapana venosa* shell: A, between the operculum height (Ho) and the aperture height (Ha); B, between the operculum width (Do) and the diameter of the last whorl (Ds)

At a high level of correspondence between the parameters of the operculum and the size of *R. venosa* shell, there are individual and repeated deviations. The highest Ho value (62.5 mm) was noted in a specimen with Hs of 115.5 mm, Ha of 102.0 mm, Ds of 102.0 mm, Da of 57.8 mm, and Do of 55.5 mm. The largest mollusc in our sample (with Hs of 135.0 mm, Ha of 115.2 mm, and Ds of 101.0 mm) has Ho of 56.8 mm, but the highest Do, 58.6 mm. These and several other individuals exhibited the phenomenon of a hypertrophied wide operculum (Figs 6A, B, 8A–C, 10D). This anomaly was registered only in male *R. venosa* and is typical for older individuals from the Donuzlav Bay, while in other areas, it is rare and much less pronounced (Fig. 8C).

The proportions of the operculum and the phenomenon of its abnormal width can be quantitatively assessed by the ratio of the parameters Do and Ho (Table 3).

Table 3. Indicators of the width-to-height ratio of *Rapana venosa* operculum (Do/Ho) of the areas of the Donuzlav Bay (DB) and Sevastopol bays (SB) and the entire sample (DB+SB) by sex groups (N, number of individuals; F, females; M, males; J, juveniles; M, mean values; σ , standard deviation)

| Sex | Area | | | | | | | | | | | |
|-----------|-----------------------|----|------|----------|----------------------|-----|------|----------|-----------|-----|------|----------|
| | The Donuzlav Bay (DB) | | | | Sevastopol bays (SB) | | | | DB + SB | | | |
| | Min–max | N | M | σ | Min–max | N | M | σ | Min–max | N | M | σ |
| J | – | – | – | – | 0.54–0.7 | 10 | 0.61 | 0.04 | 0.54–0.7 | 10 | 0.61 | 0.04 |
| F | 0.66–0.81 | 14 | 0.71 | 0.05 | 0.48–0.76 | 48 | 0.67 | 0.06 | 0.48–0.81 | 62 | 0.68 | 0.055 |
| M | 0.63–1.13 | 31 | 0.81 | 0.14 | 0.53–0.9 | 87 | 0.72 | 0.07 | 0.53–1.13 | 118 | 0.74 | 0.07 |
| F + M | 0.63–1.13 | 45 | 0.77 | 0.14 | 0.48–0.9 | 135 | 0.70 | 0.07 | 0.48–1.13 | 180 | 0.72 | 0.09 |
| J + F + M | 0.63–1.13 | 45 | 0.77 | 0.14 | 0.48–0.9 | 145 | 0.69 | 0.07 | 0.48–1.13 | 190 | 0.71 | 0.09 |

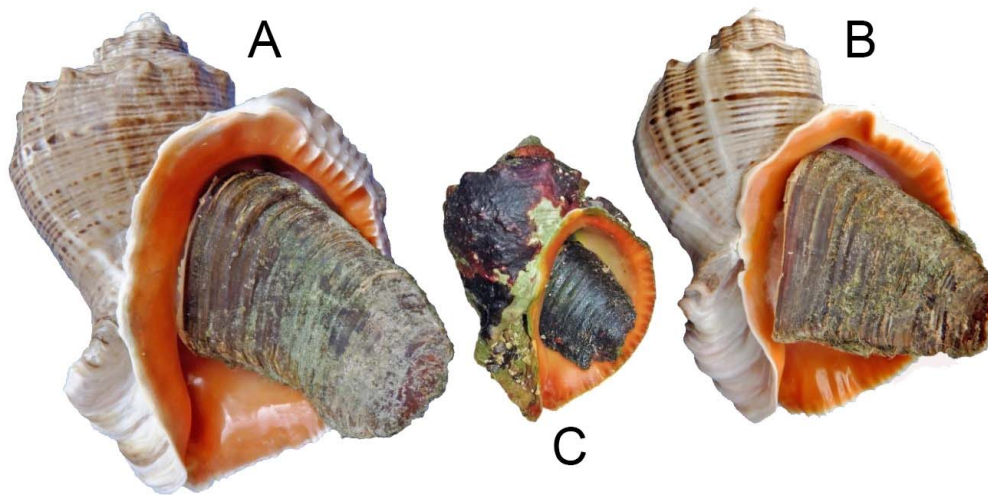


Fig. 8. Specimens of *Rapana venosa* males with an abnormally wide operculum. A, B, shells from the Donuzlav Bay; 10 years old. A: Hs, 107.8 mm; Ho, 48 mm; Do, 57 mm. B, Hs, 96.3 mm; Ho, 46 mm; Do, 52.2 mm. C, living specimen from the Solenaya Bay (Sevastopol); 8 years old; Hs, 64.5 mm; Ho, 26.5 mm; Do, 23.8 mm

The highest Do/Ho value, 1.19 (57.0/48.0 mm), was recorded in a 9-year-old male from the Donuzlav Bay with Hs of 107.8 mm, Ha of 91.0 mm, Ds of 80.1 mm, and Da of 42.0 mm (Fig. 8A). In Sevastopol bays, Do/Ho does not exceed 0.9 (23.8/26.5 mm) (Table 3), as in an 8-year-old male with Hs of 64.5 mm (Fig. 8B). In Sevastopol bays, the morphological parameters of *R. venosa* shells are characteristic of the Crimean coast; the operculum has characteristic shape and proportions as well. Do/Ho value of 0.7 for the rapa whelk in this area (Table 3) can be considered mean for the Crimea. *R. venosa* individuals from the Donuzlav Bay up to 5 years old have similar mean Do/Ho values as well. An example is Do/Ho of 0.67 (33.8/50.3 mm) of a fairly large (Hs of 108.8 mm) 3-year-old male *R. venosa* (Fig. 2A).

Do/Ho for females has lower values than for males, and this is especially pronounced in the rapa whelk from the Donuzlav Bay (Table 3). With age, the “expansion” of *R. venosa* operculum increases, but in older specimens, individual characteristics are more pronounced (Fig. 9A, B). The relationship between Do/Ho and age is stronger for males ($R^2 = 0.4325$) (Fig. 9B) than for females ($R^2 = 0.0365$) (no plot is shown).

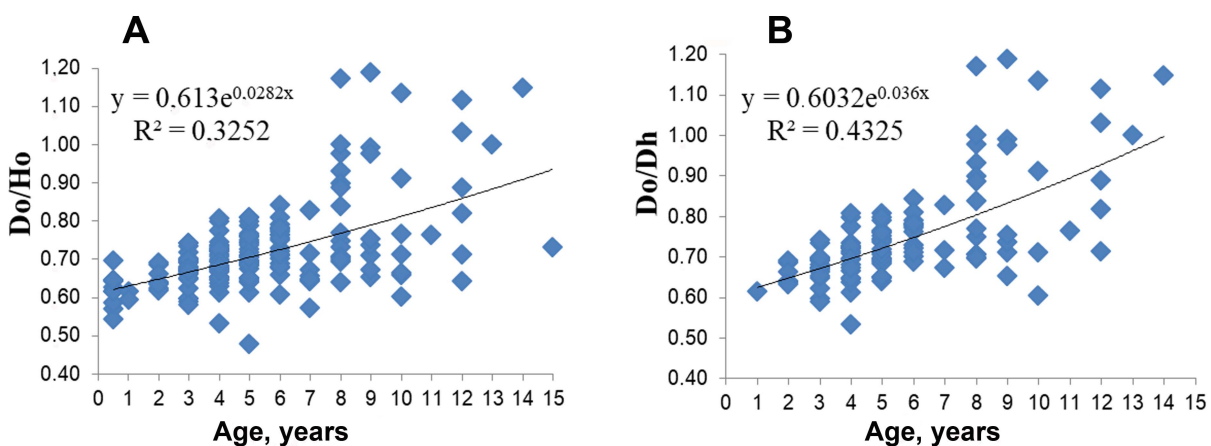


Fig. 9. Plots of Do/Ho dependence of *Rapana venosa* on the age of individuals: A, for the entire sample; B, for males

Based on the data in Table 3, the operculum of the mature rapa whelk with $Do/Ho > 0.81$ ($M + \sigma$) should be considered abnormally wide. Only 6-year-old males and older specimens have such Do/Ho values, and their proportion is 11.6% (22 ind.) of the total sample, 37.8% (17 ind.) of the sample from the Donuzlav Bay, and 3.5% (5 ind.) of the sample from Sevastopol bays. According to the results of the analysis of variance, Do/Ho distribution in the general sample by sex is not normal (Shapiro–Wilcoxon test, significance level of $P < 0.05$). Therefore, to compare two groups (all males vs. all females), Mann–Whitney rank test was applied. The differences between the samples in the median values of Do/Ho are statistically highly significant (at $P < 0.001$) and amount to 0.715 and 0.672 for males and females, respectively, *i. e.*, sex differences in Do/Ho are obvious.

According to the results of morphometric analysis of the operculum of females from two areas (the Donuzlav Bay and Sevastopol bays), the mean values of Do/Ho between groups do not differ statistically significantly (parametric test, $P > 0.05$). At the same time, the normal distribution of variants in the samples is observed (Shapiro–Wilcoxon test is passed, $P = 0.096$), and the variants are quite evenly and compactly grouped around the mean value (Fig. 10A–C). Do/Ho variation indicators, $M \pm \sigma$, are 0.71 ± 0.05 for the Donuzlav Bay and 0.67 ± 0.06 for Sevastopol bays (Table 3).

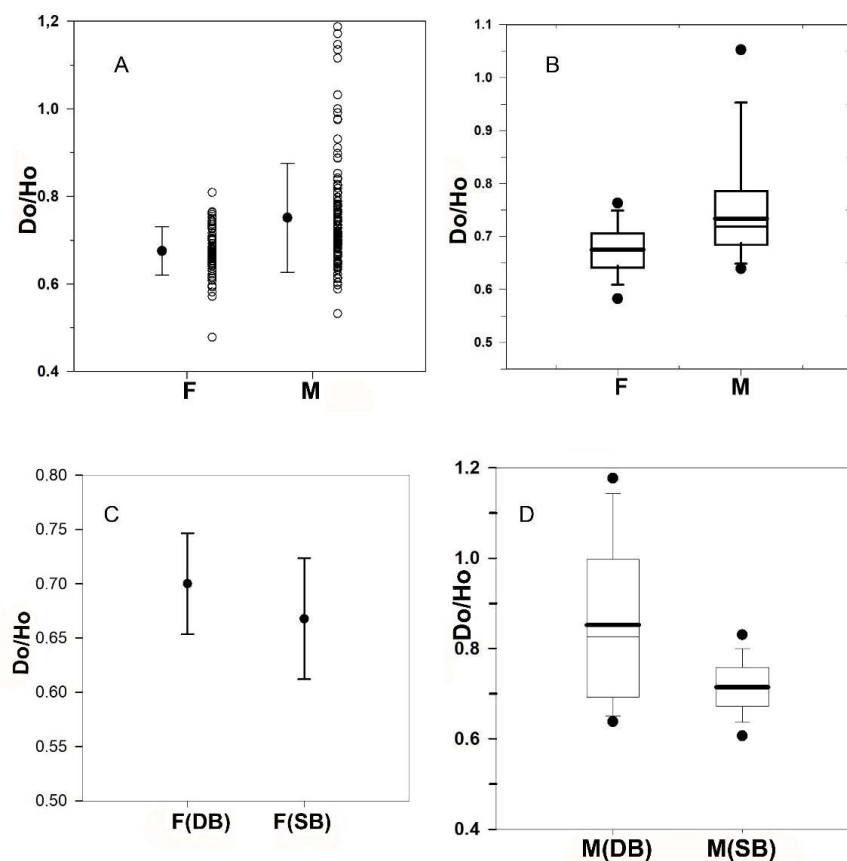


Fig. 10. Graphs of variation characteristics of Do/Ho for *Rapana venosa*: A, B, for females (F) and males (M) of the entire sample; C, for females (F); D, for males (M) of the Donuzlav Bay (DB) and Sevastopol bays (SB). A, C: bold points show mean values (M); “whiskers” show ranges from mean values ($M \pm \sigma$). B, D: the lower and upper boundaries of the boxes correspond to 25% and 75% of the total number of measurements; “whiskers” are the intervals of the dispersion spread; bold points are the percentiles of the total number of measurements [5th (bottom) and 95th (top)]; the bold line inside the boxes is the mean value; the thin line is the median

When analyzing samples of males from two areas, it was established as follows: the median values differ significantly (rank test, $P < 0.001$) due to the special ratio of the operculum morphometric characteristics in individuals from the Donuzlav Bay. Do/Ho median for male *R. venosa* from this bay is 0.826, while for males from Sevastopol bays, the value is 0.710. This allows us to say that morphological deviations in the operculum proportions are inherent only in males. Those are more pronounced in the environmental conditions of the Donuzlav Bay: the upper limit of Do/Ho values (95th percentile) exceeds 1.1 (Table 3; Figs 9, 10D). The results of testing using the quantile method for extreme variants (possible statistical outliers) to belong to the sample showed that all the outliers in Do/Ho in some rapa whelk from the Donuzlav Bay statistically belong to the sample (for $P = 0.05$) and cannot be discarded in variational analysis as random anomalies.

The coefficient of variation (CV) of Do/Ho for the sample of males from the Donuzlav Bay was 21.2%, and for the sample from Sevastopol bays, 9.1%. For samples of females, CV values were even lower: 6.6% for the Donuzlav Bay and 8.4% for Sevastopol bays. The results obtained allow suggesting that, despite the significant variability in the initial data, we are dealing with a single sample of males from the Donuzlav Bay. For other groups (both females and males), the assertion that in each case this is a single sample is even more confirmed.

The shape of *R. venosa* operculum changes in accordance with changes in the growth rate of the mollusc. This relation can be seen especially clearly in spawning annual marks on the shell (Fig. 11). Those are noticeable on the shell surface cleaned of fouling by their orange-red color emphasizing the relief of an axial ridge, which corresponds to the stage of growth interruption and thickening of the outer edge of the aperture associated with spawning. A decrease in the distance between the marks on the shell and growth lines on the operculum corresponds to a drop in growth rates, and *vice versa*; this reflects age-related changes and (or) food availability. *R. venosa* individuals in Fig. 11 show an abnormally high increase in the shell and operculum growth in the year of sampling against the backdrop of a natural decrease in the rate of shell growth with age. The line of the outer edge from the nucleus to the inner side of the operculum is a conventional graph of the mollusc growth rate. An increase in the slope steepness of this line relative to an imaginary midline connecting the nucleus and the center of the inner edge corresponds to the stage of accelerating growth and increasing the operculum height (Fig. 11B–D).

Morphological changes in *R. venosa* operculum occur as a result of attacks by predators and damage to the protective outer layer of the mollusc (Figs 12, 13). In the Black Sea, such predators are crabs *Carcinus aestuarii* Nardo, 1847 and *Eriphia verrucosa* (Forskål, 1775). Damage remains on the shell as scars, even if it was inflicted at the early stages of the shell formation (Fig. 12A). Interestingly, the rapa whelk operculum, the foot, and the gland forming the operculum can be damaged to varying degree. As a result, a horny “pearl” can be formed on the mollusc foot next to the operculum – a round formation with a convex surface and an oval depression on the inside providing attachment to the foot (Fig. 12B). On the inner side of the operculum, an irregularly shaped “blister” can be formed (Figs 12C, 13B).

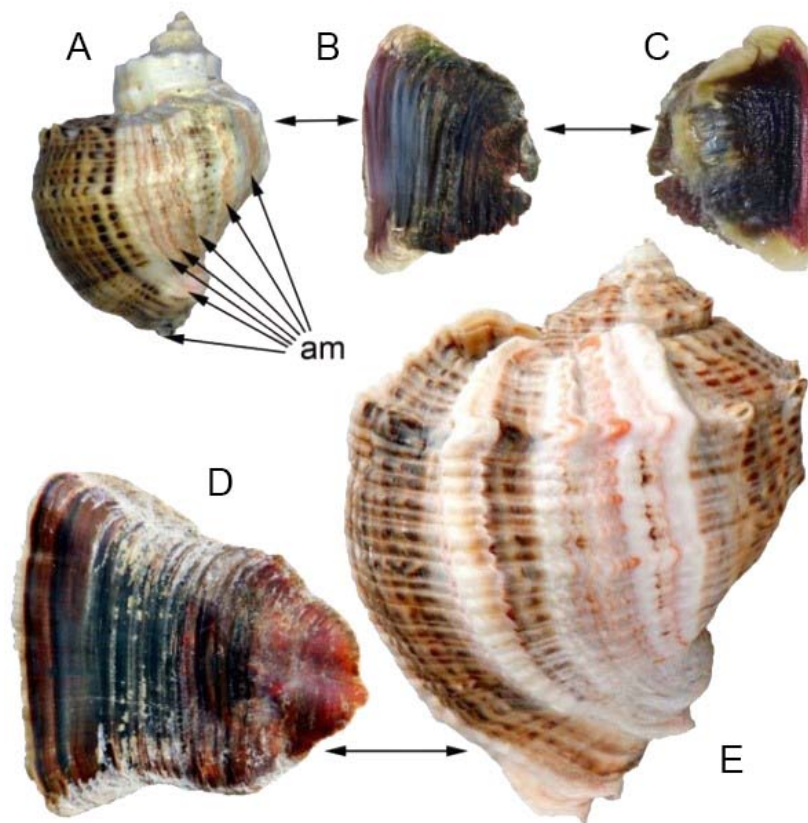


Fig. 11. Shells (A, E) of *Rapana venosa* (M, 9 years old) with annual spawning marks (am) and their opercula (B–D). A, the specimen from the Kazachya Bay (Sevastopol); Hs, 64 mm. B, C, its operculum (Ho, 26.5 mm; Do, 19.5 mm): B, outer side; C, inner side. D, outer side of the operculum (Ho, 55.5 mm; Do, 54.1 mm) of the specimen from the Donuzlav Bay, Hs, 115.5 mm, E

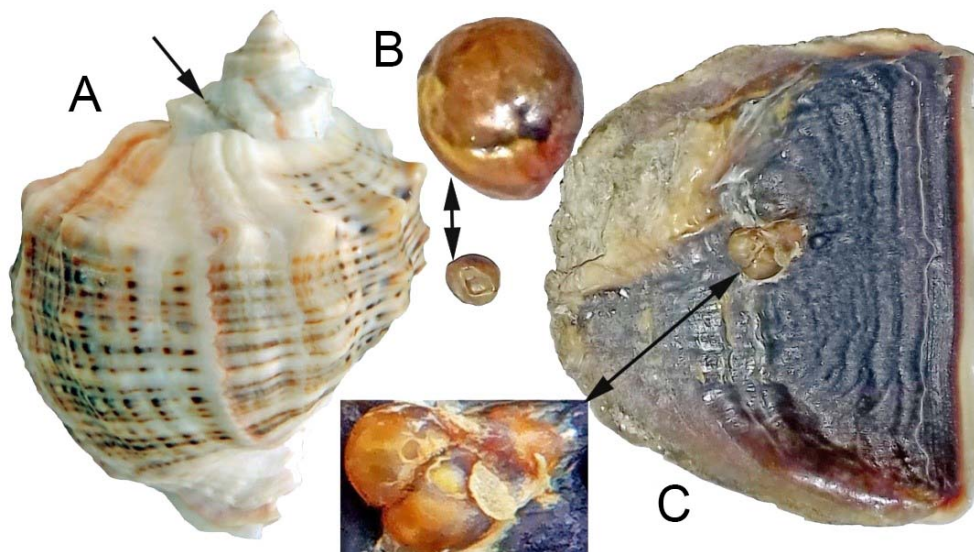


Fig. 12. A, specimen of *Rapana venosa* male; 8 years old; Hs, 88.2 mm; with damage at the apex (shown by the arrow). B, horny "pearl" of $4.2 \times 3.3 \times 2.9$ mm [enlarged view from above; bottom view (below) on the same scale as the operculum]. C, operculum (inner side) of this individual (Ho, 43.1 mm; Do, 32.3 mm) with a "blister" of 5.2×3.8 mm

Shell damage that occurs in the first year can manifest itself throughout the life of the mollusc *via* the formation of ray “tracing” on the outer surface of the operculum (Fig. 13A). After rough damage to the shell (Fig. 13C) and almost complete detachment of the operculum from the attachment site on the foot, the rapa whelk can generate a new, duplicate operculum attached to the first one (Fig. 13D, E). If the operculum is severely damaged or completely detached, it can be regenerated in an aberrant form (Fig. 13F, G).

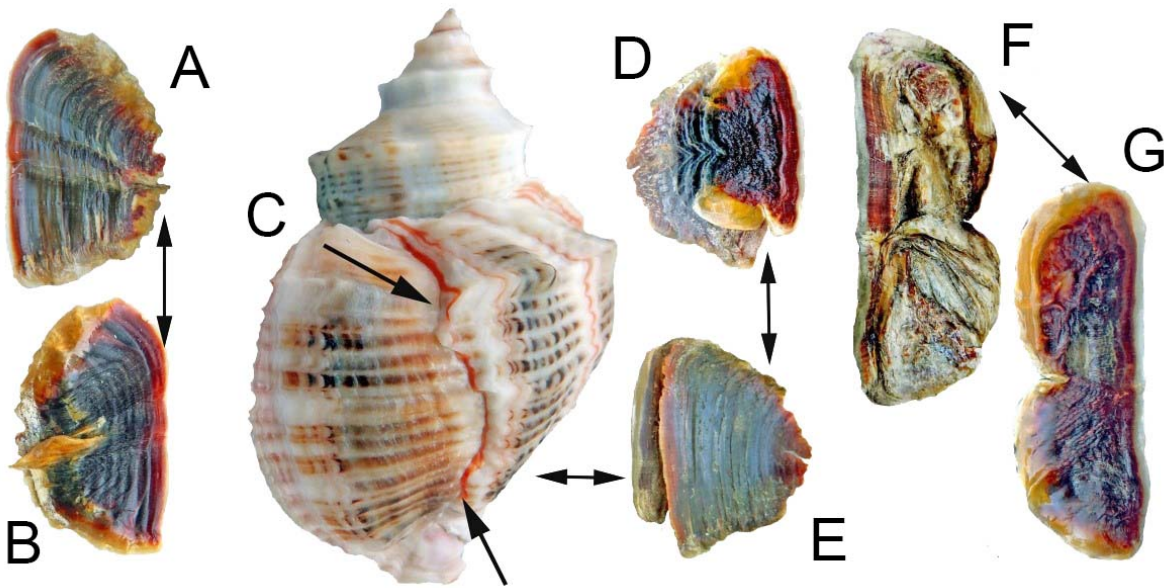


Fig. 13. A, B, operculum of *Rapana venosa* female; 12 years old; Hs, 74.5 mm; Ho, 34.2 mm; Do, 22 mm; with double-ray “tracing” of damage along the outer surface (A) and a “blister” on the inner side (B). C, *R. venosa* individual; M; 7 years old; Hs, 74.3 mm; with rough damage on the last whorl (shown by arrows). D, inner; E, outer side of its regenerated “duplicated” operculum (Ho, 28.6 mm; Do, 21.8 mm). F, outer; G, inner side of the regenerated operculum (Ho, 50 mm; Do, 18.5 mm) of *R. venosa*; male; 9 years old; Hs, 122 mm

DISCUSSION

In general terms, *R. venosa* operculum corresponds to the description for representatives of *Rapana* genus: large, horny, with a nucleus shifted to the outer edge and concentric growth lines [Golikov et al., 1972]. The deeper examination of the morphology of the rapa whelk operculum allows us to more fully assess the functionality and variability of this exosomatic organ.

Flexible and smooth edges of the operculum, which do not grow to the foot, act as a cuff and contribute to its tight adjacency to the inner surface of the aperture; also, those provide the ability to retract the soft body deep inside the shell (Fig. 3). This “option” is extremely important in defense against crabs capable of breaking off significant fragments of the shell, especially at the stage of active growth of the mollusc, when its thickness is insufficient to withstand the efforts of a predator [Bondarev, 2013]. The operculum allows *R. venosa* not only to protect itself from the intrusion of a predator, but also to maintain a special environment of the mantle fluid which ensures the normal functioning of the rapa whelk under adverse conditions [Bondarev, 2013].

The ribbed structure of the inner surface increases the adhesive area of the operculum and the foot and allows it to more effectively resist mechanical stress in various directions, preventing breaking off. Horseshoe-shaped ridges, the number of which rises with the mollusc growth, are not annual rings. V. Chukhchin [1961] was the first to draw attention to this fact; according to him, even juveniles with a shell height of 10–20 mm may have 5 “rings” on the operculum, as well as adult rapa whelk with Hs of 70–80 mm. However, determining *R. venosa* age, especially age of old individuals, by spawning marks is quite laborious (due to the need for cleaning the shell surface of fouling), and sometimes, it is simply impossible (if the shell surface is severely damaged by boring parasites). Moreover, in some habitats, *R. venosa* is characterized by weakly visible spawning marks. These circumstances force researchers to continue attempts to use growth lines on the operculum to determine the mollusc age [Choi, Ryu, 2009]. Based on the analysis of the content of stable oxygen isotopes in shell carbonates, it was established that the obtained data for determining individual age corresponded to the results of calculating the years of life of *R. venosa* specimens using spawning marks. As assumed, single coincidences of the number of “rings” on the operculum and the established age of the mollusc are accidental [Kosyan, Antipushkina, 2011]. Studying the growth of layers in cross sections under a microscope, counting the number of visible “rings” on the operculum, and assessment of their correspondence to annual marks of *H. trunculus* shell also led to the conclusion that it is impossible to use these morphological elements of the operculum to determine the age of the mollusc [Vasconcelos et al., 2012].

Our data show as follows: the number of “rings” on the inner side of *R. venosa* operculum increases with age (from 2 to 12), and the values may coincide, mainly for the age group of 5–7-year-old rapa whelk, since most individuals (82%) have 5–7 “rings” (Table 2). According to our material, 1-year-old molluscs (Table 2) and even younger ones [Chukhchin, 1961] can form the operculum with 5 “rings.” The proportion of individuals with 5 “rings” on the operculum is 55% of the sample, but their age is from 1 to 8 years. Thus, obviously, the correspondence between the number of “rings” and the number of years is random, and determination of *R. venosa* age cannot be based on counting the “rings” of the operculum.

Based on a comparison of the time of damage to the shell and regeneration of the operculum, we can say that *R. venosa* is capable of complete restoration of the operculum with 6 “rings” within a year (Fig. 13). As already noted, after rough damage to the shell by a predator (Fig. 13C) and almost complete detachment of the operculum from its attachment site on the foot, the mollusc is able to form a new, duplicate operculum attached to the old one (Fig. 13E, F). A 9-year-old male (Hs of 122 mm), with the shell bearing traces of a severe attack by a predator at 8 years, has the operculum that is not fully restored (Fig. 13D, E). However, taking into account the width (18.5 mm) and thickness (0.95 mm), probably, this is a newly formed operculum, since in males of this age and size from the Donuzlav Bay the operculum is 2–3 times wider and up to 2 times thicker.

The formation of the previously undescribed horny “pearl” and “blisters” on *R. venosa* operculum (Fig. 12B) seems to occur according to the same principle as the well-known mineral and organic influx in bivalves when glands or tissues are irritated and start secreting dense covering material layer by layer.

Already in the first months of shell formation, the proportions of the operculum (Do/Ho) correspond to the shape inherent in sexually mature individuals (Table 3). In the first 3 years, the growth rate of *R. venosa* is maximum, and this determines the subtriangular shape of the operculum (Figs 2A, 5A–C).

An age-related decrease in growth rates and abrasion of the nucleus area result in a change in shape to a more oval one (Fig. 5D–F). A rise in the relative operculum width with increasing age is more pronounced in males (Fig. 9B). The lowest Do/Ho values were recorded in females, 0.48 (in a 5-year-old rapa whelk with Hs of 62.1 mm from Sevastopol bays). The maximum Do/Ho values, 0.76 for females of the same area (Table 3), were also registered in a 5-year-old *R. venosa* with a shell height of 64.5 mm. Against the backdrop of individual growth characteristics, a general tendency for the relative width of the operculum (Do/Ho) to rise as the size of *R. venosa* shell increases can be traced for the entire sample (Fig. 9).

Of particular interest is the phenomenon of an abnormally wide operculum, found in *R. venosa* mainly from the Donuzlav Bay (Figs 6, 8, 11D). Such a shape of the operculum, with the width that can exceed the width of the shell aperture, has not previously been described for any Muricidae representatives or even for any Gastropoda species. The operculum thickness in abnormal individuals (1.0–1.9 mm) is 1.5–2.5 times greater than the mean value for the sample, 0.74 mm (Table 1). Since this anomaly in development was found in males alone, it is logical to assume that it is driven by the rapa whelk sex. Male *R. venosa* have a fairly large penis (Fig. 2B), which can be damaged by predators during copulation. Such an adaptation, as the operculum with a wide and free edge not attached to the body (Fig. 2B), can be an effective additional protection for the penis, even if the soft body is not retracted inside the shell which occurs during copulation. The Mediterranean green crab *C. aestuarii*, the most widespread rapa whelk predator in the Donuzlav Bay, is capable of causing significant damage to the soft body and even to rather thick-walled shell of *R. venosa* (Fig. 13C). Attacks of *C. aestuarii* on the rapa whelk were repeatedly observed by the author during the sampling of material. Apparently, increased pressure from crabs on this mollusc in the Donuzlav Bay is the reason for higher abundance of males with an abnormally wide operculum there (53%) than in Sevastopol bays (5.8%). It takes time for a wide operculum to be formed. Accordingly, individuals with abnormal Do/Ho are 6 years old and more, and the highest values are recorded in specimens of 9 years old and more. A significant proportion (53%) of individuals with an abnormally wide operculum among males from the Donuzlav Bay indicates that this phenomenon is not a random deviation from the norm, but the result of morphogenesis initiated by predators. This is confirmed by the analysis using the quantile method for extreme variants (possible statistical outliers) to belong to the sample. Specifically, it showed that all outliers in Do/Ho belong to the sample of *R. venosa* from the Donuzlav Bay and cannot be discarded as random anomalies (for $P = 0.05$). Despite the significant variability in the data in the sample of males from the Donuzlav Bay ($CV = 21.2\%$), we are dealing with a single sample. For other studied groups of *R. venosa*, CV of Do/Ho does not exceed 9.1%; therefore, the assertion that in each case the sample is single is even more confirmed.

According to molecular genetic studies, *R. venosa* in new habitats has an extremely low level of genetic variability compared to that for populations from its native range [Slynko et al., 2020; Xue et al., 2018]. However, with genetic monomorphism in the Black Sea, the rapa whelk demonstrates a wide polymorphism of its shell [Bondarev, 2010, 2015, 2016; Chukhchin, 1961; Slynko et al., 2020] and gonads [Bondarev, 2015]. The occurrence of a previously undescribed variant of the “expanded” operculum shows a new facet of the potential for morphological variability of *R. venosa*.

Conclusion. The operculum of *Rapana venosa* is an exosomatic organ changing its morphology with growth and age and demonstrating both regenerative capabilities and the morphogenetic potential of the species. A striking manifestation of this potential is the formation of a hypertrophied large operculum, with the proportions not being characteristic of any other Muricidae species and Gastropoda

in general. The formation of an abnormally wide and thickened operculum in the rapa whelk can be explained by increased pressure from predators. The presence of an abnormal operculum exclusively in male *R. venosa* suggests that this feature is sex-driven and results from the adaptation, possibly promoting protection for the reproductive organ from predators.

The discovery of the ability to regenerate the operculum expands the understanding of the physiological capabilities of the rapa whelk. The phenomenon of the operculum formation with a unique shape for gastropods is another manifestation of morphological plasticity, which made *R. venosa* one of the most successful invasive species in the modern marine environment.

This work was carried out within the framework of IBSS state research assignment "Regularities of formation and anthropogenic transformation of biodiversity and biological resources of the Sea of Azov–Black Sea basin and other areas of the World Ocean" (No. 121030100028-0).

Acknowledgement. The author is grateful to the anonymous reviewers for their constructive comments which helped to improve the quality of the article. The author expresses special gratitude to PhD A. Petrov (IBSS) for valuable advice and productive discussion of statistical data processing.

REFERENCES

1. Bondarev I. P. The shell morphogenesis and intraspecific differentiation of *Rapana venosa* (Valenciennes, 1846). *Ruthenica*, 2010, vol. 20, no. 2, pp. 69–90. (in Russ.)
2. Bondarev I. P. Structure of *Rapana venosa* (Gastropoda, Muricidae) population of Sevastopol bays (the Black Sea). *Morskoj biologicheskij zhurnal*, 2016, vol. 1, no. 3, pp. 14–21. (in Russ.). <https://doi.org/10.21072/mbj.2016.01.3.02>
3. Golikov A. N., Starobogatov Ya. I., Skarlato O. A. Tip mollyuski – Mollusca. In: *Opredelitel' fauny Chernogo i Azovskogo morei*. Vol. 3: *Chlenistonogie (krome rakoobraznykh), mollyuski, iglokozhiye, shchetinkochelyustnye, khordovye*. Kyiv : Naukova dumka, 1972, pp. 60–249. (in Russ.)
4. Drapkin E. I. Novyi mollyusk v Chernom more. *Priroda*, 1953, no. 9, pp. 92–95. (in Russ.)
5. Chukhchin V. D. Rost rapany (*Rapana bezoar* L.) v Sevastopol'skoi bukhte. *Trudy Sevastopol'skoi biologicheskoi stantsii*, 1961, vol. 14, pp. 169–177. (in Russ.). <https://repository.marine-research.ru/handle/299011/5503>
6. Chukhchin V. D. *Funktsional'naya morfologiya rapany*. Kyiv : Naukova dumka, 1970, 139 p. (in Russ.). <https://repository.marine-research.ru/handle/299011/1125>
7. Chukhchin V. D. *Ekologiya bryukhonogikh mollyuskov Chernogo morya*. Kyiv : Naukova dumka, 1984, 176 p. (in Russ.). <https://repository.marine-research.ru/handle/299011/5646>
8. *Alien Species Alert: Rapana venosa (Veined Whelk)* / R. Mann, A. Occhipinti, J. M. Harding (Eds). Copenhagen, Denmark : ICES, 2004, 14 p. (ICES Cooperative Research Report ; no. 264). <https://doi.org/10.17895/ices.pub.5471>
9. Bondarev I. P. Dynamics of *Rapana venosa* (Valenciennes, 1846) (Gastropoda: Muricidae) population in the Black Sea. *International Journal of Marine Science*, 2014, vol. 4, no. 3, pp. 42–56.
10. Bondarev I. P. Ecomorphological analyses of marine mollusks' shell thickness of *Rapana venosa* (Valenciennes, 1846) (Gastropoda: Muricidae). *International Journal of Marine Science*, 2013, vol. 3, no. 45, pp. 368–388.

11. Bondarev I. P. Sexual differentiation and variations sexual characteristics *Rapana venosa* (Valenciennes, 1846). *International Journal of Marine Science*, 2015, vol. 5, no. 19, pp. 1–10.
12. Choi J.-D., Ryu D.-K. Age and growth of purple whelk, *Rapana venosa* (Gastropoda: Muricidae) in the West Sea of Korea. *Korean Journal of Malacology*, 2009, vol. 25, no. 3, pp. 189–196.
13. Keppens M., Dhondt K., Mienis H. K. The variability of the operculum in *Nuccella lapillus* (Gastropoda, Muricidae) from a colony in Audresselles, France. *Vita Malacologica*, 2008, vol. 7, pp. 15–20.
14. Kosyan A. R., Antipushkina Zh. A. Determination of *Rapana venosa* individuals' ages based on the $\delta^{18}\text{O}$ dynamics of the shell carbonates. *Oceanology*, 2011, vol. 51, no. 6, pp. 1021–1028. <http://dx.doi.org/10.1134/S0001437011060075>
15. Kosyan A. R. Comparative analysis of *Rapana venosa* (Valenciennes, 1846) from different biotopes of the Black Sea based on its morphological characteristics. *Oceanology*, 2013, vol. 53, no. 1, pp. 47–53. <https://doi.org/10.1134/S0001437013010074>
16. SigmaPlot 15.0 : [site]. 2023. URL: <https://sigmaplot.software.informer.com/15.0> [accessed: 07.04.2023].
17. Slynko E. E., Slynko Y. V., Rabushko V. I. Adaptive strategy of *Rapana venosa* (Gastropoda, Muricidae) in the invasive population of the Black Sea. *Biosystems Diversity*, 2020, vol. 28, no. 1, pp. 48–52. <https://doi.org/10.15421/012008>
18. Vasconcelos P., Gharsallah I. H., Moura P., Zamouri-Langar N., Gaamour A., Misraoui H., Jarboui O., Gaspar M. B. Appraisal of the usefulness of operculum growth marks for ageing *Hexaplex trunculus* (Gastropoda: Muricidae): Comparison between surface striae and adventitious layers. *Marine Biology Research*, 2012, vol. 8, iss. 2, pp. 141–153. <https://doi.org/10.1080/17451000.2011.616896>
19. Xue D. X., Graves J., Carranza A., Sylantyev S., Snigirov S., Zhang T., Liu J.-X. Successful worldwide invasion of the veined rapa whelk, *Rapana venosa*, despite a dramatic genetic bottleneck. *Biological Invasions*, 2018, vol. 20, pp. 3297–3314. <https://doi.org/10.1007/s10530-018-1774-4>

**ФУНКЦИОНАЛЬНАЯ МОРФОЛОГИЯ
И МОРФОЛОГИЧЕСКАЯ ИЗМЕНЧИВОСТЬ
ОПЕРКУЛУМА *RAPANA VENOSA* (GASTROPODA, MURICIDAE)**

И. П. Бондарев

ФГБУН ФИЦ «Институт биологии южных морей имени А. О. Ковалевского РАН»,
Севастополь, Российская Федерация
E-mail: igor.p.bondarev@gmail.com

Брюхоногий моллюск *Rapana venosa* распространился из западной части Тихого океана в Чёрное и Средиземное моря и прибрежные районы по обе стороны Атлантического океана во многом благодаря своей экологической и морфологической пластичности. Исследованию вариативности раковины рапаны посвящены многочисленные работы. Функциональная морфология и морфологическая изменчивость оперкулула *R. venosa* изучены недостаточно, описание этого экзосоматического органа приводится только схематично. На основе анализа выборки из 190 экз. *R. venosa*, собранных в двух районах Чёрного моря, дано детальное описание и показаны тренды морфологической изменчивости оперкулула в зависимости от возраста и размера особей. Оценены характеристики, определяющие нормальное и aberrantное развитие

оперкула. Впервые показано, что *R. venosa* имеет регенеративные возможности, вплоть до восстановления утраченной крышечки, и морфогенетический адаптационный потенциал оперкула. Проявлением такого потенциала является формирование гипертрофированно крупной крышечки, форма которой не характерна ни для одного другого вида мурицид и гастропод в целом. Аномальный размер и форма крышечки, вероятно, являются защитной реакцией на давление хищников, прежде всего крабов. Ранее неизвестная способность регенерировать оперкулум расширяет представления о физиологических возможностях рапаны. Феномен формирования крышечки уникальной среди гастропод формы — ещё одно проявление морфологической пластичности, позволившей *R. venosa* занять место среди наиболее успешных видов-вселенцев в современной морской среде.

Ключевые слова: вариабельность, крышечка, морфология, регенерация, *Rapana venosa*

UDC [599.5:502.172](268.45.04)

MARINE MAMMALS OF THE KOLA BAY, BARENTS SEA

© 2023 A. A. Zaytsev, A. R. Troshichev, M. V. Pakhomov, and A. P. Yakovlev

Murmansk Marine Biological Institute of the Russian Academy of Sciences, Murmansk, Russian Federation

E-mail: yanmos@yandex.ru

Received by the Editor 24.02.2022; after reviewing 24.06.2022;
accepted for publication 04.08.2023; published online 01.12.2023.

Despite the fact that publications focused on marine mammals of the Barents Sea are quite numerous, relevant data on their habitat in the Kola Bay area are scarce. The latest work detailing this aspect dates back to 1997. At the same time, protected species of marine mammals (listed in the Red Data Book of the Russian Federation) occur in the bay waters. With the progressive implementation of the Integrated Development of the Murmansk Transport Hub project, the anthropogenic load on the Kola Bay water area may increase multifold. Therefore, research on marine mammals occurring in its waters becomes more and more relevant. This paper provides an updated list of marine mammals registered in the Kola Bay, which is compiled on the basis of published data and observations of the authors.

Keywords: Kola Bay, Barents Sea, marine mammals, protected species

In the Kola Bay, Russia's northernmost ice-free seaport is located, as well as the region's largest naval and industrial complexes. The port of Murmansk is the base of the nuclear-powered icebreaker fleet. The Northern Sea Route starts there. However, the intensity of shipping in this area is relatively low [Serova, 2018], but the situation may change over time due to growing interest in the Arctic region. Within the framework of the Integrated Development of the Murmansk Transport Hub project, it is planned to construct a year-round maritime transport hub based on the port of Murmansk. The implementation requires dredging, reconstruction and modernization of the existing port infrastructure on the Kola Bay eastern coast, and construction of an oil terminal and a coal transshipment complex on its western coast [Skufyina, Serova, 2017]. To date, the Lavna coal terminal is under intensive construction, and bored piles for future pouring stations are being installed. A diving study of the seabed is carried out with the removal of foreign objects. Backfilling with rocky soil is underway. The slope has been strengthened with large stones [Chekunkov, 2022]. The center for the construction of large-capacity offshore structures, built in the Belokamenka village, is a key facility for the industry being created in Russia – the production of LNG equipment. This center consists of five main sectors: the site for gravity-based structures, *inter alia* two dry docks; the topsides site; marine infrastructure facilities; engineering support facilities; and a residential complex and administrative facilities [LNG Construction Center, 2022].

All the above suggests as follows: over time, the anthropogenic load on the Kola Bay water area and, accordingly, on its biota will definitely increase. Despite the fact that studies of the bay have more than a century-old history, publications focused on marine mammals occurring in its waters

are scarce [Deryugin, 1915; Pleske, 1887; Smirnov, 1903; Zyryanov, Egorov, 2010]. The only relatively modern work providing a description of the marine mammal species recorded in the Kola Bay is the monograph [Goryaev, 1997]. This situation is mostly due to the lack of fishing for marine mammals in this area and due to the sporadic nature of their occurrence.

The anthropogenic load observed and little research into the issue indicate the need for regular study of marine mammals in the Kola Bay. This is especially true for species listed in the Red Book of the Russian Federation and in the IUCN (International Union for Conservation of Nature) Red List.

MATERIAL AND METHODS

Murmansk Marine Biological Institute of the RAS (MMBI RAS) has at its disposal two biotechnical aquatic complexes located on the Kola Bay coast – in the vicinity of Gadzhievo and Polyarny towns. There, the staff of the institute conducts year-round research on true seals. The availability of motor boats and the access to the bay made it possible to observe wild marine mammals both in nearby and relatively distant sites of the water area. In 2011, we made the first attempts to carry out the research, and in 2018, the observations became systematic. The results presented in this paper were obtained in 2011–2021. The study areas were predominantly the northern and central Kola Bay, where marine mammals are most often recorded. Animals were registered from the shore and during route observations. From the shore, as a rule, marine mammals were noted accidentally – during research unrelated to the surveys. Route observations were carried out in two directions – from Cape Tonya to Toros Island and from Cape Tonya to Salny Island (Fig. 1). Due to weather conditions and limited navigation of small vessels in the Kola Bay during the polar night, the surveys at this time were not strictly periodic.

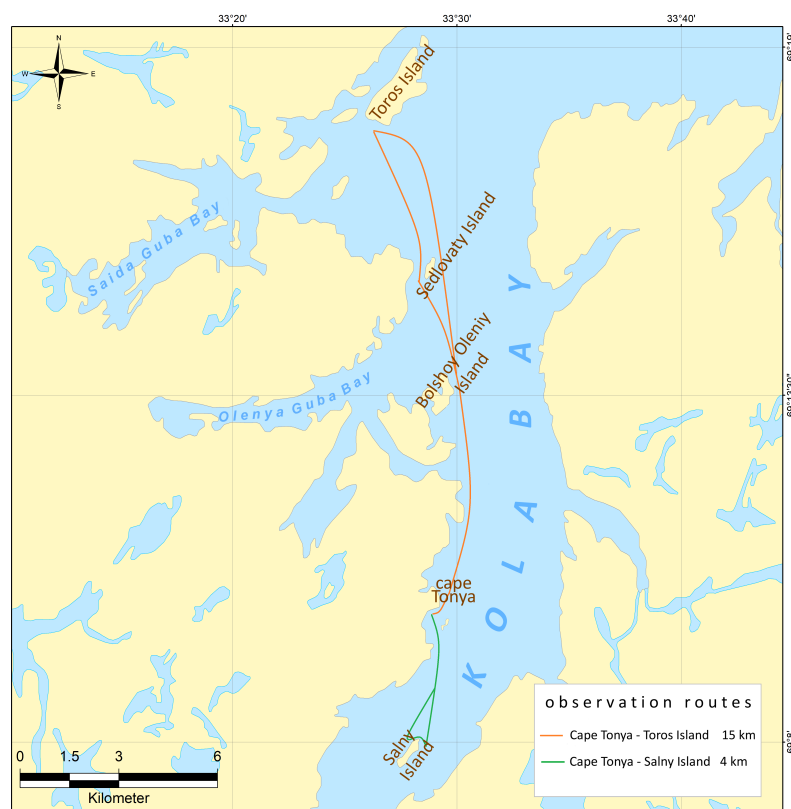


Fig. 1. Scheme of observation routes

RESULTS AND DISCUSSION

Literature data and our observations [Deryugin, 1915; Goryaev, 1997; Pleske, 1887; Smirnov, 1903; Tomilin, 1957, 1962; Zaytsev et al., 2018; Zyryanov, Egorov, 2010] evidence for the following: in the waters of the Kola Bay and the adjacent area, 14 species of marine mammals belonging to five families can be recorded.

1. Oceanic dolphins Delphinidae Gray, 1821 (order Cetacea Brisson, 1762, suborder Odontoceti Flower, 1867). Two species – the white-beaked dolphin *Lagenorhynchus albirostris* (Gray, 1846) and the killer whale *Orcinus orca* (Linnaeus, 1758).
2. Porpoises Phocoenidae Gray, 1825 (order Cetacea, suborder Odontoceti). One species – the harbor porpoise *Phocoena phocoena* (Linnaeus, 1758).
3. Monodontidae Gray, 1821 (order Cetacea, suborder Odontoceti). One species – the beluga whale *Delphinapterus leucas* (Pallas, 1776).
4. Rorquals Balaenopteridae Gray, 1864 (order Cetacea, suborder Mysticeti Flower, 1864). Five species – the humpback whale *Megaptera novaeangliae* (Borowski, 1781), the fin whale *Balaenoptera physalus* (Linnaeus, 1758), the sei whale *Balaenoptera borealis* (Lesson, 1828), the blue whale *Balaenoptera musculus* (Linnaeus, 1758), and the common minke whale *Balaenoptera acutorostrata* (Lacépède, 1804).
5. True seals Phocidae Gray, 1825 (order Carnivora Bowdich, 1821, suborder Caniformia Kretzoi, 1938). Five species – the harbor seal *Phoca vitulina* (Linnaeus, 1758), the grey seal *Halichoerus grypus* (Fabricius, 1791), the harp seal *Pagophilus groenlandicus* (Erxleben, 1777), the ringed seal *Pusa hispida* (Schreber, 1775), and the bearded seal *Erignathus barbatus* (Erxleben, 1777).

Out of the species above, only seven were registered during our surveys.

Delphinidae. The white-beaked dolphin is the northernmost representative of its genus [Kinze, 2018] and one out of two species of the genus found in the Barents Sea [Kovacs et al., 2009]. It is the most frequently recorded native cetacean (Fig. 2) [Fall, Skern-Mauritzen, 2014; Goryaev, 2017; Klepikovskiy et al., 2012]. This marine mammal inhabits temperate and subarctic waters of the North Atlantic and is recorded in both shelf and coastal water areas [Kinze, 2018]. It is listed in the Red Data Book of the Russian Federation as a rare, vulnerable species [Perechen' ob"ektov zhivotnogo mira, 2020].

In the Kola Bay, white-beaked dolphins are found irregularly. In 2011–2017, these animals were registered only during the summer–autumn period [Zaytsev et al., 2018]; in 2018–2021, they were not recorded at all. Until 2018, there was no mention of this species in the Kola Bay in the literature.



Fig. 2. White-beaked dolphins in the Kola Bay, 15.09.2011 (photo by I. Gabay)

The population status of the killer whale in the Barents Sea has not been sufficiently studied, which is primarily due to the sporadic nature of its appearance [Aars et al., 2016; Kovacs et al., 2009]. There are references to the fact that the killer whale is a common species in the Kola Bay and can be observed in Kildin Island vicinity [Deryugin, 1915; Goryaev, 1997]. Over the entire period of our research, we were unable to confirm the entry of this marine mammal into the bay waters: all reports that killer whales occur in local areas turned out to be false. Most often, other representatives of this family or common minke whales were mistaken for them.

Phocoenidae. The harbor porpoise is one of the smallest cetacean species in the Barents Sea (Fig. 3), inhabiting mainly coastal waters [Aars et al., 2016; Bjørge, Tolley, 2018; Kovacs et al., 2009]. The geography of its distribution is quite wide and covers waters from the equator to the Arctic [Lockyer, 2003]. The Barents Sea is inhabited by the North Atlantic subspecies *P. p. phocoena* (Linnaeus, 1758).

The harbor porpoise, along with the common minke whale, is the most frequently encountered cetacean in the Kola Bay [Goryaev, 1997]. Its mass entries are often related to abundance of food items (with no pronounced seasonal periodicity) [Deryugin, 1915; Goryaev, 1997; Tomilin, 1957]. Our surveys show a picture similar to that from the literature data: in different years, animals are found in various seasons (Table 1).



Fig. 3. The harbor porpoise in the Kola Bay, 12.07.2018 (photo by A. Troshichev)

Monodontidae. The distribution of the beluga whale in the Barents Sea has a pronounced seasonality closely related to changes in ice conditions throughout the year [Matishov, Ognetrov, 2006; Ognetrov et al., 2003]. In the literature, there is a reference on beluga whales entering the Kola Bay in summer months [Goryaev, 1997]. However, during our observations, we did not register this species in the bay water area.

Balaenopteridae. Representatives of this family tend to occur in the Barents Sea waters during summer feeding. At the same time, some species can stay there for wintering [Aars et al., 2016; Tomilin, 1962]. The most frequently observed species are the common minke whale, the fin whale, and the humpback whale [Aars et al., 2016; Skern-Mauritzen et al., 2011]. The fin whale and the humpback whale prefer open waters and are found in the western, central, and northern Barents Sea, while the common minke whale can usually be observed in coastal areas [Aars et al., 2016; Burdin et al., 2009; Marine Mammals, 2017]. In the Barents Sea, the fin whale is represented by the northern subspecies *B. p. physalus* (Linnaeus, 1758). It is listed in the Red Data Book of the Russian Federation as a species of uncertain status [Perechen' ob'ektov zhivotnogo mira, 2020] and in the IUCN Red List, as vulnerable (VU) [Cooke, 2018a]. The humpback whale is listed in the Red Data Book of the Russian Federation

as recovering [Perechen' ob'ektov zhivotnogo mira, 2020], and in the IUCN Red List, as a species of least concern (LC) [Cooke, 2018b]. The only mention in the literature we have come across on the entry of humpback whales into the Kola Bay is the publication of Yu. Goryaev [1997] with reference to L. Breitfuss (1903). Also, in the work on the Kola Bay fauna and the conditions of its existence, K. Deryugin [1915] highlights the probability of this species entering the water area. Moreover, there are references to the fact as follows: in the Murman coastal area and in the Kola Bay, the sei whale and the blue whale, which are rarer for the Barents Sea, can be encountered [Deryugin, 1915; Goryaev, 1997; Pleske, 1887].

Table 1. The results of the registration of marine mammals when following the route Cape Tonya – Toros Island – Cape Tonya

| Date | Time of the route | <i>Balaenoptera acutorostrata</i> | <i>Phocoena phocoena</i> | <i>Halichoerus grypus</i> |
|------------|-----------------------------|--|---|---|
| 12.07.2018 | 17:00–18:00, 20:30–22:20 | Northwest of Sedlovaty Island, 1 individual | Northwest of Sedlovaty Island, 10–15 individuals | In the water near Sedlovaty Island, 1 individual |
| 21.07.2018 | 20:00–21:00, 22:00–23:00 | – | – | – |
| 16.08.2018 | 17:00–18:00, 18:00–19:00 | – | – | In the water near Bolshoy Oleny Island, 1 individual |
| 08.09.2019 | 13:35–14:55, 15:00–16:00 | North of Bolshoy Oleny Island, 1 individual | Northeast of Cape Tonya, 15 individuals | Northeast of Bolshoy Oleny Island, 1 individual |
| 14.06.2020 | 21:00–22:00, 23:00–00:10 | – | – | Northeast of Sedlovaty Island, 1 individual; Devkina Pozhny Bay, 1 individual |

During our surveys, only two species representing this family were registered – the common minke whale and the humpback whale. Interestingly, the common minke whale is the only species of baleen whales which regularly occurs in the bay (Table 1). As for the humpback whale (Fig. 4), we observed its appearance near Shurinov Island of the Kola Bay in March 2016.



Fig. 4. The humpback whale in the Kola Bay, 01.03.2016 (photo by A. Troshichev)

Phocidae. The harbor seal is one of the most common pinnipeds in coastal waters [Burdin et al., 2009; Teilmann, Galatius, 2018]. In Russia, it is a protected species [Zyryanov, Kavtsevich, 2014]. The Barents Sea is inhabited by the Atlantic subspecies of the harbor seal *P. v. vitulina* (Linnaeus, 1758) [Berta, Churchill, 2012]. On the Kola Peninsula coast, harbor seals are encountered in the area from Varangerfjord in the west to the Ivanovskaya Bay in the east [Zyryanov, Egorov, 2010].

In the Kola Bay, the harbor seal is registered mainly in spring in its northern water area – in the Pala, Olenya, and Sayda bays, as well as in the Ekaterininskaya Harbor [Zyryanov, Egorov, 2010]. During our observations, not a single individual of this species was reliably identified.

The grey seal, the same as the harbor seal, is a coastal species, but it spends more time away from the coast [Aars et al., 2016]. The Barents Sea is inhabited by the Atlantic subspecies of the grey seal *H. g. atlantica* (Nehring, 1866) [Berta, Churchill, 2012; Olsen et al., 2016], listed in the Red Data Book of the Murmansk region as a rare species [Kavtsevich, Erokhina, 2014]. This marine mammal is registered throughout the Barents Sea coast of the Kola Peninsula [Vishnevskaya et al., 1990].

For the Kola Bay, only single cases of this species encounter are described [Goryaev, 1997]. According to the results of our surveys, the grey seal is the most common pinniped for this area. Its massive aggregations were observed on the northern tip of Salny Island and in the northeast of Domashny Island; the abundance of simultaneously registered individuals sometimes exceeds 30. For the first time, the grey seal haulout on Salny Island was recorded in autumn 2011 (Table 2). Mass haulouts are registered only in the autumn–winter period (in the northern and central Kola Bay), and single encounters occur year-round (Fig. 5).



Fig. 5. Grey seals in the Kola Bay (photo by A. Troshichev)

The harp seal, the ringed seal, and the bearded seal are pagophilic species, *i. e.*, these animals prefer to live on ice. That is why their distribution in the Barents Sea has a pronounced seasonality (with a reference to ice conditions) [Ognetov et al., 2003; Svetochev, Svetocheva, 2018].

Usually, the appearance of harp seals near the Murmansk coast occurs during their migration from the White Sea to summer feeding grounds and back [Svetochev, Svetocheva, 2018]. In the literature, there are reports of many harp seals entering the Kola Bay – with the abundance of registered individuals exceeding 500 [Goryaev, 1997]. During our observations, not a single harp seal was reliably identified.

Table 2. Observations of the grey seal haulout on Salny Island

| Year | Date | Time | Abundance of individuals | Note |
|-------|-------|--------------|--|---|
| 2011 | 01.06 | 13:30 | 0 | |
| | 17.11 | 14:10, 15:10 | 11 | Footprints of seals were noted in the snow above the high tide |
| 2018 | 18.04 | 15:00 | 1 | The grey seal lied on a rock in the littoral zone |
| | 02.05 | 15:30 | 2 | One individual in the water, and another one in the littoral |
| | 12.07 | 16:15 | 0 | |
| | 21.07 | 04:10 | 0 | |
| | 16.08 | 14:30 | 0 | |
| | 09.10 | 13:50 | 0 | |
| | 11.10 | 12:50 | 2 | Both animals were in the water |
| | 14.10 | 12:00 | 1 | In the water |
| | 09.11 | 13:00 | 2 | One individual in the water, and another one in the littoral |
| 14.11 | 12:00 | 1 | In the water | |
| 2019 | 27.02 | 11:00 | 10 | Nine individuals on the coast, and one individual in the water |
| | 10.04 | 13:40 | 0 | There were no footprints on fresh snow |
| | 26.04 | 13:40 | 0 | |
| | 24.05 | 19:40 | 0 | |
| | 03.09 | 17:00 | 0 | |
| | 08.09 | 11:00 | 2 | In Pitkov Bay (2 km west of Salny Island), 6–7 grey seals were observed |
| | 24.10 | 11:40 | 10 | All seals were in the water near the coast |
| | 12.11 | 14:30 | 20 | There were 15 seals on the coast and 5 in the littoral zone |
| 22.11 | 11:00 | 40 | About 30 seals were on the coast, in the littoral zone, and a few more seals were in the water | |
| 2020 | 09.02 | 11:20 | 30 | Most of the animals were on the coast |
| | 26.08 | 12:40 | 5 | One seal was seen 1–1.5 km north of Salny Island, and four more were registered in Pitkov Bay |
| | 07.11 | 12:30 | 2 | Two individuals in the water |
| | 11.11 | 11:20 | 4 | In the water |
| 2021 | 18.02 | 13:30 | 20 | All seals were in the water |

Unlike harp seals, bearded seals and ringed seals do not form mass aggregations in the Barents Sea. These marine mammals are recorded throughout the Murmansk coast (mostly single individuals), and they can enter river estuaries and lower reaches [Aars et al., 2016; Ognetrov et al., 2003]. Both species are found in the Kola Bay, but the nature of the encounters is sporadic. There are references to the fact that ringed seals occur at the estuaries of the Tuloma and Kola rivers [Goryaev, 1997].

During our surveys, the bearded seal was encountered twice, both times in summer. Both times, this marine mammal was noted on the outer parts of the cage of MMBI aquatic complex and was at the stage of molting.

We recorded the ringed seal twice in the Sayda Bay. Moreover, according to photographic evidence from eyewitnesses, single individuals lay on the ice at the estuaries of the Tuloma and Kola rivers.

Although the species composition of marine mammals in the Kola Bay is quite diverse [Goryaev, 1997], the species that occur there either regularly or permanently are not as abundant as the species inhabiting the open areas of the Barents Sea. Out of them, there are previously mentioned

animals – the common minke whale, the harbor porpoise, and the grey seal. Most marine mammals enter this water area searching for food; the exception is some pinnipeds which arrange seasonal haulouts there. Comparing the results of our observations and the literature data, we can conclude as follows: over the past two decades, the species composition of marine mammals in the Kola Bay has undergone certain changes, primarily concerning pinnipeds (Table 3). During the entire period of our surveys, the harbor seal, the harp seal, and the beluga whale were not encountered, although in 1996 these species were considered common for the Kola Bay [Goryaev, 1997].

Table 3. Comparison of the species composition of marine mammals recorded during observations and indicated in the literature

| Species | Mentioned in the literature | Recorded during observations in 1996. [Goryaev, 1997] | Recorded during observations in 2011–2021 |
|--|-----------------------------|---|---|
| White-beaked dolphin <i>L. albirostris</i> | – | – | + |
| Killer whale <i>O. orca</i> | + | – | – |
| Harbor porpoise <i>P. phocoena</i> | + | + | + |
| Beluga whale <i>D. leucas</i> | + | + | – |
| Humpback whale <i>M. novaeangliae</i> | + | – | + |
| Fin whale <i>B. physalus</i> | + | – | – |
| Sei whale <i>B. borealis</i> | + | – | – |
| Blue whale <i>B. musculus</i> | + | – | – |
| Common minke whale <i>B. acutorostrata</i> | + | + | + |
| Harbor seal <i>P. vitulina</i> | + | + | – |
| Grey seal <i>H. grypus</i> | + | + | + |
| Harp seal <i>P. groenlandicus</i> | + | + | – |
| Ringed seal <i>P. hispida</i> | + | – | + |
| Bearded seal <i>E. barbatus</i> | + | + | + |

The Kola Bay ichthyofauna includes species that serve as food items for many marine mammals. Out of them, there are juveniles of the Atlantic cod *Gadus morhua* Linnaeus, 1758, the haddock *Melanogrammus aeglefinus* (Linnaeus, 1758), and the Atlantic herring *Clupea harengus* Linnaeus, 1758 which sometimes occurs en masse [Karamushko, 2009]. As noted, during periods of a mass herring migration, there is an increase in encounters of marine mammals. An example is the observation of white-beaked dolphins in the bay waters in 2011: the occurrence of these animals coincided with reports of a mass herring migration. During that period, common minke whales were also observed several times [Zaytsev et al., 2018].

The occurrence of various marine mammals in the Kola Bay waters depends not only on changes in their food supply, but also on environmental processes in other areas of the Barents Sea. Specifically, the regularity of white-beaked dolphins entering the bay in 2011–2017 could result from changes in the distribution of their food items and their pursuit of alternative prey species [Aars et al., 2016]. An increase in the number of observations of the grey seal and its regular seasonal haulouts on Salny Island indicate the restoration of its population in the Barents Sea. This assumption can be supported by the highlights in the work of K. Deryugin [1915] that rich seal haulouts were recorded on Salny Island earlier.

Conclusion. Despite the increasing anthropogenic load, marine mammals continue to enter the Kola Bay waters, *inter alia* during their feeding. Over the past two decades, the occurrence and species composition of coastal marine mammal (primarily pinnipeds) have obviously changed. An increase in the abundance of a predator, the grey seal whose diet may include birds and mammals, can result in serious faunal changes in the coastal areas of the Kola Bay and the entire Barents Sea. In this regard, the relevance of research aimed at monitoring the state of coastal populations of marine mammals on the Barents Sea coast of the Kola Peninsula increases.

The work was carried out within the framework of the state research assignment "Ecology and physiology of marine mammals of the Arctic seas" [no. 121091600101-6 (16.09.2021), FMEE-2021-0009].

REFERENCES

- Burdin A. M., Filatova O. A., Hoyt E. *Marine Mammals of Russia : a guidebook*. Kirov : Volgo-Vyatskoye Publishing House, 2009, [215] p. (in Russ.)
- Vishnevskaya T. Yu., Bychkov V. A., Konkakov A. A., Mishin V. L. *Grey Seal. Biology and Present Status of Populations*. Apatity : Kol'skii nauchnyi tsentr AN SSSR, 1990, 48 p. (Preprint. Okhrana prirody / Kol'skii nauchnyi tsentr AN SSSR). (in Russ.)
- Goryaev Yu. I. Morskije mlekoopitayushchie. In: *Kol'skii zaliv: okeanografiya, biologiya, ekosistemy, pollyutanty* / G. G. Matishov (Ed.). Apatity : Kol'skii nauchnyi tsentr RAN, 1997, pp. 155–160. (in Russ.)
- Goryaev Yu. I. Distribution of marine mammals in the Barents Sea in April and May 2016. *Trudy Kol'skogo nauchnogo tsentra RAN*, 2017, vol. 8, no. 2–4, pp. 88–95. (in Russ.)
- Deryugin K. M. *Fauna Kol'skogo zaliva i usloviya ee sushchestvovaniya*. Petrograd : Tipografiya Imperatorskoi akademii nauk, 1915, 929 p. (Zapiski Imperatorskoi akademii nauk, series 8, 1915, vol. 34, no. 1). (in Russ.)
- Zyryanov S. V., Kavtsevich N. N. Obyknoventsi tyulen' *Phoca vitulina* Linnaeus, 1758 (barentsevomorskaya populyatsiya). In: *Red Data Book of the Murmansk Region*. Kemerovo : Asia-print, 2014, pp. 565–566. (in Russ.)
- Kavtsevich N. N., Erokhina I. A. Seryi tyulen' atlanticheskii *Halichoerus grypus* Fabricius, 1791. In: *Red Data Book of the Murmansk Region*. Kemerovo : Asia-print, 2014, pp. 566–567. (in Russ.)
- Karamushko O. V. Ikhtiofauna zaliva. In: *Kol'skii zaliv: osvoenie i ratsional'noe prirodopol'zovanie* / G. G. Matishov (Ed.). Moscow : Nauka, 2009, pp. 249–264. (in Russ.)
- Klepikovskiy R. N., Lukin N. N., Mishin T. V. Observation of marine mammals in the south of the Barents Sea in May–June, 2011. In: *Marine Mammals of the Holarctic : collection of scientific papers after the seventh international conference*. Moscow : Marine Mammal Council, 2012, vol. 1, pp. 303–306. (in Russ.)
- Matishov G. G., Ognetrov G. N. *White Whale Delphinapterus leucas of the Russia Arctic Seas*. Apatity : Kol'skii nauchnyi tsentr RAN, 2006, 295 p. (in Russ.)
- Marine Mammals. Russian Arctic and Far East : atlas*. Moscow : Arctic Scientific Center, 2017, pp. 91–108. (in Russ.)
- Ognetrov G. N., Matishov G. G., Vorontsov A. V. *Ring Seal of the Russia Arctic Seas* / N. N. Kavtsevich (Ed.). Murmansk : MIP-999, 2003, 38 p. (in Russ.)
- Perechen' ob'ektov zhivotnogo mira, zanesennykh v Krasnuyu knigu Rossiiskoi Federatsii*. Prilozhenie k prikazu Ministerstva prirodnykh resursov i ekologii Rossiiskoi

- Federatsii ot 24.03.2020 No. 162 “Ob utverzhenii Perechnya ob”ektov zhivotnogo mira, zanesennykh v Krasnyuyu knigu Rossiiskoi Federatsii”. Opublikovan 02.04.2020 na ofitsial’nom internet-portale pravovoi informatsii <http://www.pravo.gov.ru>. (in Russ.)
14. Pleske F. D. *Kriticheskii obzor mlekopitayushchikh i ptits Kol’skogo poluoostrova*. Saint Petersburg : Tipografiya Imperatorskoi akademii nauk, 1887, 536 p. (in Russ.)
 15. Svetochev V. N., Svetocheva O. N. *The Harp Seal: Biology, Ecology, Harvesting* / N. N. Kavtsevich (Ed.). Apatity : Murmanskii morskoi biologicheskii institut KNTs RAN, 2018, 174 p. (in Russ.)
 16. Serova N. A. The role of the Murmansk transport hub in the development of the Arctic zone of the Russian Federation. *Vestnik Kol’skogo nauchnogo tsentra RAN*, 2018, vol. 10, no. 2, pp. 123–127. (in Russ.). <https://doi.org/10.25702/KSC.2307-5228.2018.10.2.123-127>
 17. Skufyina T. P., Serova N. A. Aktual’nye aspekty razvitiya Murmanskogo transportnogo uzla. *Transport Rossiiskoi Federatsii*, 2017, no. 5 (72), pp. 19–22. (in Russ.)
 18. Smirnov N. A. *O morskoy zverinoy promysle na russkikh sudakh : otchet po komandirovкам Nestora Smirnova* / Komitet dlya pomoshchi pomoram Russkogo Severa. Ekspeditsiya dlya nauchno-promyslovykh issledovaniy u beregov Murmana. Saint Petersburg : Tipo-lit. I. Usmanova, 1903, pp. 128–153. (in Russ.)
 19. Tomilin A. G. Kitoobraznye. In: *Zveri SSSR i prilozhashchikh stran* / V. G. Geptner (Ed.). Moscow : AN SSSR, 1957, vol. 9, pp. 756. (in Russ.)
 20. Tomilin A. G. *Kitoobraznye fauny morei SSSR : spravochnoe izdanie* / E. N. Pavlovsky (Ed.). Moscow : AN SSSR, 1962, 211 p. (in Russ.)
 21. LNG Construction Center. The world’s first facility for “mass production” of natural gas liquefaction trains on gravity-based structures (GBS). In: *NOVATEK* : [site], 2021. (in Russ.). URL: <https://www.novatek.ru/ru/business/cskms/> [accessed: 20.02.2022].
 22. Chekunkov A., glava Minvostokrazvitiya Rossii: “My budem i dal’she podderzhivat’ stroitel’sтво porta “Lavna”, chtoby proekt byl realizovan v polnoi mere”. In: *Pravitel’sтво Murmanskoi oblasti* : [official site]. 2022. (in Russ.). URL: <https://gov-murman.ru/info/news/443536/> [accessed: 18.02.2022].
 23. Aars J., Belikov S., Frie A. K., Kovacs K., Klepikovskiy R., Skern-Mauritzen M., Svetochev V. 4.3.7 Marine mammals. In: *Joint Norwegian–Russian Environmental Status 2013*. Report on the Barents Sea Ecosystem. Part II Complete report / M. M. McBride, J. R. Hansen, O. Korneev, O. Titov (Eds.). Bergen, Norway : IMR, 2016, pp. 212–224. (IMR/PINRO Joint Report Series ; no. 2).
 24. Berta A., Churchill M. Pinniped taxonomy: Review of currently recognized species and subspecies, and evidence used for their description. *Mammal Review*, 2012, vol. 42, iss. 3, pp. 207–234. <https://doi.org/10.1111/j.1365-2907.2011.00193.x>
 25. Bjørge A., Tolley K. A. Harbor porpoise *Phocoena phocoena*. In: *Encyclopedia of Marine Mammals*. 3rd edition / B. Würsig, J. G. M. Thewissen, K. M. Kovacs (Eds.). London ; San Diego, CA ; Cambridge, MA ; Kidlington, Oxford (GB) : Academic Press : Elsevier Inc., 2018, pp. 448–451. <https://doi.org/10.1016/B978-0-12-804327-1.00144-8>
 26. Cooke J. G. *Balaenoptera physalus*. In: *The IUCN Red List of Threatened Species*, 2018a, e.T2478A50349982. <http://dx.doi.org/10.2305/IUCN.UK.2018-2.RLTS.T2478A50349982.en>

27. Cooke J. G. *Megaptera novaeangliae*. In: *The IUCN Red List of Threatened Species*, 2018b, e.T13006A50362794. <http://dx.doi.org/10.2305/IUCN.UK.2018-2.RLTS.T13006A50362794.en>
28. Fall J., Skern-Mauritzen M. White-beaked dolphin distribution and association with prey in the Barents Sea. *Marine Biology Research*, 2014, vol. 10, iss. 4, pp. 957–971. <http://doi.org/10.1080/17451000.2013.872796>
29. Lockyer C. Harbour porpoises (*Phocoena phocoena*) in the North Atlantic: Biological parameters. *NAMMCO Scientific Publications*, 2003, vol. 5, pp. 71–90. <http://dx.doi.org/10.7557/3.2740>
30. Kinze C. C. White-beaked dolphin: *Lagenorhynchus albirostris*. In: *Encyclopedia of Marine Mammals*. 3rd edition / B. Würsig, J. G. M. Thewissen, K. M. Kovacs (Eds). London ; San Diego, CA ; Cambridge, MA ; Kidlington, Oxford (GB) : Academic Press : Elsevier Inc., 2018, pp. 1077–1079.
31. Kovacs K. M., Haug T., Lydersen C. Marine mammals of the Barents Sea. In: *Ecosystem Barents Sea* / E. Sakshaug, G. Johnsen, K. M. Kovacs (Eds). Trondheim, Norway : Tapir Academic Press, 2009, pp. 453–496.
32. Olsen M. T., Galatius A., Biard V., Gregersen K. M., Kinze C. C. The forgotten type specimen of the grey seal [*Halichoerus grypus* (Fabricius, 1791)] from the island of Amager, Denmark. *Zoological Journal of the Linnean Society*, 2016, vol. 178, iss. 3, pp. 713–720. <https://doi.org/10.1111/zoj.12426>
33. Teilmann J., Galatius A. Harbor seal: *Phoca vitulina*. In: *Encyclopedia of Marine Mammals*. 3rd edition / B. Würsig, J. G. M. Thewissen, K. M. Kovacs (Eds). London ; San Diego, CA ; Cambridge, MA ; Kidlington, Oxford (GB) : Academic Press : Elsevier Inc., 2018, pp. 451–455. <https://doi.org/10.1016/B978-0-12-804327-1.00145-X>
34. Skern-Mauritzen M., Johannesen E., Bjørge A., Øien N. Baleen whale distributions and prey associations in the Barents Sea. *Marine Ecology Progress Series*, 2011, vol. 426, pp. 289–301. <https://doi.org/10.3354/meps09027>
35. Zaytsev A. A., Yakovlev A. P., Pakhomov M. V. An observation of *Lagenorhynchus albirostris* (Delphinidae, Odontoceti) in Kola Peninsula, Barents Sea in 2011. *Nature Conservation Research*, 2018, vol. 3, no. 4, pp. 88–90. <https://doi.org/10.24189/ncr.2018.034>
36. Zyryanov S. V., Egorov S. A. Status of the harbour seal (*Phoca vitulina*) along the Murman coast of Russia. *NAMMCO Scientific Publications*, 2010, vol. 8, pp. 37–46. <https://doi.org/10.7557/3.2670>

МОРСКИЕ МЛЕКОПИТАЮЩИЕ КОЛЬСКОГО ЗАЛИВА БАРЕНЦЕВА МОРЯ

А. А. Зайцев, А. Р. Трошичев, М. В. Пахомов, А. П. Яковлев

Мурманский морской биологический институт Российской академии наук,

Мурманск, Российская Федерация

E-mail: yanmos@yandex.ru

Несмотря на то, что публикации, посвящённые морским млекопитающим Баренцева моря, встречаются достаточно часто, актуальные данные об их численности в прибрежных водах Кольского залива довольно скудны. Последняя работа, подробно описывающая этот аспект, датирована 1997 г. В то же время в воды залива заходят в том числе и охраняемые (занесённые

в Красную книгу России) виды морских млекопитающих. Учитывая то, что по мере осуществления проекта «Комплексное развитие Мурманского транспортного узла» антропогенная нагрузка на акваторию Кольского залива и всего мурманского побережья может многократно возрасти, исследования морских млекопитающих, встречающихся в местных водах, приобретают большую актуальность. В работе представлены данные о видовом составе и частоте встречаемости различных видов морских млекопитающих в Кольском заливе, собранные на основе литературных источников и наблюдений авторов.

Ключевые слова: Кольский залив, Баренцево море, морские млекопитающие, охраняемые виды

UDC [581.526.325:574.3](262.5)

SPATIAL AND TEMPORAL DYNAMICS OF THE PHYTOPLANKTON BIOMASS IN THE SURFACE LAYER OF THE BLACK SEA

© 2023 I. V. Kovalyova¹, Z. Z. Finenko¹, and V. V. Suslin²

¹A. O. Kovalevsky Institute of Biology of the Southern Seas of RAS, Sevastopol, Russian Federation

²Marine Hydrophysical Institute of RAS, Sevastopol, Russian Federation

E-mail: ila.82@mail.ru

Received by the Editor 21.07.2021; after reviewing 21.09.2021;
accepted for publication 04.08.2023; published online 01.12.2023.

The spatial and temporal variability of phytoplankton biomass in the surface layer of the Black Sea during an 18-year period is analyzed, and the effect of the main currents in the sea on the spatial and temporal dynamics of phototrophic phytoplankton biomass is assessed. Regular long-term chlorophyll concentration data were used, obtained from satellite observations with SeaWiFS and MODIS-Aqua/Terra instruments in the Black Sea for 1998–2015. The role of macro- and microcirculations in the spatial and temporal variability of phytoplankton biomass is estimated. A gain in wind activity and a drop in water temperature from October to March, which lead to an increase in the depth of the mixed upper layer and the intensity of the main synoptic circulations, become a significant factor promoting winter–spring phytoplankton bloom. As revealed, a decrease in the mean water temperature in the cold season to +7...+8 °C, lasting for more than six weeks in the deepwater zone, leads to the intensive biomass development in spring. It was established that the mean phytoplankton biomass for 18 years in the western and eastern cyclonic cycles is (38.0 ± 17.8) and (37.7 ± 16.8) mg C·m⁻³, respectively, and in the Batumi anticyclone, (38.2 ± 18.0) mg C·m⁻³. As a rule, the Rim Current carries phytoplankton formed at the shelf zone along the coastline and almost does not mix with deep waters. In the cyclonic cycles, winter–spring phytoplankton bloom is observed on average for six weeks. Intensive bloom in the area of the flow of northwestern rivers, recorded in May–June, extends to the Bosphorus, while in the cold season, it can penetrate into the deep-sea area in the form of micro-eddies. In winter and spring, the Sevastopol anticyclonic eddy stood out as a separate zone in terms of biomass development. The role of anthropogenic load is most significant in the coastal zone. However, the effect of coastal waters on the deep-sea area is possible in late autumn and winter.

Keywords: phytoplankton biomass, synoptic circulation, Black Sea, spatial variability of phytoplankton biomass, water temperature, depth of the mixed layer

As known, one of the key indicators of the ecological state of the marine ecosystem is the level of phytoplankton biomass. Its development and variability reflect CO₂ transport from the atmosphere to the ocean, hydrochemical regime of water bodies, and carbon cycle in them. Phytoplankton development is affected by several factors: climate, anthropogenic load, and interaction between autotrophs and heterotrophs. Phytoplankton of the Black Sea is widely studied both in coastal and deep-sea areas [Arashkevich et al., 2015; Berseneva et al., 2004; Finenko et al., 2018, 2019; Mikaelyan, 2018; Mikaelyan et al., 2015]. However, there was no analysis of spatial changes in the biomass of phototrophic plankton throughout the Black Sea. The effect of the main water circulations in the sea surface

layer on the variability of phytoplankton biomass was not considered as well. Vertical convection currents of water masses, seasonal geostrophic circulations, large-scale cyclonic gyres, anticyclonic eddies, and the Rim Current form conditions for rise and transfer of nutrients and, accordingly, for formation, transfer, and localization of phytoplankton biomass in certain sites of the water area. To assess the effect of macrocirculations on the spatial distribution of phytoplankton, regular observations covering large water areas are required. Bio-optical models developed to estimate chlorophyll *a* concentration using satellite data are most convenient for solving this problem. There are various methods for establishing phytoplankton biomass [Eppley et al., 1977; Menden-Deuer, Lessard, 2000]; however, the most common technique is biomass estimation by chlorophyll *a* content. To determine phytoplankton biomass in carbon units, data on chlorophyll *a* concentration, temperature, and light conditions are required; then, chlorophyll–organic carbon ratio is calculated. In algae, this ratio depends on their taxonomic composition, light intensity, and concentration of nutrients [Finenko et al., 2003; Geider, 1987]. In our work, phototrophic phytoplankton biomass was quantified using a previously developed model [Finenko et al., 2018] allowing to calculate changes in the specific content of chlorophyll *a* in algae organic matter in various sea areas for long time series. Analysis of the spatial and long-term dynamics of phytoplankton biomass will help in assessing the effect of local and global, natural and anthropogenic factors on its variability.

The aim of the work is to analyze the spatial and temporal variability of phytoplankton biomass in the surface layer of the Black Sea over an 18-year period and assess the effect of main sea currents on the spatial and temporal dynamics of phototrophic phytoplankton biomass.

MATERIAL AND METHODS

Chlorophyll *a* concentration was calculated from satellite observations for the entire Black Sea water area for the period of 1998–2015. To estimate chlorophyll content, we applied an algorithm that was developed for the Black Sea with the inclusion of the sea brightness coefficient in three spectral channels [Suslin, Churilova, 2016]. Second-level data were obtained using the SeaWiFS (1998–2010) and MODIS-Aqua/Terra (2000–2015) instruments. The measurements were carried out on a spatial grid of 0.025° in latitude and 0.035° in longitude and averaged over a two-week period for the entire sea surface. The mean relative error in retrieving chlorophyll concentration applying the specified algorithm for the deepwater area of the Black Sea according to MODIS-Aqua/Terra and SeaWiFS data was 40% [Suslin et al., 2018].

To calculate phytoplankton biomass, we used our model developed earlier; it is based on the relationship between light absorption in the visible area of the spectrum and the specific content of chlorophyll *a* in ten species of marine planktonic algae representing different taxonomic groups [Finenko et al., 2018]. This model includes the following parameters: chlorophyll *a* concentration, intensity of solar radiation reaching the sea surface, and light absorption by algae. Phytoplankton biomass (*B*) in organic carbon units ($\text{mg C}\cdot\text{m}^{-3}$) was calculated by the equation:

$$B = \text{Chl}_0 / \text{Chl} : C,$$

where Chl_0 is chlorophyll *a* concentration in the surface layer obtained from satellite data averaged over a two-week period (1998–2015) ($\text{mg}\cdot\text{m}^{-3}$);

$\text{Chl} : C$ is chlorophyll–organic carbon ratio in algae.

To estimate the thickness of the upper quasi-homogeneous layer and the depth of the upper mixed layer, the model from [Dorofeev, Sukhikh, 2017] was used.

The depth of the zone of photosynthesis was determined by a model including the vertical light attenuation at a wavelength of 490 nm [Suslin et al., 2017].

Values of temperature in the surface layer and intensity of photosynthetically active radiation within the range of 400–700 nm were acquired from satellite observations obtained from second-level standard satellite products: SeaWiFS for 1998–1999 (<http://podaac.jpl.nasa.gov/sst/>) and MODIS-Aqua/Terra for 2000–2015 (<https://oceancolor.gsfc.nasa.gov/>).

RESULTS AND DISCUSSION

Spatial variability of seasonal and interannual dynamics of phytoplankton biomass in the deepwater area of the Black Sea. Analysis of the long-term seasonal dynamics of biomass in the deep-sea area in 1998–2015 revealed two main, as a rule, periods of its increase: in late November–February and in mid-spring. Spatial variability of the biomass of the Black Sea phytoplankton throughout the year is presented using data from 2009 as an example (Fig. 1).

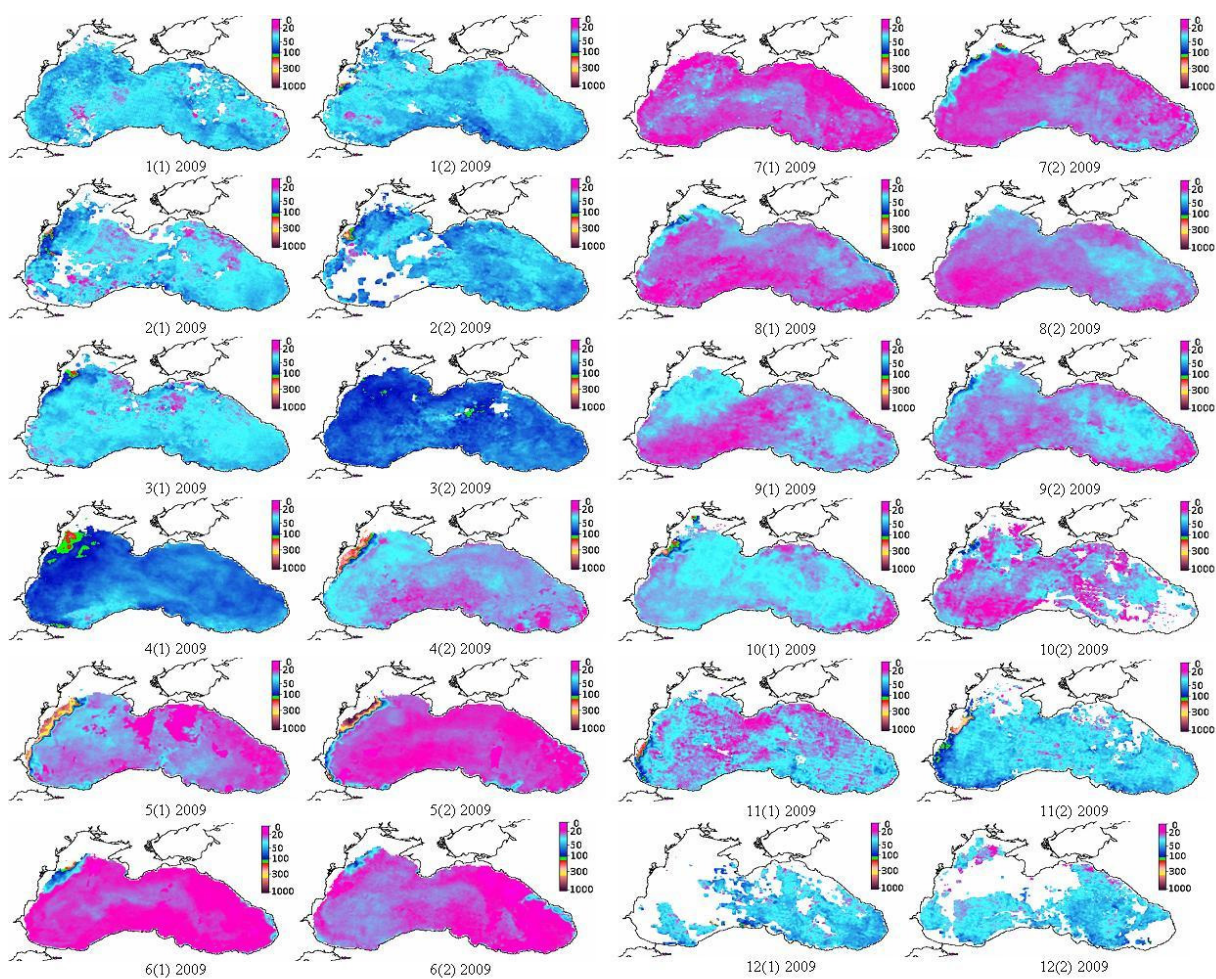


Fig. 1. Seasonal variability of phytoplankton biomass ($\text{mg C}\cdot\text{m}^{-3}$) during 2009 every first and second half of the month in the Black Sea water area

Usually, biomass values begin to increase in late October–November, and local spots of phytoplankton are observed throughout the sea. The period of wind effect in late October and November, when the depth of the mixed layer rises to 19–23 m, precedes the winter increase in phytoplankton biomass. During these months, a mosaic distribution of phytoplankton biomass values was noted almost throughout the entire sea, resulting from both macro- and microcirculations and varying in most years within the range of 20–70 $\text{mg C}\cdot\text{m}^{-3}$ (Figs 1, 2). An important role in the spatial distribution of phytoplankton in autumn and winter is played by the western coastal zone, from which a significant part of its biomass is transferred to the deep-sea area. The wind regime creates turbulent micro-eddies and meanders in the surface layer and transfers them in space. During the cold period, the effect of coastal sea areas on deepwater ones is most pronounced (Figs 1, 2). The water temperature in the surface layer in October–December remains relatively high compared to the temperature at depth, and the thermocline is not completely destroyed; therefore, the involvement of nutrient-rich water masses in the convection current and their entry into the euphotic layer are minor. For this reason, there is no significant increase in biomass up to December. By late December–January, convection in the surface layer, according to calculated data of satellite measurements, covers depths approximately down to 25–28 m. In December and January, the field of biomass becomes almost homogeneous throughout the sea (Fig. 2). Usually, the maximum phytoplankton biomass is recorded in January; less often, in December or February.

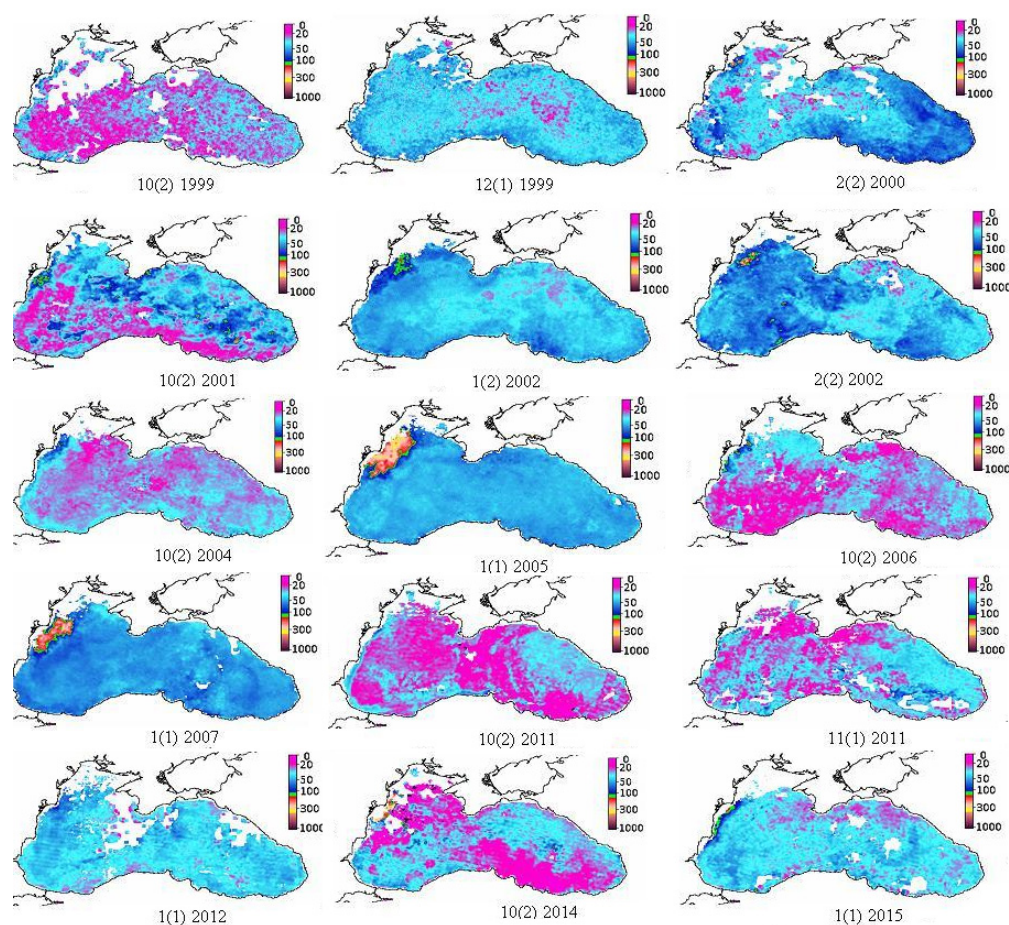


Fig. 2. Spatial variability of phytoplankton biomass ($\text{mg C}\cdot\text{m}^{-3}$) under the effect of circulations during increased mixing of water masses in autumn months and winter increase in phytoplankton biomass in the Black Sea in different years

Maximum values vary from 50 to 100 mg C·m⁻³. On average over an 18-year period, for the entire deep-sea area, phytoplankton biomass in winter is (51.52 ± 10.08) mg C·m⁻³. From February–early March, biomass decreases, which may be due to the involvement of phytoplankton by convection currents below the zone of photosynthesis. On most maps, it is reflected as a mosaic distribution of values over the entire surface of the Black Sea which vary within the range of 20–100 mg C·m⁻³ (Fig. 3). The maximum depth of water mixing, averaging 28–30 m, is usually observed in February. In some years, the depths of mixing in December and February exceeded 30 m in the deepwater zone and the slope of depth; for some areas, the mean values reached (36 ± 6) m. Moreover, in the western cyclonic gyre, the depths of convective mixing are higher compared to those in the eastern Black Sea. The occurrence of convective currents in the second half of February–early March can be caused, in addition to wind activity, by a decrease in water temperature and the leveling-off of the temperature gradient between the surface and deep-sea area. The mixing process involves layers from the sea depths, and this leads to an increase in concentration of nutrients in the upper mixed layer. The cold intermediate layer, which separates the upper quasi-homogeneous layer from nutrient-rich deep waters, is located at a depth of 30–100 m [Ivanov, Belokopytov, 2011]. At the same time, the upper boundary of the layer of maximum gradients of nitrate and phosphate concentration is located at 30–60 m [Krivenko, Parkhomenko, 2014]. From late March, a decrease in water temperature stops, wind activity drops, turbulent flows weaken, and irradiance increases, which leads to the spring bloom of phytoplankton. Thus, due to the rise of nutrients into the euphotic layer during convection in February–March, spring development of phytoplankton in deep-sea areas reaches its maximum values in the year, 100 mg C·m⁻³ or more.

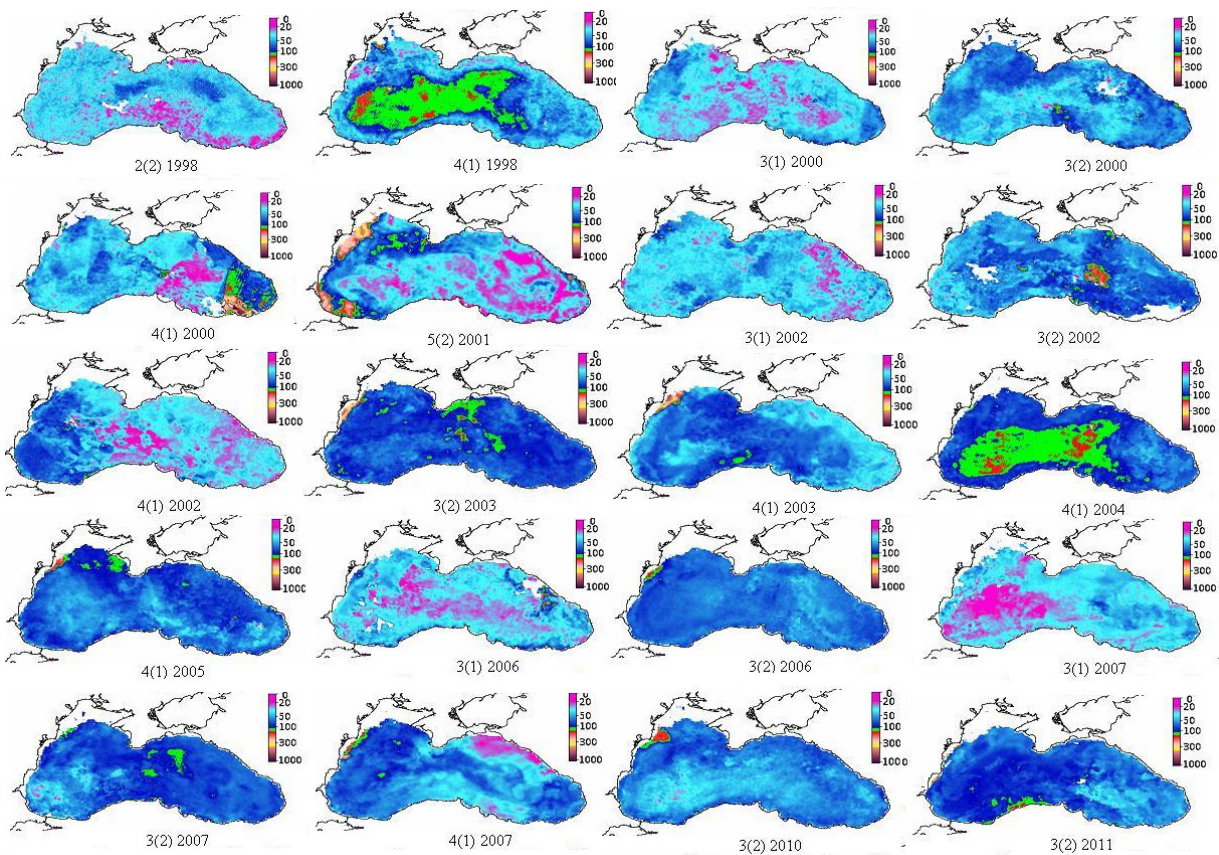


Fig. 3. Spatial variability of phytoplankton biomass (mg C·m⁻³) under the effect of circulations during the spring increase in phytoplankton biomass in the Black Sea in different years

During most years, the maximum values of phytoplankton biomass in spring were noted closer to centers of the cyclonic gyres. Based on the results of satellite observations averaged for the western and eastern cyclonic gyres, it was established as follows. In years with the mean water temperature in the deep-sea area during the cold season decreasing to the value below $+8\text{ }^{\circ}\text{C}$ for six weeks or more, intensive development of phytoplankton biomass is observed in spring. In years with the mean water temperatures above $+8\text{ }^{\circ}\text{C}$ or with the temperature decreasing to the value below $+8\text{ }^{\circ}\text{C}$ for no more than one month in winter, weak biomass growth is usually recorded in spring. At the same time, the spring bloom is less pronounced in years with prolonged mean water temperature below $+7\text{ }^{\circ}\text{C}$ during the cold season than in the case of a long period of winter temperature at $+7\dots+8\text{ }^{\circ}\text{C}$. Therefore, conditions for convective mixing and transfer of nutrients into the zone of photosynthesis are the most favorable when the temperature in the upper quasi-homogeneous layer is leveled off with the temperature in the cold intermediate layer. At lower temperatures, cold surface waters can form zones with strong downward flows, and this leads to a deepening of the upper quasi-homogeneous layer zone well below the zone of photosynthesis. As a result, chlorophyll concentration and phytoplankton biomass decrease. In the central sea, apparently, mixing is limited by the pycnocline. Moreover, the cold intermediate layer can become denser. During this period, wind effect and dynamic processes in water masses are of high importance. Specifically, in 2003, the water temperature in winter dropped below $+7\text{ }^{\circ}\text{C}$ for two months only in the western cyclonic gyre, while in the eastern one, the decrease lasted no more than a month. Accordingly, in the center of the eastern gyre, the spring bloom was approximately twice as intense as the bloom in the western gyre. These observations indicate that the condition for intensive development of phytoplankton in spring is the mean water temperature in the range of $+7\dots+8\text{ }^{\circ}\text{C}$ for more than six weeks during the cold season.

From late April–May, the values of phytoplankton biomass decrease in the deepwater zone. Throughout summer and early autumn, according to data averaged for the area, those are usually within the range of $12\text{--}42\text{ mg C}\cdot\text{m}^{-3}$. A rise in mean values in some years to $27\text{--}42\text{ mg C}\cdot\text{m}^{-3}$ can be recognized as a weak third maximum in the seasonal dynamics of biomass. The research [Finenko et al., 2018] indicates the occurrence of three biomass maximums: the winter, spring, and summer–early autumn ones. However, the latter maximum was not annual, and the mean values for the area were below $40\text{ mg C}\cdot\text{m}^{-3}$. In the deepwater zone, temperature and density stratifications are formed, and the exchange of water masses with shelf waters is minimum.

The effect of synoptic circulations on the distribution of phytoplankton biomass. About a month after the spring bloom, a decrease in biomass begins and gradually spreads across the water area with cyclical variations from the eastern area to the western one. Phytoplankton bloom in the deepwater zone usually lasts about a month [Finenko et al., 2018]. The cyclicity in variations in phytoplankton biomass, from two weeks to a month, can result from water movement in large cyclonic gyres, the western and eastern ones. This variability corresponds to the seasonal cycle of geostrophic circulation [Belokopytov, 2004]. The circulation is characterized by a common cyclonic movement with a variable center in the western or eastern Black Sea or with two pronounced gyres [Belokopytov, 2004]. The cyclicity observed throughout the year has a particularly noticeable effect on the variability of biomass in late autumn, winter, and spring, with the most pronounced processes of new formation and successive death of phytoplankton (Figs 2, 3). As follows from this circulation cycle, the periods we identified, with a mosaic distribution of phytoplankton biomass in November–December and February–March, occurring *prior* to the winter and spring blooms, coincide with a merger of two cyclonic gyres, shift in the center

of cyclonic rotation, and general increase in speeds of currents [Ivanov, Belokopytov, 2011]. In January–February, according to hydrophysical data, the eastern gyre is more pronounced. However, increased speeds of water movement and the mixing seem to prevent phytoplankton organisms, that formed biomass during the winter bloom, from being localized separately in the cycle or in its center. Phytoplankton are usually distributed along the periphery of the gyre or spread throughout the sea. In a layer down to 200 m, the horizontal structure of currents is strongly interconnected vertically; therefore, circulation throughout the entire water column has common features [Ivanov, Belokopytov, 2011], and in these months, a seasonal correlation is registered between surface and deep currents [Korotaev et al., 2006]. This may contribute to phytoplankton distribution in the water column to greater depths and beyond the zone of photosynthesis. During the spring bloom, on the contrary, biomass is more often concentrated in the gyres. In most years, the values of phytoplankton biomass established in the eastern Black Sea spread to the western sea in late March and April (Fig. 3). For summer period, due to high stratification in the water column and low current speeds [Ivanov, Belokopytov, 2011], a homogeneous field of low concentrations of phytoplankton biomass is characteristic. However, in some months of the warm season, the transport of waters with low concentrations of phytoplankton in accordance with the centers of cyclonic rotation can be noted. Thus, according to our research, phytoplankton biomass is formed, transferred, and localized under the effect of seasonal cycles of alternating changes in intensity of the eastern and western cyclonic gyres.

It is worth noting as follows. The distribution and formation of phytoplankton biomass in the Black Sea also occur in local anticyclonic eddies along the Rim Current and the movement of large cyclonic gyres. For example, the Sevastopol anticyclonic eddy [Ivanov, Belokopytov, 2011] is distinguished as a separate zone. During the spring bloom, lower or higher phytoplankton concentrations are registered there; during the winter bloom, usually lower ones. Intensive development of phytoplankton in this zone was observed in the second half of March or in the first half of April (in 1999, 2000, 2003, 2005, 2010, 2011, and 2012). Usually, the bloom in the Sevastopol micro-gyre lasted no more than two weeks, and the biomass values were 2–2.5 times higher than in the western cyclonic gyre (Fig. 3). Only in 2013 and 2015, phytoplankton concentration in the Sevastopol anticyclonic eddy was 2 times lower than in the deepwater zone. There was one significant increase in biomass – in 2001, in the second half of May; it was presumably affected by the widespread distribution of the Danube River flood (Fig. 3). In other years, in spring, changes in the analyzed indicator occurred according to the same pattern as in the deep-sea area. In winter, in this site of the water area, a homogeneous field of biomass with a western circulation is recorded, which may indicate an intensive mixing of these two zones and a temporary disappearance of the anticyclone as a separate zone for the development of phytoplankton biomass. Over the entire study period, only in 2001, 2012, 2014, and 2015, the Sevastopol anticyclonic eddy was characterized by lower biomass values in some winter months. In summer, as a rule, it was not distinguished as a separate zone; there, concentrations of phytoplankton biomass were lower than in the deep-sea area. In the Batumi anticyclone, according to 18-year studies, the values of biomass differed from those for the rest of the deep-sea area in the first half of April 2000 and 2006, in the first half of May 2001, and in the winter of 2003. During these years, intense phytoplankton bloom occurred there against the backdrop of low biomass values in the deep-sea area. In other years, the variability of values was similar. In April 2000, there was an outbreak of phytoplankton both in the coastal zone along the East Pontic Mountains (the values reached $1,000 \text{ mg C}\cdot\text{m}^{-3}$) and in the Batumi gyre ($300 \text{ mg C}\cdot\text{m}^{-3}$). In May 2001, in the shelf zone in the Batumi area, biomass increased to $200 \text{ mg C}\cdot\text{m}^{-3}$. In the indicated months in 2003

and 2006, the values did not exceed $100 \text{ mg C}\cdot\text{m}^{-3}$, but were approximately twice as high as in the eastern cyclonic gyre. According to data averaged for the area over 18 years, in the western cyclonic gyre, phytoplankton biomass was $(38.0 \pm 17.8) \text{ mg C}\cdot\text{m}^{-3}$; in the eastern cyclonic gyre, $(37.7 \pm 16.8) \text{ mg C}\cdot\text{m}^{-3}$; and in the Batumi gyre, $(38.2 \pm 18.0) \text{ mg C}\cdot\text{m}^{-3}$.

The importance of circulations in the occurrence of phytoplankton blooms was considered by other researchers as well [Kubryakov et al., 2019]. In August 2015, in the southeastern Black Sea, there were a sharp disturbance in the physical structure of waters and an isopycnic mixing, with the latter one caused by a shift in inertial currents under the effect of strong winds; this led to an increase in chlorophyll concentration [Kubryakov et al., 2019]. However, according to our calculations and satellite observation data (Fig. 4), in August 2015, a slight increase in phytoplankton biomass in the eastern anticyclonic gyre was registered: up to $27 \text{ mg C}\cdot\text{m}^{-3}$ on average for the area, against the backdrop of $13\text{--}20 \text{ mg C}\cdot\text{m}^{-3}$ in June and July. Only in the center of the anticyclone, the values rose to $50 \text{ mg C}\cdot\text{m}^{-3}$. At the same time, there was no significant increase in biomass in the eastern sea. Phytoplankton development was the same as in most years. Over an 18-year period, the greatest increase in biomass in the deep-sea area was observed in 2001 in summer (in particular, up to $38 \text{ mg C}\cdot\text{m}^{-3}$ in August), but its reasons require separate analysis. Also, for the deepwater zone, a sudden outbreak of phytoplankton development was noted in late August–early September 2012 (Fig. 4).

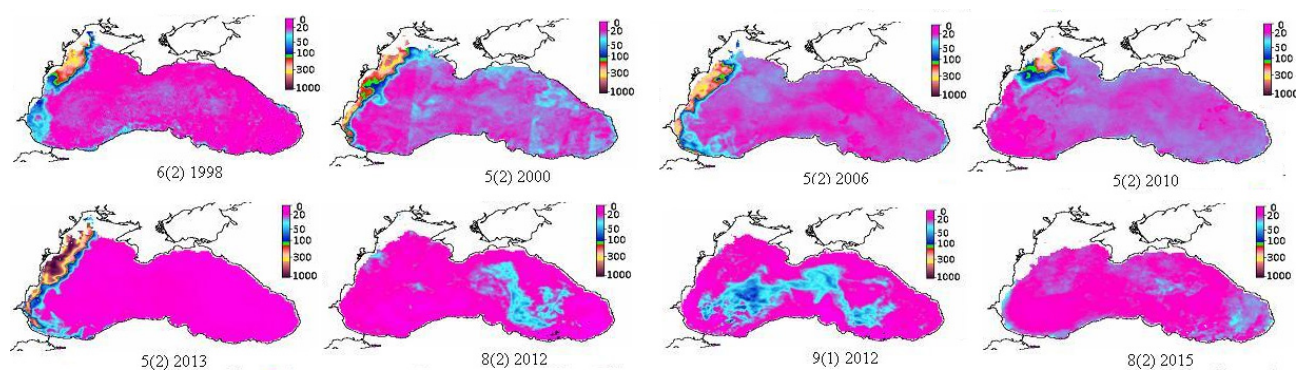


Fig. 4. Spatial variability of phytoplankton biomass ($\text{mg C}\cdot\text{m}^{-3}$) under the effect of circulations during summer months and in the Danube flood period in the Black Sea in different years

The bloom began approximately in the center of the eastern cyclonic gyre; within two weeks, it spread to the western one. Maximum values in the center of the western cyclonic gyre reached $70\text{--}80 \text{ mg C}\cdot\text{m}^{-3}$. At the same time, according to data averaged for the entire area, the values did not exceed $35 \text{ mg C}\cdot\text{m}^{-3}$, and this did not lead to a rise in biomass in general during summer. On the contrary, since 2012, the biomass of phytoplankton became to decrease in summer and dropped on average by 1.4 times in the deepwater zone and by 1.2–1.4 times in the slope of depth of the western Black Sea and almost along the entire shelf zone (compared to that in previous years). In the deep-sea area, over an 18-year period, negative trends in the values of phytoplankton biomass were recorded in spring and summer; no significant trends were found in winter and autumn [Finenko et al., 2019]. This decrease, as pointed out in the research [Finenko et al., 2019], is not associated with changes in temperature and light conditions. The only exceptions were the area of the Danube River drainage, where there was a rise

in phytoplankton biomass by 1.3 times in recent years in summer, and the Gulf of Burgas area, with an increase by 1.14 times. Over 18 years in the Danube area, according to year-round regular two-week data, biomass rose by 33% compared to the initial level, with its high variability (when assessed by Fisher's exact test at $p \leq 0.1$). This may indicate a rise in the trophic level of this area, which is likely to result from an increase in anthropogenic load.

Typically, increased biomass values extended to the boundaries of cyclonic gyres and the slope of depth, and in some cases, to the coast of the Crimea. However, according to long-term observations, due to differences in the density and salinity of shelf waters and waters of the central Black Sea, their separation occurred, and this did not lead to an increase in phytoplankton biomass in the deep-sea area.

The role of the Rim Current in shaping the development of phytoplankton in shelf waters. In the coastal zone, mainly in the area of the Danube River drainage and somewhat less in the area of the Dniester and Dnieper rivers, from late April–May, there is a significant rise in biomass caused by spring floods. Within two months, increased phytoplankton biomass, following the direction of the Rim Current, reaches the Bosphorus Strait, but, as a rule, does not spread further to the east (see Fig. 4). Most of desalinated waters is carried into the Sea of Marmara.

The period of the summer bloom on the western shelf lasted until September–October. Against the backdrop of increased concentrations, usually, there were two peaks: in May–June and in September–October (two times less one). In some cases, biomass values reached 300–1,000 mg C·m⁻³; on average, in the area of the Danube River drainage, the values were about 100 mg C·m⁻³ in summer. As water masses move towards the Bosphorus Strait, phytoplankton biomass decreases. A re-increase in its values in the western coastal zone occurs in winter, but with lower concentrations and area of distribution than in late spring. Fairly high values of phytoplankton biomass persist there throughout the year, while the level of biomass in other coastal areas in winter is usually lower than in the deepwater zone. Changes along the southern and eastern shelves occur in most years according to the same pattern as in the deep-sea area, and phytoplankton concentrations vary within the same limits. Only the northeastern coast is characterized by the lowest biomass values throughout the year, especially in summer. This may be due to the highest speed of the Rim Current [Ivanov, Belokopytov, 2011] in this site of the water area and the low depth of the mixed layer, averaging (5.0 ± 3.7) m, according to our calculations. The maximum of chlorophyll and biomass off the Crimean and Caucasian coasts in summer occurs on average at a depth of 29 m. The maximum speed of current is observed in the surface layer, 10–25 m [Ivanov, Belokopytov, 2011]. Apparently, this leads to water stratification in terms of movement speeds and to weak stirring.

Throughout a year, especially in summer, the Rim Current [Ivanov, Belokopytov, 2011] promotes biomass distribution along the shelf zone, practically without mixing with the deep-sea area. An exception may be the formation of eddy circulations transported to the open sea in late autumn and winter. Therefore, the effect of coastal waters on the deepwater zone is possible precisely during this period. In spring, during floods, the values of phytoplankton biomass are high, and those can spread to the slope of depth; however, temperature and density differences and low wind activity prevent mixing of shelf waters and deep-sea ones.

Conclusion. The movement of the main surface currents and mixing processes play an important role in the spatial distribution of phytoplankton biomass in the Black Sea. We showed the effect of large synoptic gyres on the periodicity of bloom shift from one cyclonic gyre to another, with a duration of about a month. Deep vertical circulations of water caused by temperature and wind regimes in winter,

determine the occurrence of winter and spring maximum of phytoplankton biomass. One of the key conditions for its intense bloom in the deepwater zone in spring is a drop in the mean water temperature in the cold season to +7...+8 °C for more than six weeks. These conditions contribute to an increase in vertical circulation of water masses and transfer of nutrients into the euphotic layer. According to the data of spatial changes over an 18-year period, the spring–summer bloom in the shelf zone did not go beyond the slope of depth and did not penetrate into the deep-sea area. Only in certain cases, high phytoplankton concentrations during heavy spring floods on the northwestern shelf were observed off the Crimean coast; on the southeastern shelf, those penetrated into the Batumi anticyclone. In the warm season, most of phytoplankton biomass formed at the drainage of northwestern rivers spreads to the Bosphorus Strait and is carried out of the Black Sea. In autumn from October and in winter, the bloom can cover the western cyclonic gyre and contribute to phytoplankton development in the surface layer of the central Black Sea.

This work was carried out within the framework of state research assignment “Functional, metabolic, and toxicological aspects of hydrobionts and their populations existence in biotopes with different physical and chemical regimes” (No. 121041400077-1, IBSS), partly within the framework of state research assignment “Development of methods of operational oceanology based on interdisciplinary studies of the processes of formation and evolution of the marine environment and mathematical modeling using data from remote and contact measurements” (No. 0827-2018-0002, MHI), and partly within the framework of the project of the Russian Foundation for Basic Research and the city of Sevastopol “Strategies for adaptation of phytoplankton and its consumption by microzooplankton under climate change and anthropogenic load on the Black Sea coastal ecosystems (Sevastopol area)” (No. 20-45-920002).

REFERENCES

1. Arashkevich E. G., Louppova N. E., Nikishina A. B., Pautova L. A., Chasovnikov V. K., Drits A. V., Podymov O. I., Romanova N. D., Stanichnaya R. R., Zatsepin A. G., Kuklev S. B., Flint M. V. Marine environmental monitoring in the shelf zone of the Black Sea: Assessment of the current state of the pelagic ecosystem. *Okeanologiya*, 2015, vol. 55, no. 6, pp. 964–970. (in Russ.). <https://doi.org/10.7868/S0030157415060015>
2. Belokopytov V. N. *Termokhalinnaya i gidrologo-akusticheskaya struktura vod Chernogo morya* : avtoref. dis. ... kand. geogr. nauk : 11.00.08 / MGI NAN Ukrainy. Sevastopol, 2004, 24 p. (in Russ.)
3. Berseneva G. P., Churilova T. Ya., Georgieva L. V. Seasonal variability of the chlorophyll and phytoplankton biomass in the western part of the Black Sea. *Okeanologiya*, 2004, vol. 44, no. 3, pp. 389–398. (in Russ.)
4. Ivanov V. A., Belokopytov V. N. *Oceanography of the Black Sea*. Sevastopol : EKOSI-Gidrofizika, 2011, 212 p. (in Russ.)
5. Krivenko O. V., Parkhomenko A. V. Upward and regeneration fluxes of inorganic nitrogen and phosphorus of the deep-water areas of the Black Sea. *Zhurnal obshchei biologii*, 2014, vol. 75, no. 5, pp. 394–408. (in Russ.)
6. Mikaelyan A. S. *Vremennaya dinamika fitoplanktona glubokovodnogo basseina Chernogo morya*. [dissertation]. Moscow, 2018, 266 p. (in Russ.)
7. Suslin V. V., Churilova T. Ya., Lee M., Moncheva S., Finenko Z. Z. Comparison of the Black Sea chlorophyll *a* algorithms for SeaWiFS and MODIS instruments. *Fundamental'naya i prikladnaya gidrofizika*, 2018, vol. 11, no. 3, pp. 64–72. (in Russ.). <https://doi.org/10.7868/S2073667318030085>
8. Finenko Z. Z., Kovalyova I. V., Suslin V. V. A new approach to estimate phytoplankton

- biomass and its variability in the Black Sea surface water layer based on satellite data. *Uspekhi sovremennoi biologii*, 2018, vol. 138, no. 3, pp. 294–307. (in Russ.). <https://doi.org/10.7868/S0042132418030079>
9. Finenko Z. Z., Mansurova I. M., Suslin V. V. Dynamics of chlorophyll *a* concentration in the Black Sea on satellite data. *Morskoj biologicheskij zhurnal*, 2019, vol. 4, no. 2, pp. 87–95. (in Russ.). <https://doi.org/10.21072/mbj.2019.04.2.09>
10. Dorofeev V. L., Sukhikh L. I. Study of long-term variability of Black Sea dynamics on the basis of circulation model assimilation of remote measurements. *Izvestiya. Atmospheric and Oceanic Physics*, 2017, vol. 53, no. 2, pp. 224–232. <https://doi.org/10.1134/S0001433817020025>
11. Eppley R. W., Harrison W. G., Chisholm S. W., Stewart E. Particulate organic matter in surface waters off Southern California and its relationship to phytoplankton. *Journal of Marine Research*, 1977, vol. 35, pp. 671–696.
12. Finenko Z. Z., Hoepffner N., Williams R., Piontkovski S. A. Phytoplankton carbon to chlorophyll *a* ratio: Response to light, temperature and nutrient limitation. *Morskoj ekologicheskij zhurnal*, 2003, vol. 2, no. 2, pp. 40–64. <https://repository.marine-research.ru/handle/299011/707>
13. Geider R. J. Light and temperature dependence of the carbon to chlorophyll *a* ratio in microalgae and cyanobacteria: Implications for physiology and growth of phytoplankton. *New Phytologist*, 1987, vol. 106, iss. 1, pp. 1–34. <https://doi.org/10.1111/j.1469-8137.1987.tb04788.x>
14. Korotaev G., Oguz T., Riser S. Intermediate and deep currents of the Black Sea obtained from autonomous profiling floats. *Deep Sea Research Part II: Topical Studies in Oceanography*, 2006, vol. 53, iss. 17–19, pp. 1901–1910. <https://doi.org/10.1016/j.dsr2.2006.04.017>
15. Kubryakov A. A., Zatsepin A. G., Stanichny S. V. Anomalous summer–autumn phytoplankton bloom in 2015 in the Black Sea caused by several strong wind events. *Journal of Marine Systems*, 2019, vol. 194, pp. 11–24. <https://doi.org/10.1016/j.jmarsys.2019.02.004>
16. Menden-Deuer S., Lessard E. J. Carbon to volume relationships for dinoflagellates, diatoms, and other protist plankton. *Limnology and Oceanography*, 2000, vol. 45, iss. 3, pp. 569–579. <https://doi.org/10.4319/lo.2000.45.3.0569>
17. Mikaelyan A. S., Pautova L. A., Chasovnikov V. K., Mosharov S. A., Silkin V. A. Alternation of diatoms and coccolithophores in the north-eastern Black Sea: A response to nutrient changes. *Hydrobiologia*, 2015, vol. 755, iss. 1, pp. 89–105. <https://doi.org/10.1007/s10750-015-2219-z>
18. Suslin V., Churilova T. A regional algorithm for separating light absorption by chlorophyll-*a* and coloured detrital matter in the Black Sea, using 480–560 nm bands from ocean colour scanners. *International Journal of Remote Sensing*, 2016, vol. 37, no. 18, pp. 4380–4400. <https://doi.org/10.1080/01431161.2016.1211350>
19. Suslin V. V., Slabakova V. K., Churilova T. Ya. Diffuse attenuation coefficient for downwelling irradiance at 490 nm and its spectral characteristics in the Black Sea upper layer: Modeling, *in situ* measurements and ocean color data. *Proceedings of SPIE : 23rd International Symposium on Atmospheric and Ocean Optics: Atmospheric Physics*, 2017, vol. 10466, art. no. 104663H (13 p.). <https://doi.org/10.1117/12.2287367>

**ПРОСТРАНСТВЕННАЯ И ВРЕМЕННАЯ ДИНАМИКА
БИОМАССЫ ФИТОПЛАНКТОНА
В ПОВЕРХНОСТНОМ СЛОЕ ЧЁРНОГО МОРЯ**

И. В. Ковалёва¹, З. З. Финенко¹, В. В. Суслин²

¹ФГБУН ФИЦ «Институт биологии южных морей имени А. О. Ковалевского РАН»,
Севастополь, Российская Федерация

²ФИЦ «Морской гидрофизический институт РАН», Севастополь, Российская Федерация
E-mail: ila.82@mail.ru

Проведён анализ пространственной и временной изменчивости биомассы фитопланктона в поверхностном слое Чёрного моря за 18-летний период и оценено влияние основных течений в море на пространственную и временную динамику биомассы фототрофного фитопланктона. Используются регулярные многолетние данные концентрации хлорофилла, полученные по спутниковым наблюдениям с помощью приборов SeaWiFS и MODIS-Aqua/Terra за период с 1998 по 2015 г. в Чёрном море. Оценена роль макро- и микроциркуляций в пространственно-временной вариабельности биомассы фитопланктона. Усиление ветровой активности и снижение температуры воды с октября по март, приводящие к увеличению глубины перемешивания верхнего слоя и интенсивности основных синоптических циркуляций, становятся существенным фактором, который способствует возникновению зимнего и весеннего цветения фитопланктона. Выявлено, что понижение средней температуры воды в холодный сезон до +7...+8 °C на протяжении более чем полутора месяцев в глубоководной зоне приводит к интенсивному развитию биомассы весной. Установлено, что средняя биомасса фитопланктона за 18-летний период в западном и восточном циклонических круговоротах составляет $(38,0 \pm 17,8)$ и $(37,7 \pm 16,8)$ мг С·м⁻³ соответственно, в Батумском антициклоне — $(38,2 \pm 18,0)$ мг С·м⁻³. Основное черноморское течение, как правило, переносит фитопланктон, образовавшийся у шельфовой зоны, вдоль береговой линии, мало смешиваясь с водами глубоководной акватории. В циклонических круговоротах зимне-весеннее цветение фитопланктона наблюдается в среднем на протяжении полутора месяцев. Интенсивное цветение в районе стока северо-западных рек, регистрируемое в мае — июне, распространяется до пролива Босфор, тогда как в холодный сезон может в виде микровихрей проникать в глубоководную зону. В зимние и весенние месяцы Севастопольский антициклонический вихрь выделялся как отдельная зона в развитии биомассы. Роль антропогенной нагрузки наиболее существенна в прибрежной зоне. При этом влияние прибрежных вод на глубоководную зону в некоторой степени возможно поздней осенью и зимой.

Ключевые слова: биомасса фитопланктона, синоптические циркуляции, Чёрное море, пространственная изменчивость биомассы фитопланктона, температура воды, глубина перемешанного слоя

UDC 57.087:591.148(269.4)

**USING THE VERTICAL SOUNDING METHOD
FOR RECORDING BIOLUMINESCENCE
IN THE ANTARCTIC SECTOR OF THE ATLANTIC OCEAN**

© 2023 **L. A. Melnik, A. V. Melnik, O. V. Mashukova, and V. V. Melnikov**

A. O. Kovalevsky Institute of Biology of the Southern Seas of RAS, Sevastopol, Russian Federation

E-mail: melniklidi@gmail.com

Received by the Editor 16.02.2021; after reviewing 17.06.2021;
accepted for publication 04.08.2023; published online 01.12.2023.

Bioluminescence is an essential element in the functioning of the pelagic community, which is associated with the key ecological role of light in the life of hydrobionts, *inter alia* in the formation of their spatial heterogeneity. The luminescence of marine hydrobionts is a manifestation of their vital activity in the form of electromagnetic radiation in the spectrum visible area, and its kinetic patterns are closely related to mechanism generating their chemical reactions and metabolic processes. Global warming, which undoubtedly has affected the Atlantic sector of Antarctica, caused serious structural and functional alterations in the pelagic community with repercussion on marine bioluminescence, an expressive indicator of environmental conditions. We aimed at studying the possibility of using the method of multiple vertical sounding by the hydrobiophysical complex “Salpa-M,” with simultaneous capture of biophysical and hydrological parameters at one station, to investigate the structure and length of fields of luminescence in Antarctic waters. The paper provides the technique for analyzing structural characteristics of bioluminescence, as well as material obtained during the 79th Antarctic expedition on-board the RV “Akademik Mstislav Keldysh.” The core of the sounding method is raising (or lowering) the bathyphotometer “Salpa-M” at a constant speed in a given layer [usually, it is the upper productive (0–200 m) or the photic (0–100 m) layer] in the RV’s drift. Planktonic bioluminescent organisms, which are the main contributors to the formation of the bioluminescent potential of the pelagic, mostly illuminate when stimulated. Therefore, a bathyphotometer moving at a constant speed creates a standard level of the mechanical stimulation of bioluminescent organisms, and this allows to compare correctly the results of measurements for the vertical structure of the field of bioluminescence carried out in different areas and under various weather conditions (rolling, wind drift, *etc.*). The paper presents a fairly large data set of the integral bioluminescent signal at different horizons. Primary data on bioluminescence intensity, temperature values, electrical conductivity, and photosynthetically active radiation were obtained at 18 hydrographic stations in the studied water area of the Atlantic sector of Antarctica. The article considers an important issue related to the change in seawater bioluminescence in the Atlantic sector of Antarctica studied by the vertical sounding at different levels with a bioluminescent probe. When investigating bioluminescence, its vertical variability in the upper productive layer was determined in relation to features of plankton distribution. As a result, it was found out that the luminescence of Antarctic waters in the photic layer of this area occurs within the range from 8.4×10^{-12} to $104.42 \times 10^{-12} \text{ W} \cdot \text{cm}^{-2} \cdot \text{L}^{-1}$. Bioluminescence peaks (up to $104 \times 10^{-12} \text{ W} \cdot \text{cm}^{-2} \cdot \text{L}^{-1}$) were recorded under the thermocline at a 45-m depth in the areas of concentration of the salp *Salpa thompsoni* Foxton, 1961 near the hydrological front, at a distance of about 6–7 miles on either its side. It is shown that the method of vertical sounding in Antarctic waters allows expressing the fields and the structure of aggregations of luminescent organisms.

Keywords: bioluminescence intensity, Atlantic sector of Antarctica, euphotic zone, vertical sounding, plankton

In Antarctic waters, the most important fishery object is the Antarctic krill *Euphausia superba* Dana, 1852, which forms the basis of the diet of numerous consumers. Its reserves in the Southern Ocean amount to hundreds of millions of tons [Samyshev, 1991]. This species is most common in the circumpolar belt between the Antarctica and the polar front [Nicol, Foster, 2016; Nicol et al., 2000]. To date, assessing the state of krill communities is one of the priority areas of research in the Atlantic sector of Antarctica [Spiridonov, Uryupova, 2009; Sprong, Schalk, 1992].

Krill aggregations luminesce due to bioluminescent photophores located on the body of each crustacean: one pair, on the eyestalks; another pair, on the hips of the second and seventh thoracopods; and individual organs, on four segments of the pleon. These organs periodically luminesce for 2–3 s. Bioluminescence is clearly visible in the dark. It is electromagnetic radiation in the visible area of the spectrum, and its kinetic patterns are closely related to mechanism of the chemical reactions and metabolic processes that generate them [Harvey, 1957]. There are many bioluminescent species of hydrobionts: dinoflagellates, radiolarians, and various mobile multicellular animals from polyps, jellyfish, and ctenophores to squids, crustaceans, and fish [Labas, Gordeeva, 2003]. IBSS researchers discovered the ability to luminesce in 364 phyto- and zooplankton species; out of them, 164 turned out to be bioluminescent organisms, and in 137 species, bioluminescence was shown for the first time [Tokarev, 2006]. Bacteria found in seawater at different latitudes, from tropical to polar ones, are bioluminescent organisms as well. In the open ocean, there are on average up to 1,000 cells of luminescent bacteria per 1 L of seawater [Gitelson, 1976].

In terms of energy, bioluminescence of zooplankton is obviously higher than that of phytoplankton or bacteria. Various krill species are characterized by the highest intensity and duration of bioluminescence (up to 22 s) [Tokarev, Sokolov, 2001].

The vertical sounding method for determining the level of bioluminescence can be used for rapid assessment of species diversity and spatial distribution of bioluminescent organisms in the analyzed water area.

We aimed at studying the possibility of applying the method of multiple vertical sounding with a hydrobiophysical complex “Salpa-M,” with simultaneous capture of biophysical and hydrological parameters at one station, to investigate structure and length of fields of luminescence in Antarctic waters.

MATERIAL AND METHODS

Data were obtained in February 2020 (122 soundings at 18 stations in the 79th cruise of the RV “Akademik Mstislav Keldysh”) (Fig. 1). Measurements of a field of bioluminescence were carried out day and night with a probe “Salpa-M” [Tokarev et al., 2016]. This biophysical complex has six measuring and service channels:

- 1) bioluminescence (measurement range from 10^{-12} to 10^{-8} W·cm⁻²·L⁻¹);
- 2) temperature (measurement range from –2 to +35 °C);
- 3) pressure (measurement range from 0 to 2 MPa);
- 4) photosynthetically active radiation;
- 5) information transmission and remote operation control;
- 6) control and signaling.

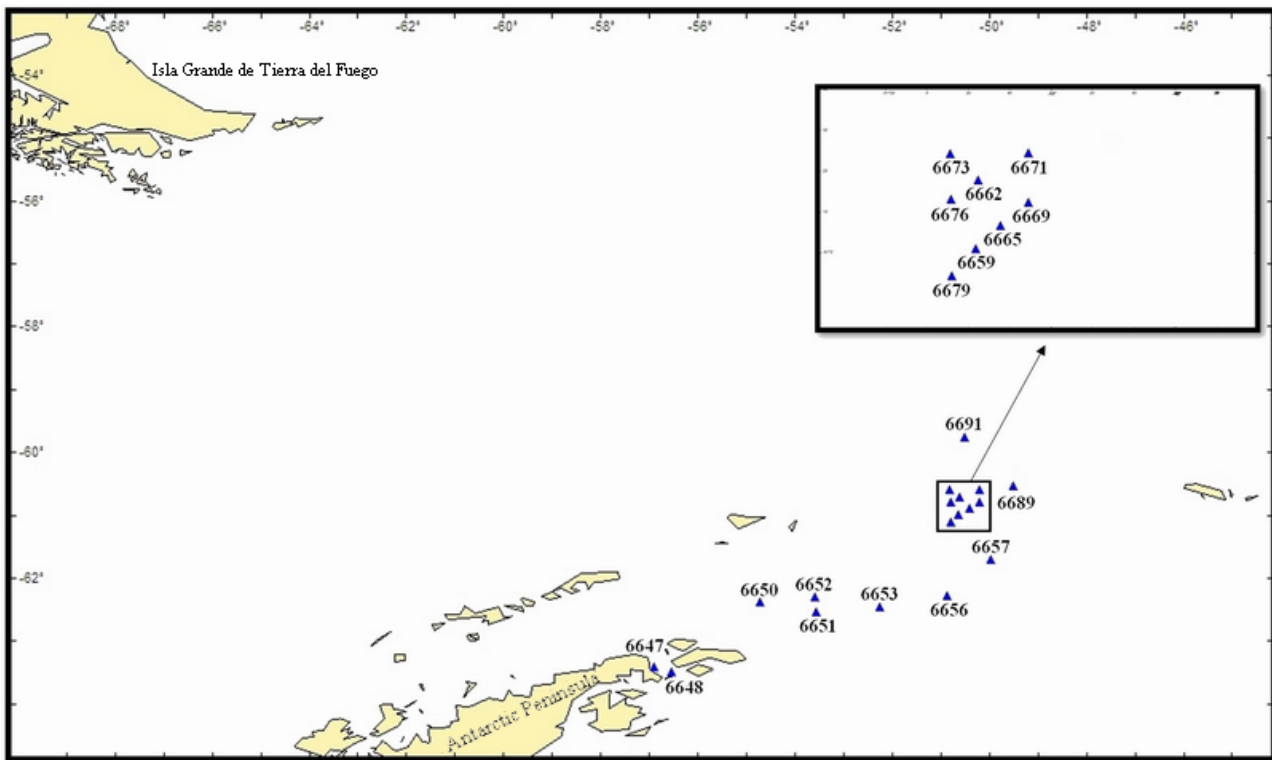


Fig. 1. Map of stations

The measuring channel of bioluminescence intensity. It consists of a measuring chamber, a luminescence collector, a photodetector, a control device, and an interface device, with the latter one used to measure temperature and pressure. The transfer of bioluminescent organisms to an active state in which they luminesce (the irritation) is carried out mechanically; the measuring chamber is used. It consists of eight blade impellers which are located in two groups of four impellers each, spaced apart along the axis.

To reduce the effect of sunlight, four rows of blackened impellers – two groups of rows of mutually perpendicular angles of attack – form a mobile luminescence trap and provide a weakening of light energy by 2×10^7 times with minimal resistance to the incoming water flow. During the axial movement of the bioluminescence probe, the studied incoming water flow enters the measuring chamber. Passing through four rows of blade impellers, water is thoroughly mixed, and bioluminescent organisms it contains are irritated. The latent period (the time before microorganisms begin to luminesce after their irritation) is determined by their species composition. To measure the bioluminescent potential, the time spent by a bioluminescent organism in an active state in the volume of the flow chamber has to exceed the latent period and the duration of its luminescence. Interestingly, the time of occurrence of microorganisms in the measuring chamber after mechanical effect is determined by the flow rate of water through this chamber. When solving the problem of bioluminescence recording, a preliminary analysis of the hydrodynamic flow of water through the measuring chamber was carried out. It showed the need for formation of a turbulent flow in the middle part of the chamber. The discreteness of measurements of characteristics by this complex when probing “down” at a speed of $1.2 \text{ m}\cdot\text{s}^{-1}$ was 0.25 m. The value was integrated

with software up to 1 m. It is worth noting that the special design of the light pipe forming a conical radiation pattern ensures the transfer of bioluminescence energy of microorganisms from the entire volume of the measuring chamber to the photodetector.

The photodetector. Bioluminescence is low-intensity pulses of light energy. Its measurement is carried out with a photomultiplier tube FEU-71 characterized by a high anode sensitivity ($1,000 \text{ A}\cdot\text{lm}^{-1}$) against the backdrop of a supply voltage of $< 1,000 \text{ V}$. The measuring signal of the photomultiplier tube is fed *via* a repeater and subsequent amplification to an interface – an analog-to-digital converter. The information signal is filtered with a constant time of 1–5 s, and this is controlled from a Salpa-T, P shell. The measuring channels for bioluminescence intensity, temperature, electrical conductivity, and hydrostatic pressure are the core ones for the complex.

The habitat of the Antarctic krill is separated from other areas of the ocean by the Antarctic polar front. It is an effective barrier to the spread of marine organisms, and it makes the Southern Ocean a largely isolated ecosystem. The total light effect created by the Antarctic krill is called a field of bioluminescence. Other luminescent hydrobionts make a significant contribution to its formation as well. As a physical field, it is characterized by energy intensity and frequency spectrum. Since this field is formed by biological objects, it is also characterized by biological features: the number of flashes of individual organisms that make this field up and the heterogeneous structure of their distribution in time and space.

When studying bioluminescence of Antarctic waters, we used the method of multiple (5 to 10) sounding of the photic layer of the pelagic zone (1–80 m). Its advantages over other techniques of investigating marine bioluminescence are as follows:

- ability to study the mosaic nature of the spatial distribution of the field of bioluminescence simultaneously with the background characteristics of the environment;
- constant level of effect on the environment and irritation of luminescent organisms;
- possibility to analyze in detail the vertical structure of bioluminescent populations;
- no effect of surface waves on the signal recorded;
- fairly simple solution to the issue of isolating the daily component of the bioluminescence registered.

RESULTS

Hydrological characteristics of the area. At the mesoscale studied site in the Weddell Sea, a hydrological front was detected [Morozov et al., 2020]. It was formed between warmer waters with cold subsurface layer and colder advective waters entering this site from the shallow western Powell Basin (the northwestern Weddell Sea). The research showed that the northern Powell Basin contains relatively warm waters. The frontal zone extended from southwest to northeast in the latitude range from 58° to 61° . The hydrological front was especially pronounced in the photic zone where the temperature difference in the upper layer reached 2°C [Morozov et al., 2020].

Bioluminescence. The investigation was carried out on a unified grid of stations approved by the general program of scientific research in the 79th Antarctic expedition on the RV “Akademik Mstislav Keldysh.” Bioluminescence was measured day and night. To exclude the phenomenon of photo-inhibition, we calculated the coefficients of daily variability for intensity of the field of bioluminescence; with these conversion factors, all data were reduced to those for night time.

In 2020, the analyzed water area was characterized by a seasonal outbreak in abundance of the salp *Salpa thompsoni* Foxton, 1961. This jellyfish-like species absolutely prevailed in zooplankton composition in the area of the southern branch of the Antarctic Circumpolar Current, the Bransfield Strait current, the Antarctic Peninsula coastal waters, and uplifts bordering the Powell Basin from the northwest [Morozov et al., 2020]. The background biomass of euphausiids, including the Antarctic krill, estimated from the Bongo net catches in a 200–0-m layer was two orders of magnitude lower, and the background biomass of other groups was several orders of magnitude lower. These data can be interpreted as a manifestation of the negative effect of the salp outbreak in abundance on the number of other groups of meso- and macrozooplankton.

Table 1 provides data on the mean amplitude indicators of fields of bioluminescence at 18 stations in the studied area in 2020. The highest level was recorded at sta. 6679 (in the southern Powell Basin) in the area of salp aggregation: the value reached $104.42 \times 10^{-12} \text{ W}\cdot\text{cm}^{-2}\cdot\text{L}^{-1}$.

Table 1. Volume of sampled material for bioluminescence measurement (2020)

| Station No. | Depth of sounding, m | Date | Station start time | Mean bioluminescence, $10^{-12} \text{ W}\cdot\text{cm}^{-2}\cdot\text{L}^{-1}$ | Maximum bioluminescence, $10^{-12} \text{ W}\cdot\text{cm}^{-2}\cdot\text{L}^{-1}$ | Level of maximum bioluminescence, m | Mean temperature, °C | Mean salinity, ‰ |
|-------------|----------------------|-------|--------------------|---|--|-------------------------------------|----------------------|------------------|
| 6647 | 35 | 13.02 | 14:58 | 25.93 | 38.98 | 11 | +0.69 | 34.29 |
| 6648 | 46 | 13.02 | 18:22 | 5.75 | 17.52 | 46 | +1.65 | 35.5 |
| 6650 | 65 | 14.02 | 15:54 | 12.56 | 25.65 | 8 | +0.22 | 33.94 |
| 6651 | 65 | 14.02 | 22:53 | 5.14 | 17.52 | 35 | +0.62 | 33.72 |
| 6652 | 75 | 15.02 | 17:40 | 4.51 | 15.99 | 58 | +0.49 | 33.9 |
| 6653 | 85 | 16.02 | 16:05 | 6.76 | 25.78 | 3 | +0.39 | 33.56 |
| 6656 | 65 | 17.02 | 14:43 | 4.61 | 10.25 | 65 | +0.77 | 33.25 |
| 6657 | 64 | 18.02 | 08:53 | 4.79 | 10.25 | 63 | +0.58 | 33.14 |
| 6659 | 71 | 19.02 | 00:09 | 4.75 | 10.25 | 4 | +0.69 | 33.81 |
| 6662 | 70 | 19.02 | 06:44 | 4.61 | 8.4 | 67 | +1.25 | 33.7 |
| 6665 | 78 | 19.02 | 13:38 | 6.97 | 21.03 | 24 | +0.4 | 33.85 |
| 6669 | 75 | 19.02 | 22:11 | 11.41 | 103.4 | 45 | +1.15 | 33.61 |
| 6671 | 75 | 20.02 | 03:33 | 4.41 | 12.04 | 61 | +1.9 | 33.79 |
| 6673 | 79 | 20.02 | 10:53 | 8.05 | 19.49 | 10 | +1.36 | 34 |
| 6676 | 65 | 20.02 | 15:52 | 11.44 | 25.66 | 18 | +0.22 | 33.95 |
| 6679 | 74 | 20.02 | 23:15 | 11.13 | 104.42 | 45 | +1.15 | 33.62 |
| 6689 | 75 | 23.02 | 16:45 | 2.71 | 13.77 | 26 | +1.97 | 33.24 |
| 6691 | 75 | 24.02 | 07:40 | 1.85 | 8.4 | 12 | +2.13 | 33.32 |

A layer of increased level of bioluminescent potential was registered at a 40–50-m depth, with a single-maximum vertical structure of bioluminescence. Intense outbreaks in this area (against the backdrop of low krill abundance) may be due to high abundance of *S. thompsoni*, since the salp is capable of forming outbreaks of such a potential. As moving north, bioluminescence intensity decreased noticeably. Specifically, at sta. 6676, the level was already $25.66 \times 10^{-12} \text{ W}\cdot\text{cm}^{-2}\cdot\text{L}^{-1}$. A layer of increased bioluminescent potential was formed at a depth of 15–20 m. At a more northern station, sta. 6673, the value was $19.49 \times 10^{-12} \text{ W}\cdot\text{cm}^{-2}\cdot\text{L}^{-1}$ (Fig. 2).

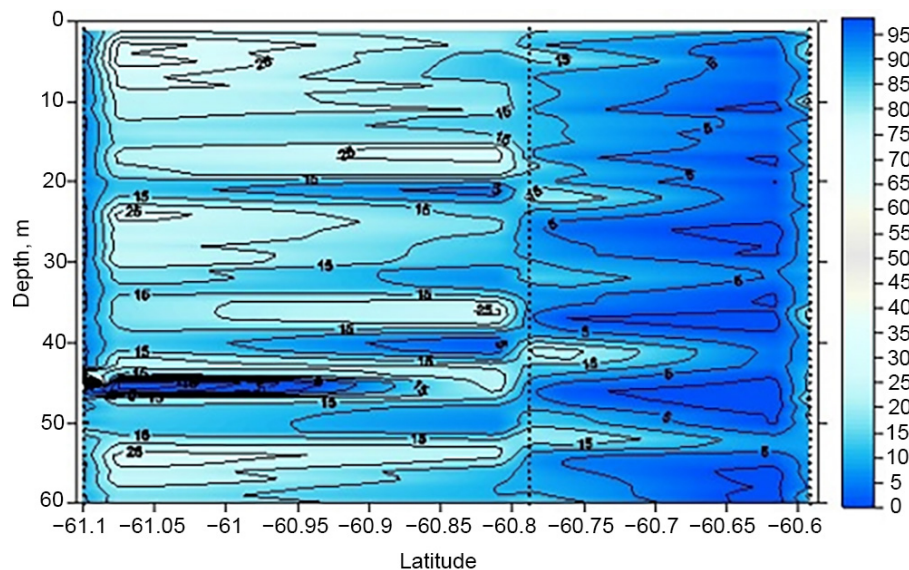


Fig. 2. Bioluminescence: spatial section at stations 6679, 6676, 6673

A layer of increased bioluminescent potential was also recorded at a 10-m depth. The vertical structure of bioluminescence at sta. 6676 and 6673 was similar. Sta. 6647 and 6648 were performed in the Antarctic Sound separating the Joinville Island group from the northeastern tip of the Antarctic Peninsula. In the studied water area, the vertical structure of bioluminescence was characterized by the presence of certain peaks. At sta. 6647, the peak of intensity ($25.93 \times 10^{-12} \text{ W}\cdot\text{cm}^{-2}\cdot\text{L}^{-1}$) occurred at a depth of 11 m. At sta. 6648, the peak of intensity ($5.75 \times 10^{-12} \text{ W}\cdot\text{cm}^{-2}\cdot\text{L}^{-1}$) was registered deeper, at 46 m. The mean level of bioluminescence at sta. 6647 was $38.98 \times 10^{-12} \text{ W}\cdot\text{cm}^{-2}\cdot\text{L}^{-1}$, and the value was significantly higher than that at sta. 6648 ($17.52 \times 10^{-12} \text{ W}\cdot\text{cm}^{-2}\cdot\text{L}^{-1}$). Sounding at sta. 6651 was carried out at the same time as at sta. 6679 (22:00–23:00), and the mean level of bioluminescence at sta. 6651 did not exceed $5.14 \times 10^{-12} \text{ W}\cdot\text{cm}^{-2}\cdot\text{L}^{-1}$. Fig. 3 shows mean profiles of bioluminescence, temperature, and salinity values obtained at sta. 6679 and 6651.

In the northwestern Weddell Sea, six stations were performed at different time of the day. The maximum level of bioluminescence ($25.65 \times 10^{-12} \text{ W}\cdot\text{cm}^{-2}\cdot\text{L}^{-1}$) was recorded at sta. 6650 at a 8-m depth. The minimum one ($15.99 \times 10^{-12} \text{ W}\cdot\text{cm}^{-2}\cdot\text{L}^{-1}$) was noted at sta. 6652 at a 58-m depth. The maximum mean level of bioluminescence in the studied water area was registered at sta. 6653 ($25.78 \times 10^{-12} \text{ W}\cdot\text{cm}^{-2}\cdot\text{L}^{-1}$). The vertical structure of bioluminescence at sta. 6650 and 6653 was multi-peaked, and the values were evenly distributed over the entire probing depth. At sta. 6652, a single-maximum vertical structure of bioluminescence was observed.

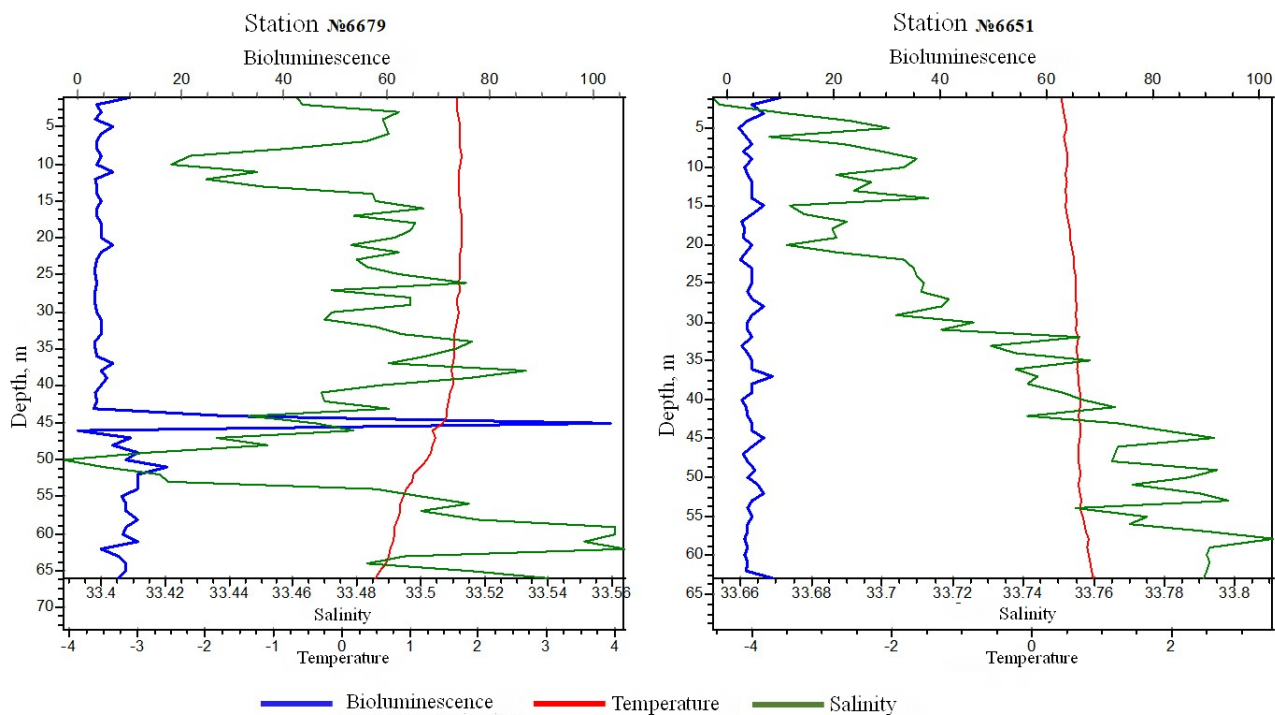


Fig. 3. Vertical profiles of temperature ($^{\circ}\text{C}$), salinity (‰), and bioluminescence ($\times 10^{-12} \text{ W}\cdot\text{cm}^{-2}\cdot\text{L}^{-1}$)

DISCUSSION

The results of this study convincingly showed that the method of multiple sounding with a hydro-biophysical complex “Salpa-M,” with simultaneous capture of biophysical and hydrological parameters at one station, is much more effective than other techniques [Kim et al., 2006] for analyzing the structure and extent of fields of luminescence. Among the existing methods for measuring bioluminescence signals in the water column (towing photometers, hanging them on a given horizon, probing certain layers, installing special devices on the bottom, *etc.*), towing and probing are recognized as the most promising and accurate ones [Biolymnestsiya v okeane, 1992]. Their advantage is the registration of bioluminescence by a bathyphotometer moving at a constant speed. Towing can only be used when the RV is moving (at a speed of no more than 4 knots) and on a limited number of horizons, usually in the range of the upper 10 m. The core of the sounding method is raising (or lowering) a bathyphotometer at a constant speed in a given layer (as a rule, the epipelagic or photic one) in the RV’s drift.

Thus, applying this method in Antarctic waters is a new opportunity to record the fields and structure of aggregations of krill, salp, and other luminescent organisms.

As found, in Antarctic, one of the main characteristics inherent in the vertical structure of fields of bioluminescent is their stratification which is determined both by the parameters of the pelagic community (species composition, chorological structure, and so on) and the features of water masses. The depth of the layer or layers of maximum luminescence intensity and their number are key characteristics of fields of bioluminescence as well. To date, there is lack of knowledge in the horizontal extent of layers of maximum luminescence intensity for the salp, the mosaic nature of its distribution

at the small-scale level, and the daily, inter-day, seasonal, and inter-annual variability of luminescence intensity. The analysis of this factor, new in the ecology of luminescent hydrobionts, involves carrying out horizontal tows with simultaneous biological sampling and acoustic sounding.

Conclusion. The method of multiple vertical sounding with the hydrobiophysical complex “Salpa-M” turned out to be quite effective in studying the structure and extent of fields of luminescence in Antarctic waters. In 2020, in the Antarctic area investigated, instead of krill fields, salp fields were observed, which may be associated with both climate change and active fishing. The krill creates fields of bioluminescence as continuous flashes of individual crustaceans. The salp forms a completely different field of bioluminescence: its vertical structure is a single-maximum one.

This work was carried out within the framework of IBSS state research assignment “Comprehensive studies of the current state of the ecosystem of the Atlantic sector of the Antarctic” (No. 121090800137-6) and “Structural and functional organization, productivity, and sustainability of marine pelagic ecosystems” (No. 121040600178-6).

Acknowledgement. The authors express their sincere gratitude to the crew and the captain of the RV “Akademik Mstislav Keldysh” for their effective assistance in carrying out this research.

REFERENCES

1. *Biolyuminescentsiya v okeane*. Saint Petersburg : Gidrometeoizdat, 1992, 283 p. (in Russ.)
2. Gitelson I. I. *Zhivoi svet okeana*. Moscow : Nauka, 1976, 120 p. (in Russ.)
3. Labas Yu. A., Gordeeva A. V. Nerazgadannaya Darwinom biolyuminescentsiya. *Priroda*, 2003, no. 2, pp. 25–31. (in Russ.)
4. Morozov E. G., Frey D. I., Polukhin A. A., Krechik V. A., Artemiev V. A., Gavrikov A. V., Kasian V. V., Sapozhnikov F. V., Gordeeva N. V., Kobylansky S. G. Mesoscale variability of the ocean in the northern part of the Weddell Sea. *Okeanologiya*, 2020, vol. 6, no. 5, pp. 663–679. (in Russ.). <https://doi.org/10.31857/S0030157420050184>
5. Samyshev E. Z. *Antarctic Krill and the Structure of the Plankton Community in Its Areal*. Moscow : Nauka, 1991, 168 p. (in Russ.). <https://repository.marine-research.ru/handle/299011/1462>
6. Spiridonov V. A., Uryupova E. F. Antarktika i Yuzhnyi okean segodnya: k pyatidesyatoi godovshchine Dogovora ob Antarktike. *Rossiya v okruzhayushchem mire*, 2009, no. 12, pp. 125–150. (in Russ.)
7. Tokarev Yu. N., Sokolov B. G. Effect of physical and biological factors on forming of small-scale structure of bioluminescent and acoustic fields in the Black and Mediterranean seas. *Gidrobiologicheskii zhurnal*, 2001, vol. 37, no. 2, pp. 3–13. (in Russ.)
8. Tokarev Yu. N. *Osnovy biofizicheskoi ekologii gidrobiontov*. Sevastopol : EKOSI-Gidrofizika, 2006, 342 p. (in Russ.). <https://repository.marine-research.ru/handle/299011/9076>
9. Tokarev Yu. N., Evstigneev P. V., Mashukova O. V. *Planktonnye biolyuminescenty Mirovogo okeana: vidovoe raznoobrazie, kharakteristiki svetoizlucheniya v norme i pri antropogennom vozdeistvii*. Simferopol : N.Orianda, 2016, 347 p. (in Russ.). <https://repository.marine-research.ru/handle/299011/7926>
10. Harvey E. N. *A History of Luminescence from the Earliest Times Until 1900*. Philadelphia : American Philosophical Society, 1957, 692 p. (Series: Memoirs of the American Philosophical Society ; vol. 44). <https://doi.org/10.5962/bhl.title.14249>
11. Kim G., Lee Y.-W., Joung D.-J., Kim K.-R., Kim K. Real-time monitoring of nutrient concentrations and red-tide outbreaks in the southern

- sea of Korea. *Geophysical Research Letters*, 2006, vol. 33, iss. 13, art. no. L13607 (4 p.). <https://doi.org/10.1029/2005GL025431>
12. Nicol S., Constable A. J., Pauly T. Estimates of circumpolar abundance of Antarctic krill based on recent acoustic density measurements. *CCAMLR Science*, 2000, vol. 7, pp. 87–99. <https://www.ccamlr.org/ru/node/72892>
13. Nicol S., Foster J. The fishery for Antarctic krill: Its current status and management regime. In: *Biology and Ecology of Antarctic Krill*. Cham, Switzerland : Springer, 2016, pp. 387–421. https://doi.org/10.1007/978-3-319-29279-3_11
14. Sprong I., Schalk P. H. Acoustic observations on krill spring–summer migration and patchiness in the northern Weddell Sea. *Polar Biology*, 1992, vol. 12, iss. 2, pp. 261–268. <https://doi.org/10.1007/BF00238268>

ИСПОЛЬЗОВАНИЕ МЕТОДА ВЕРТИКАЛЬНОГО ЗОНДИРОВАНИЯ ДЛЯ РЕГИСТРАЦИИ БИОЛЮМИНЕСЦЕНЦИИ В АНТАРКТИЧЕСКОМ СЕКТОРЕ АТЛАНТИЧЕСКОГО ОКЕАНА

Л. А. Мельник, А. В. Мельник, О. В. Машукова, В. В. Мельников

ФГБУН ФИЦ «Институт биологии южных морей имени А. О. Ковалевского РАН»,

Севастополь, Российская Федерация

E-mail: melniklidi@gmail.com

Биоломинесценция — существенный элемент функционирования пелагического сообщества, что связано с важнейшей экологической ролью света в жизни гидробионтов, в том числе в формировании их пространственной неоднородности. Свечение морских гидробионтов — это проявление их жизнедеятельности в форме электромагнитного излучения в видимой области спектра, кинетические закономерности которого тесно связаны с механизмом порождающих их химических реакций и процессов метаболизма. Глобальное потепление, охватившее и Атлантический сектор Антарктики, вызвало серьёзные структурно-функциональные изменения пелагического сообщества, которые отражаются на морской биоломинесценции — экспрессивном показателе состояния среды. Целью работы было изучить возможность применения метода многократного вертикального зондирования гидробиофизическим комплексом «Сальпа-М» с одновременной фиксацией биофизических и гидрологических параметров на одной станции для исследования структуры и протяжённости полей свечения антарктических вод. В статье представлены метод изучения структурных характеристик биоломинесценции и материалы, полученные во время 79-й антарктической экспедиции на НИС «Академик Мстислав Келдыш». Суть метода зондирования состоит в подъёме (или опускании) батифотометра «Сальпа-М» с постоянной скоростью в заданном слое [обычно это верхний продуктивный (0–200 м) или фотический (0–100 м) слой] в дрейфе судна. Планктонные биоломинесцентцы, вносящие основной вклад в формирование биоломинесцентного потенциала пелагиали, высвечиваются, как правило, только при раздражении. Именно поэтому движущийся с постоянной скоростью батифотометр создаёт стандартный уровень их механического раздражения, что позволяет корректно сравнивать результаты измерений вертикальной структуры поля биоломинесценции, выполняемых в разных регионах и при различных погодных условиях (качка, ветровой снос и т. д.). В работе представлен набор данных об интегральном биоломинесцентном сигнале на разных горизонтах. На 18 гидрографических станциях в исследуемой акватории Атлантического сектора Антарктики были получены первичные данные интенсивности биоломинесценции, значений температуры, электропроводности и фотосинтетически активной радиации. В статье рассмотрен важный вопрос, который связан с изменением биоломинесценции морской воды в Атлантическом секторе Антарктики, изученной методом вертикального зондирования на разных уровнях с помощью биоломинесцентного зонда. При исследовании биоломинесценции выполняли определение вертикальной изменчивости свечения в верхнем продуктивном слое в связи с особенностями распределения планктона. В результате было установлено, что свечение антарктических вод в фотическом слое этого

района происходит в пределах от $8,4 \times 10^{-12}$ до $104,42 \times 10^{-12}$ Вт·см⁻²·л⁻¹. Пики биолюминесценции (до 104×10^{-12} Вт·см⁻²·л⁻¹) фиксировали под термоклином на глубине 45 м в зонах концентрации сальпы *Salpa thompsoni* Foxton, 1961 вблизи гидрологического фронта, на расстоянии около 6–7 миль по обе стороны от него. Показано, что метод вертикального зондирования в антарктических водах даёт возможность экспресс-регистрации полей и структуры скопления светящихся организмов.

Ключевые слова: интенсивность биолюминесценции, Атлантический сектор Антарктики, фотический слой, вертикальное зондирование, планктон

UDC 597.2/.5-15(282.257.6)

THE STRUCTURE OF COASTAL ICHTHYOPLANKTON IN THE AREA OF THE DUDINKA RIVER CONFLUENCE (EASTERN SAKHALIN)

© 2023 O. N. Mukhametova

Sakhalin Branch of the Russian Federal Research Institute of Fisheries and Oceanography (SakhNIRO),
Yuzhno-Sakhalinsk, Russian Federation
E-mail: olga.sakhniro@gmail.com

Received by the Editor 06.11.2021; after reviewing 12.06.2022;
accepted for publication 04.08.2023; published online 01.12.2023.

The structure of ichthyoplankton complex and features of early fish ontogeny were analyzed in the coastal area off the Eastern Sakhalin. The study area is characterized by strong variations of temperature and salinity in May–July. Minimum temperature (+0.4 °C) was registered at a depth of 20 m in May, and maximum one (+15.7 °C) was recorded at a depth of 3 m in September. During the entire study period, salinity varied from 3.5 PSU in littoral zone close to the Dudinka River mouth to 31 PSU at a depth of 13–20 m. Eggs and larvae of 17 fish species from 5 families, typical for the Eastern Sakhalin, were identified in ichthyoplankton. Pleuronectidae species prevailed in taxonomic list with ratio of 71%. *Gadus chalcogrammus* eggs and larvae (71% of total value) prevailed in the second decade of May; *Clupea pallasii* bottom eggs (70%), in the third decade of May; and Pleuronectidae eggs and larvae (91–100%), in June–September. Mean ichthyoplankton abundance decreased from 52 ind. \cdot m⁻³ in littoral zone to 21–22 ind. \cdot m⁻³ above depths of 5–10 m and 13 ind. \cdot m⁻³ above 20 m. The proportion of dead *G. chalcogrammus* eggs and Pleuronectidae eggs did not exceed the values obtained for the Northeastern Sakhalin and was lower than in Aniva Bay. In May, the proportion of *G. chalcogrammus* and *Hippoglossoides robustus* prelarvae with pathologies increased. It could be caused by the development of eggs at late stages in adverse conditions. Maximum species diversity was observed in June. Seventy-seven percent of cumulative abundance was composed by eggs of four species, *G. chalcogrammus*, *H. robustus*, *Myzopsetta punctatissima*, and *Limanda aspera*.

Keywords: fish eggs, fish larvae, ichthyoplankton, abundance, species diversity, Eastern Sakhalin

Southeastern Sakhalin waters are inhabited by more than 100 fish species [Dyldin et al., 2021], and out of them, 79 are found in trawl catches. In terms of the number of species (16) and biomass (up to 47–60% of the total value), righteye flounders Pleuronectidae Rafinesque, 1815 prevail. Codfishes Gadidae Rafinesque, 1810 and sculpins Cottidae Bonaparte, 1831 have a high biomass as well (up to 32–44% and 6–11%, respectively). The abundance of species with a long life cycle – the Alaska pollock *Gadus chalcogrammus* Pallas, 1814, the Bering flounder *Hippoglossoides robustus* Gill & Townsend, 1897, the yellowfin sole *Limanda aspera* (Pallas, 1814), the Sakhalin sole *Limanda sakhalinensis* Hubbs, 1915, and the starry flounder *Platichthys stellatus* (Pallas, 1787), as well as sculpins of the genus *Myoxocephalus* Tilesius, 1811 – can remain relatively stable for a long time [Shuntov, Temnykh, 2018; Shuntov et al., 1993]. The abundance of species with a shorter cycle – the Pacific herring *Clupea pallasii* Valenciennes, 1847, the Far Eastern capelin

Mallotus villosus (Müller, 1776), the saffron cod *Eleginus gracilis* (Tilesius, 1810), and the Japanese anchovy *Engraulis japonicus* Temminck & Schlegel, 1846 (a migrant fish) – experiences significant fluctuations [Davydova, 1994; Velikanov, 2006].

In the Southeastern Sakhalin coastal areas, ichthyoplankton is formed both by eggs and larvae of marine fish species occurring in shallow waters because of drift and by resident species reproducing off the coast. For many years, off the eastern coast of Sakhalin, only research vessel studies of ichthyoplankton were carried out during the hydrological spring (May–June); these investigations were aimed at assessing the stocks of *G. chalcogrammus* and less often *H. robustus*. Off the southeastern coast of Sakhalin Island, the largest spawning grounds for these species are located in the Terpeniya Bay. The main egg aggregations are formed both in the central bay above isobaths of 60–70 m [Shuntov et al., 1993; Tarasyuk, Pushnikov, 1982; Zverkova, 2003] and north of N48° off the western coast [Moukhametov, Chastikov, 2013]. *G. chalcogrammus* and *H. robustus* spawning coincides in time and space [Moukhametov, Chastikov, 2015; Mukhametov, Mukhametova, 2017]. Drift of eggs and larvae of these two species has a similar direction, and increases in their concentrations in coastal areas usually occur simultaneously [Mukhametova, 2020a, b].

During the warm period of the year, the role of shallow waters in fish reproduction increases. The coastal area of Southeastern Sakhalin becomes a spot for formation of spawning aggregations of many Pleuronectidae, *Cl. pallasii*, *M. villosus*, and the Japanese smelt *Hypomesus japonicus* (Brevoort, 1856) [Kim Sen Tok, 2011]. The mean abundance of ichthyoplankton can be high, 300–400 ind.·m⁻³ and more [Moukhametova, Moukhametov, 2013]. In the area of the southeastern coast between N46° and N48°, eggs and larvae of 37 species from 14 families were identified in ichthyoplankton. Due to a rise in the diversity and abundance of fish in the Terpeniya Bay [Kim Sen Tok, 2002], there was an increase in species diversity and abundance of fish from south to north, mainly due to representatives of Pleuronectidae. Similar changes were noted in ichthyoplankton. The total concentrations of ichthyoplankton and the proportion of Pleuronectidae rose in a northerly direction. With a generally high abundance of eggs of the longsnout flounder *Myzopsetta punctatissima* (Steindachner, 1879) south of N47°, the predominant forms also included eggs and larvae of *Pl. stellatus* and *E. japonicus*. The maximum abundance of ichthyoplankton was recorded in August. North of N47°, eggs and larvae of *G. chalcogrammus*, *H. robustus*, *Cl. pallasii*, and *L. aspera* dominated. This area, in comparison with the southern one, was characterized by the fact that the peak abundance of ichthyoplankton was shifted to May–June [Mukhametova, 2014, 2020a, b].

Despite the high significance of shallow areas of the Southeastern Sakhalin in the reproduction of coastal and marine fish, data on the development of their eggs and larvae are scarce. The aim of this work is to describe ichthyoplankton in a coastal area off the eastern Sakhalin Island, at the confluence of the Dudinka River. The objectives of the research included studying seasonal changes in ichthyoplankton species composition, abundance, and diversity, as well as the development of eggs and larvae of abundant fish species depending on the environmental conditions.

MATERIAL AND METHODS

Ichthyoplankton was sampled in the inshore site at the confluence of the Dudinka River from May to October 2020. For sampling, an ichthyoplankton conical net (50 cm in diameter) with an inlet area of 0.2 m² and a mesh of 0.35 mm was used [Rass, Kazanova, 1966]. The stations were located at isobaths of 0–0.5 m (littoral), 5 m, 10 m, and 20 m. From the second decade of May to late June, during mass

spawning of coastal fish species, surveys were carried out every ten days. In July, due to bad weather conditions, there were two surveys – in the second and third decades. From August to October, sampling was carried out monthly. Once a calendar season, samples were taken from four sections (in the second decade of May, in the third decade of July, and in October); in other periods, from two central sections (Fig. 1). A total of 104 ichthyoplankton samples were taken in 10 surveys.

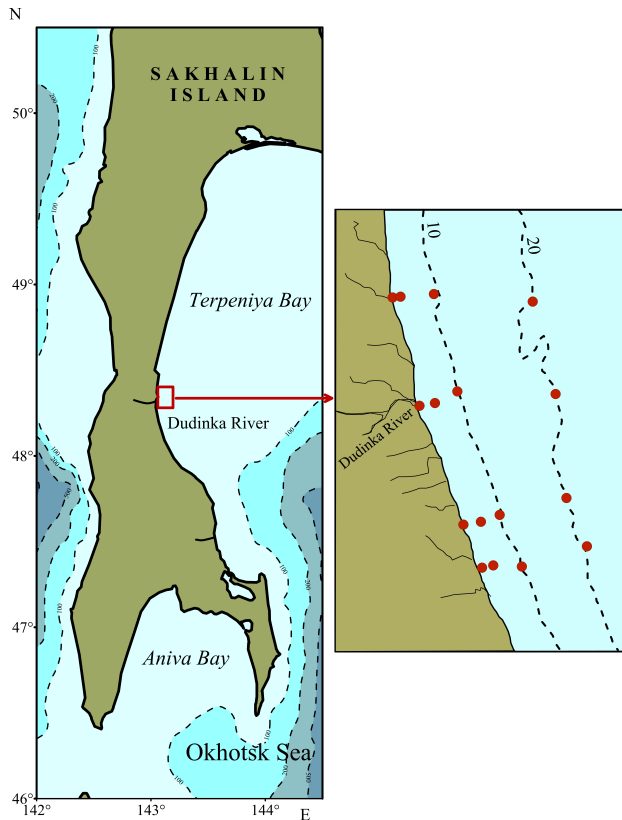


Fig. 1. Scheme of ichthyoplankton sampling in the inshore site at the confluence of the Dudinka River in 2020

Above depths of 5–20 m, the ichthyoplankton net was lifted from a motor boat vertically from the bottom to the surface. In the littoral zone, 100 L of seawater were poured through the net [Rukovodstvo po metodam, 1983]. Samples were fixed with 4% formaldehyde solution.

For vertical catches, ichthyoplankton abundance was calculated *per* 1 m³ by the formula:

$$N = (n \times 5) / S ,$$

where N is ichthyoplankton abundance in 1 m³, ind.·m⁻³;

n is ichthyoplankton abundance in the catch, ind.;

S is the distance covered by the net, m;

5 is the coefficient for reducing the net inlet area to 1 m².

During sampling in the littoral zone, the abundance was determined by the formula:

$$N = n \times 10 ,$$

where N is ichthyoplankton abundance, ind.·m⁻³;

n is ichthyoplankton abundance in the catch, ind.;

10 is the coefficient for reducing the abundance to 1 m³.

At each station, YSI Model 85 probe was used to measure temperature, salinity, and oxygen concentration from the surface to the bottom with a resolution of 1 m. Oxygen was measured only in May–June. For the analysis, we used temperature and salinity values averaged for each survey in the layer from the bottom to the surface, in the surface and near-bottom horizons. Data on wind direction and force were taken from the weather archive of the website <https://rp5.ru/> [2021].

Ichthyoplankton samples were processed in a laboratory under an Olympus SZX10 binocular equipped with an eyepiece micrometer. Eggs and larvae of each species were measured to the nearest 0.01 mm. The stages of egg development were determined according to conventional methods [Rass, Kazanova, 1966]. When identifying disorders in embryos and larvae, we were guided by descriptions of normal development and pathologies in the early fish ontogeny [Davydova, 1994; Pertseva-Ostroumova, 1961].

The taxonomy of species is given in accordance with the WoRMS database [2021]. To identify dominance classes, the Lubarsky scale was used. According to it, species with a relative abundance of 64–100% were absolute dominants; 36–64%, dominants; and 16–36%, subdominants [Bakanov, 2005]. The period when the total proportion of eggs and larvae of a given species accounted for at least 50% of all studied species was considered as the time of mass spawning of fish and development of the early stages of ontogenesis.

For statistical processing, MS Office Excel data analysis package was used. To assess the significance of the difference between the means, the Student's *t*-test was applied.

Based on the data obtained on ichthyoplankton species composition and abundance, a dominance–diversity curve was constructed [Odum, 1983; Whittaker, 1975], and ecological indices were calculated [Margalef, 1958; Pielou, 1966; Shannon, Weaver, 1949; Simpson, 1949] (Table 1).

Table 1. Indices of biodiversity used for the description of ichthyoplankton

| Index | Calculation | Designations | References |
|--------------------------|---|---|--------------------------------------|
| Shannon–Wiener diversity | $H = -\sum p_i \times \log_2 p_i$ | p_i is the proportion of the <i>i</i> -th species in abundance | Odum, 1983; Shannon, Weaver, 1949 |
| Pielou's evenness | $E = \frac{H}{\log_2 S}$ | H is the Shannon–Wiener diversity index; S is the number of species | Odum, 1983; Pielou, 1966 |
| Simpson's diversity | $D = \sum_i^s \left(\frac{n_i}{N}\right)^2$ | n_i is the abundance of the <i>i</i> -th species; N is the total abundance | Odum, 1983; Simpson, 1949 |
| Margalef's diversity | $D_{Mg} = (S - 1) / \ln N$ | S is the number of species; N is the total abundance of individuals | Margalef, 1958; Odum, 1983 |

RESULTS AND DISCUSSION

The ecosystem of the Terpeniya Bay, *inter alia* ichthyoplankton transport, is structurally affected by waters of the East Sakhalin Current penetrating from the east, a complex system of eddies, and an alongshore current off the western coast, mainly of the south direction [Pak et al., 2017; Shevchenko et al., 2020]. In the Dudinka River vicinity, as well as in the previously studied inshore sites located to the south, there was a noticeable variability in environmental parameters, especially

in the spring hydrological season. It was due to the mixing of warmer desalinated surface water with colder and saltier seawater from the bottom horizons, which results from coastal upwellings and downwellings formed under the effect of offshore western winds and surge eastern winds [Shevchenko et al., 2021]. Apparently, the formation of coastal flows is affected mainly by southeastern and eastern winds and an alongshore current with a meridional orientation [Shevchenko et al., 2021].

During the ichthyoplankton surveys, the temperature averaged for the entire water column, increased from +5.8 °C in May to +13.3 °C in October with an approximation reliability value (R^2) of 0.92. Until August, water warming occurred simultaneously with an increase in air temperature with a correlation coefficient (R) equal to 0.93. The absolute minimum for the study period (+0.4 °C) was recorded at a depth of 20 m in May, and the maximum (+15.7 °C) was registered at a depth of 3 m in September. Throughout the study period, reduced salinity values were noted in the water area, on average 26.2–30.4 PSU. The minimum (3.5 PSU) was observed in the first decade of June at the Dudinka River mouth; the maximum (31 PSU and more), at the bottom, at a depth of 13–20 m. A trend towards a decrease in salinity was revealed at the height of the flood, from late May to early June ($R^2 = 1$), and during the flood period, in September–October ($R^2 = 0.93$) [Onishchenko, 1987]. Strong desalination affected mainly the mouth areas, where eggs and larvae of euryhaline fish species with bottom eggs develop, such as *H. japonicus*, *M. villosus*, and *Cl. pallasii*. At the same time, significant temperature fluctuations were recorded throughout the studied inshore site on spawning grounds and in nursery areas of both coastal and marine fish. Because of the formation of coastal upwellings under the effect of southwestern winds, there were cases of sharp drops in temperature – to subzero values in May and from +12 °C to +2...+3 °C in July. Eastern winds prevailing in spring cause additional transport of eggs and larvae of marine species to the coastal area. A positive relationship was found between the mean ichthyoplankton abundance and northern and eastern winds ($R = 0.69$). A negative relationship was revealed with the predominance of winds of the southeast–west section ($R = -0.65$). Ichthyoplankton abundance also depended on wind speed ($R = 0.64$). Maximum density values of ichthyoplankton at depths of 0–0.5 m were recorded in May–June during the predominance of northern and eastern winds and at the highest average speeds, 3.9–4.5 m·s⁻¹. The obtained correlation coefficients indicate a significant effect of wind transport of ichthyoplankton in the study area and the predominance of transport from the north–east section.

Fluctuations in temperature and salinity, as well as the effect of shockwaves, including a swell typical for this area, are not optimal conditions for the development of planktonic communities, in particular, pelagic eggs and early fish larvae [Pertseva-Ostroumova, 1961; Tarasyuk, 1994]. A factor positively affecting ichthyoplankton structure in the Dudinka River area can be the proximity to the vast shelf protected from the east by the Terpeniya Peninsula, which is characterized by better warming than open southern areas [Lozhkin et al., 2018; Shevchenko et al., 2020]. The East Sakhalin Current branch flowing into the Terpeniya Bay and the powerful Poronay River flowing along the western coast [Pak et al., 2017] contribute to the supply of nutrients into the water column. This results in high phytoplankton biomass [Mukhametova et al., 2022], which serves as the starting food for fish larvae [Kim Sen Tok et al., 2017] and increases productivity of organisms representing other trophic levels – zooplankton, benthos, and fish.

Fish eggs and larvae were recorded in the inshore site in the confluence of the Dudinka River from May to September. In total, 17 fish species from 5 families were identified in ichthyoplankton. In addition to pelagic eggs, the catches included bottom eggs of the Pacific herring *Cl. pallasii*

and the crested flounder *Pseudopleuronectes schrenki* (Schmidt, 1904). The occurrence of bottom eggs in the water column is common for species with littoral spawning grounds – *Cl. pallasii*, *M. villosus*, *H. japonicus*, and the Japanese icefish *Salangichthys microdon* (Bleeker, 1860) – during their mass spawning [Mukhametova, 2020b; Mukhametova, Balanov, 2013]. By the number of species (12; $\approx 71\%$ of the taxonomic composition), representatives of the family Pleuronectidae prevailed. In October, there was no ichthyoplankton in the catches. The period of the increased species abundance lasted from May to late July and was accompanied by minor fluctuations: the number of species was 7–10. Except for several low-boreal flounder species [the yellow striped flounder *Pseudopleuronectes herzensteini* (Jordan et Snyder, 1901), the Black plaice *Pseudopleuronectes obscurus* (Herzenstein, 1890), *Ps. schrenki*, and *M. punctatissima*], characteristic of ichthyocenes and ichthyoplankton complexes of the southern Sea of Okhotsk and the Tatar Strait, identified species were typical for the Eastern Sakhalin shelf. Many Pleuronectidae species were represented by both eggs and larvae.

In May, the maximum ichthyoplankton abundance, $61.17 \text{ ind.}\cdot\text{m}^{-3}$, was observed (Table 2). Same month, the highest heterogeneity in its spatial distribution was noted, due to the predominance of adventive, marine species (mainly eggs of *G. chalcogrammus* and *H. robustus*) and low intensity of fish spawning in shallow waters. The standard deviation in May was twice the mean ichthyoplankton abundance. In June–August, the development of spawning of flounders representing the coastal complex resulted in a more even distribution of catches. However, variations in the abundance of eggs and larvae by stations remained quite high throughout the study period. A significant decrease in concentrations began in August against the backdrop of the completion of spawning of pelagophilic fish.

Table 2. Species composition, abundance, and indices of the ichthyoplankton species diversity in the in-shore site at the confluence of the Dudinka River in 2020 (numerator denotes eggs, % of the total abundance of eggs; denominator denotes larvae, % of the total abundance of larvae)

| Taxon | May | June | July | August | September | Mean for the entire period, % |
|---|-----------------------|---------------------|---------------------|-------------------|------------------|-------------------------------|
| Clupeidae | | | | | | |
| Pacific herring <i>Clupea pallasii</i> Valenciennes, 1847 | $\frac{12.67}{0.79}$ | $\frac{1.63}{0}$ | – | – | – | $\frac{7.50}{0.30}$ |
| Gadidae | | | | | | |
| Alaska pollock <i>Gadus chalcogrammus</i> Pallas, 1814 | $\frac{61.03}{62.88}$ | $\frac{3.75}{1.96}$ | $\frac{1.55}{0}$ | $\frac{3.28}{0}$ | – | $\frac{35.47}{24.15}$ |
| Cottidae | | | | | | |
| Elegant sculpin <i>Bero elegans</i> (Steindachner, 1881) | – | $\frac{0}{39.22}$ | – | – | – | $\frac{0}{8.00}$ |
| Threaded sculpin <i>Gymnocanthus pistilliger</i> (Pallas, 1814) | $\frac{0}{0.40}$ | – | – | – | – | $\frac{0}{0.15}$ |
| Liparidae | | | | | | |
| Striped seasnail <i>Liparis latifrons</i> Schmidt, 1950 | $\frac{0}{0.40}$ | – | – | – | – | $\frac{0}{0.15}$ |
| Pleuronectidae | | | | | | |
| Blackfin flounder <i>Glyptocephalus stelleri</i> (Schmidt, 1904) | – | – | $\frac{1.70}{0.75}$ | $\frac{21.31}{0}$ | $\frac{2.22}{0}$ | $\frac{1.05}{0.30}$ |

Continue on the next page...

| Taxon | May | June | July | August | September | Mean for the entire period, % |
|--|-----------------------|----------------------|-----------------------|-------------------|------------------------|-------------------------------|
| Bering flounder <i>Hippoglossoides robustus</i> Gill & Townsend, 1897 | $\frac{25.33}{34.76}$ | $\frac{0.12}{1.96}$ | – | – | – | $\frac{14.24}{13.53}$ |
| Yellowfin sole <i>Limanda aspera</i> (Pallas, 1814) | – | $\frac{23.46}{0.98}$ | $\frac{12.33}{67.41}$ | $\frac{75.41}{0}$ | $\frac{97.78}{100.00}$ | $\frac{11.52}{28.99}$ |
| Sakhalin sole <i>Limanda sakhalinensis</i> Hubbs, 1915 | – | $\frac{4.81}{0}$ | $\frac{0.30}{0}$ | – | – | $\frac{1.21}{0}$ |
| Far Eastern smooth flounder <i>Liopsetta pinnifasciata</i> (Kner, 1870) | $\frac{0}{0.77}$ | – | – | – | – | $\frac{0}{0.29}$ |
| Longhead dab <i>Myzopsetta proboscidea</i> (Gilbert, 1896) | – | $\frac{5.18}{0.98}$ | – | – | – | $\frac{1.25}{0.20}$ |
| Longsnout flounder <i>Myzopsetta punctatissima</i> (Steindachner, 1879) | $\frac{0.35}{0}$ | $\frac{27.61}{6.86}$ | $\frac{81.72}{31.09}$ | – | – | $\frac{18.98}{13.84}$ |
| Starry flounder <i>Platichthys stellatus</i> (Pallas, 1787) | $\frac{0.44}{0}$ | $\frac{3.79}{15.69}$ | $\frac{0.30}{0}$ | – | – | $\frac{1.21}{3.20}$ |
| Alaska plaice <i>Pleuronectes quadrituberculatus</i> Pallas, 1814 | $\frac{0.15}{0}$ | – | – | – | – | $\frac{0.08}{0}$ |
| Yellow striped flounder <i>Pseudopleuronectes herzensteini</i> (Jordan et Snyder, 1901) | $\frac{0.03}{0}$ | $\frac{10.07}{2.94}$ | $\frac{2.10}{0.75}$ | – | – | $\frac{2.76}{0.90}$ |
| Black plaice <i>Pseudopleuronectes obscurus</i> (Herzenstein, 1890) | – | $\frac{0}{23.53}$ | – | – | – | $\frac{0}{4.80}$ |
| Cresthead flounder <i>Pseudopleuronectes schrenki</i> (Schmidt, 1904) | – | $\frac{19.58}{5.88}$ | – | – | – | $\frac{4.73}{1.20}$ |
| Eggs, ($M \pm \sigma$) ind.·m ⁻³ | 59.21 ± 126.2 | 23.54 ± 15.81 | 15.65 ± 14.41 | 3.81 ± 4.13 | 1.41 ± 2.02 | 21.11 ± 23.31 |
| Larvae, ($M \pm \sigma$) ind.·m ⁻³ | 1.97 ± 1.49 | 0.80 ± 0.92 | 2.09 ± 3.40 | – | 0.09 ± 0.14 | 0.99 ± 1.00 |
| Total ichthyoplankton, ($M \pm \sigma$) ind.·m ⁻³ | 61.17 ± 125.89 | 26.60 ± 16.46 | 17.73 ± 15.03 | 3.81 ± 4.13 | 1.50 ± 2.16 | 22.10 ± 24.10 |
| Number of species | 10 | 12 | 7 | 3 | 2 | 17 |
| Indices | | | | | | |
| Shannon–Wiener diversity | 1.393 | 2.837 | 1.092 | 0.944 | 0.146 | – |
| Pielou's evenness | 0.419 | 0.791 | 0.389 | 0.596 | 0.146 | – |
| Simpson's diversity | 0.454 | 0.177 | 0.610 | 0.615 | 0.959 | – |
| Margalef's diversity | 2.188 | 3.353 | 2.087 | 1.494 | 2.466 | – |

The greatest contributors to the total abundance of ichthyoplankton were Pleuronectidae representatives, which dominated most of the study period. A decrease in their proportion was revealed only in May: in the second decade, with the high concentration of *G. chalcogrammus* eggs, and in the third decade, with the massive appearance of *Cl. pallasii* bottom eggs in the water column.

Throughout the study, fish eggs accounted for 88–100% of the total abundance of ichthyoplankton. In different periods, the predominating forms (absolute dominants, dominants, and subdominants) were eggs of the Alaska pollock *G. chalcogrammus*, *H. robustus*, *M. punctatissima*, the yellowfin sole *L. aspera*, and the blackfin flounder *Glyptocephalus stelleri* (Schmidt, 1904). In May, eggs of *G. chalcogrammus* prevailed, accounting for 61% of the total abundance of eggs. In June, against the backdrop of a rise

in spawning intensity of coastal species of the family Pleuronectidae, the dominant group included *M. punctatissima* eggs (39%). In July, *M. punctatissima* eggs accounted for 82% of all fish eggs recorded. In August and September, eggs of *L. aspera* were the absolute dominant, 75 and 98%, respectively.

The larval composition was dominated mainly by species with a high abundance of eggs: *G. chalcogrammus* and *H. robustus* in May; *Pl. stellatus* in June; and *L. aspera* and *M. punctatissima* in July and September. In June, the larval composition was characterized by an increase in abundance of sublittoral species with bottom and benthic eggs – the elegant sculpin *Bero elegans* (Steindachner, 1881) (39% of the total abundance of larvae) and *Ps. obscurus* (24%). In May and June, the proportion of larvae in the total abundance of ichthyoplankton remained at the level of 3%. In July, a rise up to 12%, caused by mass hatching of *L. aspera* and *M. punctatissima*, was registered. An increase in the concentration of eggs of these species began in the previous period. The mean abundance of *M. punctatissima* eggs rose from 0.2 ind. \cdot m⁻³ in May to 7.1 ind. \cdot m⁻³ in June and 12.8 ind. \cdot m⁻³ in July. In May, there were no *L. aspera* eggs; in June and July, their abundance was 2.1 and 1.9 ind. \cdot m⁻³, respectively.

By the number of species, the Dudinka River area was inferior to coastal waters south of N48°, where the taxonomic list could include eggs and larvae of 20–23 fish species, due to the reproduction of southern migrants in summer [Mukhametova, 2014]. At the same time, the abundance of eggs and larvae of *G. chalcogrammus* and many Pleuronectidae at the confluence of the Dudinka River was significantly higher due to the proximity of this area to the main spawning grounds located to the northeast of the inshore site [Kim Sen Tok, 2011; Zverkova, 2003]. In the Dudinka River area, the abundance of *G. chalcogrammus* eggs averaged for May–October exceeded that in the area of the Dolinka River, which is located 50 km to the south, by more than 100 times, while the abundance of larvae was more than 1,000 times higher. The abundance of *H. robustus* eggs was 7 times higher, and the abundance of its larvae was 32 times higher. The abundance of *L. aspera* eggs and larvae was 19 and 161 times higher, respectively. The mean abundance of *Pl. stellatus* eggs exceeded its concentration in the Dolinka River area by 248 times; *M. punctatissima* eggs, by 8 times; and *L. sakhalinensis* eggs, by 11 times. Interestingly, larvae of these species were not revealed in the Dolinka River area.

For species represented in ichthyoplankton in the Dudinka River vicinity, typical spawning is the one under conditions of sea salinity, except for *Cl. pallasii*, whose spawning occurs in a wide range of salinity, and *L. pinnifasciata*, whose eggs tolerate slight desalination [Pertseva-Ostroumova, 1961]. Sexually mature individuals of several coastal flounder species (*Pl. stellatus*, *L. obscura*, and *M. punctatissima*) can be found in highly desalinated areas, but their eggs and larvae develop only at sea salinity.

In Southeastern Sakhalin, spawning and the maximum abundance of larvae of most fish occur in the hydrological spring, a period of good food supply (phytoplankton and larval forms of invertebrates). A slow increase in water temperature in the coastal area of Southeastern Sakhalin [Shevchenko et al., 2021] is the reason for the prolonged hydrological spring – from early May to late July [Pishchalnik, Bobkov, 2000]. At the same time, the warming of shallow areas, which affects the timing of mass spawning of fish, may differ from the long-term average one for a period from 8–10 days to 3–4 weeks [Lozhkin et al., 2018]. Accordingly, it is quite difficult to establish clear boundaries of biological seasons. Off the southeastern coast of Sakhalin, the summer composition of ichthyoplankton can be formed from late June to late July [Mukhametova, 2020a, b]. Depending on the geographic location of the area, the spawning period and the number of seasonal spawning groups for the same species can vary significantly. Among Pleuronectidae representatives, an increase in the number of such groups was recorded from north to south [Dyakov, 2011].

In the inshore site at the confluence of the Dudinka River, four groups of species were distinguished based on the seasonality of spawning and the presence of eggs and larvae in plankton (Table 3).

Table 3. Ecological groups of ichthyoplankton in the inshore site at the confluence of the Dudinka River in 2020 (grey cells show the period of occurrence; red cells show the periods of maximum concentrations of eggs and larvae; numerator denotes the proportion of total eggs of the species; denominator denotes the proportion of larvae)

| Taxon | Stage of development | Habitat characteristic | Biotope | Bio-geographical region | Hydrological season | | | | | | | | | |
|--|----------------------|------------------------|---------|-------------------------|---------------------------|---------------------------|---------------------------|---------------------------|---------------------------|---------------------------|---------------------------|---------------------------|---------------------------|--|
| | | | | | Spring | | | | | | | Summer | | |
| | | | | | V | | VI | | | VII | | VIII | IX | |
| | | | | | 2 nd decade | 3 rd decade | 1 st decade | 2 nd decade | 3 rd decade | 2 nd decade | 3 rd decade | 3 rd decade | 2 nd decade | |
| Winter-spring spawning | | | | | | | | | | | | | | |
| <i>Gymnocanthus pistilliger</i> | larvae | coastal | SL | AB | 100 | | | | | | | | | |
| <i>Liopsetta pinnifasciata</i> | larvae | coastal | SL | LB | 100 | | | | | | | | | |
| <i>Liparis latifrons</i> | larvae | marine | EL | WB | 100 | | | | | | | | | |
| <i>Pleuronectes quadrituberculatus</i> | eggs | marine | EL | WB | 100 | | | | | | | | | |
| Spring spawning | | | | | | | | | | | | | | |
| <i>Hippoglossoides robustus</i> | eggs, larvae | marine | EL | AB | 99.7 95.6 | 0.3 4.4 | | | | | | | | |
| <i>Gadus chalcogrammus</i> | eggs, larvae | marine | EL | WB | 95.4 97.5 | | 3.8 2.5 | | 0.6 0 | | 0.2 0 | | | |
| <i>Clupea pallasii</i> | eggs, larvae | coastal | N | AB | 92.0 100 | | 8.0 0 | | | | | | | |
| <i>Pseudopleuronectes obscurus</i> | larvae | coastal | SL | LB | | 100 | | | | | | | | |
| <i>Pseudopleuronectes schrenki</i> | eggs, larvae | coastal | EL | LB | | | 100 100 | | | | | | | |
| <i>Bero elegans</i> | larvae | coastal | SL | LB | | | | 100 | | | | | | |
| <i>Myzopsetta proboscidea</i> | eggs, larvae | coastal | SL | HB | | | | 100 100 | | | | | | |
| <i>Limanda sakhalinensis</i> | eggs | coastal | EL | WB | | | 90.1 | | 9.9 | | | | | |
| <i>Platichthys stellatus</i> | eggs, larvae | coastal | SL | AB | 14.8 0 | | 82.5 87.5 | | 2.7 12.5 | | | | | |
| <i>Pseudopleuronectes herzensteini</i> | eggs, larvae | coastal | SL | LB | | 0.4 0 | 91.8 75.0 | | 7.8 25.0 | | | | | |
| <i>Myzopsetta punctatissima</i> | eggs, larvae | coastal | SL | LB | 0.9 0 | | 44.8 14.4 | | 54.3 85.6 | | | | | |
| Spring-summer spawning | | | | | | | | | | | | | | |
| <i>Limanda aspera</i> | eggs, larvae | coastal | EL | WB | | | 68.9 1.0 | | 14.8 95.8 | | 11.0 0 | 5.3 3.2 | | |
| Summer spawning | | | | | | | | | | | | | | |
| <i>Glyptocephalus stelleri</i> | eggs, larvae | marine | EL | WB | | | | | 38.6 100 | | 59.1 0 | 2.3 0 | | |

Note. Biotope: EL, elittoral; SL, sublittoral; N, neritic. Biogeographical region: AB, arctic-boreal species; HB, high-boreal; WB, wide-boreal; LB, low-boreal.

The group with winter–spring spawning was represented by larval forms of two coastal species, *G. pistilliger* and *L. pinnifasciata*, adventive larvae of the striped seasnail *Liparis latifrons* Schmidt, 1950, and eggs of the Alaska plaice *Pleuronectes quadrituberculatus* Pallas, 1814. Eggs and larvae of this group off the southeastern coast of Sakhalin massively occur in April. Accordingly, by the beginning of research, their abundance in the Dudinka River area was already at its minimum.

The most extensive group was the one with a predominance of spring spawning: it included 11 species (65% of the species composition). This group covered both coastal and marine forms. The typically adventive ones, *G. chalcogrammus* and *H. robustus*, are characterized by earlier spawning away from weakly warmed shallow waters. Therefore, the abundance of their eggs and larvae in the coastal area was maximum in the early hydrological spring, in May. Out of coastal species, the group with early spring spawning included *Cl. pallasii*, which is distributed in Arctic-boreal waters and approaches littoral spawning grounds for spawning earlier than other coastal species.

The maximum abundance of eggs and larvae of most spring-spawning species belonging to Pleuronectidae was recorded in June, except for one Cottidae representative, *B. elegans*. Among them, species with short (within one decade) and long (up to three months) periods of eggs and larvae laying in plankton stood out. Three low-boreal species, *Ps. obscurus*, *Ps. schrenki*, and *B. elegans*, whose main range is to the south, had a short-term occurrence, as well as one high-boreal species, the longhead dab *Myzopsetta proboscidea* (Gilbert, 1896), which is highly abundant off the Northeastern Sakhalin coast [Mukhametov, Mukhametova, 2017] and in the northern Sea of Okhotsk. In the Terpeniya Bay, these species are not abundant [Kim Sen Tok, 2011]. Their abundance in ichthyoplankton is also low. Apparently, spawning and development of pelagic larvae occur within a short period of time. Eggs and larvae of many coastal Pleuronectidae species with spring spawning were characterized by a fairly long period of occurrence – two to three months (Table 3). This group included *L. sakhalinensis*, *Pl. stellatus*, *Ps. herzensteini*, and *M. punctatissima*, often highly abundant in coastal ichthyocenes and, accordingly, in ichthyoplankton of Sakhalin waters.

In terms of the nature of spawning in the Dudinka River area, *L. aspera* stood out. This species usually replaces *M. punctatissima* in the composition of dominants, since the peak of *L. aspera* spawning occurs later. In 2020, in the studied inshore site, a high abundance of *L. aspera* eggs and larvae was registered in June, and it coincided with a high abundance of eggs and larvae of the spring-spawning species, *Pl. stellatus*, *L. sakhalinensis*, and *Ps. herzensteini*. However, *L. aspera* differed from the listed species in the fact that its early stages of development continued to occur until mid-September. This gives grounds to distinguish it from the general group of coastal flounders as a species with a long spring–summer spawning. The occurrence of *L. aspera* eggs and larvae lasted up to four months. The long period of its spawning in this area is related to the availability of two spawning approaches to the Terpeniya Bay. For this species, the duration of occurrence of the early stages of development in the surface layers is estimated at 130 days [Tarasyuk, 1997].

Gl. stelleri is classified as a species with summer spawning. When larvae appeared in July, the highest concentrations of eggs in this area were recorded in August, and single eggs were found in September. Since *Gl. stelleri* eggs are registered off the northeastern coast of Sakhalin in June at depths of 50 m or more, it can be assumed as follows: in the Terpeniya Bay, spawning begins in the same period or earlier, but at a distance from the coast. With a low abundance of eggs on spawning grounds, those are not likely to be revealed in the coastal area.

In the studied inshore site, we did not note the development of an autumn ichthyoplankton complex. In the waters of the Eastern Sakhalin, this complex includes larvae of Irish lords of the genus *Hemilepidotus* Cuvier, 1829 and greenlings, mainly of the genus *Hexagrammos* Tilesius, 1810.

Some species in the Dudinka River area had a longer period of occurrence of early stages of development compared to that for other areas. Eggs and larvae of *M. punctatissima*, *Ps. herzensteini*, and *Gl. stelleri* were registered in the inshore site during three months. Even eggs and larvae of *Pl. stellatus*, a species with a short spawning period (mass spawning, about 20 days; in total, about 45 days) [Yusupov, 2011], had a long period of occurrence in the studied inshore site – from May to late July. Long-term spawning of *G. chalcogrammus* is recorded off the northeastern coast of Sakhalin, while for *L. aspera*, it is known in the Terpeniya Bay [Shuntov et al., 1993; Tarasyuk, 1997].

Adventive, marine species, *H. robustus*, *G. chalcogrammus*, *Pl. quadrituberculatus*, and *Gl. stelleri*, were characterized by the maximum abundance in the inshore site at final stages of egg development. In many areas of Sakhalin, *H. robustus* spawning, which lasts in the northern Sea of Okhotsk from mid-May to mid-July [Yusupov, 2018], coincides in time and space with *G. chalcogrammus* spawning [Moukhametov, Chastikov, 2015]. *H. robustus* spawning grounds are located mainly at depths exceeding 30 m in the northeastern Terpeniya Bay, and in recent years, in its northwestern area as well [Moukhametov, Chastikov, 2015; Tarasyuk, Pushnikov, 1982]. Considering the long period of development of *G. chalcogrammus* and *H. robustus* eggs [Yusupov, 2018; Zverkova, 2003], it can be assumed as follows: in the areas adjacent to the inshore site, their spawning began no later than in mid-April. The maximum abundance of *G. chalcogrammus* and *H. robustus* eggs in the Dudinka River vicinity was registered at the initial stages of seasonal desalination of the coastal area, which occurred in the second decade of May only in the surface layers, while in the deeper ones, rather stable thermohaline conditions persisted [Shevchenko et al., 2021]. The alongshore current of the south direction, as well as northern, northeastern, and eastern winds with a total frequency of 91%, blowing even at a not very high speed, on average $4.5 \text{ m}\cdot\text{s}^{-1}$, could maintain a fairly stable movement of ichthyoplankton to the south and southwest.

Eggs of the species that reproduce directly in shallow waters, *M. punctatissima* and *Pl. stellatus*, formed aggregations at the initial stages. Some species had relatively high abundance of both initial and final stages throughout the study period. Specifically, the development stages I and III for *L. aspera* had close proportions, more than 40%, already in mid-June. By the end of June, the proportion of stage I (41%) slightly exceeded the proportion of stage III (32%). By mid-July, there was a reduction in the final stages. In late July, stage IV had the highest contribution, 29%, while the relative abundance of other stages remained at 21–26%. In June, with the maximum frequency of surveys, it was impossible to register the predominance of the development stage I, which could result from a constant arrival of *L. aspera* eggs from northern areas, where its main reproduction ground is located [Kim Sen Tok, 2002, 2011]. The high relative contribution of the development stage I for *L. aspera* was registered only from late August, during residual spawning. A similar proportion of development stages was established for *Ps. herzensteini*, with the difference that the abundance of eggs of this species decreased already in July.

The spatial distribution of ichthyoplankton by depth was determined by the seasonal features of fish reproduction in Eastern Sakhalin waters. According to the indicator averaged over May–September, the most productive depths were the minimum ones: the value was about $52 \text{ ind}\cdot\text{m}^{-3}$. Above 5–10-m isobaths, mean concentrations of ichthyoplankton remained at the level of $21\text{--}22 \text{ ind}\cdot\text{m}^{-3}$; to a depth

of 20 m, the values decreased by almost half, to 13 ind. \cdot m⁻³. In shallow areas, mainly fish eggs were found. Larvae were rare. From May to late June, higher densities of ichthyoplankton were observed at the water's edge. The maximum abundance of eggs, more than 260 ind. \cdot m⁻³, was recorded in mid-May (Fig. 2).

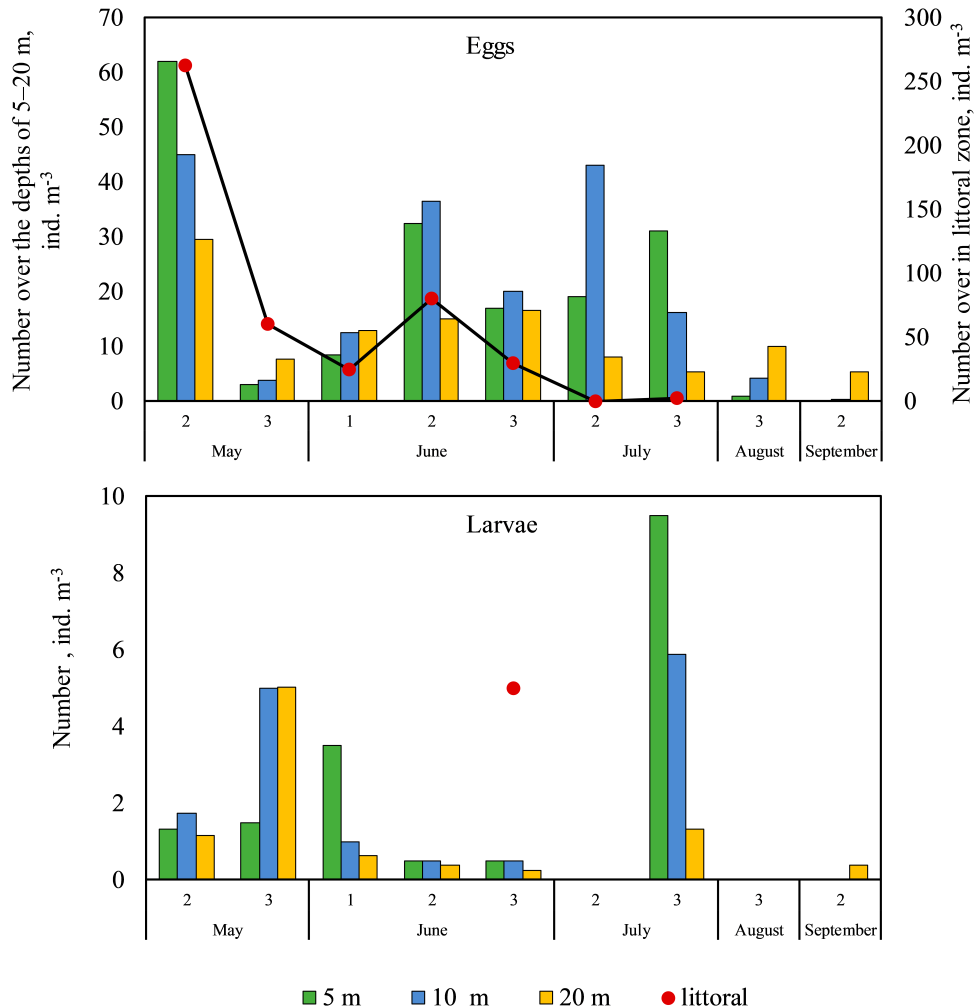


Fig. 2. Dynamics of ichthyoplankton abundance (ind. \cdot m⁻³) at isobaths of 0.5–20 m in the inshore site at the confluence of the Dudinka River in May–September 2020 (numbers on the abscissa are decades)

Pelagic eggs of most Pleuronectidae and *G. chalcogrammus* arrived to minimum depths with surge winds. Bottom eggs dominated during mass spawning of *Cl. pallasii* (in May) and *Ps. schrenki* (in early June). In July, an increase in egg concentrations was noted in the depth range of 5–10 m; in August and September, above isobaths of more than 10 m. In May, similar densities of larvae were recorded in the entire depth range of 5–20 m. In early June, a rise in concentrations was recorded at 5-m isobath due to mass hatching of *Ps. obscurus*. The maximum abundance of larvae occurred in late July, when larvae of several coastal flounder species, *L. aspera*, *M. punctatissima*, and *Ps. herzensteini*, were characterized by high densities.

At the beginning of the study (the second decade of May), the abundance of *G. chalcogrammus* and *H. robustus* eggs reached its maximum values. Eggs at the final stages of development (III and IV) predominated: their total proportion exceeded 93% for *G. chalcogrammus* and 86% for the Bering flounder.

In the early hydrological spring, when coastal water areas are still slightly warmed up and exposed to fresh-water runoff, fish with pelagic eggs (*H. robustus*, *G. chalcogrammus*, *Pl. quadrituberculatus*, and *Gl. stelleri*) spawn outside the 50-m isobath. Flounders of the coastal complex, *Pl. stellatus*, *M. punctatissima*, *L. aspera*, *L. sakhalinensis*, and *Ps. herzensteini*, also begin spawning at depths exceeding 15–20 m. At this stage, the coastal water area becomes a spot of high concentrations of eggs and larvae of species that lay bottom eggs on littoral spawning grounds. In the Dudinka River area, out of these species, only *Cl. pallasii* was found. In other areas, this niche can also be occupied by *M. villosus* and *H. japonicus* [Mukhametova, 2020a]. In May, maximum concentrations are formed in the littoral zone due to the transport of pelagic eggs of marine species by prevailing eastern winds and currents. In June, the role of 5–10-m isobaths increases. In July, the main concentrations of ichthyoplankton shift to depths of 5–10 m. At the height of the hydrological summer, in August, as the water column warms up, the spawners begin to move deeper. The reproductive value of shallow waters decreases. The main concentrations of eggs and larvae from residual spawning are formed above isobaths of 10–20 m (Fig. 2).

The survival rate of early stages of fish development is one of the significant indicators of spawning efficiency, which determine the productivity of recruitment. The formation of embryonic pathologies and high mortality of eggs and larvae under natural conditions can be caused by sudden fluctuations in temperature and salinity, storms, lack of food items, *etc.* Under adverse conditions, egg mortality can reach 90–100% [Davydova, 1994]. In the inshore site at the confluence of the Dudinka River, average mortality of *G. chalcogrammus* eggs (29.2%) coincided with average mortality in the Northeastern Sakhalin waters (29%); the value for *L. aspera* was lower (19.5% vs. 30.2%) [Davydova, Cherkashin, 2007]. In May in the Dudinka River area, the proportion of non-viable eggs of *G. chalcogrammus* (1.6%) and *H. robustus* (1.8%) was also lower than in the Aniva Bay (8.3% for *G. chalcogrammus* and 2.1% for *H. robustus*). At the same time, the proportion of postembryonic disorders was quite high, especially for *H. robustus* (Table 4).

Table 4. Larvae characteristics of abundant fish species during periods of high abundance in the inshore site at the confluence of the Dudinka River in 2020

| Species | Month | Decade | Length, mm, min–max $M \pm \sigma$ | Mean weight of 1 individual, mg, $M \pm \sigma$ | Prelarvae, % | Prelarvae with pathologies, % |
|------------------------------------|-------|-----------------|--|---|-----------------|-------------------------------------|
| <i>Gadus chalcogrammus</i> | May | 2 nd | $\frac{2.20-5.15}{3.78 \pm 0.84}$ | 0.510 ± 0.418 | 70.6 | 5.9 |
| | | 3 rd | $\frac{3.2-5.9}{4.51 \pm 0.66}$ | 0.460 ± 0.177 | 100.0 | – |
| <i>Hippoglossoides robustus</i> | May | 2 nd | $\frac{1.24-4.87}{3.33 \pm 1.20}$ | 0.223 ± 0.139 | 72.2 | 38.9 |
| | | 3 rd | $\frac{3.5-5.3}{4.60 \pm 0.72}$ | 0.257 ± 0.106 | 76.9 | – |
| <i>Limanda aspera</i> | July | 3 rd | $\frac{0.9-3.5}{2.15 \pm 0.69}$ | 0.050 ± 0.019 | 69.0 | 48.3 |
| <i>Myzopsetta punctatissima</i> | | | $\frac{1.1-4.2}{2.16 \pm 0.59}$ | 0.049 ± 0.034 | 10.0 | 20.0 |
| <i>Platichthys stellatus</i> | June | 1 st | $\frac{1.8-4.05}{2.85 \pm 0.80}$ | 0.139 ± 0.086 | – | 14.3 |
| <i>Pseudopleuronectes obscurus</i> | | | $\frac{2.3-3.1}{2.72 \pm 0.33}$ | 0.063 ± 0.025 | 100.0 | – |

Apparently, a simultaneous increase in the abundance of *G. chalcogrammus* and *H. robustus* individuals with pathologies (these species have similar spawning areas and the direction of drift of the early stages of development) is related to the exposure of their eggs and larvae to adverse conditions. In May in the inshore site, the most common types of effect, that reduced the survival rate of fish eggs and larvae, were the effect of waves and sudden fluctuations in temperature and salinity in the area of upwellings and downwellings. Considering the long period of egg development at low temperatures and significant distances of their transport, adverse factors could affect fish eggs and larvae outside the inshore site as well.

The mortality rate for eggs of coastal Pleuronectidae was higher, and this may be due to the high intensity of spawning directly in the inshore site and the predominance of the initial stages of development, more sensitive to any effect, throughout the study period. However, the conditions for egg development in the area of the Dudinka River confluence can be considered more favorable than in southern areas. In Aniva Bay, the proportion of non-viable eggs of *L. aspera* in the second decade of July exceeded mortality rate in the Dudinka River area by half (46% vs. 23%); that of *M. punctatissima* in the second decade of June, by more than 2.5 times (44% vs. 17%). Pleuronectidae embryos before leaving their membranes and larvae at the stage of transition to exogenous nutrition turned out to be more vulnerable. The proportion of non-viable larvae (14–48%) was comparable to egg mortality rate or higher (17–30%). An increase in mortality rate at the early stages of embryogenesis in the inshore site coincided with the known critical periods [Chambers et al., 2001].

Compared to the values for coastal lagoon waters of the southeastern Sakhalin Island [Mukhametova, Balanov, 2013], the period of occurrence of ichthyoplankton in the Dudinka River vicinity lasted a month longer, and the greatest species diversity was formed a month later. The values of the indices of diversity (2.84), evenness (0.79), and species richness (3.35) were the highest in June – with the maximum number of species (12) and with the abundance (26.60 ± 16.46 ind.·m⁻³), close to the mean value for the period (Table 2). High biotic diversity during this period was also indicated by the minimum value of the Simpson index (0.18). The relatively low values of species richness indices in this study area were due to a decrease in the number of species in the ichthyofauna of the Far Eastern seas in shallow areas compared to the number for deep-water ones [Ashikhmina, 2009]. The minimum diversity and evenness of ichthyoplankton were observed in September, when *L. aspera* eggs and larvae dominated in the catches, and the dominance index reached 0.96.

The ichthyoplankton dominance–diversity curve for the Eastern Sakhalin occupies a high position on the graph (Fig. 3).

The shape of the ichthyoplankton dominance–diversity curve is close to the “MacArthur’s broken-stick model” which characterizes natural communities. Most species were evenly distributed in ranked order of dominance. The proportion of eggs and larvae of four abundant species, *G. chalcogrammus*, *M. punctatissima*, *H. robustus*, and *L. aspera*, accounted for 77% of the cumulative abundance. The next eight species accounted for 22% of the cumulative abundance, and the last five ones accounted for only 0.4%. A sharp decline in abundance began only with *Ps. obscurus*, which occupied the 13th position in the ranked list. The presence of a few high-abundant species and many low-abundant ones is a characteristic feature of boreal communities [Odum, 1983].

In general, the basis of the community in the Dudinka River area was formed by the early stages of development of four fish species with different status and characteristics of abundance dynamics. In May, the main concentrations, existing for a short time (within the second decade), were produced by eggs

and larvae of *G. chalcogrammus* and *H. robustus* transported from seaward areas: 72 and 28 ind. \cdot m⁻³, respectively. By the third decade of May, the mean concentration of *G. chalcogrammus* eggs decreased by 24 times, and that of *H. robustus* eggs, by 9.5 times. In June and July, eggs and larvae of resident species, *M. punctatissima* and *L. aspera*, dominated; these species do not form aggregations with high densities, but have a relatively stable abundance for several months. Decade concentrations of *M. punctatissima* eggs and larvae from early June to late July varied from 6.3 to 15.8 ind. \cdot m⁻³. Variations in *L. aspera* abundance were more pronounced. From mid-June to September, the total abundance of eggs and larvae of this species varied within 0.9–11.9 ind. \cdot m⁻³. The dominant forms were common for Eastern Sakhalin [Davydova, Cherkashin, 2007; Moukhametov, Chastikov, 2013]. Analysis of the structure and indicators of species abundance for ichthyoplankton in the inshore site at the confluence of the Dudinka River allows us to classify it as a typical natural community.

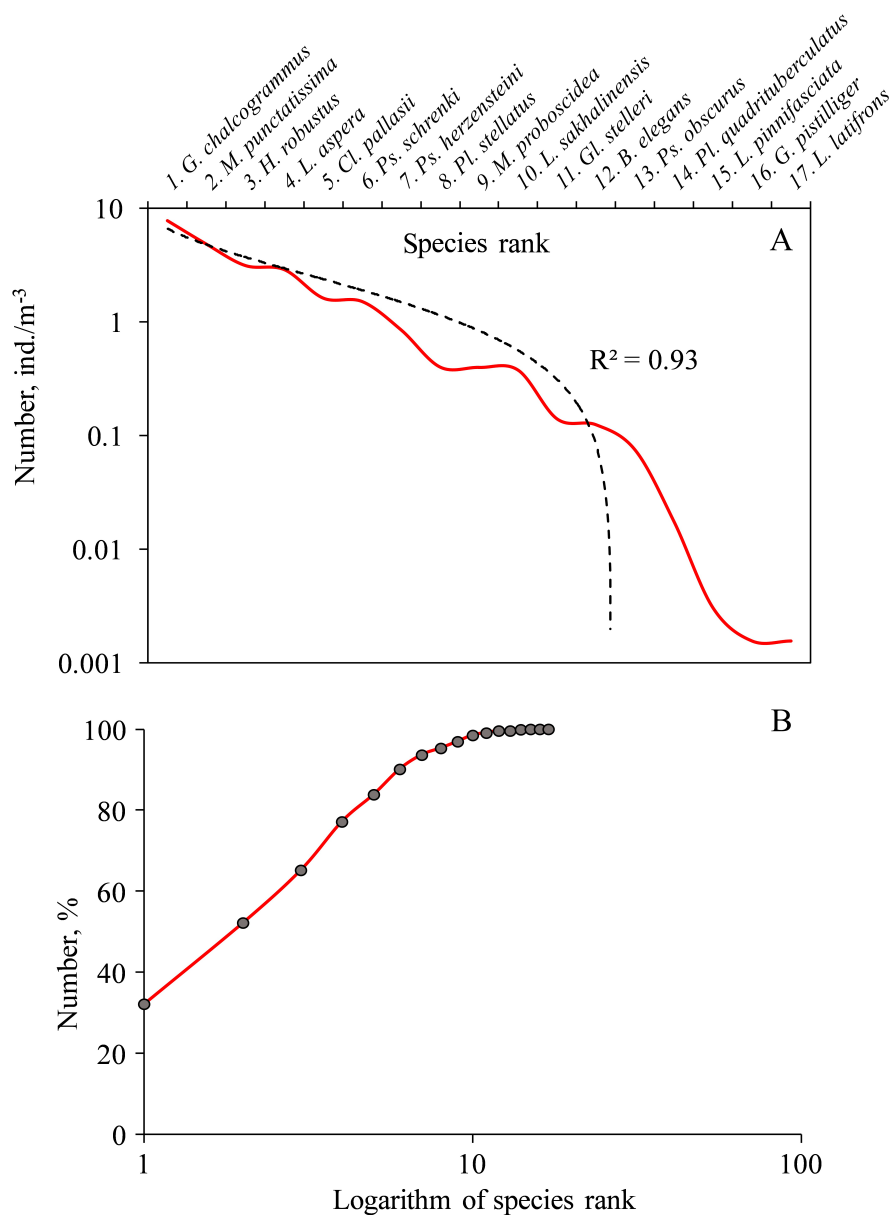


Fig. 3. Dominance–diversity curve (A) and species accumulation curve (B) in the inshore site at the confluence of the Dudinka River in 2020

Conclusion. Development of ichthyoplankton in the Dudinka River area occurred under conditions of significant temperature fluctuations resulting from the formation of coastal upwellings and downwellings during surge phenomena. Maximum fluctuations in temperature were observed throughout the hydrological spring, from May to July; fluctuations in salinity, in June, during the flood period. An additional negative effect in spring was the one of waves and swell caused by the passage of cyclones.

Ichthyoplankton in the Dudinka River vicinity included eggs and larvae of 17 fish species from 5 families typical for the Eastern Sakhalin waters. Their occurrence was limited to the period from May to September. Of the cumulative abundance, 77% were eggs and larvae of four species: *Gadus chalcogrammus*, *Myzopsetta punctatissima*, *Hippoglossoides robustus*, and *Limanda aspera*.

Spawning of most fish in the inshore site and adjacent areas occurred during the spring hydrological season rich in food resources. In May, the maximum abundance of ichthyoplankton, 61 ind. \cdot m⁻³, was recorded, while in August, with the end of the spawning period of pelagophilic fish, a significant drop was observed, down to 3.5 ind. \cdot m⁻³. The abundance averaged for the study period decreased from 52 ind. \cdot m⁻³ in the littoral zone to 21–22 ind. \cdot m⁻³ above depths of 5–10 m and to 13 ind. \cdot m⁻³ above a depth of 20 m.

In the second decade of May, eggs of adventive, marine species dominated in terms of abundance, *G. chalcogrammus* (71% of the total value) and *H. robustus* (28%); in late May, bottom eggs of *Clupea pallasii* (70%); and in June–September, eggs and larvae of Pleuronectidae (91–100%). The abundance of eggs and larvae of *G. chalcogrammus* and Pleuronectidae in the Dudinka River area was significantly higher than in areas south of N48°. An increase in concentrations resulted from the proximity of the studied inshore site to the main spawning grounds of many fish species.

Species with spring spawning dominated, accounting for 65% of the species composition. This group covered both adventive, marine forms (mainly *G. chalcogrammus* and *H. robustus*), which gave high abundance in May, and coastal ones (*Platichthys stellatus*, *M. punctatissima*, *Limanda sakhalinensis*, and *Pseudopleuronectes herzensteini*). The adventive species with pelagic eggs were characterized by a predominance of the final stages of development. Resident species were distinguished by a high abundance of eggs at the initial stages of development, which indicated spawning within the inshore site.

The proportion of dead eggs of *G. chalcogrammus* and Pleuronectidae flounders did not exceed the values for the Northeastern Sakhalin waters and was lower than in Aniva Bay. In May, an increase in the proportion of prelarvae with pathologies was recorded for *G. chalcogrammus* and *H. robustus*, and this could be caused by exposure to adverse conditions.

Indices of diversity had the highest values in June – with the maximum number of species (12) and with the abundance (26.60 ± 16.46) ind. \cdot m⁻³, close to the mean value for the study period. In this month, 78% of the total abundance were eggs and larvae of three subdominants, *M. punctatissima* (27%), *L. aspera* (23%), and *Pseudopleuronectes schrenki* (19%).

The shape of the ichthyoplankton dominance–diversity curve was close to the “MacArthur’s broken-stick model” which characterizes natural communities. Most species were evenly distributed in ranked order of dominance.

REFERENCES

1. Ashikhmina E. V. Otsenka vidovogo raznoobraziya ikhtiofauny zaliva Petra Velikogo (Yaponskoe more). *Trudy Instituta sistemnogo analiza RAN*, 2009, vol. 42, pp. 273–284. (in Russ.)
2. Bakanov A. I. Kolichestvennaya otsenka dominirovaniya v ekologicheskikh soobshchestvakh. In: *Kolichestvennye metody ekologii i gidrobiologii* : sbornik nauchnykh trudov, posvyashchennyi pamyati A. I. Bakanova / G. S. Rozenberg (Ed.). Tolyatti : SamNTs RAN, 2005, pp. 37–67. (in Russ.)
3. Velikanov A. Ya. Novaya volna migratsii ryb yuzhnykh shirot k beregam Sakhalina. *Vestnik Sakhalinskogo muzeya*, 2006, no. 1 (13), pp. 265–278. (in Russ.)
4. Davydova S. V. Vstrechaemost' ikry dal'nevostochnoi sardiny i yaponskogo anchousa v zalive Petra Velikogo (Yaponskoe more). *Izvestiya TINRO*, 1994, vol. 115, pp. 130–136. (in Russ.)
5. Dyakov Yu. P. *Flatfish (Pleuronectiformes) of the Far Eastern Seas of Russia*. Petropavlovsk-Kamchatsky : Izd-vo KamchatNIRO, 2011, 433 p. (in Russ.)
6. Zverkova L. M. *Mintai. Biologiya, sostoyanie zapasov*. Vladivostok : TINRO-Tsentr, 2003, 248 p. (in Russ.)
7. Kim Sen Tok. Resursy donnykh ryb zalivov Aniva i Terpeniya. *Rybnoe khozyaistvo*, 2002, no. 1, pp. 39–41. (in Russ.)
8. Kim Sen Tok. The main features of spatial distribution and commercial resources of abundant fishes in sublittoral zone of Terpeniye Bay and south-eastern coast of Sakhalin Island. *Voprosy rybolovstva*, 2011, vol. 12, no. 4 (48), pp. 648–667. (in Russ.)
9. Lozhkin D. M., Tshay Zh. R., Shevchenko G. V. Satellite monitoring of temperature conditions near the mouths of spawning rivers in the southern part of Sakhalin Island. *Issledovanie Zemli iz kosmosa*, 2018, no. 5, pp. 15–22. (in Russ.). <https://doi.org/10.31857/S020596140003232-6>
10. Moukhametova O. N. Ptichiye Lake as a model of the formation of lagoon ichthyoplankton complexes (Southeast Sakhalin). *Vladimir Ya. Levanidov's Biennial Memorial Meetings*, 2014, vol. 6, pp. 453–463. (in Russ.)
11. Mukhametova O. N. Ichthyoplankton in the southeastern inshore area of Sakhalin Island in 2019. *Vestnik Sakhalinskogo muzeya*, 2020a, no. 4 (33), pp. 113–130. (in Russ.)
12. Moukhametova O. N. Ichthyoplankton of the nearshore area in the east part of Aniva Bay in 2018. *Transactions of the SakhNIRO. Water Life Biology, Resources Status and Condition of Inhabitation in Sakhalin–Kuril Region and Adjoining Water Areas*, 2020b, vol. 16, pp. 39–60. (in Russ.)
13. Mukhametova O. N., Balanov A. A. *Ikhtio-plankton lagunnykh ozer yugo-vostochnoi chasti ostrova Sakhalin*. Yuzhno-Sakhalinsk : Sakhalinskii nauchno-issledovatel'skii institut rybnogo khozyaistva i okeanografii, 2013, 188 p. (in Russ.)
14. Moukhametova O. N., Moukhametov I. N. Ichthyoplankton of nearshore area of Aniva Bay. *Transactions of the SakhNIRO. Water Life Biology, Resources Status and Condition of Inhabitation in Sakhalin–Kuril Region and Adjoining Water Areas*, 2013, vol. 14, pp. 180–197. (in Russ.)
15. Onishchenko N. I. *Vodnye resursy Sakhalina i ikh izmeneniya pod vliyaniem khozyaistvennoi deyatel'nosti*. Vladivostok : DVO AN SSSR, 1987, 151 p. (in Russ.)
16. Pak E. A., Hapov D. S., Dubina V. A. Submesoscale abiotic factors in coastal marine ecosystems of the Terpeniya Bay (Okhotsk Sea). *Nauchnye trudy Dal'rybvтуza*, 2017,

- vol. 40, no. 1, pp. 17–21. (in Russ.)
17. Pertseva-Ostroumova T. A. *Razmnozhenie i razvitie dal'nevostochnykh kambal*. Moscow : Izd-vo Akad. nauk SSSR, 1961, 484 p. (in Russ.)
 18. Pishchalnik V. M., Bobkov A. O. *Okeanograficheskii atlas shel'fovoi zony ostrova Sakhalin* : nauchnoe izdanie : [in 2 pts]. Yuzhno-Sakhalinsk : SakhGU, 2000, pt 1, 174 p. (in Russ.)
 19. *Pogoda v 240 stranakh mira* : [site]. (in Russ.). URL: <http://www.rp5.ru> [accessed: 25.07.2021].
 20. Rass T. S., Kazanova I. I. *Metodicheskoe rukovodstvo po sboru ikrinok, lichinok i mal'kov ryb*. Moscow : Pishchevaya promyshlennost', 1966, 43 p. (in Russ.)
 21. *Rukovodstvo po metodam gidrobiologicheskogo analiza poverkhnostnykh vod i donnykh otlozhenii*. Leningrad : Gidrometeoizdat, 1983, 239 p. (in Russ.)
 22. Tarasyuk S. N. O vozmozhnykh prichinakh, obuslavlivayushchikh urozhainost' pokolenii zheltoperoi kambaly. In: *Rybokhozyaistvennye issledovaniya v Sakhalino-Kuril'skom raione i sopredel'nykh akvatoriyakh* : sbornik nauchnykh trudov / SakhNIRO. Yuzhno-Sakhalinsk : Sakhalinskoe oblastn. kn. izd-vo, 1994, pp. 23–32. (in Russ.)
 23. Tarasyuk S. N. *Biologiya i dinamika chislennosti osnovnykh promyslovykh vidov kambal Sakhalina* : avtoref. dis. ... kand. biol. nauk : 03.00.10. Vladivostok, 1997, 22 p. (in Russ.)
 24. Tarasyuk S. N., Pushnikov V. V. *Ekologiya neresta paltusovidnoi kambaly v zalivakh Aniva i Terpeniya*. In: *Ekologiya i usloviya vosproizvodstva ryb i bespozvonochnykh dal'nevostochnykh morei i severo-zapadnoi chasti Tikhogo okeana*. Vladivostok : TINRO, 1982, pp. 58–62. (in Russ.)
 25. Shevchenko G. V., Tshay Zh. R., Chastikov V. N. Features of oceanological conditions on the southeastern shelf of Sakhalin Island according to surveys on standard sections and satellite observations. *Okeanologicheskie issledovaniya*, 2020, vol. 48, no. 2, pp. 51–68. (in Russ.). [https://doi.org/10.29006/1564-2291.JOR-2020.48\(2\).4](https://doi.org/10.29006/1564-2291.JOR-2020.48(2).4)
 26. Shevchenko G. V., Chastikov V. N., Polupanov P. V. Oceanological studies in assessing the receiving capacity of coastal waters in the areas of the mouths of spawning rivers on the southeastern coast of Sakhalin Island. *Transactions of the SakhNIRO. Water Life Biology, Resources Status and Condition of Inhabitation in Sakhalin–Kuril Region and Adjoining Water Areas*, 2021, vol. 17, pp. 132–147. (in Russ.)
 27. Shuntov V. P., Volkov A. F., Temnykh O. S., Dulepova E. P. *Mintai v ekosistemakh dal'nevostochnykh morei*. Vladivostok : TINRO, 1993, 426 p. (in Russ.)
 28. Shuntov V. P., Temnykh O. S. Long-term average biomass and dominant fish species in the bottom biotopes of the Okhotsk Sea. Part 1. Composition and quantitative ratio of species on shelves in different areas of the sea. *Izvestiya TINRO*, 2018, vol. 193, pp. 3–19. (in Russ.). <https://doi.org/10.26428/1606-9919-2018-193-3-19>
 29. Yusupov R. R. Reproduction and embryonic development of starry flounder *Platichthys stellatus* (Pleuronectidae) in the Tauyskaya Bay (northern Okhotsk Sea). *Izvestiya TINRO*, 2011, vol. 166, pp. 38–53. (in Russ.)
 30. Yusupov R. R. Embryonic and larval development of Bering flounder *Hippoglossoides robustus* (Pleuronectidae) in the northern Okhotsk Sea. *Izvestiya TINRO*, 2018, vol. 194, pp. 42–53. (in Russ.). <https://doi.org/10.26428/1606-9919-2018-194-42-53>
 31. Chambers R. Ch., Witting D. A.,

- Lewis S. J. Detecting critical periods in larval flatfish populations. *Journal of Sea Research*, 2001, vol. 45, iss. 3–4, pp. 231–242. [https://doi.org/10.1016/S1385-1101\(01\)00058-2](https://doi.org/10.1016/S1385-1101(01)00058-2)
32. Davydova S. V., Cherkashin S. A. Ichthyoplankton of the eastern shelf of Sakhalin Island and its use as an environmental state indicator. *Journal of Ichthyology*, 2007, vol. 47, iss. 6, pp. 438–448. <https://doi.org/10.1134/S0032945207060033>
33. Dyldin Yu. V., Fricke R., Hanel L., Vorobiev D. S., Interesova E. A., Romanov V. I., Orlov A. M. Freshwater and brackish water fishes of Sakhalin Island (Russia) in inland and coastal waters: An annotated checklist with taxonomic comments. *Zootaxa*, 2021, vol. 5065, no. 1, pp. 1–92. <https://doi.org/10.11646/zootaxa.5065.1.1>
34. Kim Sen Tok, Mukhametov I. N., Zavarzin D. S., Chastikov V. N., Latkovskaya E. M., Tskhai Zh. R., Korneev E. S., Koreneva T. G. Reproductive conditions of walleye pollock *Theragra chalcogramma* (Gadidae) off the northeastern coast of Sakhalin Island, Sea of Okhotsk. *Journal of Ichthyology*, 2017, vol. 57, iss. 6, pp. 893–907. <https://doi.org/10.1134/S003294521706008X>
35. Margalef R. Information theory in ecology. *General Systems*, 1958, vol. 3, pp. 36–71.
36. Moukhametov I. N., Chastikov V. N. Marine ichthyoplankton off Northern Sakhalin at after ice-thawing season. In: *Proceedings of the 28th International Symposium on Okhotsk Sea and Sea Ice*. Mombetsu, Hokkaido, 2013, pp. 332–335.
37. Moukhametov I. N., Chastikov V. N. Peculiarities of spatial distribution of Alaska pollock' and Bering flounder's eggs off Eastern Sakhalin in 2012 and 2014 years. In: *The 30th International Symposium on Okhotsk Sea and Sea Ice*. Mombetsu, Hokkaido, 2015, pp. 227–230.
38. Mukhametov I. N., Mukhametova O. N. Species composition and distribution of ichthyoplankton in the waters of north-east Sakhalin. *Journal of Ichthyology*, 2017, vol. 57, iss. 6, pp. 846–859. <https://doi.org/10.1134/S0032945217050137>
39. Mukhametova O., Atamanova I., Motylkova I., Konovalova N. Plankton communities of inshore area of southeastern Sakhalin (Sea of Okhotsk). In: *The 36th International Symposium on the Okhotsk Sea & Polar Oceans*. Mombetsu, Hokkaido, 2022, pp. 156–159.
40. Odum E. P. *Basic Ecology*. Philadelphia : Saunders College Publishing, 1983, 325 p.
41. Pielou E. C. Shannon's formula as a measure of specific diversity: Its use and misuse. *American Naturalist*, 1966, vol. 100, no. 914, pp. 463–465. <https://doi.org/10.1086/282439>
42. Shannon C. E., Weaver W. *The Mathematical Theory of Communication*. Urbana : University of Illinois Press, 1949, 144 p.
43. Simpson E. H. Measurement of diversity. *Nature*, 1949, vol. 163, pp. 688. <https://doi.org/10.1038/163688a0>
44. Whittaker R. H. *Communities and Ecosystems*. 2nd revise edition. New York : MacMillan Publishing Co., 1975, 385 p.
45. *World Register of Marine Species* : [site]. URL: <http://www.marinespecies.org/> [accessed: 27.10.2021].

СТРУКТУРА ПРИБРЕЖНОГО ИХТИОПЛАНКТОНА В РАЙОНЕ ВПАДЕНИЯ РЕКИ ДУДИНКА (ВОСТОЧНЫЙ САХАЛИН)

О. Н. Мухаметова

Сахалинский филиал ФГБНУ «Всероссийский научно-исследовательский институт рыбного хозяйства и океанографии» (СахНИРО), Южно-Сахалинск, Российская Федерация

E-mail: olga.sakhniro@gmail.com

Изучены структура ихтиопланктонного комплекса и особенности раннего развития массовых видов рыб на морском прибрежном полигоне у восточного побережья острова Сахалин. Для района исследований характерны значительные вариации температуры и солёности в мае — июле. Минимальная температура воды (+0,4 °C) отмечена на глубине 20 м в мае, а максимальная (+15,7 °C) — на глубине 3 м в сентябре. Солёность в течение всего периода исследований колебалась от 3,5 PSU на литорали в районе устья реки Дудинка до 31 PSU на глубине 13–20 м. В ихтиопланктоне идентифицированы икра и личинки 17 видов рыб из 5 семейств, типичных для вод Восточного Сахалина. По количеству видов преобладали представители семейства Pleuronectidae, формировавшие 71 % таксономического списка. По численности во второй декаде мая доминировали икра и личинки *Gadus chalcogrammus* (71 % суммарной величины), в третьей декаде мая — донная икра *Clupea pallasii* (70%), с июня по сентябрь — икра и личинки Pleuronectidae (91–100 %). Осреднённая за период исследований численность ихтиопланктона снижалась с 52 экз.·м⁻³ на литорали до 21–22 экз.·м⁻³ над глубинами 5–10 м и до 13 экз.·м⁻³ над глубиной 20 м. Доля мёртвых икринок *G. chalcogrammus* и камбал Pleuronectidae не превышала значений для вод Северо-Восточного Сахалина и была ниже, чем в заливе Анива. В мае у *G. chalcogrammus* и *Hippoglossoides robustus* отмечено увеличение доли предличинок с аномалиями, что может быть вызвано попаданием икры на завершающих стадиях развития в неблагоприятные условия среды. Максимальное видовое разнообразие зарегистрировано в июне. Четыре вида формировали 77 % накопленного обилия — *G. chalcogrammus*, *H. robustus*, *Myzopsetta punctatissima* и *Limanda aspera*.

Ключевые слова: икра рыб, личинки рыб, ихтиопланктон, численность, видовое разнообразие, Восточный Сахалин

UDC [504.5:620.267](268.45)

**ASSESSMENT OF RADIATION EFFECT OF ^{137}Cs , ^{134}Cs , AND ^{90}Sr
ON BIOTA OF THE BARENTS SEA
IN THE VICINITY OF HYPOTHETICAL ACCIDENT
WITH THE SUNKEN NUCLEAR SUBMARINE K-159**

© 2023 T. G. Sazykina and A. I. Kryshev

Research and Production Association “Typhoon,” Obninsk, Russian Federation

E-mail: ecomod@yandex.ru

Received by the Editor 30.11.2022; after reviewing 18.01.2023;
accepted for publication 04.08.2023; published online 01.12.2023.

Radiation effect of ^{137}Cs , ^{134}Cs , and ^{90}Sr on marine biota was modelled for early period of a hypothetical accident with the sunken nuclear submarine K-159 during its surfacing and transportation in the Barents Sea. Dynamics of radioactivity in seawater was described, using analytical 2-dimensional model of radionuclide dispersion from an instantaneous point release in seawater. Radioactive contamination of seawater and bottom sediments with ^{137}Cs , ^{134}Cs , and ^{90}Sr was calculated for distances from 200 m to 30 km from the source. Estimated dose of acute exposure accumulated within the first 10 days was close to 100 mGy for bottom fish at a 200-m distance from the accidental source of contamination. The probability of lethal effects for fish at this dose was estimated to be below 1%. Chronic exposures from ^{137}Cs , ^{134}Cs , and ^{90}Sr at a distance of 200 m from the accidental source of contamination during the first year after the accident were as follows: for bottom fish, 9.7 mGy·day⁻¹; molluscs, 11 mGy·day⁻¹; and aquatic plants, 6.3 mGy·day⁻¹. These dose rates exceed the reference level ensuring safety of marine biota. Therefore, in the vicinity of the accident site, the radiation situation cannot be considered safe for bottom fish, molluscs, and aquatic plants. At distances of more than 500 m from the accidental source of contamination, expected dose rates of chronic exposure to marine biota were below reference level. Dose rates for biota resulting from a hypothetical accident in the Barents Sea were caused mainly by external exposure from contaminated sediments and also by accumulation of long-lived radionuclides from sediments by bottom biota.

Keywords: Arctic, Barents Sea, radiation accident, modelling, marine biota, dose, acute exposure, chronic exposure

In the Arctic seas, there are a significant number of radiation hazard facilities: radioactive waste containers, dumped/sunken nuclear submarines, a nuclear-powered icebreaker, *etc.* Various scenarios of accidents during surfacing of sunken radiation hazard facilities for their transportation and disposal were developed [Sarkisov et al., 2015]. To calculate the results of radionuclide dispersion from an instantaneous point release in the Arctic marine environment, several models were used:

- NAOSIM ocean model with a grid of 28 × 28 km [Hosseini et al., 2017];
- regional model with a grid of 3 × 3 km [Antipov et al., 2015];
- ECOMOD-ARCTIC radioecological box model [Kryshev et al., 2022b; Sazykina, 1998];
- ARCTICMAR box model [Iosjpe et al., 2020].

In all the models listed, the dimensions of spatial grid and camera boxes turned out to be too large, and it was impossible to directly examine the nearest zone of radioactive contamination – the one with the highest levels of exposure to marine organisms. The methodological objective of this study is to develop techniques for assessing acute exposure to marine biota in the early period of a radiation accident. The analysis of its radioecological consequences, including radionuclide accumulation in bottom sediments and hydrobionts, was carried out using dynamic models, since in the acute period of an accident, it is incorrect to apply equilibrium coefficients of transition from seawater to bottom sediments and fish [Kryshev et al., 2022a, b; Sazykina et al., 2022].

Radiation effects on marine biota were modelled for a scenario of a hypothetical accident with a spontaneous chain reaction on the sunken submarine K-159 during its transportation in the Barents Sea to a disposal site. The nuclear submarine K-159 of the project 627A (now, B-159) sank on 30.08.2003 in the southern Barents Sea because of an emergency during its transportation for disposal. The site is in approximately 6 km from Kildin Island, on the slope of the Kildin part of the Murmansk Trench, at the entrance to the Kola Bay, at a depth of 246 m [Sarkisov et al., 2015]. For this nuclear and radiation hazard facility, there is a hypothetical possibility of a radiation accident with a spontaneous chain reaction, both when the submarine is at the bottom and when it is being surfaced for transportation, which could lead to the release of long-lived radionuclides into the marine environment [Antipov et al., 2015; Hosseini et al., 2017; Sarkisov et al., 2018]. Predictive estimates were made of radioactivity spread in seawater under different scenarios of accident, obtained using a gridpoint model with 3-km horizontal resolution [Antipov et al., 2015].

This work models the contribution of long-lived radionuclides (^{137}Cs , ^{134}Cs , and ^{90}Sr) to exposure to marine biota during the initial period of radioactive contamination of the marine environment in the nearest zone of the accident – from 200 m to 30 km from the source. The analysis is based on estimates of the release of long-lived radionuclides into the marine environment, which were obtained within the scenario of a spontaneous chain reaction in the K-159 reactor after the submarine surfacing for transportation. The following long-lived radionuclides are expected to be released into seawater: ^{137}Cs , $2.48 \cdot 10^{13}$ Bq; ^{134}Cs , $1.4 \cdot 10^9$ Bq; and ^{90}Sr , $5.72 \cdot 10^{12}$ Bq [Sarkisov et al., 2015]. The release of short-lived radionuclides into seawater was not assessed in this scenario. Determining their potential contribution to exposure to marine biota requires additional research.

The levels of radioactive contamination of seawater and bottom sediments during the movement and dispersion of the primary spot of radioactive contamination were calculated using an analytical model for distances up to 30 km from the source. The model of accidental contamination of the marine environment made it possible to determine the dose rate and absorbed dose for 10 days of exposure to marine biota and to estimate the probability of lethal effects for marine organisms in the acute period of a radiation accident from exposure to ^{137}Cs , ^{134}Cs , and ^{90}Sr near the source. In the immediate vicinity of the accident site, radioactive contamination of bottom sediments can persist for a long time. Therefore, along with the dose of acute exposure, the dose rate of chronic exposure of benthic organisms was assessed.

MATERIAL AND METHODS

When surfacing a dumped radiation hazard facility, an emergency may arise associated with radionuclide release into the marine environment. The scenario of a hypothetical accident during surfacing of the sunken nuclear submarine K-159 for its transportation and disposal is described

in the work [Sarkisov et al., 2015]. After an accident, a spot of radioactively contaminated seawater is formed near the facility and is spread with sea currents. The volumetric activity of radionuclides in the contamination spot decreases with distance from the accident site.

To describe seawater contamination during the acute period of a radiation accident, a two-dimensional model of radionuclide dispersion in seawater from an instantaneous point release was used. The dynamics of depth-averaged volumetric radionuclide activity in seawater, $\text{Bq}\cdot\text{m}^{-3}$, was calculated by the formula:

$$C_w(x, y, t) = \frac{A_0}{H} \cdot G(x, y, t) \cdot \exp\left(-\frac{w}{H} \cdot t\right), \quad (1)$$

where A_0 is the radionuclide activity released into seawater during an accident, Bq ;

H is the depth at the accident site, m ;

w is the hydraulic particle size, $\text{m}\cdot\text{s}^{-1}$;

t is the time from the moment of emergency (point) radionuclide release into seawater, s .

$G(x, y, t)$ is the dynamic function of scattering in the marine environment of a single one-time source, which is assessed by the formula [Yurezanskaya, Koterov, 2011]:

$$G(x, y, t) = \frac{1}{2 \cdot \pi \cdot \sigma_x \cdot \sigma_y} \cdot \exp\left(-\frac{(x - u_x \cdot t)^2}{2 \cdot \sigma_x^2} - \frac{(y - u_y \cdot t)^2}{2 \cdot \sigma_y^2}\right), \quad (2)$$

where x, y are the distances along coordinate axes with the center at the location of the source of contamination, m ;

u_x, u_y are speeds of currents along X- and Y-axis, respectively, $\text{m}\cdot\text{s}^{-1}$;

σ_x, σ_y are dispersion coefficients of the impurity distribution.

Dispersion coefficients of the impurity distribution were calculated by the formulas:

$$\sigma_x^2 = \alpha \cdot t^3 + \sigma_{0,x}^2; \quad \sigma_y^2 = \alpha \cdot t^3 + \sigma_{0,y}^2, \quad (3)$$

where $\alpha = 8 \cdot 10^{-9} \text{ m}^2\cdot\text{s}^{-3}$ for distances up to 10 km, and $\alpha = 2 \cdot 10^{-9} \text{ m}^2\cdot\text{s}^{-3}$ for distances more than 10 km;

σ_0 is the initial size of the radioactive contamination spot, m [Yurezanskaya, Koterov, 2011].

For a hypothetical accident with K-159, σ_0 value is taken to be equal to the submarine length, *i. e.*, $\sigma_0 = 107.4 \text{ m}$ [Sarkisov et al., 2015]. In the southern Barents Sea, the speed of the current $u_x = 0.4 \text{ m}\cdot\text{s}^{-1}$; the speed of the cross-current u_y is assumed to be zero (we consider contamination along the axis of the accident trail spread).

The specific activity of the radionuclide in the upper layer of bottom sediments, $\text{Bq}\cdot\text{kg}^{-1}$, at time t_s was determined by the formula:

$$C_s(x, y, t_s) = \int_0^{t_s} \frac{w}{\rho_s \cdot h} \cdot C_w(t) dt, \quad (4)$$

where ρ_s is the density of bottom sediments taken equal to $1,250 \text{ kg}\cdot\text{m}^{-3}$;

h is the thickness of the upper (effective) layer of bottom sediments, $h = 0.1 \text{ m}$ [MARINA II, 2003].

Large suspended particles (1 mm or more) are characterized by turbulent settling; their hydraulic size does not depend on the viscosity of the fluid and is calculated by the formula [Koterov, Yurezanskaya, 2009]:

$$w = \sqrt{\frac{4 \cdot g \cdot d_p \cdot \rho_p}{3 \cdot r \cdot \rho_w}}, \quad (5)$$

where $g = 9.8 \text{ m}\cdot\text{s}^{-2}$;

d_p is the suspended particle diameter, m;

r is the coefficient of water resistance for a spherical particle moving in it, $r = 0.45$ [Shilova, Studenov, 2017];

ρ_p is the density of suspended particles, $\rho_p = 2,600 \text{ kg}\cdot\text{m}^{-3}$;

ρ_w is the density of seawater, $\rho_w = 1,020 \text{ kg}\cdot\text{m}^{-3}$.

The settling of large particles formed during an accident at a radiation hazard facility in the sea occurs in its nearest zone, at a distance of approximately $2 \cdot \sigma_0$. When suspended particles decrease in size from 10^{-3} to 10^{-6} m, the sedimentation speed in seawater drops from 10^0 to $10^{-4} \text{ m}\cdot\text{s}^{-1}$. Small particles of radioactive contamination, comparable in size to particles of natural suspension in seawater, settle at rates corresponding to natural sedimentation. ^{137}Cs , ^{134}Cs , and ^{90}Sr can also be absorbed on natural suspension and settle together with the suspension into bottom sediments. Due to the settling of radioactive particles, in the upper layer of bottom sediments, a distributed source of radiation is formed; it affects the bottom biota both in the acute and long-term periods after accidental contamination. For the scenario under consideration, the value of w was calculated by formula (5) at $d_p = 10^{-3}$ m for distances up to 200 m from the site of the submarine K-159 sinking: $w = 0.27 \text{ m}\cdot\text{s}^{-1}$. For larger distances, w was taken equal to $10^{-4} \text{ m}\cdot\text{s}^{-1}$.

The estimated time for passage of a seawater contamination spot near an accidental source is short in the presence of a sea current and amounts to about 30 min for distances up to 200 m. With a hydraulic particle size, w , of $0.27 \text{ m}\cdot\text{s}^{-1}$ and a depth of 246 m, this time is sufficient for the formation of a contamination spot in bottom sediments. The specific activity of long-lived radionuclides in bottom sediments remains high for a long time after an accident. Therefore, when considering the effect on marine biota, it is advisable to select benthic organisms associated with benthic food chains as reference objects. As assumed in this work, the accumulation of radionuclides in benthic hydrobionts in this case is caused to a greater extent by contamination of the upper layer of bottom sediments, rather than seawater.

To determine the specific activity of a radionuclide in small hydrobionts (molluscs, zoobenthos, and aquatic plants) C_b , $\text{Bq}\cdot\text{kg}^{-1}$, one can conservatively use the linear dependence $C_b = CF_{b,s} \cdot C_s$, where $CF_{b,s}$ is the equilibrium coefficient of radionuclide transfer from bottom sediments to a hydrobiont. To calculate the dynamics of ^{137}Cs contamination of bottom fish after an accident, the equilibrium approach is not applicable [Kryshev, Ryabov, 2000]. The specific activity of a radionuclide in benthic fish C_f , $\text{Bq}\cdot\text{kg}^{-1}$, assuming that the main source of its contamination is the trophic chain associated with bottom sediments, is calculated by the equation:

$$\frac{dC_f}{dt} = -(\lambda + \varepsilon + \mu) \cdot C_f + (\varepsilon + \mu) \cdot CF_{f,s} \cdot C_s, \quad (6)$$

where λ is the radioactive decay constant, day^{-1} ;

μ is the relative increase in fish mass, day^{-1} ;

$CF_{f,s}$ is the equilibrium coefficient of radionuclide transfer from bottom sediments to fish;

ε is the parameter characterizing the metabolism and exchange of ^{137}Cs in the fish body, day^{-1} .

The procedure for ε calculation depending on fish mass and seawater temperature is described in [Kryshev, Ryabov, 2000; Sazykina et al., 2022].

For a short time after the accident, we can neglect the radioactive decay of ^{137}Cs and the decrease in its content in bottom sediments due to its penetration into deeper layers; so, we can consider the parameters μ and ε to be constant values. Then, the equation (6) has an analytical solution:

$$C_f = CF_{f,s} \cdot C_s \cdot (1 - \exp(-(\mu + \varepsilon) \cdot t)). \quad (7)$$

As a reference species of bottom fish, the European plaice *Pleuronectes platessa* Linnaeus, 1758 was chosen. With fish mass of 500 g, the calculated μ value is $6.45 \cdot 10^{-4} \text{ day}^{-1}$ [European Plaice, 2021], and $\varepsilon = 1.5 \cdot 10^{-3} \text{ day}^{-1}$. The equilibrium coefficients of ^{137}Cs transfer from bottom sediments to the Barents Sea biota are 0.22 for fish, 0.12 for molluscs, and 0.16 for aquatic plants. The values for ^{90}Sr are as follows: 0.027 for fish, 0.047 for molluscs, and 0.043 for aquatic plants [Rosnovskaya et al., 2022].

The dose rate of exposure to marine biota, $\text{mGy} \cdot \text{day}^{-1}$, was determined by the formula:

$$d_i = \beta_{int,i} \cdot C_i + \beta_{ext,i} \cdot (C_{w,i} + 0.5 \cdot \tau_s \cdot C_{s,i}), \quad (8)$$

where $\beta_{int,i}$ is the dose coefficient of internal exposure to a hydrobiont, $(\text{mGy} \cdot \text{kg})/(\text{Bq} \cdot \text{day})$;

C_i is the specific activity of the i -th radionuclide in a hydrobiont, $\text{Bq} \cdot \text{kg}^{-1}$;

$\beta_{ext,i}$ is the dose coefficient of external exposure to a hydrobiont, $(\text{mGy} \cdot \text{kg})/(\text{Bq} \cdot \text{day})$;

$C_{w,i}$ is the specific activity of the i -th radionuclide in seawater, $\text{Bq} \cdot \text{kg}^{-1}$;

$C_{s,i}$ is the specific activity of the i -th radionuclide in bottom sediments, $\text{Bq} \cdot \text{kg}^{-1}$;

τ_s is the fraction of time during which a hydrobiont is exposed to radiation from bottom sediments, taken equal to 1 for bottom fish and molluscs and 0.5 for aquatic plants.

The values of the dose coefficients were determined using the BiotaDC calculator, v.1.5.1 (<http://biotadc.icrp.org>), an annex to [ICRP Publication 136, 2017]. Marine organisms were approximated by ellipsoids with the following mass and ratios between axes: fish (the European plaice), 0.5 kg and 1/0.6/0.04; bivalves, $1.64 \cdot 10^{-2}$ kg and 1/0.5/0.5; and aquatic plants, $6.5 \cdot 10^{-3}$ kg and 1/0.01/0.01. The calculated values of dose coefficients for estimating internal and external exposure to marine organisms from ^{137}Cs , ^{134}Cs , and ^{90}Sr are given in Table 1.

Table 1. Dose coefficients for calculation of exposure to marine organisms, $(\text{mGy} \cdot \text{day}^{-1})/(\text{Bq} \cdot \text{kg}^{-1})$

| Radionuclide | The European plaice | Molluscs | Aquatic plants |
|-------------------|----------------------|----------------------|----------------------|
| Internal exposure | | | |
| ^{137}Cs | $3.77 \cdot 10^{-6}$ | $3.62 \cdot 10^{-6}$ | $3.1 \cdot 10^{-6}$ |
| ^{134}Cs | $3.34 \cdot 10^{-6}$ | $2.95 \cdot 10^{-6}$ | $2.28 \cdot 10^{-6}$ |
| ^{90}Sr | $1.34 \cdot 10^{-5}$ | $1.37 \cdot 10^{-5}$ | $1.07 \cdot 10^{-5}$ |
| External exposure | | | |
| ^{137}Cs | $7.49 \cdot 10^{-6}$ | $7.63 \cdot 10^{-6}$ | $8.16 \cdot 10^{-6}$ |
| ^{134}Cs | $2.04 \cdot 10^{-5}$ | $2.08 \cdot 10^{-5}$ | $2.15 \cdot 10^{-5}$ |
| ^{90}Sr | $2.12 \cdot 10^{-6}$ | $1.82 \cdot 10^{-6}$ | $4.8 \cdot 10^{-6}$ |

Doses of acute exposure were assessed as total absorbed doses accumulated by marine biota during the first 10 days after the accident. The distribution of the probability of lethal effects was determined by the formula [Finney, 1971]:

$$P = \frac{1}{\sqrt{2 \cdot \pi}} \cdot \int_{-\infty}^{Pr} \exp\left(-\frac{t^2}{2}\right) dt, \quad (9)$$

where the upper limit of integration of the Gauss error function is the so-called probit function which reflects the correlation between the probability of lethal effects and the absorbed dose.

The value of the probit function was calculated by the formula:

$$Pr = a_{Pr} + b_{Pr} \cdot \ln D, \quad (10)$$

where D is the dose of acute exposure, mGy.

To determine the parameters of the probit function for fish and molluscs, we used literature data on lethal effects for these hydrobionts after acute exposure at different doses [Effects of Ionizing Radiation, 1976; Polikarpov, 1964; Polikarpov, Egorov, 1986] (Table 2).

Table 2. Lethal effects of acute exposure to marine biota in relation to the absorbed dose and the calculated probit function, (mGy·day⁻¹)/(Bq·kg⁻¹)

| Dose, D, mGy | Ln(D) | % of lethality | Value of probit function |
|-----------------|--------|----------------|--------------------------|
| Fish (adult) | | | |
| 100 | 4.605 | 0.1 | 1.5 |
| 1,000 | 6.907 | 2.5 | 3.12 |
| 3,500 | 8.161 | 30 | 4.48 |
| 5,000 | 8.517 | 50 | 5 |
| 10,000 | 9.210 | 90 | 5.52 |
| Marine molluscs | | | |
| 10,000 | 9.210 | 50 | 4.75 |
| 20,000 | 9.903 | 70 | 5.5 |
| 40,000 | 10.596 | 90 | 6.28 |

Graphs of the probit function dependence on the logarithm of the absorbed dose were approximated by a linear function (Fig. 1). The values for parameters in formula (10) were as follows: $a_{Pr} = -2.74$ for fish and $a_{Pr} = -5.42$ for molluscs; $b_{Pr} = 0.89$ for fish and $b_{Pr} = 1.1$ for molluscs. The probability of lethal effects for marine organisms depending on the dose received in the first 10 days after the accident was calculated by formula (9) using standard tables [Finney, 1971; Metodika modelirovaniya, 2015].

During chronic exposure to marine biota from contaminated bottom sediments, the criterion for the occurrence of adverse radiobiological effects is the excess of the reference level of radiation dose rate for a given ecological group [ICRP Publication 108, 2008; ICRP Publication 124, 2014; Sazykina et al., 2022]. The reference level is 1 mGy·day⁻¹ for fish and aquatic plants and 10 mGy·day⁻¹ for molluscs. When the reference level is exceeded under chronic exposure throughout life of marine organisms, their health and reproductive capacity are impaired, and their lifespan is reduced [Sazykina, Kryshev, 2003; Sazykina et al., 2009].

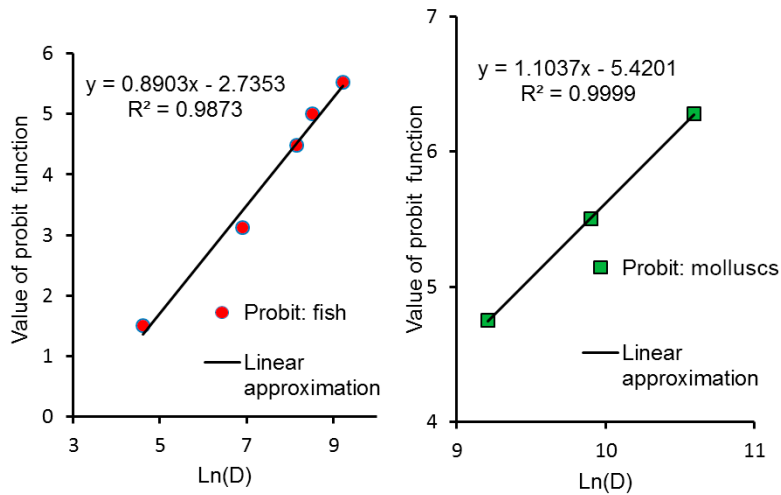


Fig. 1. Relationship between the probit function and logarithm of the acute dose (mGy) for fish (left side) and marine molluscs (right side)

RESULTS AND DISCUSSION

The calculated dynamics of water contamination with ^{137}Cs at a distance from 200 m to 30 km from the accidental source is shown in Fig. 2. In 200 m from the source, the time of passage of a contamination spot is no more than 30 min, and the maximum volumetric activity of ^{137}Cs in seawater during this period does not exceed $10^6 \text{ Bq}\cdot\text{m}^{-3}$. At a distance of 30 km, the volumetric activity of ^{137}Cs in seawater is maximum in 17 h after the accident and amounts to $6.3 \cdot 10^3 \text{ Bq}\cdot\text{m}^{-3}$. It is worth noting as follows: during the acute period of a radiation accident, comparison of calculated values for volumetric activity of ^{137}Cs in seawater with the control levels of radionuclide content in it [Poryadok rascheta, 2016] is incorrect due to the lack of equilibrium in radionuclide dispersion between the components of the marine ecosystem.

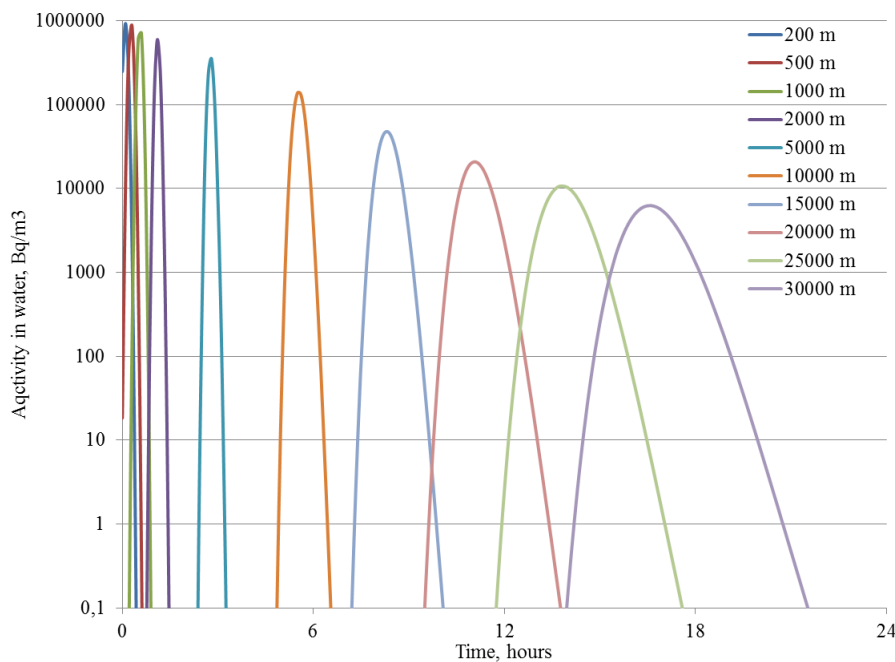


Fig. 2. Calculation of ^{137}Cs volume activity in seawater at different distances from the accidental source of contamination

The calculated dynamics of bottom sediment contamination with ^{137}Cs depending on the distance from the accidental source is presented in Fig. 3. Near the accident site (200 m), the specific activity of ^{137}Cs in the upper layer of bottom sediments can reach $1.2 \cdot 10^6 \text{ Bq}\cdot\text{kg}^{-1}$, and this exceeds the criterion for classifying this radionuclide as solid radioactive waste by 120 times. When moving away from the accident site, the estimated contamination of bottom sediments decreases significantly, since an assumption is made that the largest radionuclide-containing particles settle near the source of contamination. At a distance of 10 km from the accident site, the calculated specific activity of ^{137}Cs in bottom sediments does not exceed $150 \text{ Bq}\cdot\text{kg}^{-1}$. Unlike seawater contamination, bottom sediment contamination with ^{137}Cs slowly decreases over time, being a long-term source of exposure to benthic biota.

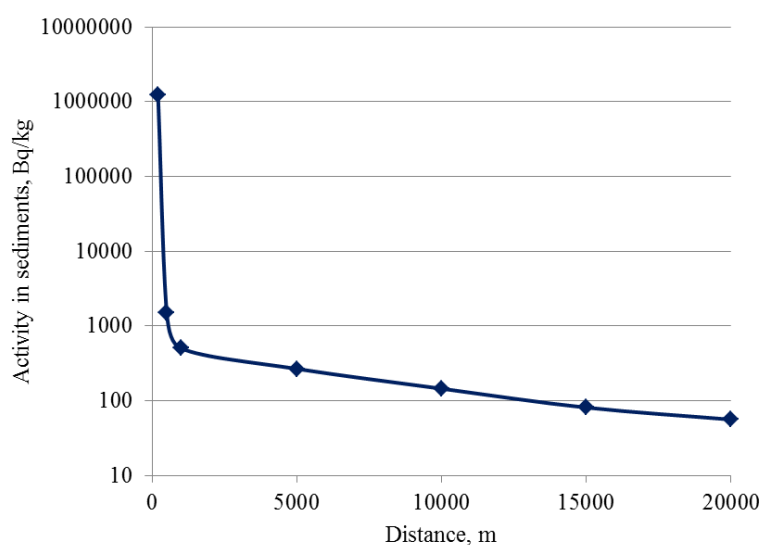


Fig. 3. Maximum activity concentrations of ^{137}Cs in bottom sediments at different distances from the accidental source of contamination

According to calculated estimates, the maximum volumetric activity of ^{90}Sr in seawater at a distance of 200 m from the accident site during the passage of the contamination spot does not exceed $2 \cdot 10^5 \text{ Bq}\cdot\text{m}^{-3}$. Contamination of bottom sediments with ^{90}Sr at a distance of 200 m from the accident site will be $2.8 \cdot 10^5 \text{ Bq}\cdot\text{kg}^{-1}$. The maximum volumetric activity of ^{134}Cs in seawater and its specific activity in bottom sediments will be $50 \text{ Bq}\cdot\text{m}^{-3}$ and $65 \text{ Bq}\cdot\text{kg}^{-1}$, respectively. The initial emergency release of ^{134}Cs into the marine environment is estimated to be 18,000 times lower than that of ^{137}Cs and 4,000 times lower than the value for ^{90}Sr [Sarkisov et al., 2015].

The accumulation of ^{137}Cs in benthic organisms is associated with its content in the upper layer of bottom sediments. The calculated specific activity of ^{137}Cs in molluscs at a distance of 200 m from the accident site is $2.6 \cdot 10^5 \text{ Bq}\cdot\text{kg}^{-1}$; in aquatic plants, the value is $1.9 \cdot 10^5 \text{ Bq}\cdot\text{kg}^{-1}$. When moving away from the accident site, their contamination decreases in proportion to the contamination of bottom sediments. As follows from formula (7), during the first 30 days after the accident, the specific activity of ^{137}Cs in benthic fish increases almost linearly; at a distance of 200 m from the source of contamination, the value rises from 400 to $6,000 \text{ Bq}\cdot\text{kg}^{-1}$. Under the conservative assumption that fish constantly occur there for several years, and the specific activity in bottom sediments does not decrease with time, the maximum (equilibrium) value of $2.4 \cdot 10^5 \text{ Bq}\cdot\text{kg}^{-1}$ is achieved no earlier than in two years after the accident.

The dose of acute exposure to bottom fish in the first 10 days after the accident is estimated at almost 100 mGy. The value of the probit function according to formula (10) is 1.36. The probability of lethal effects for fish equal to 1% is achieved with the value of the probit function of 2.67. Thus, the probability of death of bottom fish from exposure with ^{137}Cs , ^{134}Cs , and ^{90}Sr over 10 days of the acute period of the hypothetical accident under consideration is $< 1\%$.

The estimated dose rate of chronic exposure to the Barents Sea hydrobionts from long-lived radionuclides during the first year after the accident at different distances from the source of contamination is given in Table 3. In 200 m, the dose rate of chronic exposure to hydrobionts from an emergency release of ^{137}Cs is estimated to be $9.0 \text{ mGy}\cdot\text{day}^{-1}$ for fish, $9.7 \text{ mGy}\cdot\text{day}^{-1}$ for molluscs, and $5.5 \text{ mGy}\cdot\text{day}^{-1}$ for aquatic plants, with the main contributor being external exposure. The maximum dose rate of chronic exposure to hydrobionts from an emergency release of ^{90}Sr is estimated to be $0.7 \text{ mGy}\cdot\text{day}^{-1}$ for fish, $0.7 \text{ mGy}\cdot\text{day}^{-1}$ for molluscs, and $0.8 \text{ mGy}\cdot\text{day}^{-1}$ for aquatic plants. ^{134}Cs makes an insignificant contribution to the dose rate of exposure to hydrobionts, both in acute and chronic periods: no more than $1.4 \cdot 10^{-3} \text{ mGy}\cdot\text{day}^{-1}$ for fish, $1.5 \cdot 10^{-3} \text{ mGy}\cdot\text{day}^{-1}$ for molluscs, and $8.2 \cdot 10^{-4} \text{ mGy}\cdot\text{day}^{-1}$ for aquatic plants.

Table 3. Dose rate of chronic exposure to marine organisms with ^{137}Cs , ^{134}Cs , and ^{90}Sr at different distances from the accidental source of contamination, $\text{mGy}\cdot\text{day}^{-1}$

| Distance, m | Fish | Molluscs | Aquatic plants |
|-------------|---------------------|---------------------|---------------------|
| 200 | $9.7 \cdot 10^0$ | $1.1 \cdot 10^1$ | $6.3 \cdot 10^0$ |
| 500 | $1.4 \cdot 10^{-2}$ | $1.3 \cdot 10^{-2}$ | $7.9 \cdot 10^{-3}$ |
| 1,000 | $4.5 \cdot 10^{-3}$ | $4.3 \cdot 10^{-3}$ | $2.6 \cdot 10^{-3}$ |
| 5,000 | $2.4 \cdot 10^{-3}$ | $2.4 \cdot 10^{-3}$ | $1.4 \cdot 10^{-3}$ |
| 10,000 | $1.3 \cdot 10^{-3}$ | $1.3 \cdot 10^{-3}$ | $7.6 \cdot 10^{-4}$ |
| 20,000 | $7.2 \cdot 10^{-4}$ | $6.9 \cdot 10^{-4}$ | $4.3 \cdot 10^{-4}$ |

As follows from Table 3, at a distance of 500 m or greater from the source of contamination, the dose rate of exposure for all reference species is significantly lower than the reference level of safe chronic exposure ($1 \text{ mGy}\cdot\text{day}^{-1}$). Therefore, we can conclude about the local nature of the radioecological effect of a hypothetical accident with the nuclear submarine K-159 to the Barents Sea biota.

For benthic organisms that permanently inhabit the area of maximum contamination of bottom sediments (up to 200 m from the accident site), the dose rates indicated in Table 3 persist for several years. Due to the excess of the reference level of chronic exposure, these dose rates cannot be considered safe for the development of populations of bottom fish, molluscs, and aquatic plants in the immediate vicinity of the accident site.

Conclusion. The contribution of ^{137}Cs , ^{134}Cs , and ^{90}Sr to radioactive contamination of the marine environment was calculated, and dose rates on marine biota in the early period of contamination were determined for a hypothetical scenario of a radiation accident with the sunken nuclear submarine K-159.

The dose of acute exposure to bottom fish from ^{137}Cs , ^{134}Cs , and ^{90}Sr at a distance of 200 m from the accident site in the first 10 days is almost 100 mGy. The probability of lethal effects for bottom fish at such an absorbed dose is estimated to be less than 1%. Assessment of the release of short-lived radionuclides into the marine environment and their contribution to acute exposure to marine biota requires additional research within the framework of the scenario of an accident.

Contamination of bottom sediments with long-lived radionuclides slowly decreases over time, being a long-term source of exposure to benthic biota. The dose rate of chronic exposure to marine biota within the first year after the accident at a distance of 200 m from the source of contamination is estimated to be $9.7 \text{ mGy}\cdot\text{day}^{-1}$ for bottom fish, $11 \text{ mGy}\cdot\text{day}^{-1}$ for molluscs, and $6.3 \text{ mGy}\cdot\text{day}^{-1}$ for aquatic plants. These levels are higher than the reference value for dose rate of chronic exposure that ensure the safety of marine biota.

At a distance of 500 m and greater from the source of contamination, the dose rate of chronic exposure to marine biota is significantly lower than the reference level. This makes it possible to predict the local nature of the effect of a hypothetical accident on the Barents Sea ecosystem.

REFERENCES

1. Antipov S. V., Bilashenko V. P., Vysotskii V. L., Kalantarov V. E., Kobrinskii M. N., Sarkisov A. A., Sotnikov V. A., Shvedov P. A., Ibraev R. A., Sarkisyan A. S. Prediction and evaluation of the radioecological consequences of a hypothetical accident on the sunken nuclear submarine B-159 in the Barents Sea. *Atomnaya energiya*, 2015, vol. 119, iss. 2, pp. 106–113. (in Russ.)
2. Koterov V. N., Yurezanskaya Y. S. Simulation of suspended substance dispersion on the ocean shelf: Effective hydraulic coarseness of poly-disperse suspension. *Zhurnal vychislitel'noi matematiki i matematicheskoi fiziki*, 2009, vol. 49, no. 7, pp. 1245–1256. (in Russ.)
3. Kryshev A. I., Sazykina T. G., Katkova M. N., Kryshev I. I., Buryakova A. A., Pavlova N. N. Assessment of ecological risk to biota of the Stepovogo Bay of the Kara Sea after the hypothetical accidental contamination. *Radiatsionnaya biologiya. Radioekologiya*, 2022a, vol. 62, no. 4, pp. 424–433. (in Russ.)
4. *Metodika modelirovaniya rasprostraneniya avariinykh vybrosov opasnykh veshchestv. Rukovodstvo po bezopasnosti*. Utverzhdeno prikazom Federal'noi sluzhby po ekologicheskomu, tekhnologicheskomu i atomnomu nadzoru ot 20.04.2015 no. 158. Moscow : ZAO "NTTs PB", 2015, 125 p. (Normativnye dokumenty v sfere deyatel'nosti Federal'noi sluzhby po ekologicheskomu, tekhnologicheskomu i atomnomu nadzoru. Series 27. Deklarirovanie promyshlennoi bezopasnosti i otsenka riska ; iss. 11). (in Russ.)
5. Polikarpov G. G. *Radioekologiya morskikh organizmov*. Moscow : Atomizdat, 1964, 295 p. (in Russ.). <https://repository.marine-research.ru/handle/299011/12748>
6. Polikarpov G. G., Egorov V. N. *Morskaya dinamicheskaya radiokhemoekologiya*. Moscow : Energoatomizdat, 1986, 176 p. (in Russ.). <https://repository.marine-research.ru/handle/299011/7683>
7. *Poryadok rascheta kontrol'nykh urovnei sodержaniya radionuklidov v morskikh vodakh : rekomendatsii R-52.18.852-2016 / Rosgidromet*. Obninsk : FGBU "NPO "Taifun", 2016, 28 p. (in Russ.)
8. Rosnovskaya N. A., Kryshev A. I., Kryshev I. I. Determination of control levels of radionuclides ensuring acceptable environmental risk in the Barents Sea water and bottom sediments. *Morskoj biologicheskij zhurnal*, 2022, vol. 7, no. 4, pp. 70–80. (in Russ.). <https://marine-biology.ru/mbj/article/view/360>
9. Sazykina T. G., Kryshev A. I., Kryshev I. I. *Modelirovanie radioekologicheskikh protsessov v okruzhayushchei srede*. Moscow : OOO "Maska", 2022, 638 p. (in Russ.)
10. Sarkisov A. A., Antipov S. V., Vysotsky V. L., Kobrinsky M. N., Shvedov P. A., Bilashenko V. P., Khokhlov I. N. Forecast of the radioecological consequences of hypothetical accidents in nuclear and radiation hazardous objects located at the bottom of the Barents and Kara seas. *Atomnaya energiya*, 2018, vol. 125, iss. 6, pp. 343–351. (in Russ.)
11. Sarkisov A. A., Sivintsev Yu. V., Vysotskii V. L.,

- Nikitin V. S. *Atomnoe nasledie kholodnoi voyny na dne Arktiki. Radioekologicheskie i tekhniko-ekonomicheskie problemy radiatsionnoi rehabilitatsii morei*. Moscow : IBRAE RAN, 2015, 699 p. (in Russ.)
12. Shilova N. A., Studenov I. I. Peculiarities of calculation of hydraulic particle size to simulate the initial concentration of suspended substances in the estuarine areas of the Arctic seas (the case of the White Sea). *Arctic Environmental Research*, 2017, vol. 17, no. 4, pp. 295–307. (in Russ.). <https://doi.org/10.17238/issn2541-8416.2017.17.4.295>
 13. Yurezanskaya Y. S., Koterov V. N. *Modelirovaniye perenosa vzheshennykh veshchestv na okeanicheskom shel'fe*. Moscow : Lambert Academic Publishing, 2011, 116 p. (in Russ.)
 14. *Effects of Ionizing Radiation on Aquatic Organisms and Ecosystems*. Vienna : IAEA, 1976, 131 p. (IAEA Technical Report Series ; no. 172).
 15. *European Plaice (Pleuronectes platessa) of the Barents Sea: A Retrospective Review of Fishing and Research Activities for the Period 2016–2020 and a Modern Assessment of the State of Its Reserves*. Report on the Research Work. Agreement no. 18/2021 between the Polar Branch of the VNIRO (PINRO) and GELA Ltd. Murmansk : PINRO, 2021, 25 p.
 16. Finney D. J. *Probit Analysis*. 3rd edition. New York : Cambridge University Press, 1971, 333 p.
 17. Hosseini A., Amundsen I., Brown J., Dowdall M., Dyve J. E., Klein H. *Radiological Impact Assessment for Hypothetical Accident Scenarios Involving Russian Nuclear Submarine K-159*. Østerås : Statens Strålevern, 2017, 145 p. (Strålevern Rapport ; no. 12).
 18. ICRP Publication 108. Environmental protection: The concept and use of reference animals and plants. *Annals of the ICRP*, 2008, vol. 38, nos 4–6, 242 p.
 19. ICRP Publication 124. Protection of the environment under different exposure situations. *Annals of the ICRP*, 2014, vol. 43, no. 1, 58 p.
 20. ICRP Publication 136. Dose coefficients for non-human biota environmentally exposed to radiation. *Annals of the ICRP*, 2017, vol. 46, no. 2, 136 p.
 21. Iosjpe M., Amundsen I., Brown J., Dowdall M., Hosseini A., Strand P. *Radioecological Assessment After Potential Accidents with the Russian Nuclear Submarines K-27 and K-159 in the Arctic Marine Environment*. Østerås : Norwegian Radiation and Nuclear Safety Authority, 2020, 78 p. (DSA Report ; no. 7).
 22. Kryshev A. I., Ryabov I. N. A dynamic model of ¹³⁷Cs accumulation by fish of different age classes. *Journal of Environmental Radioactivity*, 2000, vol. 50, iss. 3, pp. 221–233. [https://doi.org/10.1016/S0265-931X\(99\)00118-6](https://doi.org/10.1016/S0265-931X(99)00118-6)
 23. Kryshev A. I., Sazykina T. G., Katkova M. N., Buryakova A. A., Kryshev I. I. Modelling the radioactive contamination of commercial fish species in the Barents Sea following a hypothetical short-term release to the Stepovogo Bay of Novaya Zemlya. *Journal of Environmental Radioactivity*, 2022b, vols 244–245, art. no. 106825 (9 p.). <https://doi.org/10.1016/j.jenvrad.2022.106825>
 24. *MARINA II. Update of the MARINA Project on the Radiological Exposure of the European Community from Radioactivity in North European Marine Waters*. Vol. 2. Luxembourg : Office for Official Publications of the European Communities, 2003, 364 p. (Radiation Protection ; 132).
 25. Sazykina T. G. The regional radioecological model “Arctic” for predictions of radioactive contamination of the Barents and Kara seas. In: *International Symposium on Marine Pollution*, Monaco, 5–9 October, 1998 : Extended Synopses. [Vienna] : International Atomic Energy Agency, 1998, pp. 339–340.
 26. Sazykina T. G., Kryshev A. I. EPIC database on the effects of chronic radiation in fish: Russian/FSU data. *Journal of Environmental Radioactivity*, 2003, vol. 68, iss. 1, pp. 65–87. [https://doi.org/10.1016/S0265-931X\(03\)00030-4](https://doi.org/10.1016/S0265-931X(03)00030-4)
 27. Sazykina T. G., Kryshev A. I., Sanina K. D. Non-parametric estimation of thresholds for radiation effects in vertebrate species under chronic low-LET exposures. *Radiation and Environmental Biophysics*, 2009, vol. 48, iss. 4, pp. 391–404. <https://doi.org/10.1007/s00411-009-0233-0>

**ОЦЕНКА РАДИАЦИОННОГО ВОЗДЕЙСТВИЯ ^{137}Cs , ^{134}Cs , ^{90}Sr
НА БИОТУ БАРЕНЦЕВА МОРЯ
ВБЛИЗИ ИСТОЧНИКА ЗАГРЯЗНЕНИЯ
ПРИ ГИПОТЕТИЧЕСКОЙ АВАРИИ
С ЗАТОНУВШЕЙ АТОМНОЙ ПОДВОДНОЙ ЛОДКОЙ К-159**

Т. Г. Сазыкина, А. И. Крышев

Научно-производственное объединение «Тайфун», Обнинск, Российская Федерация

E-mail: ecomod@yandex.ru

Выполнено моделирование воздействия излучения ^{137}Cs , ^{134}Cs , ^{90}Sr на морскую биоту для гипотетической аварии с самопроизвольной цепной реакцией на затонувшей подводной лодке К-159 при её подъёме и транспортировке в Баренцевом море. Для описания загрязнения морской воды в острый период аварии использована двумерная модель рассеивания радионуклидов в морской воде от мгновенного источника. Рассчитано радиоактивное загрязнение ^{137}Cs , ^{134}Cs , ^{90}Sr морской воды и донных отложений на расстояниях от 200 м до 30 км от источника. Доза острого облучения придонной рыбы от ^{137}Cs , ^{134}Cs , ^{90}Sr на расстоянии 200 м от места аварии за первые 10 дней составляет почти 100 мГр. Согласно оценке, вероятность летальных эффектов для придонной рыбы при такой поглощённой дозе — менее 1 %. Мощность дозы хронического облучения морской биоты ^{137}Cs , ^{134}Cs , ^{90}Sr в течение первого года с момента аварии на расстоянии 200 м от источника загрязнения оценена в 9,7 мГр-сут⁻¹ для придонной рыбы, 11 мГр-сут⁻¹ для моллюсков и 6,3 мГр-сут⁻¹ для водных растений. Эти уровни выше референтного значения мощности дозы хронического облучения, обеспечивающего безопасность морской биоты, поэтому нельзя рассматривать такие дозовые нагрузки как безопасные для развития популяций придонной рыбы, моллюсков и водных растений в непосредственной близости от места аварии. При удалении от источника загрязнения на 500 м и более мощность дозы хронического облучения морской биоты значительно ниже референтного уровня. Дозовые нагрузки на биоту Баренцева моря для аварийного сценария обусловлены преимущественно внешним облучением от донных отложений, а также переходом долгоживущих радионуклидов из донных отложений в придонные организмы.

Ключевые слова: Арктика, Баренцево море, радиационная авария, моделирование, морская биота, доза, острое облучение, хроническое облучение

NOTES

UDC 597.311.2(265.1)

**ON A LARGE SHORTFIN MAKO SHARK
ISURUS OXYRINCHUS (LAMNIDAE)
OBSERVED AT CABO SAN LUCAS, MEXICO
(EASTERN CENTRAL PACIFIC OCEAN)**

© 2023 **J. Brunetti¹, A. De Maddalena², M. A. Eliceche Constantini¹, and C. Calatayud¹**

¹Cabo Shark Dive, Cabo San Lucas, Baja California Sur, Mexico

²Shark Museum, Simon's Town, Cape Town, South Africa

E-mail: info@cabosharkdive.com

Received by the Editor 05.07.2023; after reviewing 02.08.2023;
accepted for publication 04.08.2023; published online 01.12.2023.

A large female shortfin mako shark, *Isurus oxyrinchus* Rafinesque, 1810, was observed on 26 March, 2023, off Cabo San Lucas, Baja California Sur, Mexico. The total length was carefully estimated at 450 cm. This shark is the third largest mako ever recorded and the second largest observed and photographed alive.

Keywords: shortfin mako shark, *Isurus oxyrinchus*, Mexico, size

The shortfin mako shark *Isurus oxyrinchus* Rafinesque, 1810 belongs to the order Lamniformes and the family Lamnidae. This shark inhabits temperate and tropical waters of the Atlantic, Pacific, and Indian oceans. It is pelagic, coastal, and oceanic, occurring at a depth range from 1 to 500 m [Compagno, 2002]. The embryonic development of this species is ovoviviparous, with 15–18-month gestation and litter size of 4–25 young. Its size at birth is 60–70 cm, and it can attain a maximum size of 585 cm. This shark feeds on bony fishes, elasmobranchs, marine turtles, squids, crustaceans, marine mammals, birds, salps, and Porifera [De Maddalena et al., 2015].

In the present article, we report a record of a huge shortfin mako encountered in March 2023 by the first author in Pacific Mexican waters.

MATERIAL AND METHODS

On the morning of 26 March, 2023, the first author, Jacob Brunetti, the co-owner of the shark diving company *Cabo Shark Dive*, was snorkeling with a group of snorkelers in the waters off Cabo San Lucas, Baja California Sur, Mexico, in the eastern central Pacific Ocean. From the boat, a 9.5-m “Robalo 2 Bertram,” sardines *Sardinops* sp. and bonitos *Sarda* sp. were used as chum to attract the sharks to the site and keep them interested around the snorkelers for viewing purposes. No other boats were present in the area. Pictures of the shark were taken by two of the snorkelers.

RESULTS AND DISCUSSION

At 10:00 a.m., with a relatively calm sea and little wind, a very large shortfin mako was observed in 1,000-m deep blue waters, 2.5 nautical miles from the coast (Fig. 1). The snorkelers were already in the water with a smaller male shortfin mako, with the total length (hereinafter TL) estimated at 150 cm, and four female blue sharks *Prionace glauca* (Linnaeus, 1758), TL ranging from 180 to 210 cm. The large mako showed no interest in the boat; it was shy towards the snorkelers and swam just once close to them. However, it showed an aggressive behavior towards the blue sharks, and it was observed attempting to catch one of them (Fig. 2). After a few minutes, the large mako left the area.



Fig. 1. The estimated 450-cm TL female shortfin mako shark *Isurus oxyrinchus* observed off Cabo San Lucas, Baja California Sur, Mexico, on 26 March, 2023. Photo by Alexander Schmidt

The underwater images show clearly the morphological features of the animal that allowed the authors to make an immediate identification of the shark as an unusually large shortfin mako *I. oxyrinchus*. These morphological features include markedly spindle-shaped body, pointed conical snout, wide caudal keels, lunate caudal fin, long gill slits, high and erect first dorsal fin, greyish blue coloration with strong metallic reflection on the flanks, and long and pointed teeth protruding from the mouth in the lower jaw [Compagno, 2002; De Maddalena et al., 2005, 2015]. The first author was also able to observe the pelvic area, which revealed the absence of claspers. He could therefore conclude that the shark was a female. On the head and the trunk, there were bite scars that were likely the result of love bites by male makos.

The size of the shark was estimated by the first author at 450 cm TL, based on the size of an estimated 200-cm blue shark, which was observed swimming close to the mako.

The estimated size of the mako observed off Cabo San Lucas is unusual for *I. oxyrinchus*. A study of 199 shortfin mako sharks showed an average TL of 171 cm [Kohler et al., 1996]. Female shortfin makos attain sexual maturity between 270- and 300-cm TL, and male makos, between 195- and 215-cm TL. This species can sometimes attain huge sizes, but records of specimens reaching and exceeding 4 m are very rare [De Maddalena et al., 2023]. The largest shortfin mako reported to date worldwide was a female caught in the late 1950s in the Aegean Sea off Marmaris, Turkey, which was estimated at 585-cm TL [Kabasakal, De Maddalena, 2011]. The second largest mako ever recorded was an estimated 500-cm-long female observed on 28 June, 2018, near Cabrera Grande, in the Balearic Islands, Spain [Lopez-Mirones et al., 2020].

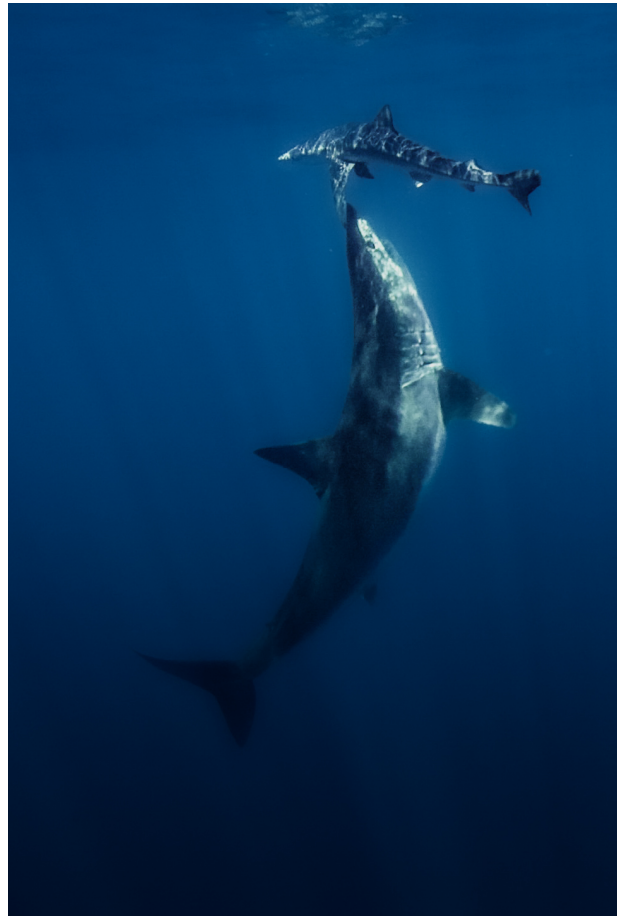


Fig. 2. The 450-cm TL female shortfin mako shark *Isurus oxyrinchus* performing a vertical approach on a 200-cm TL blue shark *Prionace glauca*. Photo by Pollo Berho

Conclusion. The estimated 450-cm TL female shortfin mako shark observed off Cabo San Lucas is one of the largest of its species recorded worldwide. It is the third largest mako ever recorded and the second largest observed and photographed alive.

REFERENCES

1. Compagno L. J. V. *Sharks of the World*. An annotated and illustrated catalogue of shark species known to date. Vol. 2 : Bullhead, mackerel and carpet sharks (Heterodontiformes, Lamniformes and Orectolobiformes). Rome : FAO, 2002, 269 p. (FAO Species Catalogue for Fishery Purposes ; no. 1).
2. De Maddalena A., Preti A., Smith R. *Mako Sharks*. Malabar : Krieger Publishing, 2005, 72 p.
3. De Maddalena A., Baensch H., Heim W. *Sharks of the Mediterranean. An Illustrated Study of All Species*. Jefferson : McFarland & Co., 2015, 204 p.
4. De Maddalena A., Bonomo M. G., Calascibetta A., Gordigiani L. On a large shortfin mako shark *Isurus oxyrinchus* Rafinesque, 1810 (Lamnidae) observed at Pantelleria (Central Mediterranean Sea). *Annales, Series Historia Naturalis*, 2023, vol. 33, iss. 1, pp. 43–48. <https://doi.org/10.19233/ASHN.2023.07>
5. Kabasakal H., De Maddalena A. A huge shortfin mako shark *Isurus oxyrinchus* Rafinesque, 1810 (Chondrichthyes: Lamnidae) from the waters of Marmaris, Turkey. *Annales, Series Historia Naturalis*, 2011, vol. 21, iss. 1, pp. 21–24.
6. Kohler N. E., Casey J. G., Turner P. A. *Length–Length and Length–Weight Relationships*

for 13 Shark Species from the Western North Atlantic. Washington D. C. : NOAA, 1996, 22 p. (NOAA Technical Memorandum NMFS-NE-110).

7. Lopez-Mirones F., De Maddalena A., Sagarmirana Van Buiten R. On a huge shortfin mako

shark *Isurus oxyrinchus* Rafinesque, 1810 (Chondrichthyes: Lamnidae) observed at Cabrera Grande, Balearic Islands, Spain. *Annales, Series Historia Naturalis*, 2020, vol. 30, iss. 1, pp. 25–30. <https://doi.org/10.19233/ASHN.2020.04>

**О КРУПНОЙ АКУЛЕ-МАКО *ISURUS OXYRINCHUS* (LAMNIDAE),
ЗАМЕЧЕННОЙ В КАБО-САН-ЛУКАС, МЕКСИКА
(ВОСТОЧНО-ЦЕНТРАЛЬНАЯ ЧАСТЬ ТИХОГО ОКЕАНА)**

Дж. Брунетти¹, А. Де Маддалена², М. А. Эличече Константини¹, К. Калатаюд¹

¹Центр погружения с акулами в Кабо, Кабо-Сан-Лукас, Южная Нижняя Калифорния, Мексика

²Музей акул, Саймонс-Таун, Кейптаун, Южная Африка

E-mail: info@cabosharkdive.com

Крупную самку акулы-мако *Isurus oxyrinchus* Rafinesque, 1810 наблюдали 26 марта 2023 г. у Кабо-Сан-Лукас, Южная Нижняя Калифорния, Мексика. Общая длина экземпляра оценена в 450 см. Эта акула является третьей по величине акулой-мако, когда-либо зарегистрированной, и второй по величине, наблюдаемой и сфотографированной живой.

Ключевые слова: акула-мако, *Isurus oxyrinchus*, Мексика, размер

UDC 582.263.3-152.632.33(262.5.04)

RESTORATION OF THE *CHARA ACULEOLATA* KÜTZING PHYTOCENOSIS IN THE TENDROVSKY BAY (BLACK SEA)

© 2023 D. D. Koroliesova

Black Sea Biosphere Reserve, Golaya Pristan, Russian Federation

E-mail: chernyakova.darya@gmail.com

Received by the Editor 25.05.2023; after reviewing 03.07.2023;
accepted for publication 04.08.2023; published online 01.12.2023.

For the *Chara aculeolata* Kützing phytocenosis in the Tendrovsky Bay of the Black Sea, long-term dynamics of growth areas and biomass of macrophytes was analyzed. Its partial degradation was observed since 1993. In 1993–2010, the area of the phytocenosis decreased from 100 to 6.3 km². In 2010–2021, elements of regenerative succession were registered. A gradual slow expansion of growth areas and an increase in algae biomass were noted over the 10-year monitoring, and a sudden significant recovery was recorded in 2021. According to the data of 2021, the *C. aculeolata* phytocenosis was distributed over an area of 36 km², and the biomass of the dominant species reached 1,800 g·m⁻². Possible reasons for the observed changes are discussed.

Keywords: Charophyta, macrophytobenthos, regenerative succession, long-term dynamics, recolonization

Charophytes are recorded from a variety of water bodies. Those algae are most typical for bottom vegetation of freshwater oligotrophic lakes [Pelechaty et al., 2019], as well as sea bays and lagoons of partially saline seas of Eurasia [Kovtun et al., 2011]. Their dense beds determine the conditions for the functioning of coastal ecosystems, form the habitat for many species of hydrobionts [Beilby et al., 2022; Sooksawat et al., 2017] and serve as an important food resource for waterbird species [Schmieder et al., 2006].

The first mentions of charophytes from the Black Sea date back to the early XX century [Pauli, 1927; Zernov, 1908]. Communities of charophyte algae were widely distributed in the northern Black Sea [Milchakova, Aleksandrov, 1999; Morozova-Vodyanitskaya, 1959; Palamar-Mordvintseva, 1998; Sadogursky, 2009]. Their development was maximum in the Karkinitzky [Morozova-Vodyanitskaya, 1959; Sadogursky, 2009], Tendrovsky, Yagorlytsky, and Dzharylgachsky bays [Cherniakov, 1995; Pogrebnyak, 1965; Tkachenko, Maslov, 2002], where their total stock was estimated at 1,176.8 thousand tones. More than 40% of this volume accounted for the Tendrovsky Bay, where *Lamprothamnium papulosum* (Wallroth) J. Groves, 1916 and *Chara aculeolata* Kützing, 1832 dominated [Pogrebnyak, 1965].

About 30 years ago, ubiquitous reduction in growth areas and decrease in the productivity of phytocenoses of charophytes were registered; in the Tendrovsky Bay, these algae degraded almost completely. After 1993, *C. aculeolata* was revealed in this bay in small areas, and it did not form characteristic phytocenoses [Cherniakov, 1995; Korolesova, 2017; Tkachenko, Maslov, 2002].

In 2010, we recorded a slight restoration of the *C. aculeolata* phytocenosis. Therefore, the aim of the research was to estimate the dynamics of restoration succession, current state, and boundaries of the phytocenosis in the shallow area of the Tendrovsky Bay.

MATERIAL AND METHODS

The Tendrovsky Bay is located in the northwestern Black Sea. It is a semi-enclosed shallow water body, naturally divided into eastern and western parts. As Charophyta communities were not noted in the western, deeper bay part, this paper presents data for the eastern one. Its total area is 365 km², and the mean depth is 1.5 m. Silty and silty-sandy sediments dominate there [Cherniakov, 1995]. The mean salinity of surface waters is 13.5‰. Their maximum temperature is observed in August and ranges within +20...+32.3 °C. In the macrophytobenthos, two types of Charophyta communities are described – *L. papulosum* and *C. aculeolata* [Korolesova, 2017; Pogrebnyak, 1965].

To study the restoration dynamics of the *C. aculeolata* community throughout the eastern Tendrovsky Bay, a square network of stations with a step of 2 km was used. The material was macrophytes sampled at network stations annually in the summer season in 2010–2021. We used a standard geobotanical technique [Kalugina-Gutnik, 1975] and laid a frame of 25 × 25 cm in triplicate at each station. Qualitative sampling was carried out with a scraper with a working width of 30 cm or manually. For bottom phytocenoses, we determined a projective cover of abundant species and their biomass (g·m⁻² wet weight).

Samples of macrophytes were washed in seawater and fixed with a 4% formalin solution or frozen at a temperature of –18 °C. Some of the algae were herbarized [Gollerbakh, Krasavina, 1983; Minicheva et al., 2014].

Macrophytes were determined down to a species level according to monographic summaries [Gollerbakh, Krasavina, 1983; Vinogradova, 1974; Zinova, 1967], and nomenclatural changes were given in accordance with AlgaeBase (<https://www.algaebase.org/>). *C. aculeolata* taxonomic status is presented according to the report of Charophyta regional flora [Borisova, Tkachenko, 2008], since the taxonomic position of the species remains not fully clarified, and published sources contain different names – *Chara intermedia* A. Braun, 1859 (syn. *Chara papillosa* Kützing, 1834) and *Chara baltica* (Hartman) Bruzelius, 1824 [Romanov et al., 2020]. The phytocenoses are named in accordance with the classification of the Black Sea bottom vegetation [Kalugina-Gutnik, 1975].

The growth area of macrophytes was calculated using the Quantum Gis software (3.28.5).

RESULTS AND DISCUSSION

The *C. aculeolata* phytocenosis belongs to monocenoses, since the biomass of the dominant species makes up more than 90% of the total biomass. In the community, 10 species of macrophytes were identified: *C. aculeolata*, *L. papulosum*, *Chaetomorpha linum* (O. F. Müller) Kützing, 1845, *Lophosiphonia obscura* (C. Agardh) Falkenberg, 1897, *Callithamnion granulatum* (Ducluzeau) C. Agardh, 1828, *Chondria capillaris* (Hudson) M. J. Wynne, 1991, *Chondria dasyphylla* (Woodward) C. Agardh, 1817, *Laurencia obtusa* (Hudson) J. V. Lamouroux, 1813, *Polysiphonia opaca* (C. Agardh) Moris & De Notaris, 1839, and *Stuckenia pectinata* (Linnaeus) Börner, 1912. The following species were characterized by the highest occurrence: red algae (Rhodophyta), *Ch. capillaris* and *L. obscura* (63 and 50%, respectively); Charophyta, *L. papulosum* (38%); and higher aquatic plants (Angiospermatophyta), *S. pectinata* (25%).

In 2010–2020, the *C. aculeolata* phytocenosis was registered on average at 6% of stations, and the area it occupied varied from 4 to 8 km², with a mean of 6.3 km². In 2021, the phytocenosis was recorded at 13 stations out of 27 studied (its occurrence was 48%); its area reached 36 km², or 10% of the total monitoring area (Fig. 1). The *C. aculeolata* community was represented by dense, almost closed beds with a projective cover of 90–100%; it was distributed along the Tendrovskaya Spit and to the northwest of Smaleny Island. By 2021, the growth area was about 40% of that of the 1960s and almost doubled the area of the mid-1990s.

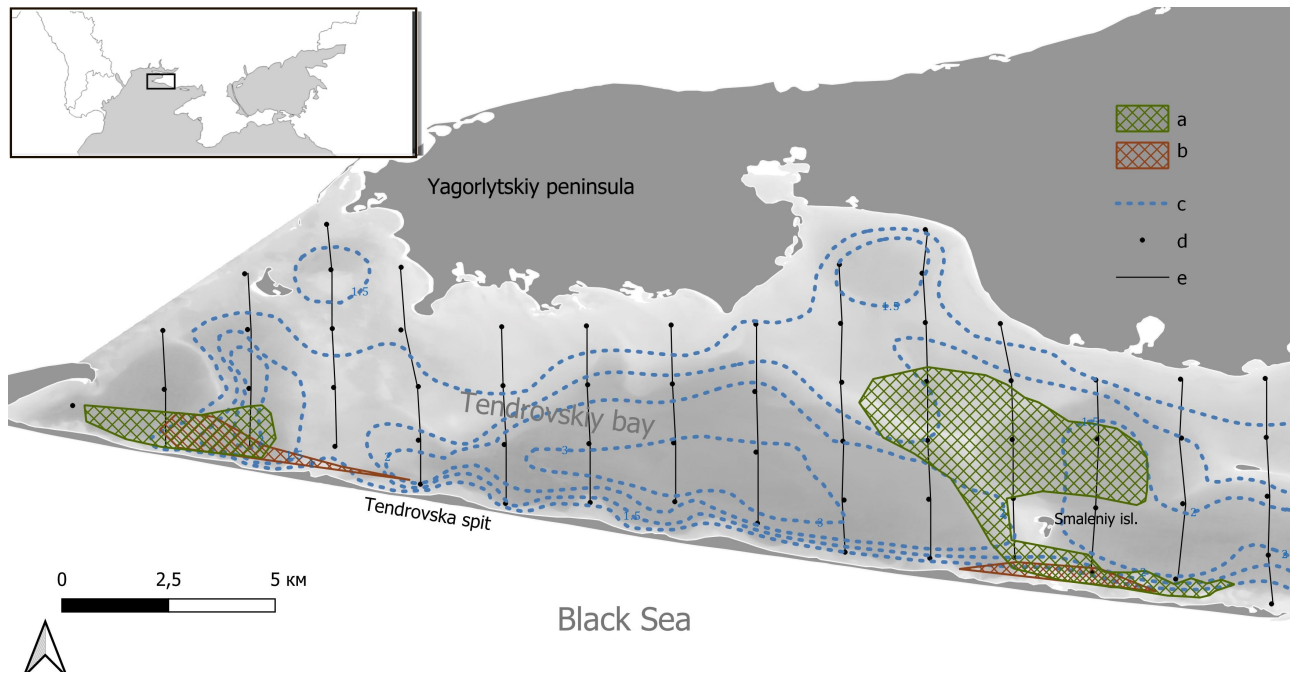


Fig. 1. Map of the *Chara aculeolata* phytocenosis distribution and monitoring stations scheme in the eastern Tendrovsky Bay: a, phytocenosis area in 2021; b, phytocenosis area in 2010–2020; c, isobaths; d, monitoring network stations; e, transects

In 2010–2016, the mean biomass of the *C. aculeolata* phytocenosis was $(485.28 \pm 221.17) \text{ g}\cdot\text{m}^{-2}$. In 2021, it reached $1,926 \text{ g}\cdot\text{m}^{-2}$, with the dominant species accounting for more than 90% of the community biomass ($1,800 \text{ g}\cdot\text{m}^{-2}$). In total, the values of the phytocenosis biomass became comparable with those of the 1960s, exceeding the values characteristic of the last decade by more than 4 times. To date, the phytocenosis restoration is observed within previously known growth boundaries (after 25 years of its partial degradation) [Pogrebnyak, 1965].

At this stage, it is impossible to identify reliably the causes of these changes. The restoration of Charophyta communities after partial or complete degradation is described in the literature for the Baltic Sea bays [Torn, Martin, 2003] and European fresh water bodies [Pefechaty et al., 2019; Sand-Jensen et al., 2017; Simons et al., 1994].

Most researchers believe that Charophyta restoration is directly driven by a decrease in the level of exposure to adverse environmental factors – anthropogenic load, eutrophication, etc. [Kovtun et al., 2011; Torn, Martin, 2003]. For the northwestern Black Sea, the restoration of communities of charophytes is also associated with their long-term cycles [Cherniakov, 1995].

The decrease in the level of eutrophication in the Tendrovsky Bay occurred long before the registration of the first elements of the restoration succession of the *C. aculeolata* phytocenosis there [Korolesova, 2017; Zaika et al., 2004]. In our opinion, *C. aculeolata* recolonization may be related to the effect of abiotic and biotic factors, including the cyclical development of Charophyta communities.

Conclusion. Based on the research carried out, elements of restorative succession and recolonization of the *Chara aculeolata* phytocenosis in the eastern Tendrovsky Bay in 2010–2021 were identified. By 2021, the biomass of the community and the area it occupied turned out to be comparable with those of the 1960s and exceeded the values recorded in the mid-1990s.

To identify the causes of the *C. aculeolata* recolonization, further investigation of a complex of biotic and abiotic factors affecting the composition and structure of Charophyta communities in the Tendrovsky Bay is required.

The work was carried out within the framework of the research assignment “Monitoring of the state of natural complexes of the Black Sea Biosphere Reserve (“Chronicle of Nature”).”

Acknowledgment. The author is grateful to PhD D. Chernyakov for his assistance in expeditionary work and recommendations on the research topic.

REFERENCES

1. Borisova E. V., Tkachenko F. P. A contribution to the flora of Charales in southwest Ukraine. *Algologia*, 2008, vol. 18, no. 3, pp. 287–298. (in Russ.)
2. Vinogradova K. L. *Ul'voye vodorosli (Charophyta) morei SSSR*. Leningrad : Nauka, 1974, 166 p. (in Russ.)
3. Gollerbakh M. M., Krasavina L. K. *Opredelitel' presnovodnykh vodoroslei SSSR* : in 14 vols. Leningrad : Nauka, Leningr. otd-nie, 1983, vol. 14 : *Kharovye vodorosli*, 190 p. (in Russ.)
4. Zaika V. E., Boltachev A. R., Zuev G. V., Kovalev A. V., Milchakova N. A., Sergeeva N. G. Floristic and faunistic changes in the Crimean Black Sea shelf after 1995–1998. *Morskoy ekologicheskij zhurnal*, 2004, vol. 3, no. 2, pp. 37–44. (in Russ.). <https://repository.marine-research.ru/handle/299011/745>
5. Zernov S. A. Otchet po komandirovke v severozapadnuyu chast' Chernogo morya dlya izucheniya fauny i sobiraniya kolleksii Zoologicheskogo muzeya Imperatorskoi akademii nauk (Odesskii zaliv, Dnepro-Bugskii liman, Karkinitiskii i Dzharylgatskii zalivy). *Ezhegodnik Zoologicheskogo muzeya Imperatorskoi akademii nauk*, 1908, vol. 13, pp. 154–166. (in Russ.)
6. Zinova A. D. *Opredelitel' zelenykh, burykh i krasnykh vodoroslei yuzhnykh morei SSSR*. Moscow ; Leningrad : Nauka, 1967, 400 p. (in Russ.)
7. Kalugina-Gutnik A. A. *Fitobentos Chernogo morya*. Kyiv : Naukova dumka, 1975, 248 p. (in Russ.). <https://repository.marine-research.ru/handle/299011/5645>
8. Korolesova D. D. Current state of the macrophytobenthos in Tendrivska and Yagorlytska Bays of Black Sea Biosphere Reserve. *Chornomorskyi botanichnyi zhurnal*, 2017, vol. 13, no. 4, pp. 457–467. (in Ukr.). <https://doi.org/10.14255/2308-9628/17.134/4>
9. Milchakova N. A., Aleksandrov V. V. Bottom vegetation at some sites of coastal salt lake Donuzlav (the Black Sea). *Ekologiya morya*, 1999, iss. 49, pp. 68–71. (in Russ.). <https://repository.marine-research.ru/handle/299011/4237>
10. Morozova-Vodyanitskaya N. V. Rastitel'nye assotsiatsii v Chernom more. *Trudy Sevastopol'skoi biologicheskoi stantsii*, 1959, vol. 11, pp. 3–28. (in Russ.). <https://repository.marine-research.ru/handle/299011/5389>
11. Palamar-Mordvintseva G. M. Charophyta of the Crimean Peninsula (Ukraine). *Al'gologiya*, 1998, vol. 8, no. 1, pp. 14–22. (in Russ.)
12. Pauli V. L. Materialy k poznaniyu biotsenozov Egorlytskogo zaliva. *Trudy Vseukrainskoi*

- gosudarstvennoi Chernomorsko-Azovskoi nauchno-promyslovoi opytnoi stantsii*, 1927, vol. 2, iss. 2, pp. 63–75. (in Russ.)
13. Pogrebnyak I. I. *Donnaya rastitel'nost' limanov Severo-Zapadnogo Prichernomor'ya i sopredel'nykh im akvatorii Chernogo morya* : avtoref. dis. ... d-ra biol. nauk. Odesa, 1965, 31 p. (in Russ.)
 14. Sadogursky S. E. Aquatic flora and vegetation in the filial "Swan Islands" of the Crimean Nature Reserve (Black Sea): Its modern state and the ways of preservation. *Zapovidna sprava v Ukraini*, 2009, vol. 15, no. 2, pp. 41–50. (in Russ.)
 15. Tkachenko F. P., Maslov I. I. Marine macrophytobenthos of Chernomorsky Biosphere Reservation. *Ekologiya morya*, 2002, iss. 62, pp. 34–40. (in Russ.). <https://repository.marine-research.ru/handle/299011/4556>
 16. Cherniakov D. A. *Pryrodno-akvalni landshaftni komplekсы Tendrivskoi ta Yehorlytskoi zatok i monitorynh yikh stanu u Chornomorskomu biosfernomu zapovidnyku* : avtoref. dis. ... kand. heohr. nauk. Kharkiv, 1995, 16 p. (in Ukr.)
 17. Beilby M. J., Bisson M. A., Schneider S. C. How characean algae take up needed and excrete unwanted ions – An overview explaining how insights from electrophysiology are useful to understand the ecology of aquatic macrophytes. *Aquatic Botany*, 2022, vol. 181, art. no. 103542 (9 p.). <https://doi.org/10.1016/j.aquabot.2022.103542>
 18. Kovtun A., Torn K., Martin G., Kullas T., Kotta J., Suursaar Ü. Influence of abiotic environmental conditions on spatial distribution of charophytes in the coastal waters of West Estonian Archipelago, Baltic Sea. *Journal of Coastal Research*, 2011, spec. iss. 64, pp. 412–416.
 19. Minicheva G., Afanasyev D., Kurakin A. *Black Sea Monitoring Guidelines. Macrophytobenthos*. [s. l. : s. n.], 2014, 92 p. URL: https://emblasproject.org/wp-content/uploads/2013/12/Manual_macrophytes_EMBLAS_ann.pdf [accessed 21.03.2023].
 20. Pełechaty M., Brzozowski M., Kaczmarek L., Kowalewski G., Nowak B., Pukacz A. The charophyte decline and recovery in Lake Lednica in response to four decades of changes in water fertility and hydrometeorological conditions. In: *11th Symposium for European Freshwater Sciences*, June 30 – July 5, 2019, Zagreb, Croatia : Abstract book. [Zagreb] : [s. n.], 2019, pp. 386.
 21. Romanov R., Korolesova D., Afanasyev D., Zhakova L. *Chara baltica* (Charophyceae, Charales) from the Black Sea Region and taxonomic implications of extrastipulodes. *Botanica*, 2020, vol. 26, iss. 2, pp. 126–137. <https://doi.org/10.2478/botlit-2020-0014>
 22. Sand-Jensen K., Bruun H. H., Baastrup-Spohr L. Decade-long time delays in nutrient and plant species dynamics during eutrophication and reoligotrophication of Lake Fure 1900–2015. *Journal of Ecology*, 2017, vol. 105, no. 3, pp. 690–700. <https://doi.org/10.1111/1365-2745.12715>
 23. Schmieder K., Werner S., Bauer H. Submersed macrophytes as a food source for wintering waterbirds at Lake Constance. *Aquatic Botany*, 2006, vol. 84, iss. 3, pp. 245–250. <http://dx.doi.org/10.1016/j.aquabot.2005.09.006>
 24. Simons J., Ohm M., Daalder R., Boers P., Rip W. Restoration of Botshol (the Netherlands) by reduction of external nutrient load: Recovery of a characean community, dominated by *Chara connivens*. *Hydrobiologia*, 1994, vol. 275, iss. 1, pp. 243–253. <https://doi.org/10.1007/BF00026715>
 25. Sooksawat N., Meetam M., Kruatrachue M., Pokethitiyook P., Inthorn D. Performance of packed bed column using *Chara aculeolata* biomass for removal of Pb and Cd ions from wastewater. *Journal of Environmental Science and Health, Part A*, 2017, vol. 52, iss. 6, pp. 539–546. <https://doi.org/10.1080/10934529.2017.1282774>
 26. Torn K., Martin G. Changes in the distribution of charophyte species in enclosed seabays of western Estonia. *Proceedings of the Estonian Academy of Sciences. Biology. Ecology*, 2003, vol. 52, iss. 2, pp. 134–140. <https://doi.org/10.3176/biol.ecol.2003.2.05>

**ВОССТАНОВЛЕНИЕ ФИТОЦЕНОЗА *CHARA ACULEOLATA* KÜTZING
В ТЕНДРОВСКОМ ЗАЛИВЕ (ЧЁРНОЕ МОРЕ)****Д. Д. Королесова**

Черноморский биосферный заповедник, Голая Пристань, Российская Федерация

E-mail: chernyakova.darya@gmail.com

Проанализирована долгосрочная динамика площадей произрастания и биомассы макрофитов фитоценоза *Chara aculeolata* Kützing в Тендровском заливе Чёрного моря. Частичную его деградацию отмечали с 1993 г. За период с 1993 по 2010 г. площадь произрастания фитоценоза сократилась с 100 до 6,3 км². В 2010–2021 гг. зарегистрированы элементы восстановительной сукцессии. Зафиксированы постепенное медленное расширение площадей произрастания и увеличение биомассы водорослей в течение 10 лет мониторинга и внезапное значительное восстановление в 2021 г. По данным 2021 г., исследуемый фитоценоз распространён на площади 36 км², биомасса доминирующего вида достигла 1800 г·м⁻². В работе обсуждаются возможные причины наблюдаемых изменений.

Ключевые слова: Charophyta, макрофитобентос, восстановительная сукцессия, многолетняя динамика, реколонизация

UDC 582.273-19(265.52)

FINDING
OF ACROSORIUM YENDOI YAMADA (DELESSERIACEAE, RHODOPHYTA),
A NEW TO KAMCHATKA SPECIES,
IN AVACHA GULF

© 2023 **O. N. Selivanova and G. G. Zhigadlova**

Kamchatka Branch of the Pacific Geographical Institute, Far Eastern Branch
of the Russian Academy of Sciences, Petropavlovsk-Kamchatsky, Russian Federation
E-mail: oselivanova@mail.ru

Received by the Editor 12.10.2022; after reviewing 12.10.2022;
accepted for publication 04.08.2023; published online 01.12.2023.

Recent finding of the red alga *Acrosorium yendoi*, new to Kamchatka, during observations in a laboratory marine aquarium, containing sediments and water from the Avacha Gulf (Southeastern Kamchatka), was supported by its discovery in this water area using the method of parallel floristic observations both under laboratory and natural conditions. *A. yendoi* was previously recorded in more southern areas of the Pacific coast of Russia (Sea of Japan), as well as in Japan, China, and Korea. As a result of our studies, the species is registered in the flora of Eastern Kamchatka, and this significantly expands the understanding of *A. yendoi* range, shifting it to the north and changing the phytogeographic characteristics of the species.

Keywords: *Acrosorium*, Kamchatka, area, aquarium research, parallel floristic observations, climate warming

The study of aquarium algae in a laboratory marine aquarium, containing soil and water from the Avacha Gulf (Southeastern Kamchatka), was initially undertaken by us as a monitoring research of this group of marine organisms that create a habitat for other hydrobionts in an artificial reservoir. However, this investigation had unexpected results. In the aquarium, algae new for this region were registered: *Lukinia dissecta* Perestenko, 1996 and *Acrosorium yendoi* Yamada, 1930 (Rhodophyta) [Selivanova, Zhigadlova, 2021, 2022]. We recognized them not as invasive aquarium elements, but as real natural species that got into the aquarium with water and soil. The occurrence of unusual algae in the aquarium was assumed to be an indicator of their actual presence in the Avacha Gulf water area and a stimulus to search and find these species in nature. Being focused on this problem, we carried out expeditionary work. Soon, our assumption about the actual growth of these algae in nature was fully confirmed for *L. dissecta*: it was registered in Kamchatka water area in June 2021 [Selivanova, Zhigadlova, 2023]. Continuing the search for new species became the aim of this study. As a result, the second species recorded in the aquarium, *A. yendoi*, was also found in natural conditions during field work in the Avacha Gulf. The finding allowed to clarify the available information about the geography of this species.

MATERIAL AND METHODS

In the course of this study, an original observation method was used in the laboratory marine aquarium in parallel with the classic sampling of algological material in nature. The method proved to be quite productive for searching and finding algal species new for the investigated region.

Algological material was sampled in the Avacha Gulf using light diving equipment from a small vessel. Aquarium and natural algae samples from Southeastern Kamchatka were identified under an Olympus CX31 light microscope. When identifying, we compared the material with the original description of a taxon and information from other publications on this species [Perestenko, 1994; Yamada, 1930; Yoshida, 1998]. Samples were photographed with an Olympus SZ-20 digital camera. The material is stored in the laboratory of hydrobiology of KB PGI FEB RAS.

RESULTS AND DISCUSSION

The studied natural samples of *A. yendoi* (Fig. 1A, B) were taken on 21 April, 2022, in the Vilyuchinskaya Bay (the Avacha Gulf), near the Cape Razdelny, from a 14-m depth, from rocky-pebble soil with sand deposits. The sampling was carried out by Ermolenko E.

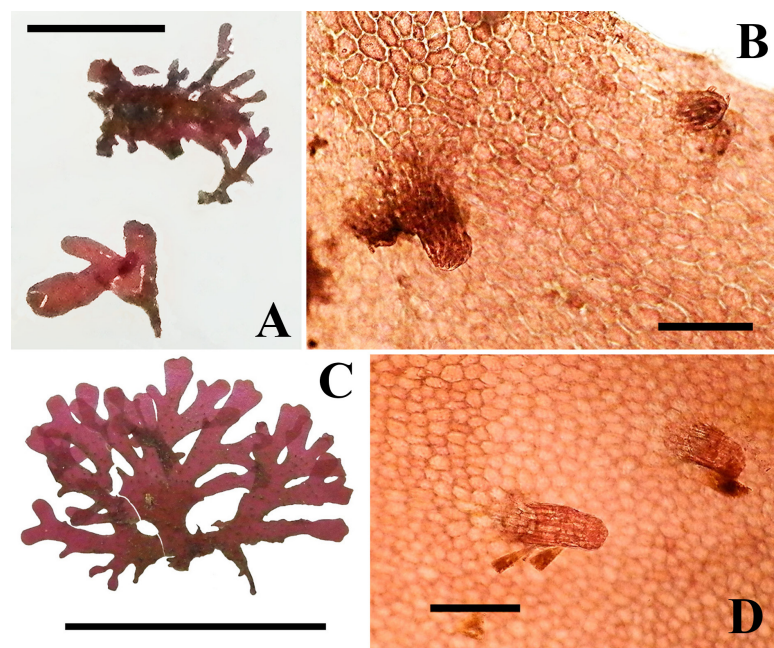


Fig. 1. *Acrosorium yendoi* Yamada, 1930 from the coastal waters of Southeastern Kamchatka (A, B) and laboratory marine aquarium (C, D): A, young natural plants; C, mature aquarium plants; B, D, fragments of the blades of natural and aquarium plants with rhizoidal outgrowths. Scale: A, 1 cm; C, 2 cm; B, D, 200 μ m

During diving works in the Vilyuchinskaya Bay, small, rather depressed young plants were sampled; those grew in early spring at a temperature of +1...+2 °C which is probably uncomfortable for them. However, their general morphology and anatomy were consistent with those of mature plants grown in the aquarium at a higher temperature, +6...+7 °C, and these ones, in turn, correspond to the original description of the species. The thallus is purple-red and membranous; it is attached to the substrate by numerous rhizoids. Branching is irregularly dichotomous. The branches intertwine using rhizoidal outgrowths. The plates have a smooth edge; microscopic one- to three-layer veins are revealed on a cross-section.

A. yendoi was originally described from Japan [Yamada, 1930] and recorded in the southern areas of the Russian Far East (Strait of Tartary and Peter the Great Gulf, Sea of Japan) [Klochkova, 1996; Kozhenkova, 2020; Perestenko, 1994]. In addition to Japan [Yoshida, 1998; Yoshida et al., 2015] and Russia, this species was registered in China [Checklist of Biota, 2008; Tseng, 2009] and Korea [Lee, Kang, 2001; Nam, Kang, 2012]. In Russian literature on phycology, *A. yendoi* is generally considered as a boreal-tropical, interzonal Pacific sub-Asian species [Perestenko, 1994] or a sub-Asian low-boreal-subtropical species [Klochkova, 1996].

In fact, the first finding of *A. yendoi* in Kamchatka was its record in the aquarium [Selivanova, Zhigadlova, 2021, 2022]. In these publications, we excluded the accidental introduction of algal spores from reliably known habitats of the species due to their geographic distance from the studied area. To explain the occurrence in the aquarium of algae unusual for the investigated water area, we assumed that spores or juvenile plants were contained in water or soil sampled for the aquarium from the Avacha Gulf. Observations on the dynamics of the aquarium ecosystem development revealed an extensive growth of algae; *Acrosorium*, with its small, creeping thallus, was so active that it almost distributed in all suitable surfaces of the substrate and became the prevailing species. Apparently, the conditions in the aquarium turned out to be favorable for its development. Temperature was most likely the limiting factor. Interestingly, it became clear relatively recently that this species is not so thermophilic. The work of Chinese researchers [Sun et al., 2010], who carried out a long-term monitoring of the biodiversity of benthic algae in the littoral zone of the Nanji Islands (National Marine Nature Reserve, South China Sea, China), showed that with a rise in water temperature, the proportion of subtropical species in a macroalgal community increased, while the proportion of moderately cold-water species noticeably decreased. Regarding *A. yendoi*, it was established as follows: its abundance in the littoral zone of the islands dropped by approximately 1.5 times over 40 years, with the transition from the category of prevailing species to the category of common ones [Sun et al., 2010]. These researchers assumed that a decrease in abundance of certain algal species results from the global climate warming. Kamchatka is also in the trend of increasing mean annual temperature of the surface layer of the Earth and World Ocean. Data obtained in a comparative analysis of two 30-year periods using the mean annual temperature curve for Petropavlovsk-Kamchatsky showed a rise in air temperature by 0.5 °C (<http://kammeteo.ru>). The water temperature increases, as the temperature of water masses rises; accordingly, the finding of species of marine hydrobionts considered to be warm-water ones is not so unexpected in Kamchatka water area. Probably, due to the climate warming, *A. yendoi* began to move north, *inter alia* to Kamchatka shores, and thus occurred in our aquarium.

Under natural conditions, this species might not have been found in the bay due to its small size, its low abundance, or simply poor knowledge on the algal flora of the region. The study of aquarium algae served as a sort of target indicator for its search in nature. To date, *A. yendoi* has been found in the Avacha Gulf water area, which allows to expand and clarify its natural range.

Conclusion. The finding of *Acrosorium yendoi* in Eastern Kamchatka waters significantly shifts the species range to the north compared to previously known one (data from more southern areas of the Pacific coast of Russia, Sea of Japan). Thus, *A. yendoi* should no longer be considered as a boreal-tropical, Pacific sub-Asian or low-boreal-subtropical species, but should be recognized as a wide-boreal Asian-Pacific species.

Acknowledgment. We express our gratitude to the crew of the boat “Larus” for the opportunity to work in the Avacha Gulf water area and to Ermolenko E. for participation in the sampling of algae.

REFERENCES

1. Klochkova N. G. *Flora vodoroslei makrofitov Tatarskogo proliva (Yaponskoe more) i osobennosti ee formirovaniya*. Vladivostok : Dal'nauka, 1996, 292 p. (in Russ.)
2. Perestenko L. P. *Red Algae of the Far-Eastern Seas of Russia*. Saint Petersburg : Olga, 1994, 331 p. (in Russ.)
3. Selivanova O. N., Zhigadlova G. G. Floristic finds in the marine laboratory aquarium. In: *Conservation of Biodiversity of Kamchatka and Coastal Waters : materials of the XXII international conference*, Petropavlovsk-Kamchatsky, 17–18 November, 2021. Petropavlovsk-Kamchatsky : Kamchatpress, 2021, pp. 66–71. (in Russ.). https://doi.org/10.53657/9785961004038_66
4. Selivanova O. N., Zhigadlova G. G. On the finding of algae new to South-eastern Kamchatka in a laboratory marine aquarium. *Biologiya morya*, 2022, vol. 48, no. 2, pp. 129–134. (in Russ.). <https://doi.org/10.1134/S1063074022020092>
5. Selivanova O. N., Zhigadlova G. G. On the distribution of marine alga *Lukinia dissecta* Perestenko (Rhodymeniaceae, Rhodymeniales) in the North Pacific. *Morskoy biologicheskij zhurnal*, 2023, vol. 8, no. 1, pp. 109–112. (in Russ.). <https://marine-biology.ru/mbj/article/view/370>
6. *Checklist of Biota of Chinese Seas* / Liu Ruiyu (Ed.). Beijing : Science Press, Academia Sinica, 2008, pp. 1–1267. [in Chinese].
7. Kozhenkova S. I. Checklist of marine benthic algae from the Russian continental coast of the Sea of Japan. *Phytotaxa*, 2020, vol. 437, no. 4, pp. 177–205. <https://doi.org/10.11646/phytotaxa.437.4.1>
8. Lee Y., Kang S. *A Catalogue of the Seaweeds in Korea*. Jeju : Cheju National University Press, 2001, 662 p. [in Korean].
9. Nam K. W., Kang P. J. *Algal Flora of Korea*. Vol. 4, no. 7 : *Rhodophyta: Florideophyceae: Ceramiales: Delesseriaceae: 22 Genera Including Acrosorium*. Incheon : National Institute of Biological Resources, 2012, 129 p.
10. Sun J., Ning X.-R., Le F., Chen W., Zhuang D. Long term changes of biodiversity of benthic macroalgae in the intertidal zone of the Nanji Islands. *Acta Ecologica Sinica*, 2010, vol. 30, iss. 2, pp. 106–112. <http://dx.doi.org/10.1016/j.chnaes.2010.03.010>
11. Tseng C. K. *Seaweeds in Yellow Sea and Bohai Sea of China*. Beijing : Science Press, 2009, 453 p. [in Chinese].
12. Yamada Y. Notes on some Japanese algae. I. *Journal of the Faculty of Science, Hokkaido Imperial University. Series 5, Botany*, 1930, vol. 1, no. 1, pp. 27–36.
13. Yoshida T. *Marine Algae of Japan*. Tokyo : Uchida Rokakuho Publishing Co., Ltd., 1998, 1222 p. [in Japanese].
14. Yoshida T., Suzuki M., Yoshinaga K. Checklist of marine algae of Japan (revised in 2015). *Japanese Journal of Phycology*, 2015, vol. 63, no. 3, pp. 129–189. [in Japanese].

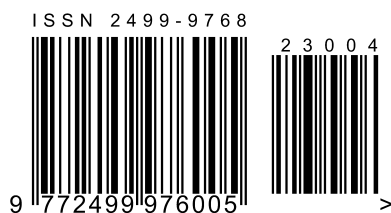
**НАХОДКА В АВАЧИНСКОМ ЗАЛИВЕ
НОВОЙ ДЛЯ КАМЧАТКИ ВОДРОСЛИ
ACROSORIUM YENDOI YAMADA (DELESSERIACEAE, RHODOPHYTA)**

О. Н. Селиванова, Г. Г. Жигadlova

Камчатский филиал Тихоокеанского института географии ДВО РАН, Петропавловск-Камчатский,
Российская Федерация
E-mail: oselivanova@mail.ru

Недавнее нахождение новой для Камчатки красной водоросли *Acrosorium yendoi* в ходе наблюдений в лабораторном морском аквариуме, содержащем грунт и воду из Авачинского залива (Юго-Восточная Камчатка), подкреплено её обнаружением в данной акватории с использованием метода параллельных флористических исследований в лабораторных и природных условиях. Ранее *A. yendoi* был известен из более южных районов тихоокеанского побережья России (Японское море), а также из Японии, Китая и Кореи. В результате наших исследований вид регистрируется во флоре Восточной Камчатки, что значительно расширяет представления об ареале *A. yendoi*, смещая его к северу и изменяя фитогеографические характеристики вида.

Ключевые слова: *Acrosorium*, Камчатка, ареал, аквариумные исследования, параллельные лабораторные и природные наблюдения, потепление климата



Вниманию читателей!

*Институт биологии южных морей
имени А. О. Ковалевского РАН,
Зоологический институт РАН*

*издают
научный журнал*

**Морской биологический журнал
Marine Biological Journal**

- МБЖ — периодическое издание открытого доступа. Подаваемые материалы проходят независимое двойное слепое рецензирование. Журнал публикует обзорные и оригинальные научные статьи, краткие сообщения и заметки, содержащие новые данные теоретических и экспериментальных исследований в области морской биологии, материалы по разнообразию морских организмов, их популяций и сообществ, закономерностям распределения живых организмов в Мировом океане, результаты комплексного изучения морских и океанических экосистем, антропогенного воздействия на морские организмы и экосистемы.
- Целевая аудитория: биологи, экологи, биофизики, гидро- и радиобиологи, океанологи, географы, учёные других смежных специальностей, аспиранты и студенты соответствующих научных и отраслевых профилей.
- Статьи публикуются на русском и английском языках.
- Периодичность — четыре раза в год.
- Подписной индекс в каталоге «Пресса России» — E38872. Цена свободная.

Заказать журнал

можно в научно-информационном отделе ИнБЮМ.
Адрес: ФГБУН ФИЦ «Институт биологии южных морей имени А. О. Ковалевского РАН», пр-т Нахимова, 2, г. Севастополь, 299011, Российская Федерация.
Тел.: +7 8692 54-06-49.
E-mail: mbj@imbr-ras.ru.

*A. O. Kovalevsky Institute of Biology
of the Southern Seas of RAS,
Zoological Institute of RAS*

*publish
scientific journal*

**Морской биологический журнал
Marine Biological Journal**

- MBJ is an open access, peer reviewed (double-blind) journal. The journal publishes original articles as well as reviews and brief reports and notes focused on new data of theoretical and experimental research in the fields of marine biology, diversity of marine organisms and their populations and communities, patterns of distribution of animals and plants in the World Ocean, the results of a comprehensive studies of marine and oceanic ecosystems, anthropogenic impact on marine organisms and on the ecosystems.
- Intended audience: biologists, ecologists, biophysicists, hydrobiologists, radiobiologists, oceanologists, geographers, scientists of other related specialties, graduate students, and students of relevant scientific profiles.
- The articles are published in Russian and English.
- The journal is published four times a year.
- The subscription index in the “Russian Press” catalogue is E38872. The price is free.

You may order the journal

in the scientific information department of IBSS.
Address: A. O. Kovalevsky Institute of Biology of the Southern Seas of RAS, 2 Nakhimov avenue, Sevastopol, 299011, Russian Federation.
Tel.: +7 8692 54-06-49.
E-mail: mbj@imbr-ras.ru.